DOE/ET/23114-80/1
(DE82008098)

SURVEY OF THE HEIGHT AND EXPOSURE VARIATION OF EMPIRICAL PARAMETERS ENTERING AN EMPIRICAL PROBABILITY DENSITY FUNCTION FOR WIND SPEED

Final Report

By
C. Eugene Buell
Robert C. Bundgaard

January 1981

Work Performed Under Contract No. AC06-79ET23114

Science Applications, Inc.
Colorado Springs, Colorado

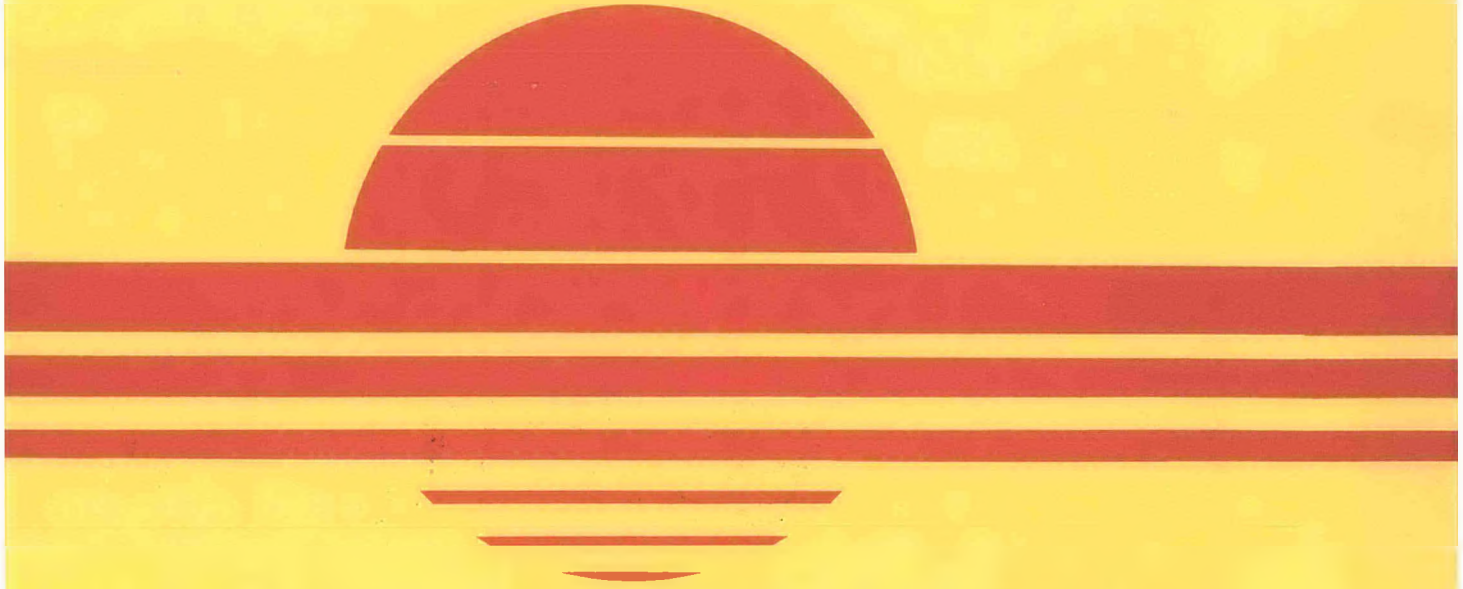

U.S. Department of Energy

Solar Energy

DISCLAIMER

DOE/ET/23114--80/1

DE82 008098

SURVEY OF THE HEIGHT AND EXPOSURE VARIATION OF EMPIRICAL PARAMETERS ENTERING AN EMPIRICAL PROBABILITY DENSITY FUNCTION FOR WIND SPEED

FINAL REPORT

C. Eugene Buell (a)
Robert C. Bundgaard (b)

Science Applications, Inc.
2860 South Circle Drive
Colorado Springs, CO 80906

January 1981

PREPARED FOR THE UNITED STATES

DEPARTMENT OF ENERGY
OFFICE OF SOLAR POWER APPLICATIONS
FEDERAL WIND ENERGY PROGRAM

DOE CONTRACT NO. DE-AC06-79ET23114

(a) Consultant
1601 Columbine Place
Colorado Springs, CO

(b) Consultant
1405 Eagle View Drive
Colorado Springs, CO

ACKNOWLEDGEMENTS

We wish to express our appreciation of the assistance rendered by Mr. Jack W. Reed in loaning the print-out of the Patrick AFB Tower 313 summaries, to Mr. Frank V. Hansen for a copy of the WSMR tower data summaries, and to the personnel of the Pacific Northwest Laboratory for several data summaries.

EXECUTIVE SUMMARY

Since the Weibull distribution is not a physically acceptable distribution function for scalar wind speed and since even the wind speed data itself is frequently bimodal, it is suggested that a mixture of two generalized Rayleigh distributions (a thoroughly acceptable distribution) be used to describe the distribution of scalar wind speed.

A reasonably extensive analysis of scalar wind speed data of several kinds is reported. Data from meteorological towers at Patrick AFB, FL, the Hanford Meteorological Station, Cape Kennedy (NASA), FL, and White Sands Missile Range, NM, were analyzed in some detail and the variation of parameters as a function of anemometer height was determined. Data from meteorological towers at nuclear power plant sites was analyzed for those cases where anemometers were located at two or more levels. Data was provided by Pacific Northwest Laboratory from locations in the northwestern U.S. where the anemometer had been located at two different elevations and the wind speed frequency tabulated separately at the different levels. In all of these cases the variation of the parameters entering the distribution function was determined as a function of height. It was found that insofar as the empirical distribution function remained of the same type from level to level, the parameter variation was reasonably well described by the frequently applied power law with the exception of the mixing proportion of the two components of the mixture of the two generalized Rayleigh distributions used.

The effect of the site exposure on the parameters of the empirical distribution function is reported for locations near Boston, MA, Washington, DC, Bridgeport and New Haven, CT, and Tucson, AZ. It was found, as expected, that site exposure was important in determing the parameters of the mixture.

Diurnal changes in the empirical distribution function parameters at Washington, DC, Montgomery, AL, and Mobile, AL, are also reported.

The two components of the mixture, each a generalized Rayleigh distribution, may be described as one that dominates the distribution of the lower scalar wind speeds and one that dominates the higher speeds, called herein the low speed and high speed components of the mixture. In any particular case, one of these mixture components may be absent. Also one or both of these components may reduce to an ordinary Rayleigh distribution or even to a degenerate (spike) distribution.

In the case of the tower data it was found that the low speed component of the mixture was dominant at the lower anemometer elevations while at the higher elevations the high speed component became dominant.

With regard to the type of distribution that appeared in the two mixture components, it may be said that the more varied the conditions included in the data collection the simpler the two mixture components. Thus, yearly data (which is affected by the annual and diurnal variation) tends frequently to be an ordinary Rayleigh distribution.

In the case of tower scalar wind speed, the high speed mixture component at the upper levels is usually a generalized Rayleigh while that at the lower levels tends to be an ordinary Rayleigh.

At "sheltered" locations, i.e., those located on terrain noticeably lower than the surrounding hilltops, the low speed mixture component is strongly dominant and tends to be an ordinary Rayleigh distribution or even degenerate. At "exposed" locations, i.e., those located at roughly the general hilltop level, the high speed component is dominant and tends to be a generalized Rayleigh distribution.

As far as the annual variation of the parameters and the type of distribution appearing in the mixture components is concerned, the low speed component is more frequent in summer and the high speed component more frequent in winter. The type of distribution function for these mixture components seems to be more or less consistent as far as seasonal variation

is concerned. A notable feature of the monthly distribution function is that the generalized Rayleigh distribution function appears more frequently than in the annual data.

The diurnal variation of parameters and the distribution types is more extreme than for the annual variation. As expected, the early morning scalar wind speed distribution is dominated by the low speed component which tends to be an ordinary Rayleigh distribution and very frequently can be described as degenerate (a "spike" at zero wind speed, calm). The afternoon winds are dominated by the high speed component which is most frequently a generalized Rayleigh distribution.

TABLE OF CONTENTS

LIST OF TABLES

LIST OF FIGURES

INTRODUCTION

PREVIOUS RESEARCH

The problem of describing the probability density function for the scalar wind speed is of long standing. Hesselberg and Björkdal (1929) consider wind speeds as an aspect of turbulence (speeds measured almost instantaneously and sampled frequently over a short period of record, several minutes) while Wagner (1929) considers the case of wind speeds sampled daily over a long period of record (several years). Turbulence theory considerations lead Hesselberg and Björkdal to conclude that the scalar wind speed probability density function should be that of a generalized Rayleigh distribution. Wagner starts with the assumption that the wind vector is distributed as a bivariate normal distribution (general) and derives the corresponding distribution for the scalar wind speed (and direction, also). Both conclude that their results do not satisfactorily describe the observed data and suggest that the data requires that the probability density function should be that of a mixture of two or more distributions with different parameters.

The work of Hesselberg and Björkdal and of Wagner was essentially neglected. There was a revival of interest in the subject in the 1950s (Brooks et al. (1950), Davies (1958), Dinkelacker (1949) Essenwanger (1959), Gloyne (1959), Guterman (1961), to mention some) but attention was confined to either the circularly normal case for the wind velocity vector or to probability density functions of special form in the case of the scalar wind speed.

Current interest in the scalar wind speed distribution for power (and other) applications has lead to many proposed probability density functions (p.d.f.). Luna and Church (1974) suggest a log-normal p.d.f. (see also Buell, 1976); Widger (1976 and 1977) a square-root-normal; Boehm (1976) approximates an observed wind speed p.d.f. with seven different functions; Beardsley (1980) suggests the inverse Gaussian p.d.f. The greatest current interest is centered on the Weibull p.d.f. [see Justus, Hargraves, and Yalcin (1976), Justus, Hargraves, Mikhail, and Garber (1978), Justus (1978),

Hennessey (1977)]. Extensions or generalizations of the Weibull p.d.f. by introduction of an additional parameter have been made by Stewart and Essenwanger (1978) and by Van der Auwera, de Meyer, and Malet (1980) while Takle and Brown (1977) introduce a parameter to account for the occurrence of calms. There are serious objections to nearly all of these p.d.f.'s as applied to the scalar wind speed. First, except for some special values of the parameters, they are physically impossible (see Appendix A for details). Second, they are all unimodal (one maximum) while there are many cases in which the observed scalar wind speed p.d.f. is bimodal (two distinct maxima) (see Appendix B).

PRESENT PROBLEM

The objective of this report is to reconsider the suggestions of Hesselberg and Björkdal (1929) and Wagner (1929) (namely to use as the probability density function for wind speed a mixture of two generalized Rayleigh distributions) and to investigate the behavior of the parameters that are involved under various conditions, particularly as a function of anemometer height above the ground.

ORGANIZATION OF THIS REPORT

The remaining sections of this introduction are devoted to a brief explanation of details regarding the empirical probability density function being used including the physical significance of the parameters involved and several items regarding the behavior of the probability density functions of the mixture components as functions of these parameters.

Several chapters are devoted to the investigation of the behavior of the parameters as a function of anemometer height using data from instrumented towers; in particular at White Sands, NM, Hanford, WA, Cape Kennedy, FL, Patrick AFB, FL, several nuclear power plant sites, and from locations in the northwestern states for which wind speed data pertaining to different anemometer levels has been summarized. A chapter is devoted to the behavior of the parameters at station anemometer elevation as a function of the nature of the surrounding terrain, month of the year, and hour of the day.

THE EMPIRICAL FORMULA

The Wall Street Journal occasionally remarks "There is no such thing as a free lunch." Also, there is no such thing as a simple universal probability density function for wind speed in the atmosphere. An adequate empirical formula for the probability density function for wind speed should not only be simple (or at least as simple as possible to describe the data) but it should also be strictly compatible with the fact that wind speed is only a partial aspect of the two-dimensional wind velocity vector and in addition it should be derivable from bivariate distributions that are approximations which reasonably reproduce the characteristics of such a bivariate vector distribution. Some of these requirements are discussed in more detail in Appendix A and Appendix B. In particular, it is shown in Appendix B that one must be prepared to accept as a reasonable approximation to the real world a speed probability density function that can represent a mixture of two probability density functions each of which is of the simplest type that can be derived from the simplest possible bivariate probability density for a wind velocity vector. This probability density function is of the form

$$p(w) = kp_1(w;\sigma_1,w_1) + (1-k)p_2\ (w;\sigma_2,w_2) \qquad (1)$$

where $p(w)$ = the probability density function (p.d.f. hereafter) of the mixture

$p_1(w;\sigma_1,w_1)$ = the generalized Rayleigh p.d.f. for the first component of the mixture with parameters σ_1,w_1

$p_2(w;\sigma_2,w_2)$ = the generalized Rayleigh p.d.f. for the second component of the mixture with parameters σ_2,w_2

σ_1,σ_2 = the wind vector component standard deviation of a circularly normal bivariate p.d.f.

w_1,w_2 = the resultant mean wind speed of a circularly normal bivariate p.d.f.

k = the mixing fraction (k=1 implies that the mixture is entirely from the component with parameters σ_1, w_1; k=0 that it is entirely from the component with parameters σ_2, w_2). For a true mixture $0<k<1$.

The functions on the right of (1) differ only in the values that are assigned to the parameters and may be written in common form

$$p(w;\sigma,w_R) = (w/\sigma^2)\exp\left\{-(w^2+w_R^2)/2\sigma^2\right\} I_0(ww_R/\sigma^2) \qquad (2)$$

where $I_0(\cdot)$ is the modified Bessel function of zero order. (Tabulated extensively; see Abramowitz and Stegun (1964), Jahnke and Emde (1960); etc.) The infinite series for $I_0(\cdot)$ is

$$I_0(x) = 1 + (x/2)^2/(1!)^2 + (x/2)^4/(2!)^2 + \text{---} + (x/2)^{2m}/(m!)^2 + \text{---} \qquad (3)$$

It is readily seen that if $w_R=0$, one has the p.d.f. for the ordinary Rayleigh distribution

$$p(w;\sigma,0) = (w/\sigma^2)\exp\left\{-w^2/2\sigma^2\right\} \qquad (4)$$

(Note: The Rayleigh distribution is sometimes written in the form

$$p(w) = \frac{\pi}{2}\frac{w}{\bar{w}^2}\exp\left\{-\frac{\pi}{4}\left(\frac{w}{\bar{w}}\right)^2\right\}$$

where $\bar{w}$ is a mean wind speed (see Cliff, 1977). Comparing this with (4) indicates that $\bar{w}=\sigma\sqrt{\pi/2}$, which is the mean wind speed resulting from a bivariate circularly normal p.d.f. for the wind vector with resultant mean speed (w_R) of zero and a standard deviation of σ. There is a considerable difference between the mean wind speed and the resultant mean wind speed (or mean resultant wind speed). The first is the mean of the individual speeds, the second is the mean of the resultant vector. For example consider the three wind vectors with components (1,0), (0,1), (-1,-1). The three wind speed are 1, 1, $\sqrt{2}$ [$w = (u^2+v^2)^{\frac{1}{2}}$] so that the mean wind speed is (1+1+1.414)/3 = 1.13

The resultant of the three vectors concerned has components $u_R=1+0-1=0$ and $v_R=0-1+1=0$ and thence the mean components $\bar{u}=0$, $\bar{v}=0$ so that the resultant mean speed is given by $w_R=(\bar{u}^2+\bar{v}^2)^{\frac{1}{2}}=0$. The resultant mean speed is a vector and thence has a direction (except when its value is zero). The expressions mean resultant speed and resultant mean speed are exactly equivalent. If one has vectors with components (u_i,v_i), $i=1,---,n$, then the resultant vector has components $u_R=\sum u_i$, $v_R=\sum v_i$ so that the mean resultant speed is $w_R=(u_R^2+v_R^2)^{\frac{1}{2}}/n$; the mean vector has components $\bar{u}=(\sum u_i)/n$, $\bar{v}=(\sum v_i)/n$ so that the resultant mean speed is $w_R=(\bar{u}^2+\bar{v}^2)^{\frac{1}{2}}$ which is exactly the same as before.)

The p.d.f. (2) has the property of becoming a "Dirac function." As for p.d.f.'s generally, $\int_0^\infty p(w;\sigma,w_R)dw = 1$, i.e., the area under the curve is 1 regardless of the parameter values. If the parameter σ approaches zero this property is preserved. This means that for $\sigma\to 0$ the "graph" of the p.d.f. becomes an infinitely tall spike of zero width but with unit area. This will be called a degenerate case, but will be useful.

The empirical formula (1) for the wind speed p.d.f. contains five parameters which will be tabulated as the pentad $(\sigma_1,w_1,\sigma_2,w_2,k)$. Due to the fact that the p.d.f.'s for the two components of the mixture have identical functional form there is some redundancy. For example, if we replace k by 1-k and exchange σ_1,w_1 with σ_2,w_2, the mixture described is the same as the original. Thus,

(1.43, 0.00, 2.78, 3.14, 33.47) and (2.78, 3.14, 1.43, 0.00, 66.53)

are one and the same mixtures. In the above and throughout this report, the units for σ_1,w_1,σ_2, and w_2 are meters per second. The mixing ratio, k, may be expressed in percent ($0\le k\le 100$) or in fraction form ($0\le k\le 1$).

Usually, but not always, one pair of (σ,w_R) describes the p.d.f. of the mixture at low wind speed and while the other pair is predominant at high wind speed (see illustrations in Appendix C). To simplify the situation

the following convention will be used frequently: the first pair, (σ_1,w_1) will be used for the component of the mixture that describes the low wind speed range of the p.d.f. and (σ_2,w_2) for the component effective in describing the high wind speed range.

CLASSIFICATION OF CASES

It is useful to classify the various special cases that occur for special values of the parameters $\sigma_1,w_1,\sigma_2,w_2,k$. These are listed in the order of increasing number of non-zero parameter values. The first five cases are concerned with the situations in which neither of the two components of the mixture is degenerate, i.e., the p.d.f.'s concerned are either Rayleigh or generalized Rayleigh types. In the remaining cases one of the p.d.f.'s is degenerate. The degenerate cases are more than a mathematical curiosity. They apparently occur with reasonable frequency and represent situations of considerable engineering importance.

When only one component of the mixture is present, then k=0 or k=1. There are two cases of this kind:

I. $(0,0,\sigma_2,0,0)$, $(\sigma_1,0,0,0,1)$ when the p.d.f. corresponds to the ordinary Rayleigh distribution, and the special case

II. $(0,0,\sigma_2,w_2,0)$, $(\sigma_1,w_1,0,0,1)$ when the p.d.f. is that of the generalized Rayleigh distribution.

In other cases $0<k<1$. The simplest case is

III. $(\sigma_1,0,\sigma_2,0,k)$ when two ordinary Rayleigh distributions are present. And progressively

IV. $(\sigma_1,w_1,\sigma_2,0,k)$, $(\sigma_1,0,\sigma_2,w_2,k)$ when one is an ordinary Rayleigh and the other is a generalized Rayleigh, and finally

V. $(\sigma_1,w_1,\sigma_2,w_2,k)$ when both are generalized Rayleigh distribution.

The remaining cases are all degenerate in that one component of the mixture reduces to an infinite spike of weight k at w_1 or weight 1-k at w_2 in the p.d.f. (or a jump of height k at w_1 or of height 1-k at w_2 in the distribution function (D.F.)).

When the regular component is an ordinary Rayleigh distribution the cases are

VI. $(0,0,\sigma_2,0,k)$, $(\sigma_1,0,0,0,k)$, $(0,w_1,\sigma_2,0,k)$, $(\sigma_1,0,0,w_2,k)$

and when the regular component is a generalized Rayleigh distribution the cases are

VII. $(0,0,\sigma_2,w_2,k)$, $(\sigma_1,w_1,0,0,k)$, $(0,w_1,\sigma_2,w_2,k)$, $(\sigma_1,w_1,0,w_2,k)$

The impractical degenerate cases consist entirely of spikes; one of weight k at w_1 and one of weight (1-k) at w_2 in the p.d.f. (jump of height k at w_1 and one of height (1-k) at w_2 in the D.F.)

VIII. $(0,0,0,0,k)$, $(0,w_1,0,0,k)$, $(0,0,0,w_2,k)$, $(0,w_1,0,w_2,k)$.

The number of occurrences for the pentad $(\sigma_1,w_1,\sigma_2,w_2,k)$ classified as in the preceding paragraphs have been extracted from the various tables that follow and are tabulated in Table 0. The columns are headed I through VII, which correspond to the preceding cases, and one of the pentads concerned is shown. These are three types of records concerned which characterize the frequency function for scalar wind speed from which the parameters of the empirical formula were derived,; annually, monthly, and hourly. The fourth row gives the total of these three. The top half is simply a numbers count while the bottom half gives the occurrence of the cases in percent. (The data for White Sands Missile Range Tower has been omitted since it is a very special situation. If included it would add 108 cases to the monthly record type, all in case VI.)

TABLE 0. FREQUENCY OF OCCURRENCE OF THE CASES FOR THE PENTAD $(\sigma_1, w_1, \sigma_2, w_2, k)$

Type of Record	I $(0,0,\sigma_2,0,0)$	II $(0,0,\sigma_2,w_2,0)$	III $(\sigma_1,0,\sigma_2,0,k)$	IV $(\sigma_1,0,\sigma_2,w_2,k)$	V $(\sigma_1,w_1,\sigma_2,w_2,k)$	VI $(0,0,\sigma_2,0,k)$	VII $(0,0,\sigma_2,w_2,k)$	Total
				Number of Cases				
Annual	3	3	64	64	18	6	3	161
Monthly	0	6	54	81	67	9	7	224
Hourly	0	7	36	96	59	1	19	218
Total	3	16	154	241	144	16	29	603
				Percent of Cases				
Annual	1.9	1.9	39.8	39.8	11.2	3.7	1.9	
Monthly	0.0	2.7	24.1	36.2	29.9	4.0	3.1	
Hourly	0.0	3.2	16.5	44.0	27.1	0.5	8.7	
Total	0.5	2.7	25.5	40.0	23.9	2.7	4.8	

The largest fraction of occurrences from annual data are in cases III and IV with only 11.2% in case V. As the scalar wind speed record becomes more specialized (monthly and hourly) the largest fraction of occurrences shifts from cases III and IV to IV and V. In fact, the fraction of occurrences in case III decreases steadily, the more detailed the scalar wind speed record.

The "pure" cases of the ordinary Rayleigh (case I) or the generalized Rayleigh (case II) combined only account for almost 3% of the occurrences, thus emphasizing the importance of considering the p.d.f. for scalar wind speed as a mixture.

The frequency of occurrence of the degenerate cases VI and VII is in the range from 5% to 10%. These could have been eliminated and classified under cases III and IV respectively with small values of σ_1. On the other hand, the scalar wind speed frequency function data analyzed in this report is largely from meteorological towers where cases VI and VII are not expected. These cases occur frequently in the surface wind records over the southeastern states, especially during the early morning hours of the summer months.

DATA REDUCTION AND THE EMPIRICAL FORMULA

Adequate interpretation of the parameters $\sigma_1, w_1, \sigma_2, w_2, k$ in physical terms requires some insight into the details of the data reduction technique, the behavior of the empirical formula under certain conditions, and the interaction of the two.

The parameters were obtained by a least squares fit of the distribution function to the wind speed frequency table data. If (P(w) is the distribution function corresponding to the probability density function p(w), then $P(w) = \int_0^w p(x)dx$ and it represents the probability that the wind speed is less than or at most equal to the speed indicated by the argument w. In terms of the distribution functions (1) becomes

$$P(w) = kP_1(w;\sigma_1,w_1) + (1-k)P_2(w;\sigma_2,w_2) \qquad (5)$$

where $P_1(w;\sigma_1,w_1)$ and $P_2(w;\sigma_2,w_2)$ are distribution functions corresponding to the probability density functions $p_1(w;\sigma_1,w_1)$ and $p_2(w;\sigma_2,w_2)$ of (1).

First, one needs to consider the behavior of the least squares technique for determining the parameters. In geometrical terms, the least squares technique may be thought of as finding the bottom of the deepest depression in an m-dimensional hyper-surface. In the case at hand, m=5. The first step in this process is to make a rough guess as to where this is (i.e., estimate roughly the parameter values); and then to adjust these estimates until there is little or no reduction in the sum of the squares of the errors. This is straight forward enough if there is only one such minimum. It is, however, characteristic of multidimensional least squares problems of this kind that there are several relative minima; i.e., the surface displays an assembly of pot-holes not all of the same depth. To handle this kind of situation it is necessary to make several initial estimates of the parameter values and determine the minimum to which each may lead. If all initial estimates lead to the same minimum the situation is simple. If they lead to two or more distinct minima one must be prepared to make a selection. If of these several one is by far the deepest (smallest sum of squares of the errors) the choice is obvious. On the other hand, it frequently occurs that there are two (or more) minima for which the sum of the squares of the errors are not significantly different from each other. In this case the situation is ambiguous and the choice may depend on other considerations such as the simplicity of the parameter set obtained and on its physical interpretation.

Second, the empirical formula being used has some characteristics that must be considered and which are used in the location of the minimum, particularly to introduce zero values for some parameters (which greatly facilitates physical interpretation) and to introduce certain degenerate cases. Two characteristics of this kind are: (a) the fact that for small

values of w_R (compared with the associated σ) the p.d.f. changes very little from that of w_R=0 (see Appendix B for details) and (b) the fact that when $\sigma \to 0$ (regardless of the associated w_R though most frequently occurring at w_R=0) one gets "spike formation" in the p.d.f., a degenerate case (see also Appendix B). The procedure for estimating the parameters incorporates these items. Thus, a step is provided which permits immediate recognition of a case for which the parameters $(0,0,\sigma_2,w_2,k)$, $0 \leq k < 1$, is a possibility and the minimization and corresponding root mean square errors (RMSE) are computed accordingly. For the general case, $(\sigma_1,w_1,\sigma_2,w_2,k)$, all of the initial parameter estimates are usually non-zero. After convergence to the minimum it is possible that w_1 or w_2 may have converged to zero in which case nothing further is required. When w_1 or w_2 converge to non-zero values these are tested against the corresponding values of σ_1 or σ_2. If $w_1 \leq \sigma_1$ or $w_2 \leq \sigma_2$ the values w_1=0 or w_2=0 are inserted and further iterations are performed to adjust the remaining parameters and compute the new minimum mean square error. Thus, if the iteration procedure leads to $(\sigma_1,w_1,\sigma_2,w_2,k)$ and $w_1 \leq \sigma_1$, then w_1=0 and further iterations find new values of the non-zero parameters in $(\sigma_1,0,\sigma_2,w_2,k)$ and a new RMSE. If $w_2 \leq \sigma_2$ at this stage, then w_2=0 and further iterations are used to adjust the non-zero parameters in $(\sigma_1,0,\sigma_2,0,k)$ and a new RMSE. When a zero is introduced in this way for w_1 or w_2 it is usually found that the adjustments of the non-zero parameters are quite small (or zero) and the increase in the RMSE is also small (or zero).

Third, it will be noted that the data tables occasionally exhibit RMSE values that are 0 or which are very close to 0. These are not to be interpreted to mean that the model being used is unusually well chosen. The computation procedure assumes that there are more data points than there are parameters to be determined, i.e., that the scalar wind speed frequency table contains more than 5 speed class intervals. If the function being fitted is reasonably well behaved and contains the same number of parameters as data points an exact solution is theoretically possible and the RMSE would be zero. The frequency tables for scalar wind speed contain a wide variety of speed class intervals, the number usually

increasing with the height of the anemometer level, and the class intervals being uniform with height. For summer data it frequently happens that at the lowest levels there are barely a sufficient number of class intervals to provide a solution. Thus, unusually small or zero RMSE values should be interpreted as a sign of insufficient input data rather than in terms of an unusually appropriate model. (As a matter of fact, the computation technique used involves a variable augmentation of the diagonal elements of the coefficient matrix which prevents it from becoming singular so that it will produce a solution even when there are fewer data points than parameters.)

IDENTIFICATION OF COMPONENTS OF THE MIXTURE

In the discussions that follow the idea of a reasonably identifiable component of the mixture defined by the parameters of the empirical formula for the p.d.f. for scalar wind speed is used.

One way of identifying the mixture components is through the value of the mixing parameter, k. Throughout, the pentad $(\sigma_1,w_1,\sigma_2,w_2,k)$ is always arranged so that the parameters σ_1,w_1 refer to the mixture component that occurs with frequency k and σ_2,w_2 refers to the mixture component that occurs with frequency 1-k. If $k<0.5$ then the mixture component with parameters σ_1,w_1 may be called the minor or recessive component while that with parameters σ_2,w_2 could be called the major or dominant component. If $0.5<k$ the situation is reversed. This is an adequate identification terminology if one is dealing with only one such pentad.

We will have occasion to deal with sequences of such pentads in connection with the annual or diurnal variation of the p.d.f. of scalar wind speed and particularly in connection with the scaling of parameters as a function of the anemometer height. In these connections the idea of the major or minor mixture component is useful but inadequate to completely describe the situation. All of these situations involve a sequence of parameter pentads of such nature that at least some of the parameters

change progressively from one member of the sequence to the next. We will say that a component of the mixture is reasonably identifiable if such a progressive change in one or more parameters is clearly recognizable. The idea involves degree of identifiability. It is best described by some examples.

The sequence of pentads relating to the p.d.f. for scalar wind speed on the tower at the Montaque, MA, nuclear power plant site (Table 23) is

Height	σ_1	w_1	σ_2	w_2	k(%)
10	0.87	0.00	2.13	0.00	72.14
46	1.15	0.00	2.88	0.00	18.33
99	1.22	0.00	3.75	0.00	16.30
151	1.63	0.00	4.27	0.00	9.99

Both the components with parameters σ_1,w_1 and σ_2,w_2 are already identifiable in that they show a clear progression of parameter values as a function of height. At the 10m height, the pair (σ_1,w_1) is the major component while (σ_2,w_2) is minor, but at all other levels the reverse is the case. If one were to change the k at 10m to 27.86 and interchange (σ_1,w_1) and (σ_2,w_2) at that level the sequence for σ_1 would be 2.13, 1.15, 1.22, 1.63 and for σ_2 0.87, 2.88, 3.75, 4.27 and one could maintain that the 10m mixture components were incorrectly identified since the sequence of values is not as regular as in the tabulated order.

A more complex situation is illustrated by the diurnal variation of the parameters at the Washington National Airport during January (Table 33)

Hour	σ_1	w_1	σ_2	w_2	k(%)
00	0.00	0.00	3.71	0.00	11.31
03	0.76	0.00	3.74	0.00	10.85
06	1.19	0.00	3.92	0.00	20.36
09	0.53	10.95	2.62	3.31	9.74
12	3.64	0.00	2.88	5.74	32.88
15	0.00	0.00	2.77	5.02	1.89
18	0.00	0.00	2.93	3.43	2.95
21	0.00	0.00	3.74	0.00	4.55

The values of k indicate that (σ_2, w_2) represent the parameters of the major mixture component. This mixture component is also well identified even though it displays a change of structure during the daytime hours. The minor mixture component is only fairly well identified. From 15 hours through 00 hours it is a "spike" at zero speed which occurs with increasing, but small, frequency with time. At 03 and 06 hours the "spike" broadens into a peak of finite width and eventually amounts for 20.36% of occurrences. At 09 hrs. the minor mixture component changes character completely from a low speed peak to a narrow high speed peak that accounts for a small fraction of occurrences. At 12 hrs. the minor mixture component has returned to a low speed peak, but much broader and of higher most probable speed than at any other hour. The case at 09 hrs. does not belong to the same minor mixture component represented by the other hours and there is some doubt about the case at 12 hrs. One would not consider the minor mixture component well identified.

WHITE SANDS MISSILE RANGE, NM

The fundamental data on the distribution function of scalar wind speed at the White Sands Missile Range, NM, (WSMR) is taken from Hansen and Neil (1964). The observations were made during a two year period from 14 April 1958 to 29 April 1960 for five days per week in alternate weeks. Data consisted of ten-minute means observed at eight three-hour intervals throughout the day. The summaries are by month so that each monthly summary consists of from 152 to 247 observations (except for December for which only 48 observations are recorded at each level). The instrument heights above ground level are at 4.6, 11.9, 19.3, 26.6, 33.9, 41.2, 48.5 55.8, and 62.0 m. The form of the summaries is one not commonly used, namely the wind speed that was not exceeded by a specified fraction of the observations.

Figure 1 illustrates the data from Hansen and Neil (1964) for the month of April. The ordinate is scalar wind speed (m/sec); the abscissa is a probability scale derived from the ordinary Rayleigh distribution function (see Appendix D). If one applies a straight-edge through (0,0) to these curves, it is evident that they are all approximately asymptotic to a line so-drawn, i.e., the data points lie approximately on hyperbolas in standard position. As pointed out in Appendix D, this would imply that the parameter pentad $(0,0,\sigma_2,o,k)$ is an appropriate representation for the data at each level. The data for the other months is remarkably like that for April. Consequently, this parameter pentad was used for each month and each level.

The computed values of σ_2 and k for each month and level are tabulated in Tables 1 and 2. Figure 2 shows the annual variation of σ_2 at the various levels (same data as appears in Table 1). The zig-zag behavior of the data points from month to month is assumed to be due to the small data sample. This is confirmed by the December data which differs considerably from that for November and January and for which the sample size was only 48 compared to 152 for each of the adjacent months.

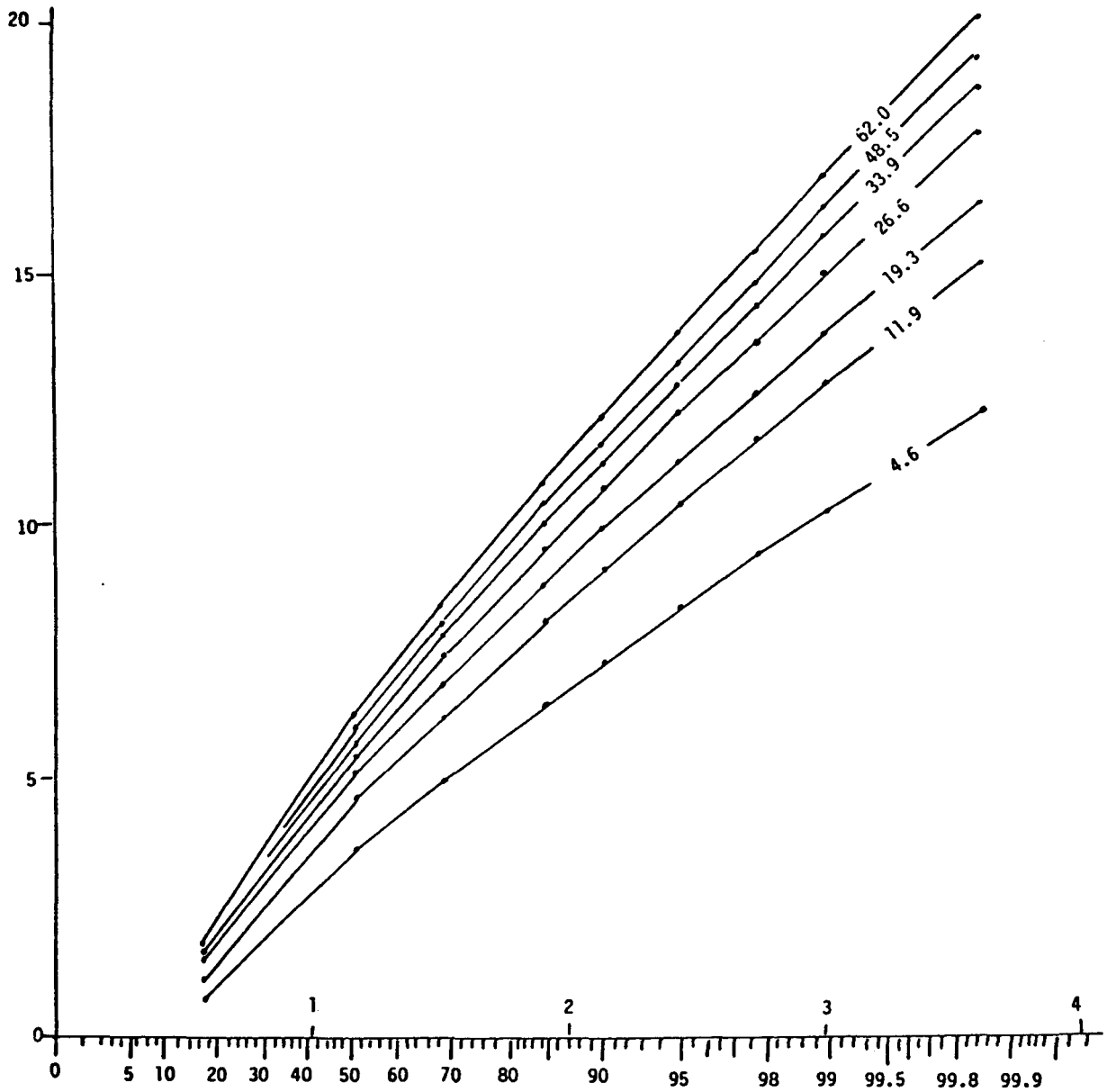

Figure 1. Probability of Wind Speed Less Than the Value Show at Levels on the WSMR Tower During April

TABLE 1. VALUES OF σ_2 FOR EACH MONTH AND LEVEL AT WSMR

Month	Height (m) 4.6	11.9	19.3	26.6	33.9	41.2	48.5	55.8	62.0
JAN	2.07	2.66	2.91	3.17	3.33	3.37	3.53	3.68	3.77
FEB	2.91	3.67	4.09	4.37	4.65	4.65	4.86	4.93	4.98
MAR	3.47	4.39	4.77	5.16	5.42	5.44	5.62	5.86	5.83
APR	2.50	3.13	3.54	3.72	3.92	3.94	4.12	4.29	4.29
MAY	2.13	2.95	3.25	3.52	3.72	3.78	3.88	4.04	4.17
JUN	2.61	2.96	3.30	3.50	3.72	3.94	3.88	4.02	4.15
JUL	2.03	2.13	2.47	2.66	2.92	2.96	3.08	3.15	3.27
AUG	2.50	2.75	2.92	3.13	3.23	3.27	3.40	3.47	3.49
SEP	1.56	2.10	2.34	2.59	2.71	2.83	2.98	3.05	3.12
OCT	2.00	2.52	2.75	2.89	3.03	3.09	3.25	3.33	3.42
NOV	2.09	2.60	3.12	3.15	3.39	3.46	3.67	3.83	3.89
DEC	1.28	1.86	2.25	2.42	2.52	2.61	2.63	2.67	2.68

TABLE 2. VALUES OF k FOR EACH MONTH AND LEVEL AT WSMR

Month	Height (m) 4.6	11.9	19.3	26.6	33.2	48.2	48.5	55.8	62.0
JAN	0.3735	0.3001	0.3220	0.3180	0.3091	0.2967	0.2818	0.2904	0.3008
FEB	0.1706	0.1598	0.1552	0.1590	0.1568	0.1590	0.1573	0.1568	0.1534
MAR	0.1504	0.1361	0.1241	0.1275	0.1256	0.1231	0.1254	0.1251	0.1108
APR	0.1423	0.1106	0.1034	0.1002	0.0991	0.1005	0.1041	0.1018	0.1110
MAY	0.1610	0.1438	0.1336	0.1348	0.1282	0.1274	0.1287	0.1197	0.1032
JUN	0.1385	0.1059	0.0926	0.0917	0.0790	0.0891	0.0878	0.0830	0.0867
JUL	(0.1181)	0.0934	0.0786	0.0881	0.0873	0.1059	0.0966	0.0902	0.0947
AUG	0.1416	0.1422	0.1432	0.1363	0.1380	0.1396	0.1476	0.1464	0.1448
SEP	0.1625	0.1259	0.1171	0.1147	0.1046	0.1217	0.1168	0.1286	0.1202
OCT	0.2765	0.1424	0.1422	0.1404	0.1393	0.1379	0.1382	0.1435	0.1423
NOV	0.3043	0.1680	0.2361	0.1698	0.1632	0.1621	0.1623	0.1608	0.1630
DEC	0.3339	0.3798	0.3105	0.2665	0.2985	0.2632	0.2605	0.2473	0.2470

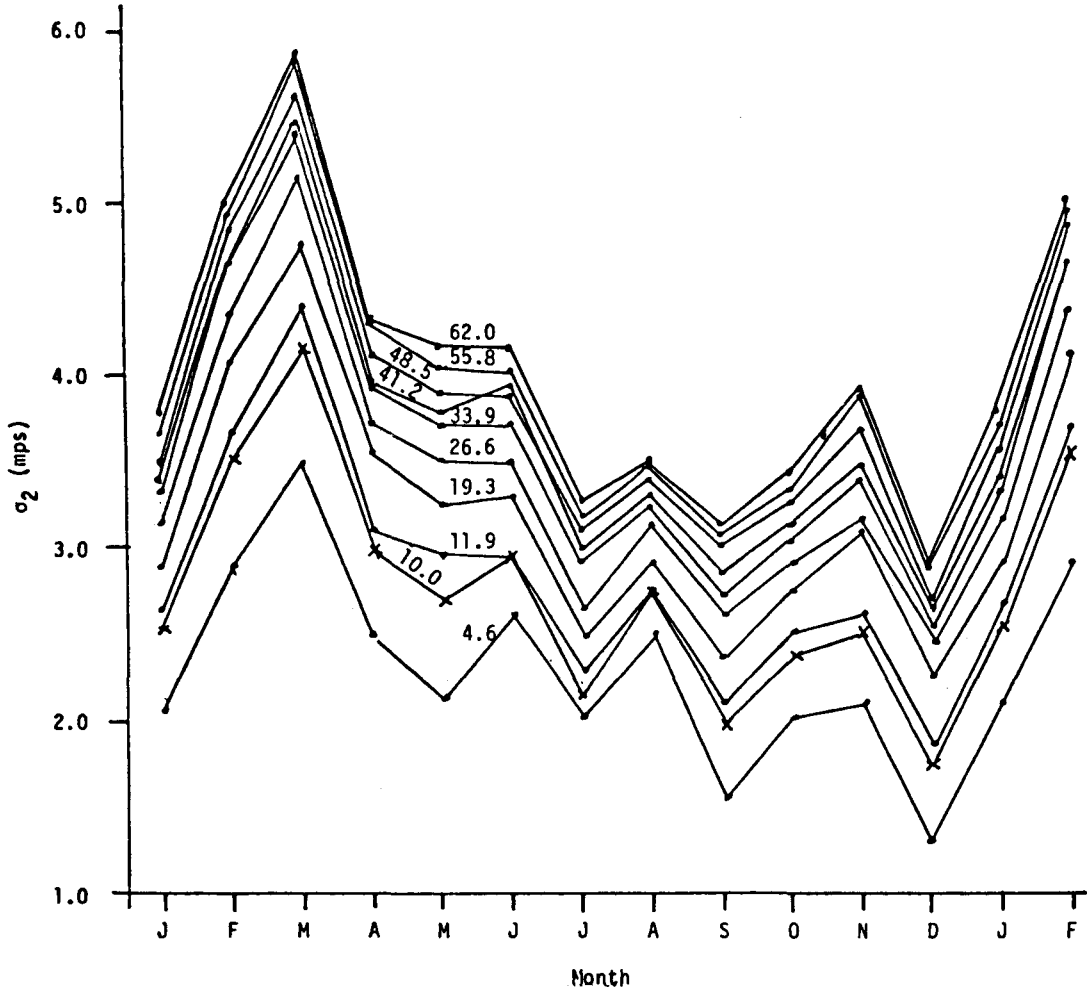

Figure 2. Values of σ_2 at WSMR Tower Levels as a Function of Month. The Value σ_o (at z=10m) from the Scaling Formula is also Shown.

The values of σ_2 were approximately by a scaling formula $\sigma=\sigma_0(z/10)^b$ where σ_0 is the value at z=10m and b is the scaling exponent. (The values of σ_0 and b were determined by a least squares fit to the logarithm of the scaling formula $\log \sigma=(\log \sigma_0)+b \log (z/10)$ which is linear in the parameters $\log \sigma_0$ and b.) The results are tabulated in Table 3. Values of σ_0 are shown in Figure 2. The monthly values of the scaling exponent, b, are shown in Figure 3 together with a curve for smoothed values and a horizontal line representing the average value of 0.214. Though the smoothed values seem to indicate annual and semi-annual oscillations, the violent zig-zags from May to October cast considerable doubt on its reality.

The values of the parameter k (the fraction of calms) from Table 2 for the months of September through March are shown in Figure 4 as a function of altitude. The outstanding features illustrated are (1) the fact that the variations of k with altitude are generally small and (2) the fact that k has a definite maximum in December and January (October and November have large k values at the 4.5m level). The curves for the months of April through August are not shown. Inspection of Table 2 indicates that they all lie rather uniformly clustered about the value k=0.1 (10%). There seems to be tendency for k to decrease slightly with increasing altitude. The general behavior of k as a function of altitude would indicate that a scaling relation similar to that used for σ_2 is not appropriate.

The annual variation of the parameter σ_0 (at z=10m) derived from the scaling formula is shown in Figure 5 together with corresponding smoothed values. The points of the zig-zag curve are the same as also shown in Figure 2 as a special insert. The rather sharp maximum in February, March, and April is the outstanding feature here. This is to be contrasted with the fact that, as shown in Figure 4, the fraction of calms (indicated by the parameter k) reached a pronounced maximum in the months just preceding (December and January). One may summarize the situation as follows: (a) Fall and early winter characterized by high frequency of calms and low wind speeds; (b) late winter and early spring by infrequent calms and high wind speeds; (c) late spring and summer by infrequent calms and low wind speeds.

TABLE 3. THE PARAMETER σ_o AT 10m AND THE SCALING EXPONENT, b, AND ITS STANDARD DEVIATION, σ_b, FROM VALUES OF σ_2 COMPUTED AT LEVELS FROM 4.6 TO 62.0m (TABLE 1) AT WSMR

Month	σ_o (10m)	b	σ_b
JAN	2.51	0.224	0.006
FEB	3.50	0.207	0.009
MAR	4.15	0.199	0.009
APR	3.00	0.206	0.008
MAY	2.70	0.245	0.013
JUN	2.97	0.178	0.014
JUL	2.23	0.199	0.018
AUG	2.73	0.134	0.006
SEP	1.96	0.261	0.008
OCT	2.38	0.198	0.006
NOV	2.35	0.237	0.010
DEC	1.73	0.281	0.026

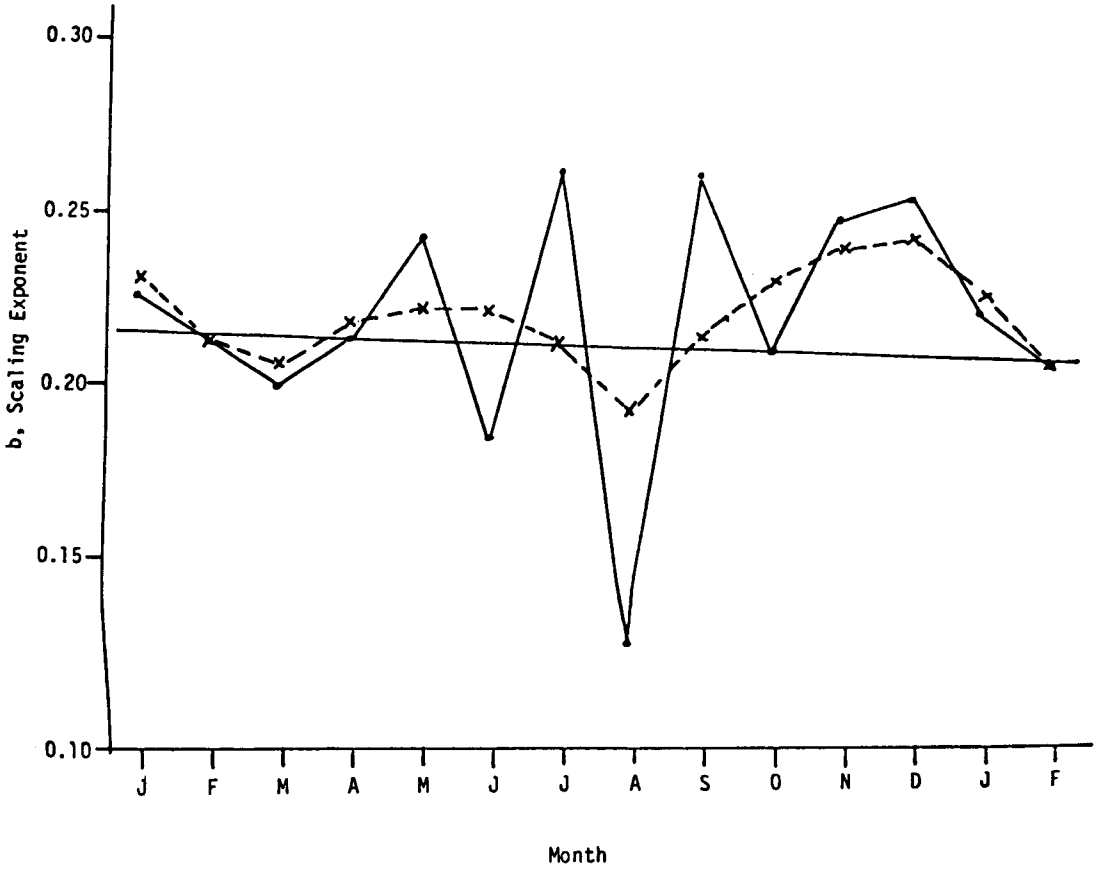

Figure 3. The Annual Variation of the Scaling Exponent, b, Evaluated at Levels from 4.6 to 62.0m on the WSMR Tower. Smoothed Values and the Mean Value are also Shown.

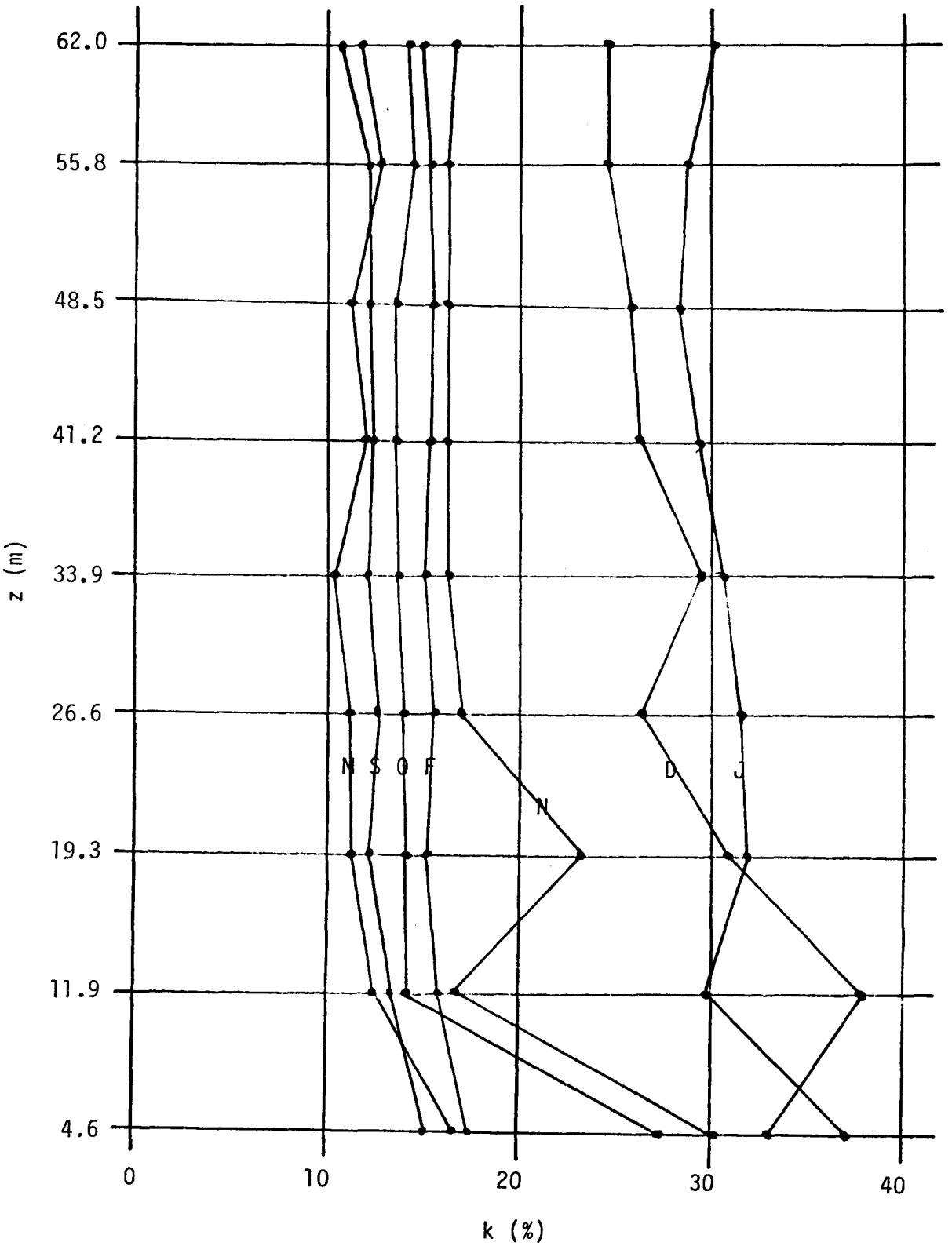

Figure 4. The Variation of the Parameter k as a Function of Altitude by Months from September Through March at the WSMR Tower

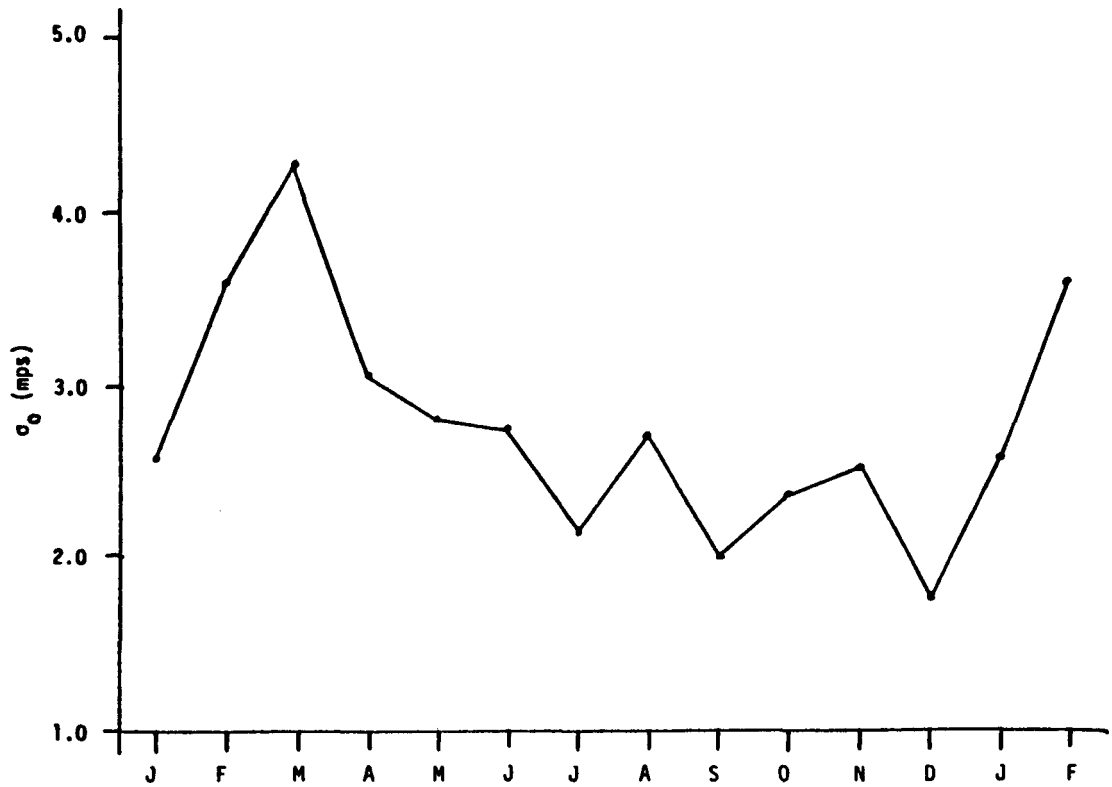

Figure 5. The Annual Variation of σ_o at 10m Evaluated at Levels from 4.6 to 62.0m on the WSMR Tower

HANFORD METEOROLOGICAL STATION

The data used to compute the parameters of the empirical wind speed p.d.f. for the Hanford Tower were extracted from the scalar wind speed frequency function tables published in Stone, Jenne, and Thorp (1972). These data are by far the most satisfactory used in that they cover a period of 15 years. Unfortunately, only three levels are summarized, 15, 60, and 121m.

The parametric representation of the p.d.f. for scalar wind speed at the WSMR Tower was exceptionally simple. The pentad required to represent the data from the Hanford Tower requires three and occasionally four parameters on a monthly basis and occasionally all five when considered on an hourly basis within months.

THE ANNUAL VARIATION

The basic pentads by month and level are tabulated in Table 4.

The columns headed Month and Level need no particular comment. The columns headed σ_1, w_1 and σ_2, w_2 refer to the parameters of the assumed mixture of circularly normal wind component bivariate distributions from which the scalar wind speed frequency function might have been derived. σ_1 and σ_2 are the vector wind component standard deviations and w_1, w_2 are the corresponding mean resultant wind speeds. (See Appendices A and B.) The value of k is the mixing ratio of these two distributions in the sense that k is the fraction attributed to the part with parameters σ_1, w_1 and 1-k the fraction due to the part described by σ_2, w_2. The column headed RMSE is the root mean square error of the empirical fit to the observed distribution function expressed in percent. The units for σ_1,w_1,σ_2,w_2 are meters per second while k is a pure number.

TABLE 4. VALUES OF σ_1,w_1,σ_2,w_2, AND k FOR THE HANFORD TOWER FOR EACH MONTH AND LEVEL AND FOR THE YEAR BY LEVELS. SEE TEXT FOR EXPLANATION OF THE COLUMN HEADINGS.

Mo.	Lvl.	σ_1	w_1	σ_2	w_2	k	RMSE
1	15	1.04	0.00	3.35	0.00	0.4981	0.74
	60	1.01	0.00	4.24	0.00	0.3678	0.68
	121	1.03	0.00	4.62	0.00	0.3889	0.81
2	15	1.11	0.00	3.37	0.00	0.3878	0.97
	60	1.05	0.00	4.37	0.00	0.2925	0.67
	121	1.09	0.00	4.87	0.00	0.3188	1.03
3	15	1.72	0.00	4.14	0.00	0.4487	0.66
	60	1.53	0.00	4.80	0.00	0.2594	0.57
	121	1.61	0.00	5.38	0.00	0.2595	0.86
4	15	1.80	0.00	4.18	0.00	0.3884	0.28
	60	1.58	0.00	4.91	0.00	0.2140	0.20
	121	1.65	0.00	5.63	0.00	0.2236	0.28
5	15	1.90	0.00	3.99	0.00	0.4147	0.23
	60	1.64	0.00	4.71	0.00	0.2228	0.23
	121	1.71	0.00	5.40	0.00	0.2380	0.17
6	15	1.13	2.86	4.02	0.00	0.3251	0.10
	60	0.99	2.03	4.95	0.00	0.2128	0.14
	121	1.18	1.92	5.68	0.00	0.2326	0.19
7	15	1.26	1.93	4.04	0.00	0.4540	0.13
	60	1.06	1.91	4.91	0.00	0.2795	0.25
	121	1.21	1.88	5.68	0.00	0.3011	0.23
8	15	1.57	1.39	3.90	0.00	0.5291	0.04
	60	1.17	1.68	4.62	0.00	0.2936	0.18
	121	1.36	1.55	5.33	0.00	0.2998	0.17
9	15	1.59	0.00	3.73	0.00	0.4934	0.43
	60	1.47	0.00	4.46	0.00	0.3028	0.39
	121	1.60	0.00	5.09	0.00	0.3115	0.56
10	15	1.21	0.00	3.39	0.00	0.4691	0.72
	60	1.17	0.00	4.31	0.00	0.3521	0.41
	121	1.17	0.00	4.78	0.00	0.3278	0.61
11	15	1.17	0.00	4.07*	0.00	0.5654	2.43
	60	1.06	0.00	4.22	0.00	0.4017	0.66
	121	1.09	0.00	4.72	0.00	0.4035	0.89
12	15	1.00	0.00	3.31	0.00	0.5159	0.80
	60	1.01	0.00	4.22	0.00	0.4016	0.85
	121	0.99	0.00	4.62	0.00	0.3972	1.21
13	15	1.37	0.00	3.71	0.00	0.4204	1.03
	60	1.32	0.00	4.57	0.00	0.2952	0.66
	121	1.35	0.00	5.18	0.00	0.3042	0.89

Table 4 is so arranged that σ_2, w_2 refer to the part of the mixture with the higher wind speeds while σ_1, w_1 represents the part due to lower wind speeds. When w_2 or w_1 is zero the value of σ_2 or σ_1 is that of the most probable wind speed for that part of the mixture. When w_1 is listed then $\sigma_1 < w_1$. This is due to the fact that whenever $w_1 \leq \sigma_1$ it is found that an equally satisfactory fit is obtained with $w_1 = 0$ (and occasionally a small change in σ_1). It is the outstanding feature of Table 4 that $w_2 = 0$ throughout. Also the general case is that the more important part of the mixture is in the higher wind speed part (i.e., $k < 0.5$ as a general rule, the exceptions being confined to a few cases at the 15m level).

(The value of σ_2 for 15m in November is marked by an asterisk. It is assumed that this is an error, but its source could not be found.)

The data for σ_2 is shown in Figure 6 as a function of the month. The reasonably smooth annual variation is evident, the maximum being in spring and early summer, the minimum being in the fall and early winter.

The parameter σ_2 scales readily as seen from Table 5 where $\sigma_0(z=10m)$ and the exponent b are tabulated (and also the standard deviation of the estimate of b, σ_b). The values of σ_0 are plotted as the bottom curve in Figure 6. It shares the same annual variation as the values of σ_2 at the observation levels. Figure 7 shows the annual variation of the scaling exponent, b. The horizontal line is drawn at the average value of b (November value omitted) of 0.153. The annual variation of b does not seem to be significant. The average value of b by month (0.153) and the value computed for the annual data (0.159) agree reasonably well.

The annual variation of the parameter k, the fraction of cases in the low speed component of the mixture, is illustrated in Figure 8. In the first place, note that the value of k at 15m is much larger than at 60 and 121m throughout the year and that the values at 60 and 121m are very nearly the same. This is an effect that would influence the scaling of the average scalar wind speed and which has been removed from the scaling of

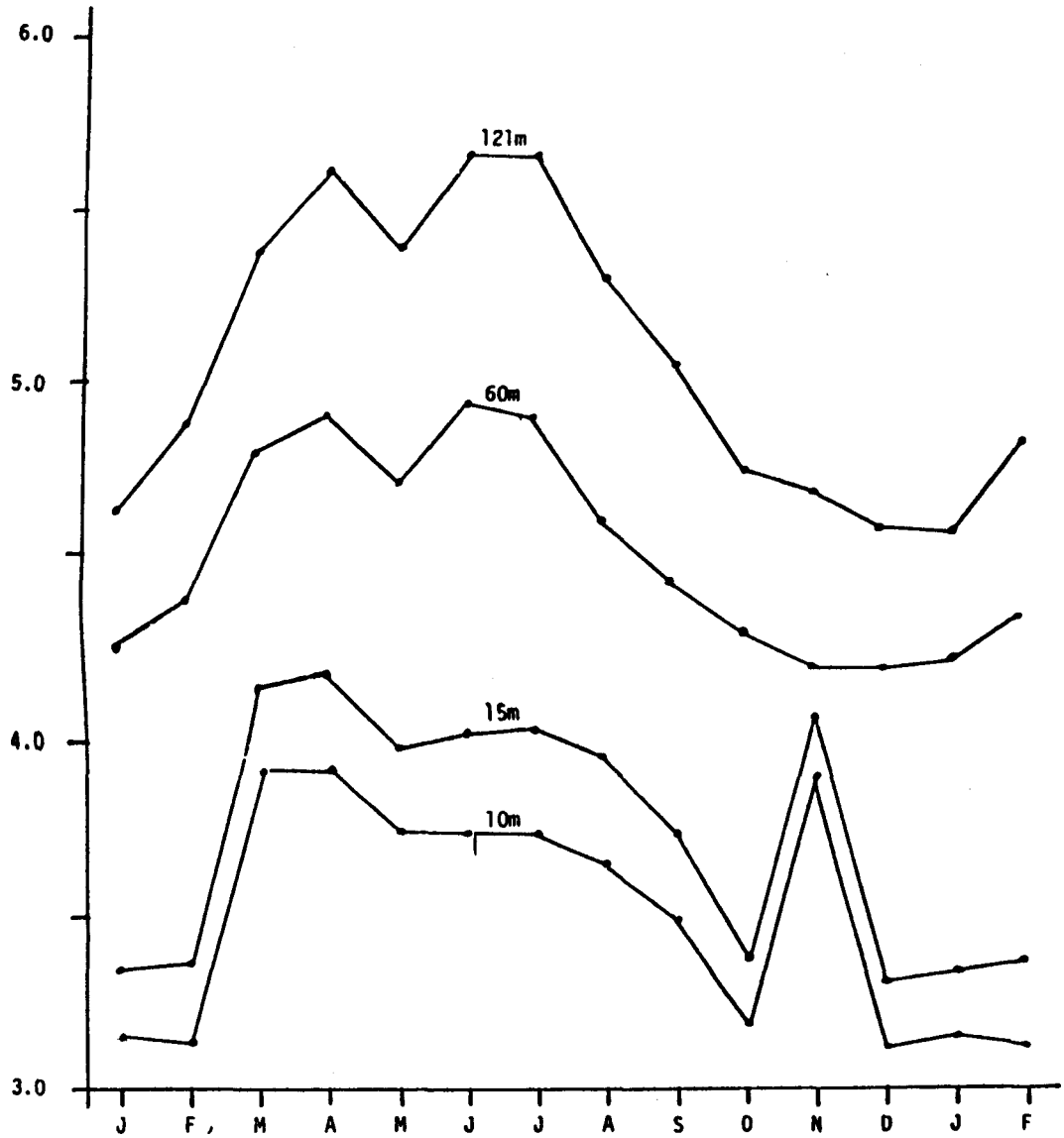

Figure 6. Annual Variation of σ_2 (w_2=0 all months) from the Hanford Tower Data. Lower Curve is for Scaled Values σ_o at 10m

TABLE 5. SCALING PARAMETERS FOR σ_2, MONTHLY AND ANNUAL DATA, HANFORD TOWER

Mo.	σ_o	b	σ_b
JAN	3.16	0.156	0.012
FEB	3.13	0.176	0.004
MAR	3.92	0.123	0.014
APR	3.92	0.139	0.020
MAY	3.74	0.141	0.019
JUN	3.74	0.163	0.011
JUL	3.74	0.163	0.016
AUG	3.65	0.146	0.020
SEP	3.49	0.146	0.015
OCT	3.18	0.166	0.006
NOV	3.91	0.065	0.033
DEC	3.11	0.162	0.012
ALL	3.47	0.159	0.007

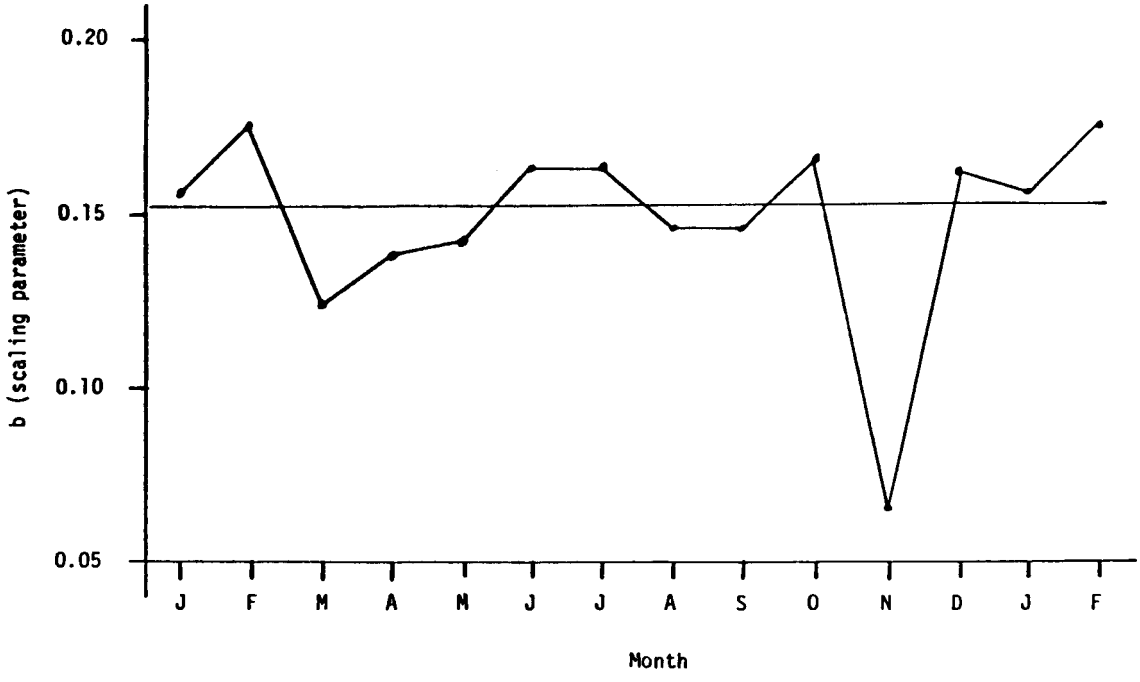

Figure 7. Annual Variation of the Scaling Parameter, b, for the Parameter σ_2 at the Hanford Tower.

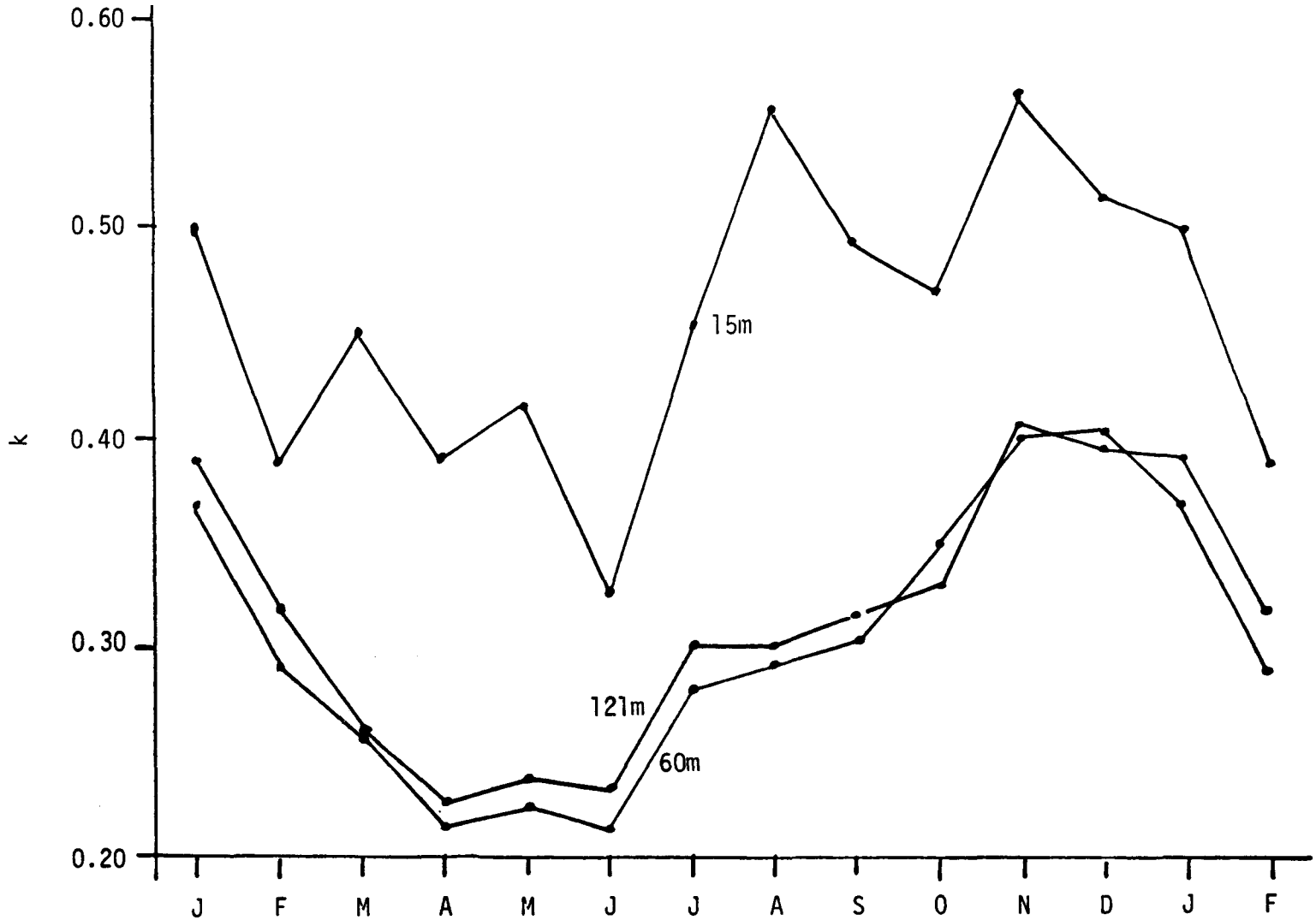

Figure 8. Annual Variation of k, the Fraction of Cases in the Low Speed Mixture Component, Hanford Tower Data

σ_2 discussed above. In the second place, note that the annual variation of k (Figure 8) is just the opposite of that of σ_2 (Figure 6). Thus, the low speed mixture component is less frequent when the high speed mixture component has its highest most probable values. Since 1-k represents the relative frequency of the high speed mixture component, one would then say that the high speed mixture component is more frequent when it has the largest most probable value.

The behavior of k with height appears to be rather uniform throughout the year. It is, however, a behavior which, on the basis of the data at only 15, 60, and 121m, does not fit an exponential scaling law. One is tempted to conjecture that, if more data were available from below 60m, a scaling law for k might be possible in these lower levels (not necessarily an exponential one) and melding into a region for which k=constant for $z>z_*$ where $z_*\leq 60$m.

The annual variation of the parameters σ_1 and w_1 for the low speed mixture component is shown in Figure 9. At all three levels one has $w_1=0$ except for the summer months. In June, July, and August (except at 15m (two branches of the curves are shown: the upper for w_1 and the lower for σ_1. If one follows the upper branch (w_1) for summer, the annual variation of the low speed mixture component resembles that of the high speed mixture component shown in Figure 6. The main distinction lies in the fact that during the summer months ($w_1\neq 0$) the value of σ_1 shows a marked decrease. This indicates that (1) the low speed mixture component becomes directionally dependent (not necessarily in a simple way) and (2) the speed p.d.f. for this mixture component has a narrow spike near the value of w_1.

It is evident from Figure 9 (or Table 4) that neither σ_1 or w_1 varies in altitude in such a way as to permit an exponential scaling law. In fact one would be tempted to simply average the values and consider σ_1 and w_1 independent of altitude (an exponential scaling law with b=0).

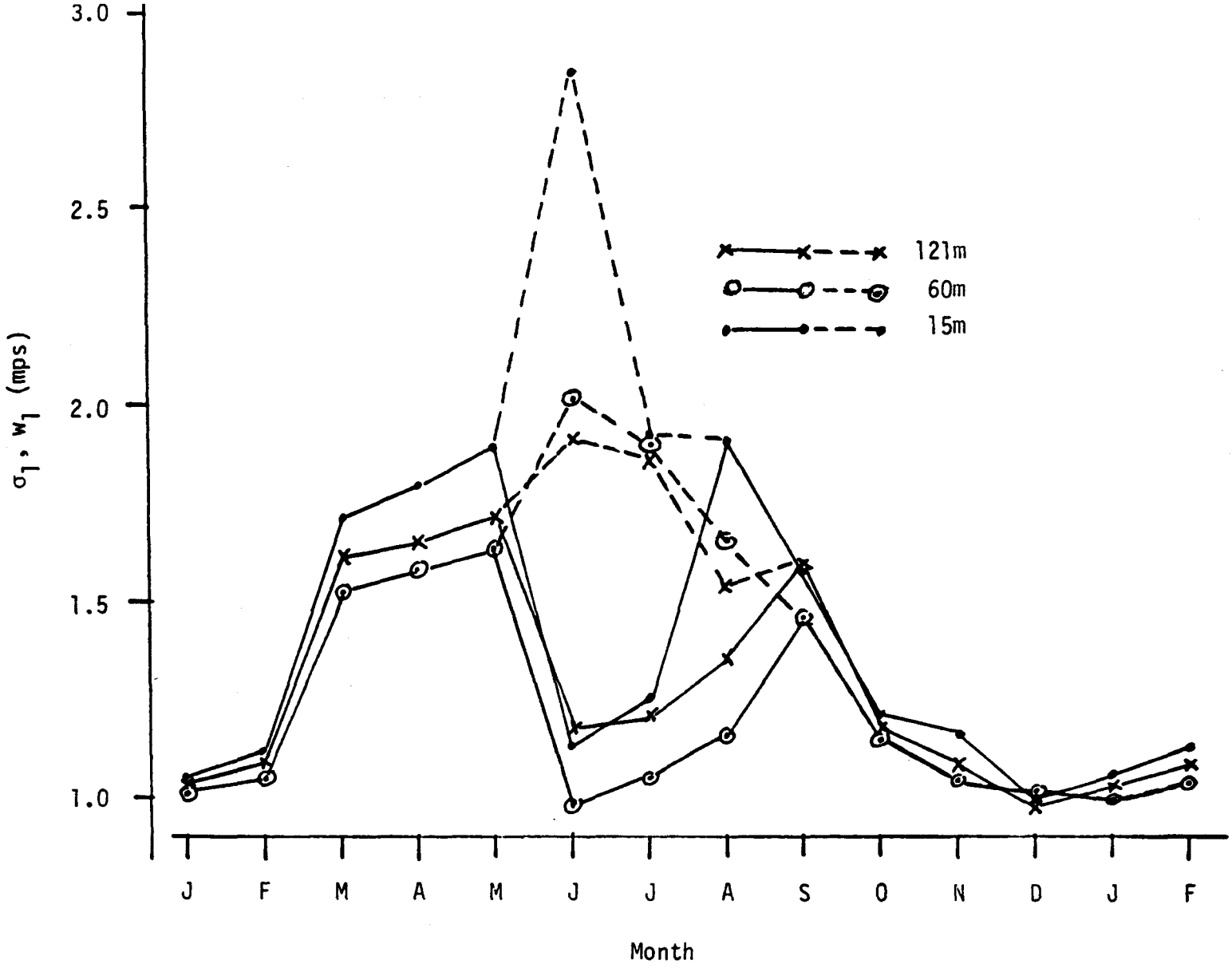

Figure 9. Annual Variation of σ_1 and w_1 ($w_1 > \sigma_1$, otherwise $w_1 = 0$), Hanford Tower

[Note: In Figure 9 and in subsequent figures in which σ_1, w_1 (or σ_2, w_2) are plotted together as a function of month or hour, the following convention has been adopted. When $w_1 \neq 0$ the minimization computations always result in $w_1 > \sigma_1$ so there are two "branches" of the curve, one for w_1 and one for σ_1. If the computations lead to $w_1 < \sigma_1$, then they proceed at once to $w_1 = 0$ since there is only an insignificant difference in the values of σ_1 (and the remaining parameters). Rather than plot these values of $w_1 = 0$, the single value of σ_1 is plotted. In the interval between successive points $w_1(t_i) = 0$ and $w_1(t_{i+1}) > \sigma_1(t_{i+1})$ (or $w_1(t_i) > \sigma_1(t_i)$ and $w_1(t_{i+1}) = 0$) the zero value of $w_1(t_i)$ (or $w_1(t_{i+1})$) is treated as though $w_1(t_i) = \sigma_1(t_i)$ (or $w_1(t_{i+1}) = \sigma_1(t_{i+1})$). Thus, the dashed line for $w_1(t)$ joins the points $\sigma_1(t_i)$ and $w_1(t_{i+1})$ (or $w_1(t_i)$ and $\sigma_1(t_{i+1})$).]

THE DIURNAL VARIATION, JANUARY

The values of the parameter $\sigma_1, w_1, \sigma_2, w_2$, and k by level and hour of day at the Hanford Tower during January are listed in Table 6. One sees immediately that $w_1 = 0$ and $w_2 = 0$ at all levels and all hours.

The hourly values of σ_2 at each level are illustrated in Figure 10. The diurnal variation at all three levels are similar to each other with some minor differences. A minimum occurs at all levels in early morning (05 to 08 hours) and increases rapidly thereafter toward a mid-day maximum. At 15 meters the maximum is narrow while at 60m it is widened on the afternoon side while at 121m it is shifted toward afternoon and also widened.

It is also evident that σ_2 is readily scaled. The scaling parameters by hour are tabulated in Table 7. The scaled value of w_o (z=10m) is shown in Figure 10 and, of course, closely follows the value of σ_2 at 15m. The scaling parameter, b, by hour of the day is shown in Figure 11. The diurnal variation of b is evident, being at a minimum around noon and a maximum in the late afternoon. This behavior, of course, is induced by the differences in the diurnal variation of σ_2 at the levels concerned.

TABLE 6. VALUES OF THE PARAMETERS $\sigma_1, w_1, \sigma_2, w_2, k$ AT THE HANFORD TOWER BY HOUR OF THE DAY AND LEVEL DURING THE MONTH OF JANUARY. THE HOUR IS LOCAL STANDARD TIME.

Hr.	Lvl.	σ_1	w_1	σ_2	w_2	k	RMSE
2	15	1.08	0.00	3.23	0.00	0.5048	0.80
	60	1.02	0.00	4.15	0.00	0.3084	0.73
	121	1.18	0.00	4.67	0.00	0.3462	1.03
5	15	1.13	0.00	3.18	0.00	0.5488	1.11
	60	0.91	0.00	3.88	0.00	0.2992	1.35
	121	0.95	0.00	4.25	0.00	0.3129	1.53
8	15	1.02	0.00	3.11	0.00	0.5345	0.86
	60	1.01	0.00	3.80	0.00	0.3377	1.38
	121	1.01	0.00	4.34	0.00	0.3429	1.24
11	15	1.03	0.00	3.76	0.00	0.5361	0.93
	60	1.11	0.00	4.58	0.00	0.5053	1.17
	121	1.12	0.00	4.98	0.00	0.5120	1.50
14	15	1.09	0.00	3.91	0.00	0.5431	1.48
	60	1.18	0.00	4.69	0.00	0.5058	1.56
	121	1.15	0.00	5.12	0.00	0.5027	1.82
17	15	1.10	0.00	3.25	0.00	0.4370	0.89
	60	1.17	0.00	4.41	0.00	0.3574	0.54
	121	1.19	0.00	5.09	0.00	0.4412	0.92
20	15	1.17	0.00	3.38	0.00	0.4488	0.59
	60	0.96	0.00	4.36	0.00	0.2944	0.53
	121	1.02	0.00	4.96	0.00	0.3463	0.94
23	15	1.00	0.00	3.10	0.00	0.4603	0.92
	60	.099	0.00	4.16	0.00	0.3122	0.72
	121	1.10	0.00	4.72	0.00	0.3475	0.89

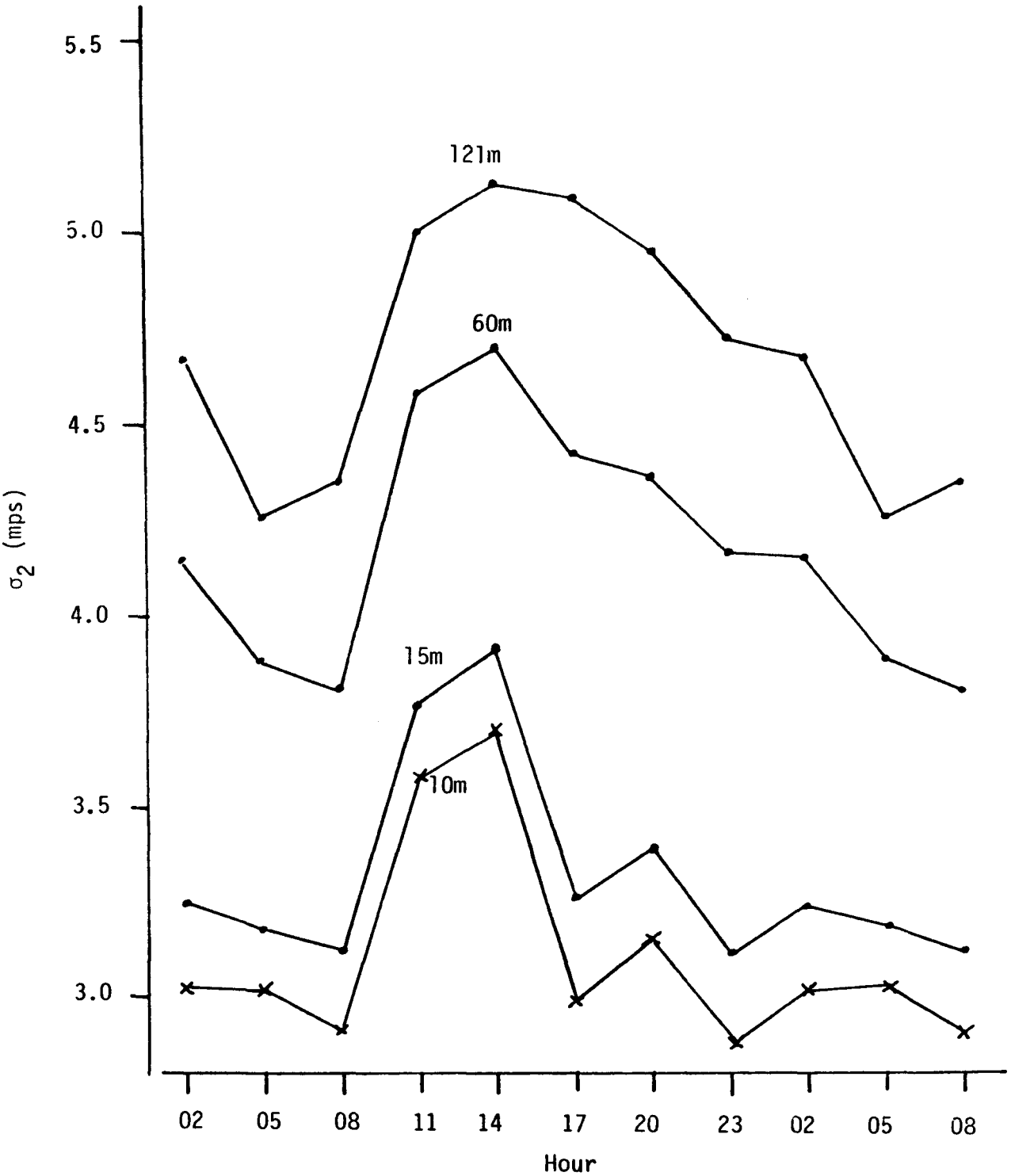

Figure 10. Diurnal Variation of σ_2, January, Hanford Tower

TABLE 7. SCALING PARAMETERS BY HOUR OF THE DAY FOR σ_2, HANFORD TOWER, JANUARY

k	w_o	b	σ_b
02	3.01	0.777	0.003
05	3.01	0.140	0.003
08	2.90	0.158	0.011
11	3.57	0.136	0.006
14	3.70	0.127	0.010
17	2.98	0.216	0.004
20	3.14	0.184	0.000
23	2.86	0.203	0.008

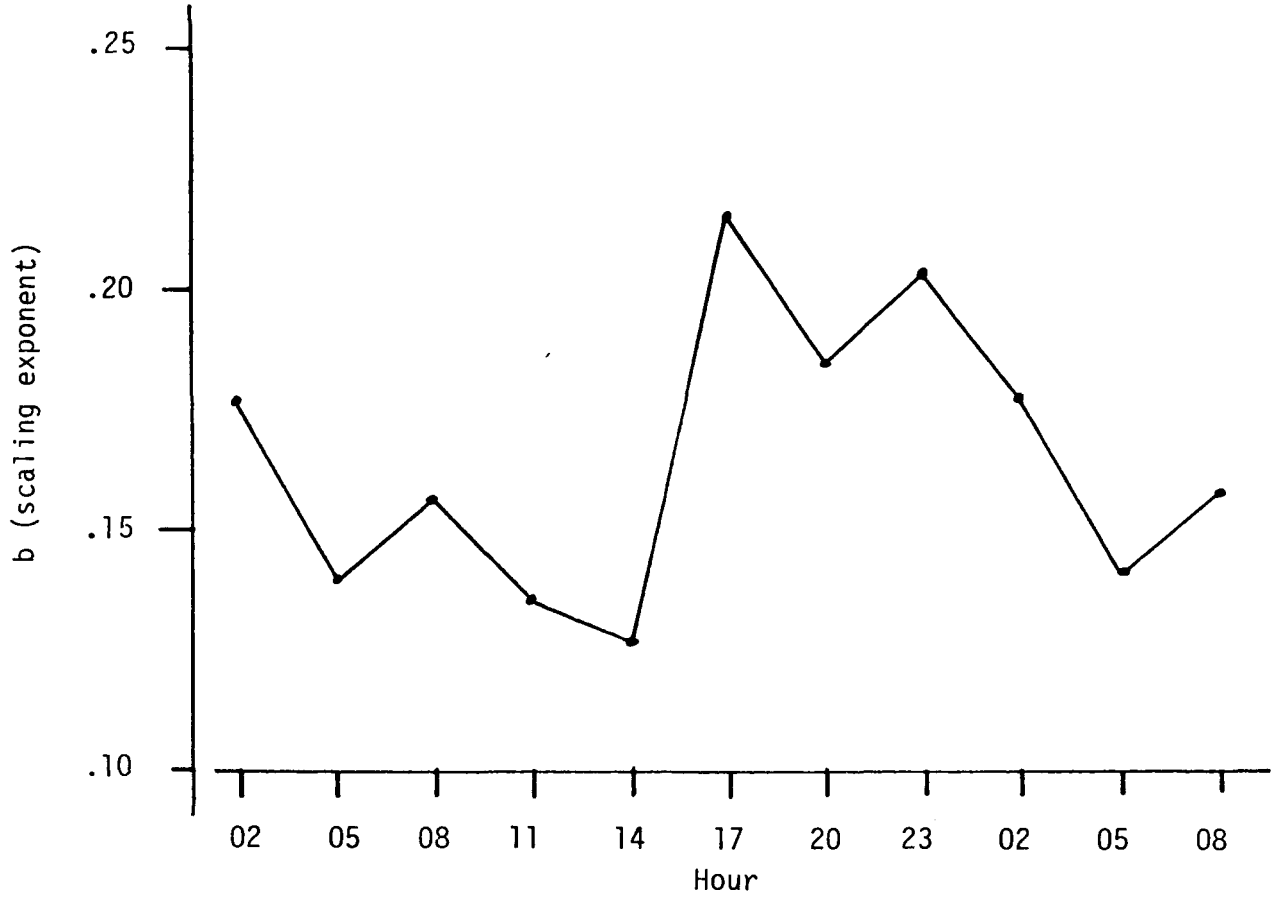

Figure 11. Diurnal Variation of the Scaling Exponent, Hanford Tower, January

The minimum of b occurs where the value of σ_2 at 15m is largest and the maximum occurs as a result of the rapid decrease of σ_2 at 15m, the less rapid decrease at 60m, and the slow decrease at 121m during the afternoon hours.

The diurnal variation of σ_1 at the three levels is shown in Figure 12. The diurnal variation at 15m is very small, and at 60 and 121m is only slightly larger. One is tempted to consider σ_1 as constant throughout the day and at all levels (scaling exponent of zero).

The diurnal variation of the mixing parameter, k, is shown in Figure 13. As was the case for the annual variation (Figure 8) the value at 15m is larger than at 60 or 121m and the values at 60 and 121m are nearly the same. In this case also one is inclined to conjecture a scaling of some kind which smoothes into a nearly constant value somewhere below the 60m level.

A good deal of the diurnal variation of the average scalar wind speed is wound up in the interaction of the variations of k and σ_2. At the 60 and 121m levels the fact that the low speed mixture component is most important around noon when also the most probable speed (σ_2) of the high speed mixture component shows a maximum tends to push the occurrence of the maximum mean wind speed at these levels into the late afternoon hours. At the 15m level the fact that the value of k is nearly constant from midnight to 14 hours allows the realization of low mean scalar wind speeds in early morning but also allows the increase in the high speed mixture component from 08 to 14 hours to be realized in the mean scalar wind speed.

THE DIURNAL VARIATION, JULY

The values of parameters $\sigma_1, w_1, \sigma_2, w_2$, k by hour of the day and level at the Hanford Tower during July are shown in Table 8. Since $w_1=w_2=0$ for January (Table 4) and $w_1 \neq 0$, $w_2=0$ for July, one would expect some appreciable differences between these months. In fact, the differences turn out to be much more than is expected.

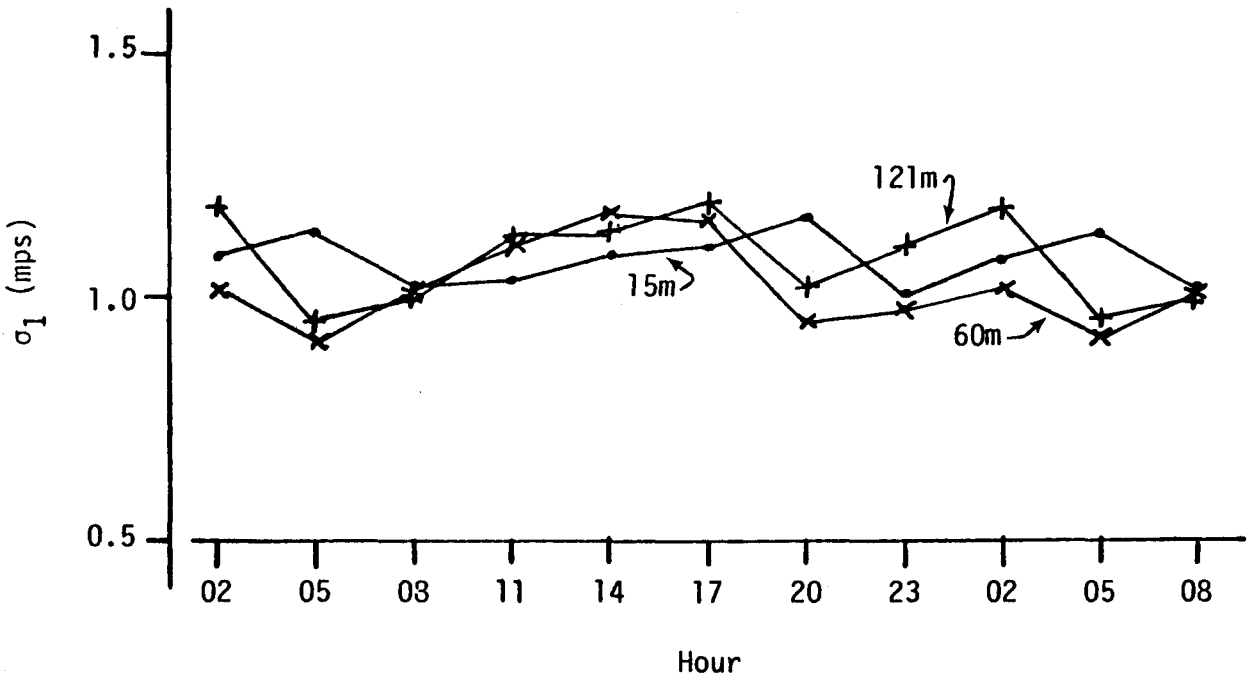

Figure 12. Diurnal Variation of σ_1, Hanford Tower, January

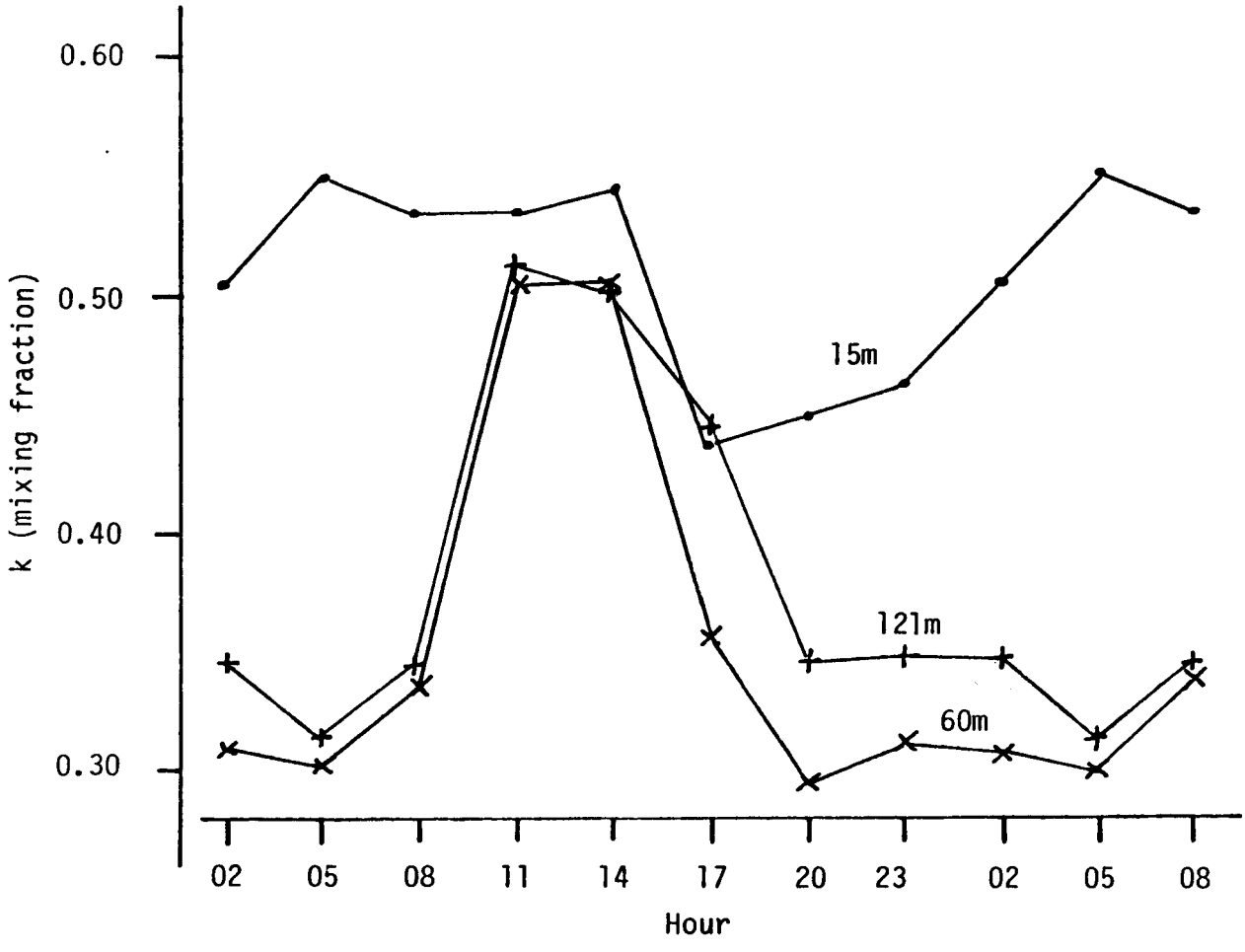

Figure 13. Diurnal Variation of k, Fraction of Cases in Low Speed Mixture Component, Hanford Tower, January

TABLE 8. VALUES OF THE PARAMETERS $\sigma_1, w_1, \sigma_2, w_2, k$ AT THE HANFORD TOWER BY HOUR OF THE DAY AND LEVEL DURING JULY

Hr.	Ht.	σ_1	w_1	σ_2	w_2	k	RMSE
02	15	0.00	0.00	1.63	3.21	0.0000	0.97
	60	2.77	0.00	2.02	5.70	0.1571	0.26
	121	3.54	0.00	2.08	7.18	0.2856	0.72
05	15	0.00	0.00	1.73	2.22	0.0507	0.56
	60	1.29	0.00	2.07	4.48	0.1522	0.52
	121	1.17	0.00	2.10	5.27	0.0962	0.79
08	15	0.99	1.08	3.27	0.00	0.6616	0.13
	60	1.51	0.00	3.90	0.00	0.6832	0.35
	121	1.47	0.00	3.98	0.00	0.6554	0.12
11	15	0.35	1.75	3.17	0.00	0.6302	0.08
	60	0.91	2.08	4.28	0.00	0.7593	0.13
	121	0.95	1.98	4.14	0.00	0.6841	0.27
14	15	0.83	2.32	4.03	0.00	0.6268	0.22
	60	0.82	2.51	4.46	0.00	0.5629	0.29
	121	0.87	2.46	4.53	0.00	0.5373	0.52
17	15	2.41	0.00	2.42	7.63	0.6473	0.14
	60	1.74	2.09	3.51	7.95	0.5644	0.52
	121	1.44	2.03	6.30	0.00	0.4034	1.06
20	15	1.44	2.25	2.00	7.27	0.3773	0.02
	60	2.26	2.97	2.17	10.15	0.3999	0.31
	121	4.14	0.00	2.27	12.60	0.4794	0.85
23	15	1.46	3.94	1.48	6.38	0.5653	0.00
	60	4.26	0.00	2.05	8.13	0.4809	0.71
	121	1.78	2.46	2.81	9.00	0.1973	0.19

Although from the monthly data (Table 4) one has w_2=0 for July, the hourly data of Table 8 indicates that w_2 is uniformly zero only during mid-day. Details of the diurnal variation of σ_2 and w_2 are shown in Figure 14. It is immediately evident that since the curves for these parameters do not show a uniform increase in value with increasing height the scaling formula is only marginally valid. Since the curves for 60m and 121m are reasonably coincident while that for 15m is somewhat lower, it might be possible to scale over a range of levels below 60m and with $b \approx 0$ above that level. The scaling parameters from the data in Table 8 are given in Table 9. The hour to hour variations of the scaling exponent, b, is so large and irregular that a detailed discussion of diurnal variation is futile.

The diurnal variation of the parameters σ_1 and w_1 is illustrated in Figure 15. To avoid confusion, these are plotted in separate strips for each level. When put in a single diagram the curves overlap. Obviously, no form of scaling is possible. A diurnal change from lower values in the morning and higher values in the afternoon is evident. The maximum also shifts to later times in the evening as the altitude increases while the minimum shifts to later times in the morning.

The diurnal variation of the mixing fraction, k, is shown in Figure 16. This differs from the annual variation (Figure 8) and the diurnal variation in January (Figure 13) in that the values at all three levels are intertwined. Thus, k is essentially independent of elevation. The diurnal variation in July is quite different from that of January, especially at the upper levels. The abrupt morning rise is common to both (but 3 hours earlier in July since it is expected to occur on "sun time" rather than standard time). Instead of a rapid decrease after the maximum, the July curves fall off rather linearly to the morning minimum. The range of values of k is also much larger in July than in January (10% to 70% rather than 30% to 60%). As a consequence, the diurnal variation of the mean wind speed in July is essentially the shift (indicated by the variation of k) from emphasis on the low speed to the high speed mixture component. It is also coupled with the fact that when the low speed mixture component dominates the speed of this mixture component is also low and when the high speed mixture component dominates its speed is also high.

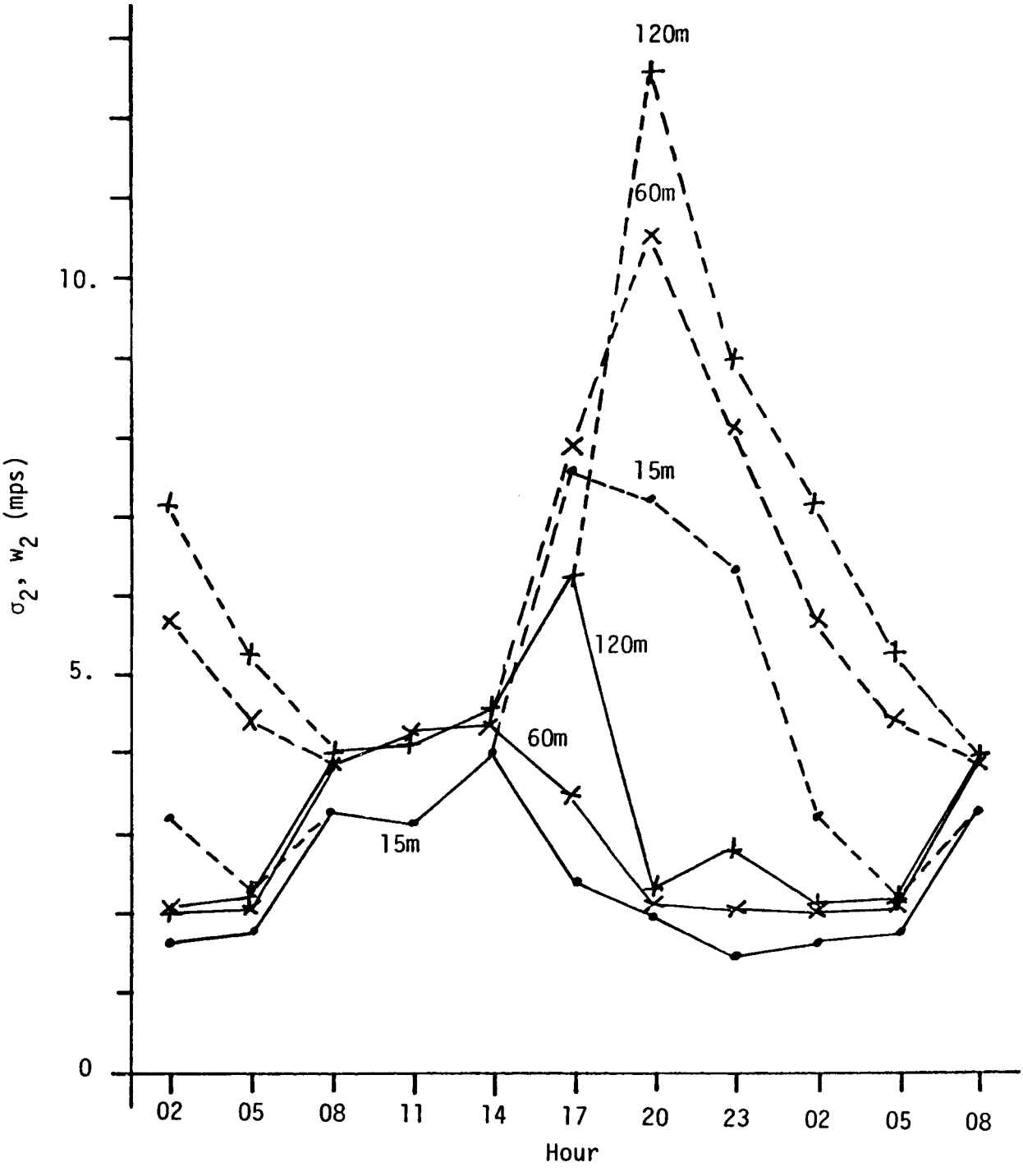

Figure 14. Diurnal Variation of σ_2, w_2, July, Hanford Tower

TABLE 9. SCALING PARAMETERS BY HOUR OF THE DAY FOR σ_2,w_2, HANFORD TOWER, JULY

	σ_2			w_2		
Hr.	w_o	b	σ_b	w_o	b	σ_b
02	1.57	0.122	0.028	2.76	0.390	0.021
05	1.68	0.098	0.027	1.92	0.427	0.068
08	3.17	0.099	0.024	--	--	--
11	3.08	0.140	0.066	--	--	--
14	3.96	0.058	0.013	--	--	--
17	1.92	0.432	0.141	7.54	0.030	--
20	1.95	0.060	0.001	6.50	0.260	0.017
23	1.28	0.297	0.053	5.98	0.166	0.007

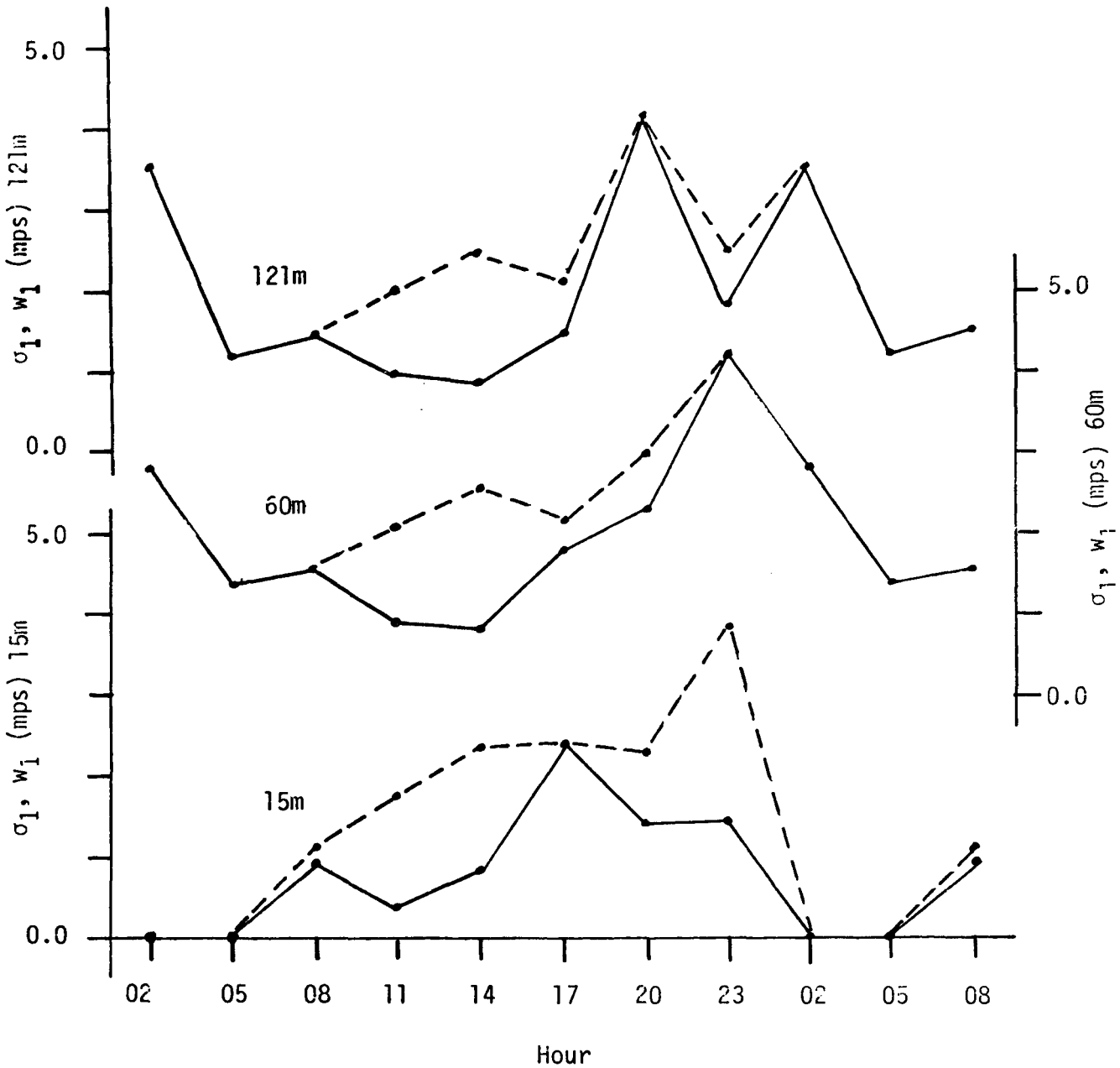

Figure 15. Diurnal Variation of σ_1, w_1, July, Hanford Tower

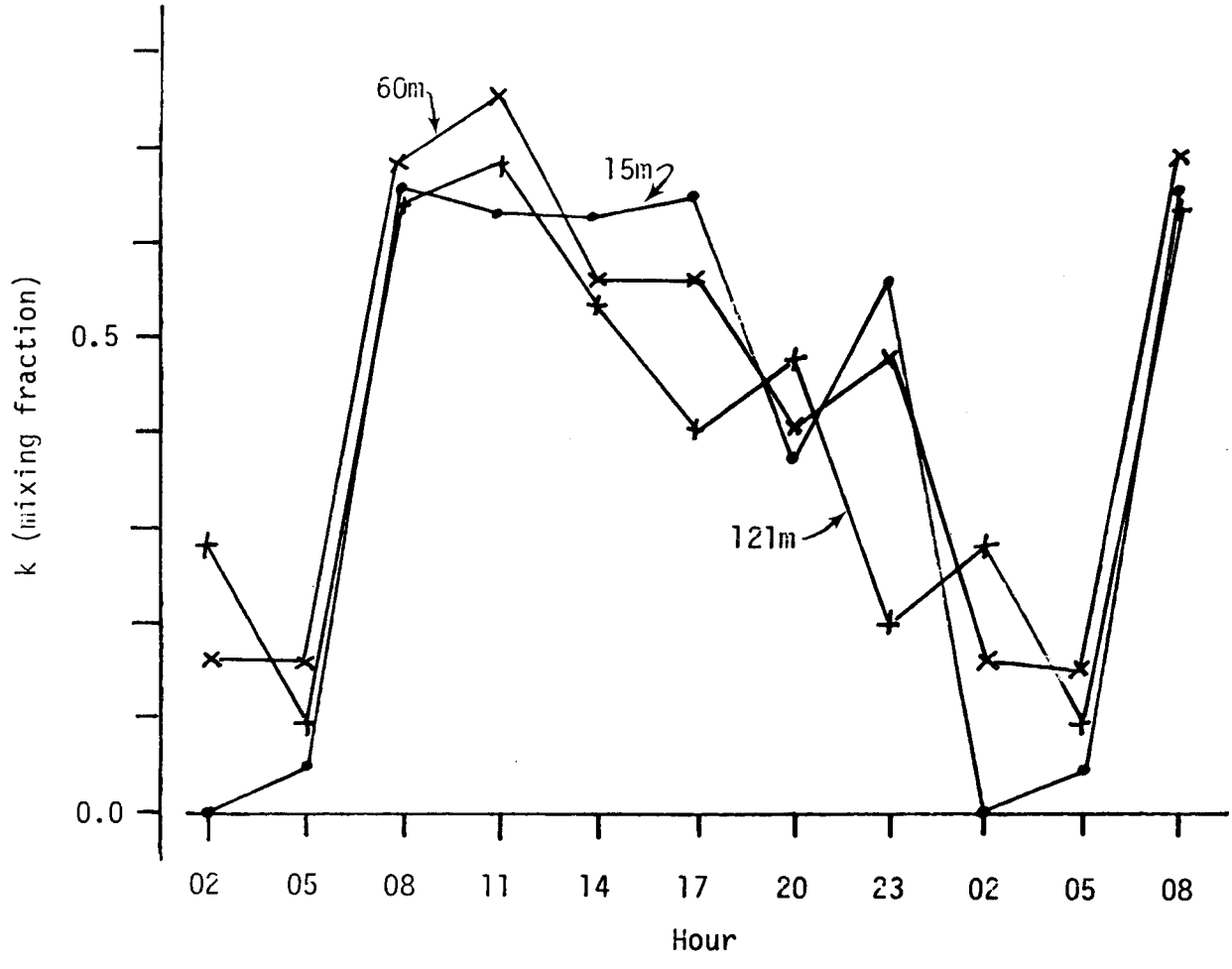

Figure 16. Diurnal Variation of the Mixing Parameter, k, July, Hanford Tower

CAPE KENNEDY TOWER

The frequency function tables from which the parameters of the empirical distribution function were computed are contained in Anon., 1971. The data covers the year 1968 and are 10 minute mean values obtained every 10 minutes throughout the day. There were actually two towers, one of 150m and another of 18m located 18m from the taller tower. The values hereafter tabulated at heights designated as 3, 10, and -18m pertain to the shorter tower; all others to the 150m tower.

The values of the parameters $\sigma_1, w_1, \sigma_2, w_2$ and k for each level for all months combined are tabulated in Table 10 and for each level by individual months in Table 11.

A comparison of the parameter values σ_2 and w_2 at the 18m level is shown in Figure 17. The values of σ_2 seem to agree fairly well except for May and January. The values of w_2 do not agree as well. Values of σ_1, w_1, and k do not agree well.

The annual variation of σ_2 and w_2 at the 60m and 120m levels are shown in Figure 18. It will be noted that (in Figure 17) the annual variation of σ_2 and w_2 is quite small (if present at all). On the other hand at both 60m and 120m both σ_2 and w_2 show some annual variation (summer minimum, winter maximum).

The values of the scaling parameters for σ_2 and w_2 at the Cape Kennedy Tower are given in Table 12. The values obtained for the annual data are indicated by ANN-A and ANN-B on the bottom line of the table. Two sets of scaling parameters were used to reflect the two different "models" appearing in Table 10; the one consisting of levels marked # for which $w_2=0$ and the other of levels marked * for which $w_2 \neq 0$. In the case A for σ_2 and B for w_2 the scaling appears to be rather reasonable. In case A for w_2 scaling is not appropriate unless b=0 is considered an acceptable parameter value. For case B for σ_2 the parameter value, b, is too large and its error, σ_b,

TABLE 10. VALUES OF PARAMETERS $\sigma_1, w_1, \sigma_2, w_2$, AND k BY ELEVATION AT CAPE KENNEDY TOWER, ANNUAL DATA

Ht.	σ_1	w_1	σ_2	w_2	k	RMSE
3	0.00	0.00	2.69#	0.00	0.1275	0.08
10	0.49	2.49	3.09#	0.00	0.1370	0.13
-18	1.00	2.95	3.36#	0.00	0.2721	0.05
18	0.40	4.21	3.51#	0.00	0.1890	0.16
30	2.80	5.15	1.66*	3.87	0.3961	0.08
60	1.60	4.83	3.34*	4.83	0.3690	0.15
90	0.42	4.61	3.44*	5.11	0.1158	0.19
120	0.42	4.54	3.52*	5.38	0.0836	0.08
150	2.27	3.86	3.03	8.04	0.5268	0.23

TABLE 11. VALUES OF PARAMETERS $\sigma_1, w_1, \sigma_2, w_2$, AND k BY ELEVATION AND MONTH AT CAPE KENNEDY TOWER

Ht.	σ_1	w_1	σ_2	w_2	k	RMSE
			JANUARY			
3	0.79	5.83	1.82	0.00	0.2184	0.01
10	--	--	--	--	--	--
-18	0.43	7.91	2.31*	2.38	0.0804	0.02
18	1.67	6.25	1.12*	2.95	0.4145	0.00
30	1.27	8.04	1.52*	4.05	0.2647	0.00
60	1.78	8.52	1.42*	4.03	0.5613	0.05
90	0.99	3.54	2.55*	7.29	0.2573	0.09
120	0.00	0.00	3.32*	6.49	0.0271	0.75
150	1.87	0.00	2.73*	7.46	0.1765	0.33
			FEBRUARY			
3	1.51	6.19	2.08	0.00	0.1936	0.02
10	--	--	--	--	--	--
-18	2.05	7.12	1.41*	2.79	0.2892	0.01
18	1.63	8.45	1.61*	3.59	0.1352	0.19
30	1.70	10.91	1.68*	5.16	0.0956	0.87
60	1.82	14.02	2.35*	5.50	0.0490	0.30
90	7.50	0.00	2.59*	6.84	0.2416	0.57
120	1.74	17.42	3.31*	6.43	0.0103	0.43
150	1.88	10.43	5.81	0.00	0.0700	0.33
			MARCH			
3	0.00	0.00	1.94*	3.86	0.2146	0.09
10	--	--	--	--	--	--
-18	1.16	8.12	1.84*	3.26	0.1277	0.00
18	1.95	6.06	1.17*	3.00	0.5728	0.02
30	2.52	7.00	1.81*	4.47	0.2828	0.14
60	5.33	0.00	1.36*	6.47	0.5026	0.63
90	0.00	0.00	4.21*	6.50	0.0000	1.52
120	2.26	0.00	3.43*	6.59	0.0165	0.80
150	2.98	9.71	4.12	0.00	0.4865	0.36
			APRIL			
3	1.03	6.25	2.28	0.00	0.1259	0.00
10	0.53	8.25	1.73*	2.67	0.0464	0.00
-18	2.13	5.00	1.41*	2.60	0.4014	0.00
18	1.75	6.46	1.37*	3.27	0.2976	0.03
30	0.74	9.59	1.90*	4.45	0.0340	0.04
60	0.00	0.00	2.35*	5.43	0.0000	0.51
90	0.00	0.00	2.60*	5.90	0.0000	0.69
120	0.00	0.00	2.98*	6.00	0.0000	0.84
150	3.83	0.00	2.83*	6.55	0.3953	0.69

TABLE 11
(continued)

Ht.	σ_1	w_1	σ_2	w_2	k	RMSE
			MAY			
3	0.00	0.00	1.62*	3.73	0.2745	0.04
10	0.00	0.00	2.78*	2.46	0.0000	0.53
-18	0.00	0.00	3.19	0.00	0.0000	0.97
18	2.13	4.85	1.95*	3.57	0.4855	0.02
30	1.83	7.22	1.61*	4.09	0.2154	0.02
60	0.36	10.31	1.95*	4.99	0.0775	0.24
90	0.00	0.00	2.61*	5.74	0.0054	0.36
120	0.00	0.00	2.93*	5.47	0.0000	0.48
150	0.00	0.00	3.10*	5.41	0.0239	0.43
			JUNE			
3	1.73	11.29	2.47	0.00	0.0267	0.46
10	5.50	0.00	1.73*	2.73	0.1338	0.23
-18	6.42	0.00	1.76*	2.55	0.1609	0.42
18	5.64	0.00	1.39*	3.52	0.2803	0.59
30	6.41	0.00	1.45*	3.96	0.2359	0.91
60	7.34	0.00	1.53*	4.80	0.2281	0.54
90	7.69	0.00	1.70*	4.78	0.2761	0.63
120	7.62	0.00	1.50*	5.22	0.3655	1.08
150	7.84	0.00	1.98*	4.81	0.3226	0.88
			JULY			
3	0.00	0.00	1.36*	2.87	0.3313	0.00
10	0.00	0.00	1.33*	3.42	0.3202	0.04
-18	0.00	0.00	1.38*	3.66	0.2154	0.03
18	0.00	0.00	1.44*	3.61	0.1981	0.12
30	0.00	0.00	1.80*	3.37	0.0631	0.24
60	0.00	0.00	1.61*	4.46	0.1636	0.16
90	0.00	0.00	1.94*	4.44	0.1056	0.12
120	0.00	0.00	2.21*	4.33	0.0485	0.13
150	0.00	0.00	2.46*	3.71	0.0000	1.22
			AUGUST			
3	0.00	0.00	1.34*	2.79	0.3134	0.00
10	0.00	0.00	1.05*	3.80	0.4162	0.00
-18	2.72	0.00	1.38*	3.26	0.5236	0.05
18	0.83	0.00	1.52	3.27	0.0444	0.02
30	0.16	0.22	1.59*	3.63	0.0214	0.25
60	0.40	8.51	1.55*	4.28	0.0197	0.00
90	0.35	5.99	1.63*	4.16	0.1387	0.04
120	0.88	4.06	2.29*	4.62	0.1951	0.26
150	1.70	8.41	1.77*	4.24	0.0673	0.03

TABLE 11
(continued)

Ht.	σ_1	w_1	σ_2	w_2	k	RMSE
			SEPTEMBER			
3	0.00	0.00	0.95*	3.80	0.3654	0.00
10	0.00	0.00	2.24*	3.35	0.0161	0.35
-18	0.00	0.00	2.15*	2.91	0.0154	0.26
18	0.00	0.00	2.04*	3.23	0.0000	0.28
30	0.00	0.00	2.06*	3.74	0.0000	0.84
60	0.94	8.77	1.90*	4.36	0.0826	0.04
90	0.36	10.31	2.17*	4.42	0.1114	0.70
120	0.38	4.71	3.82*	3.22	0.1835	0.39
150	0.00	0.00	3.24*	4.90	0.0000	1.62
			OCTOBER			
3	0.00	0.00	2.94	0.00	0.0000	0.73
10	0.00	0.00	3.43	0.00	0.0000	1.73
-18	2.57	5.00	1.26*	2.83	0.6625	0.04
18	1.63	7.59	1.52*	3.58	0.2885	0.02
30	1.56	8.49	1.75*	4.18	0.2302	0.10
60	0.46	4.38	3.25*	5.99	0.1226	0.17
90	1.39	3.79	3.22*	7.19	0.1939	0.51
120	1.93	4.51	3.21*	8.14	0.3208	0.70
150	0.00	0.00	4.11*	5.78	0.0000	0.54
			NOVEMBER			
3	1.74	4.42	1.61	0.00	0.2559	0.00
10	1.72	4.78	0.95*	2.29	0.3826	0.03
-18	1.36	7.30	1.84*	2.78	0.0871	0.00
18	0.55	2.64	2.11*	4.15	0.3665	0.11
30	1.66	7.77	1.79*	3.93	0.1326	0.02
60	1.32	4.94	3.53*	4.71	0.2869	0.17
90	1.44	9.76	2.16*	4.74	0.2464	0.68
120	0.00	0.00	3.46*	5.19	0.0000	1.07
150	2.56	9.75	2.07*	4.33	0.3964	0.57
			DECEMBER			
3	1.08	5.70	1.89	0.00	0.1706	0.00
10	0.20	7.64	2.98	0.00	0.0297	0.98
-18	1.07	7.77	1.55*	3.35	0.1695	0.00
18	1.58	5.79	1.05*	2.97	0.3445	0.01
30	1.59	7.31	1.47*	3.87	0.2896	0.03
60	3.48	0.00	2.64*	5.76	0.2136	0.29
90	2.49	7.49	4.07	0.00	0.3545	0.90
120	0.00	0.00	3.77*	6.21	0.0000	1.39
150	2.06	9.40	5.19	0.00	0.3204	0.38

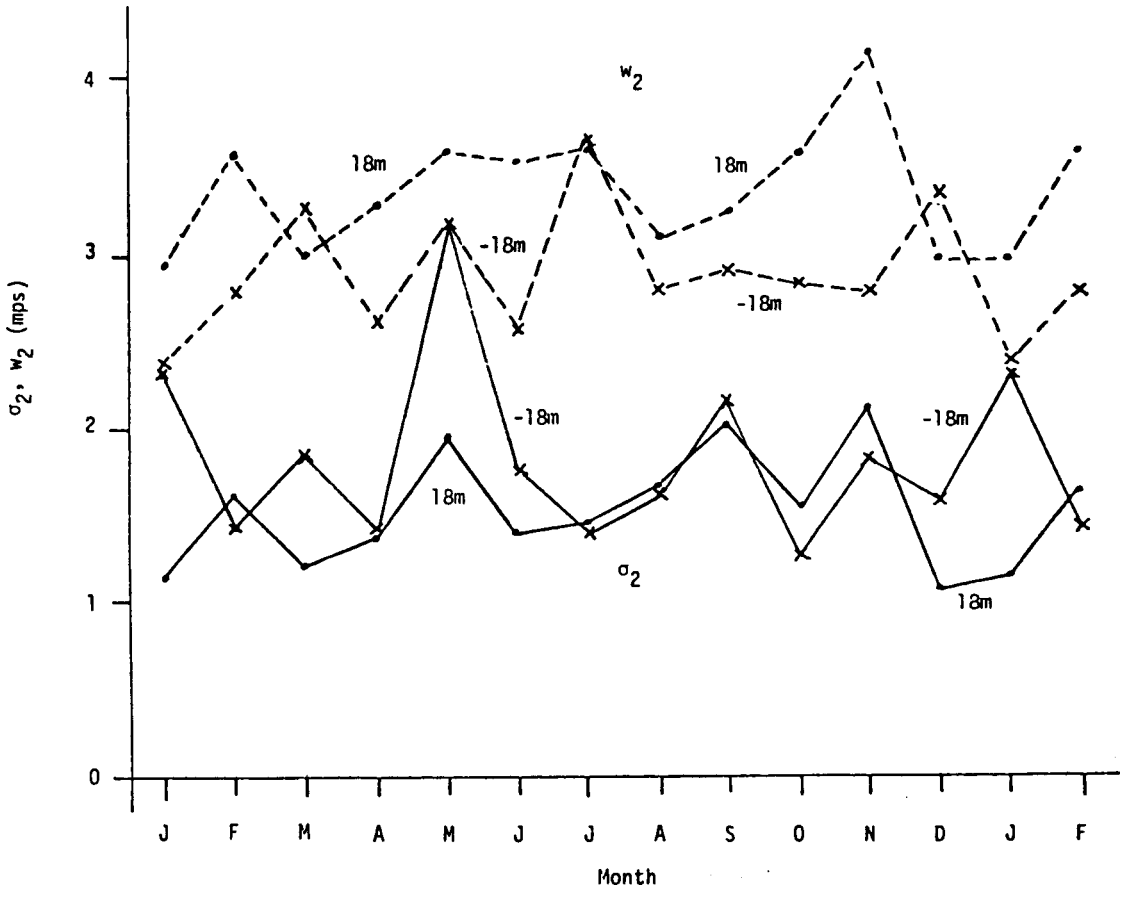

Figure 17. Values of σ_2 and w_2 by Months at the 18m Level on Both Towers at Cape Kennedy

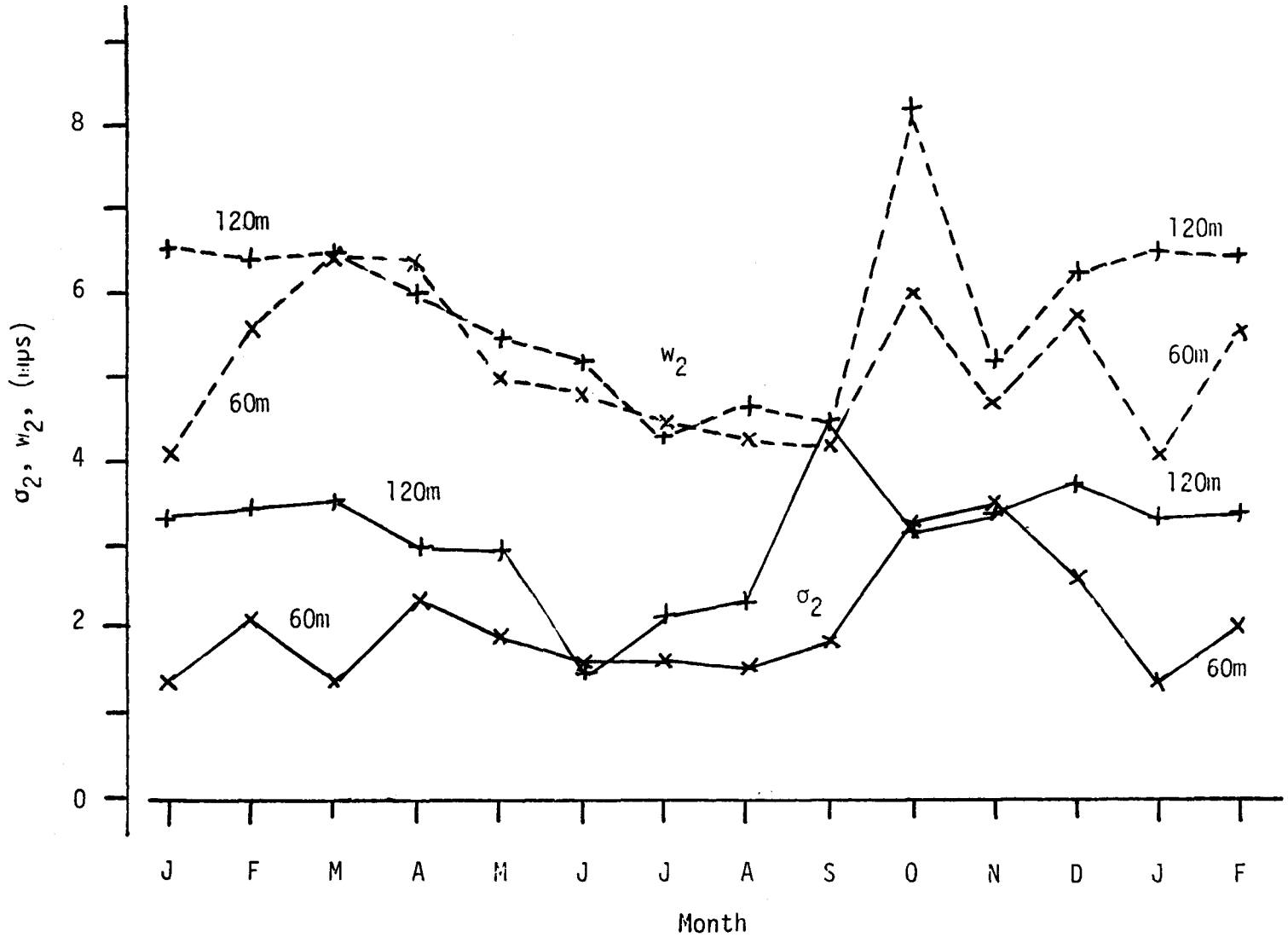

Figure 18. Annual Variation of σ_2 and w_2 at the 60 and 120m Levels on the Cape Kennedy Tower

TABLE 12. SCALING PARAMETERS FOR σ_2 AND w_2, CAPE KENNEDY TOWER

	σ_2			w_2		
Mo.	w_o	b	σ_b	w_o	b	σ_b
JAN	1.21	0.309	0.148	2.06	0.484	0.074
FEB	1.16	0.393	0.042	2.73	0.389	0.088
MAR	1.68	0.179	0.145	3.73	0.203	0.081
APR	1.38	0.279	0.051	2.59	0.361	0.044
MAY	1.95	0.120	0.064	3.50	0.168	0.054
JUN	1.56	0.026	0.047	2.74	0.249	0.047
JUL	1.44	0.148	0.029	3.35	0.094	0.025
AUG	1.33	0.124	0.041	3.33	0.110	0.019
SEP	1.70	0.224	0.066	3.47	0.061	0.046
OCT	1.06	0.502	0.062	2.66	0.393	0.083
NOV	1.39	0.286	0.121	2.78	0.234	0.066
DEC	0.87	0.590	0.109	2.56	0.386	0.058
ANN-A	3.15	0.136	0.018	--	--	--
ANN-B	0.99	0.565	0.172	3.04	0.237	0.032

is also large. This is due to the value σ_2=1.66 at 30m in Table 10. The situation at this level illustrates one of the ambiguities in the interpretation of the parameters of the d.f.; there is no difference in the fit of the empirical formula to the data between the pentad (2.80, 5.15, 1.66, 3.87, 0.3961) and the pentad (1.66, 3.87, 2.80, 5.15, 0.6039). That is, we may exchange the parameter pairs σ_1,w_1 and σ_2,w_2 provided that at the same time we replace k by 1-k, this convention guaranteeing that the k shown is the mixing fraction referring to the <u>first</u> mentioned pair. (Also we have generally tabulated values of k less than 0.5 so that the first parameter pair occurs less frequently in the mixture than the second, but this is not absolutely necessary, the previous convention is.) As tabulated, w_2=3.87, k=0.3961 fit into the trend of other values rather well while σ_1=2.80, w_1=5.15 are not very satisfactory and σ_2=1.66 is definitely out of line. On the other hand the alternate choice does not improve the situation; a σ_2=2.80 is better than 1.66 but not satisfactory, w_2=5.15 is far worse than 3.87, k=0.6039 is worse than the original value, σ_1=1.66 is an improvement over 2.80 and w_1=3.87 seems no better or worse than 5.15. In other words the exploitation of this ambiguity in the parameters leaves the situation as unsatisfactory as it was originally.

In the computation of the scaling parameters it is important that only those levels be used where the p.d.f. model indicates a common parameter usage. As pointed out above, this resulted in two different sets of scaling parameters for the annual data at Cape Kennedy. The common model cases for the computation of scaling parameters are indicated in the monthly data of Table 11 by the asterisks following the value of σ_2. Inspection of these columns indicates that all rows are marked for which $w_2 \neq 0$. In other words, there were only isolated cases of w_2=0 or occasionally two adjacent levels so that scaling parameters for these monthly cases could not be reasonably computed.

The annual variation of the scaling parameters b and w_0 for the d.f. parameters σ_2 and w_2 is shown in Figure 19 and 20 respectively. The scaling parameter, b, Figure 19, shows a strong annual variation in both cases with

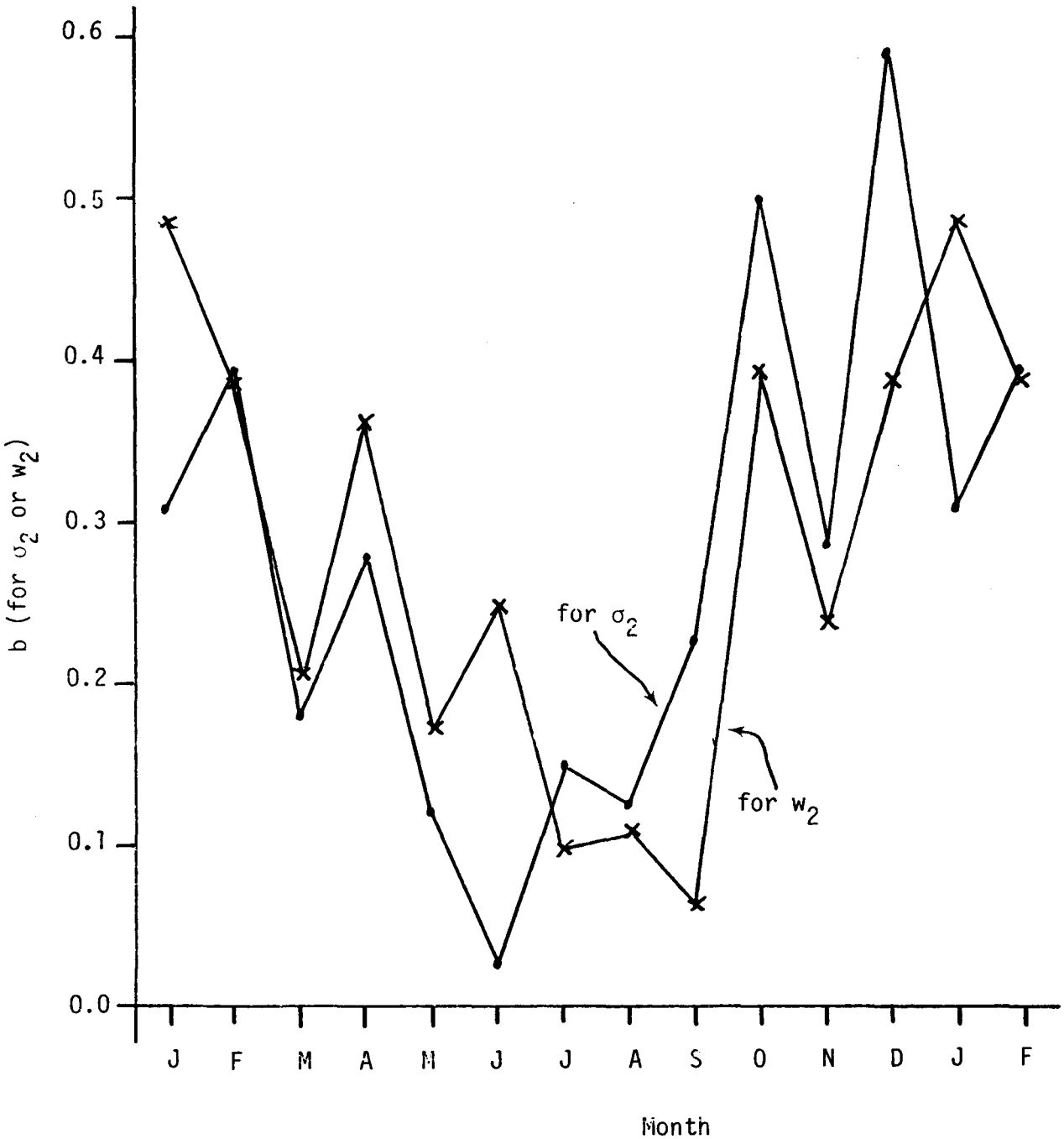

Figure 19. Annual Variation of the Scaling Parameter, b, for both σ_2 and w_2 at Cape Kennedy

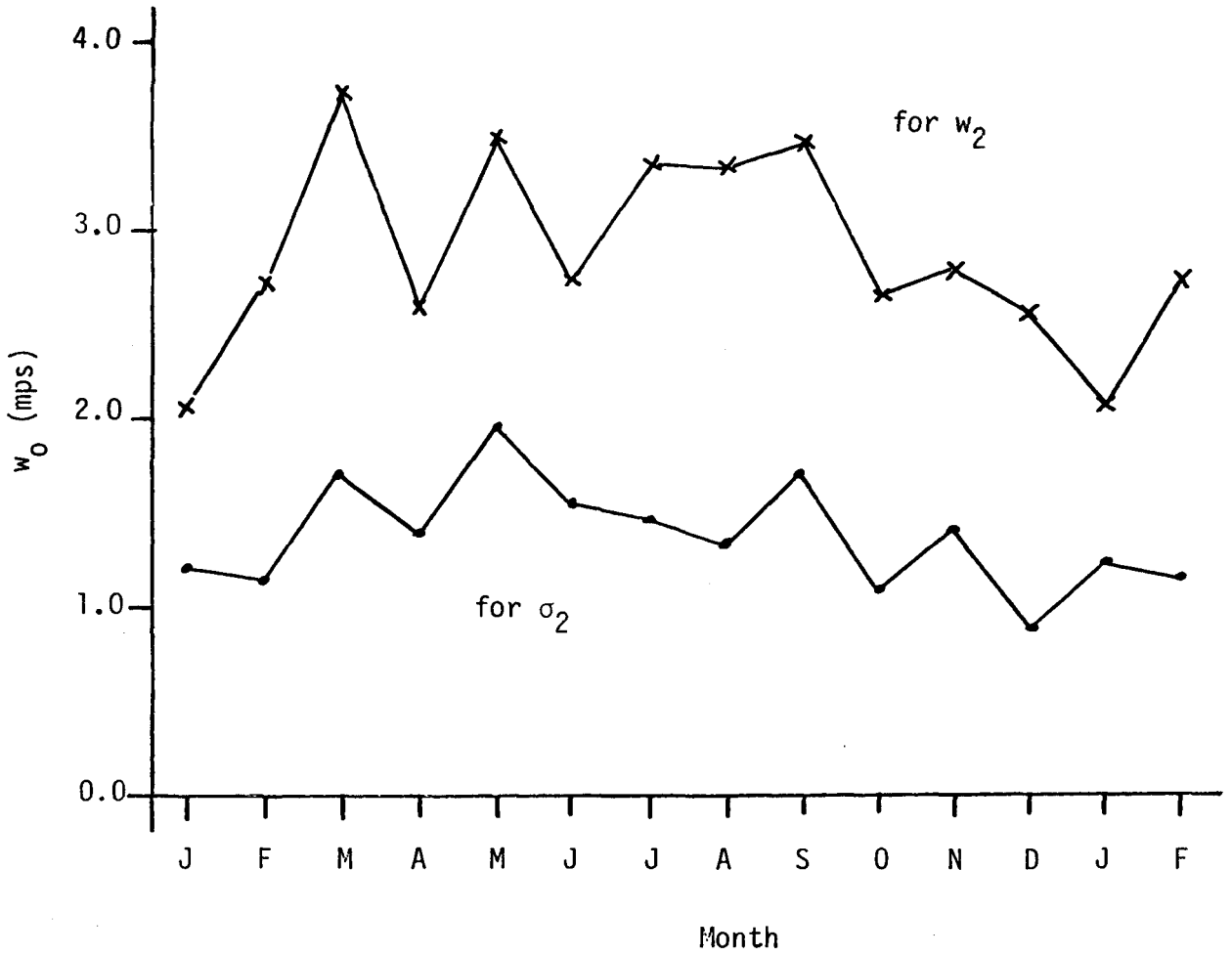

Figure 20. Annual Variation of the Scaling Parameter w_o for Both σ_2 and w_2 at Cape Kennedy

a pronounced minimum in summer and maximum in winter. The scaling parameter, w_o, Figure 20, shows only a slight annual variation but in the opposite phase, maximum in summer and minimum in the winter. Throughout, the reference level in the scaling formula has been taken as 10m (σ_2 or $w_2 \approx w_o(z/z_o)^b$, z_o=10). The combined annual variation of w_o and b for both σ_2 and w_2, then indicates summer maximum of σ_2,w_2 at low levels, a cross-over level where there is little or no annual variation, and summer minima of σ_2,w_2 at the higher levels. This is, of course, brought about by the large annual variation of b which roughly measures the rate of increase of the parameter being scaled with height (strictly the logarithm of the parameter vs the logarithm of height).

It is not without interest to note that b (for σ_2) and b (for w_2) are somewhat out of phase, b (for σ_2) being less than b (for w_2) from January through June with the reverse from July through December (nearly the same in February), and the minimum in b (for σ_2) occurring in June while that for b (for w_2) occurs in August or September. This accounts for the somewhat out of phase variation of σ_2 and w_2 (at both 60 and 120m) shown in Figure 18.

The curves for w_o (for w_2) and w_o (for σ_2) in Figure 20 are well separated, $w_2 > \sigma_2$ throughout. This is, of course, expected since in the data reduction procedure we have generally taken w_2=0 if it is found that $w_2 < \sigma_2$, i.e., the error in using w_2=0 and a slightly adjusted σ_2 is seldom larger than that for using $w_2 \neq 0$ but $< \sigma_2$. In this respect the Cape Kennedy data differs markedly from that at WSMR and Hanford where in both cases w_2=0 throughout for the monthly data.

The role of the minor mixture component (σ_1,w_1) is quite different from that played by this mixture component in the monthly data at both WSMR and Hanford. In the WSMR case $\sigma_1 = w_1 = 0$, $k \neq 0$ so that the minor mixture component is a "spike" in the p.d.f. at w=0. In the case of the Hanford monthly data the minor mixture component accounted for 20% to 50% and was always one for which the most probable speed was less than that for the

major mixture component. (The most probable speed is σ_1 (or σ_2) where w_1 (or w_2) is zero. Otherwise see Appendix F.) Thus, monthly data at Hanford is described by a major mixture component that is an ordinary Rayleigh p.d.f. which is modified by a minor mixture component of considerable importance over the low speed range of the distribution.

Inspection of the data in Table 11 indicates that the "minor" mixture component may have either a larger or smaller most probable speed than the "major" component and also need not be "minor" in the sense that $k<0.5$. By far the larger number of cases consist of those for which the most probable speed is larger than that of the major mixture component. Thus, the overall p.d.f. consists of a generalized Rayleigh p.d.f. for the major mixture component with the minor mixture component making modifications on the high speed tail of the distribution. These are, however, a number of cases where the minor component modifies the low speed end of the distribution. An example appears at once in Table 11 for the January data. At levels up to and including 60m the minor mixture component has a most probable speed much larger than that of the major mixture component while for levels above 60m it is much smaller. At 60m itself the value of k indicates that the "minor" mixture component has become "major". On the other hand it does not seem reasonable to switch the values of (σ_1,w_1) and (σ_2,w_2) and change k to 1-k since the value of σ_2 of 8.52 is too far out of line with values at higher and lower levels.

One is involved here with the limitations of the empirical formula that is being used. This formula is confined to representing a mixture of only two generalized Rayleigh distributions. The computing procedure then operates to select the most important part as indicated by the data and one other part to give the most significant modifications. Consider a hypothetical situation in which the distribution involves a major mixture component and two minor mixture components, one high speed and the other low speed. An empirical formula that can account for only two components of the mixture can then do one of two things; (1) select a minor high speed mixture component and modify the major mixture component to account for

part of the low speed mixture component it cannot explicitly represent, or (2) select a minor low speed mixture component and modify the major mixture component to account for part of the high speed mixture component if cannot explicitly represent.

It may well be that part of the zig-zag character of the scaling parameter shown in Figure 19 and Table 12 might have been smaller if this aspect of a self-consistent model had been taken in account (i.e., a value of b computed separately for those cases for which the minor component was high or low speed). On the other hand it seems scarcely worth the trouble because the small number of data values in each such determination would itself introduce large variations of a different kind.

PATRICK TOWER 313

The wind speed frequency function tables used to compute the empirical distribution function parameters are contained in Anon., 1976. The data are from the years 1971, 1973, 1975, and 1976. The Patrick Tower 313 is located about 45 km south of the Cape Kennedy Tower (NASA Launch Complex No. 39 on the Kennedy Space Center). The Kennedy Tower data are confined to the year 1968. Thus, there is no overlap in the period of record at these locations. Nonetheless their close approximity should lead to similarities in the scalar wind speed distributions observed.

The data tabulations in Anon., 1976, contained several cases of irregular occurrence of large isolated wind speeds. These were arbitrarily eliminated and adjustments made to the remaining wind speed frequencies. The results were not always satisfactory, but it was felt that the inclusion of these cases outweighed the gaps that would be left had they been entirely omitted.

The annual data for the frequency function of scalar wind speed leads to two different self-consistent sets of parameters $\sigma_1, w_1, \sigma_2, w_2, k$ which describes the data with very nearly the same accuracy. These are shown in Table 13 and are there headed A and B. The parameters for 3m elevation are the same for both cases, the remainder are different. In both cases the parameters σ_2 and w_2 are very nearly the same. The differences occur in the parameters σ_1, w_1, and k. In case A, $w_1=0$ throughout; σ_1 is nearly the same but somewhat smaller than w_2 but more than twice σ_2; k is in the range 25% to 60%. Thus, the minor mixture component represents a p.d.f. with most probable wind speed somewhat less than that of the major mixture component but rather broadly distributed. It thus adjusts the wind speed frequencies most on the low speed side of the most probable speed indicated by σ_2, w_2. In case B at 16 and 49m the minor mixture component is a p.d.f. with a narrow spike located on the high speed side of the most probable speed indicated by the major mixture component (σ_2, w_2). The corresponding values of k are 21% and 12% so its effect is appreciable. For the higher levels, 62 to 149m, $\sigma_1=w_1=0$, and k is very small or zero so that the major mixture component essentially stands alone.

TABLE 13. TWO POSSIBLE ANNUAL PARAMETER DESCRIPTIONS OF THE SCALAR WIND SPEED DISTRIBUTION AT LEVELS ON THE PATRICK TOWER

Ht.	σ_1	w_1	σ_2	w_2	k	RMSE
			(A)			
3	0.88	0.00	2.48	0.00	0.0903	0.03
16	4.29	0.00	1.59	4.08	0.2636	0.37
49	4.99	0.00	1.59	5.06	0.2816	0.52
62	4.93	0.00	1.94	6.02	0.4384	0.40
89	5.67	0.00	2.42	6.13	0.3376	0.25
120	5.78	0.00	2.52	6.40	0.4345	0.39
149	6.25	0.00	2.37	6.73	0.6005	0.52
			(B)			
3	0.88	0.00	2.48	0.00	0.0903	0.03
16	1.98	6.55	1.54	3.76	0.2069	0.01
49	1.88	8.64	1.75	4.81	0.1166	0.05
62	0.00	0.00	2.54	5.68	0.0135	0.57
89	0.00	0.00	2.97	5.91	0.0000	0.61
120	0.00	0.00	3.23	6.05	0.0004	0.67
149	0.00	0.00	3.70	6.23	0.0000	0.98

The parameters for the mixture that describes the wind p.d.f. for the mid-season months are listed in Table 14. The similarity of the situation here and that at Cape Kennedy is quite evident. The major mixture component is reasonably well defined (σ_2,w_2) and varies rather consistently with elevation; the minor mixture component plays the role of an adjustment which is effective on the high or on the low side of the most probable wind speed described by the major mixture component.

Table 15 lists the scaling formula parameters for σ_2 and w_2 from the data in Tables 13 and 14. The range of values pertaining to scaling σ_2 is quite large and reflects the fact that the highly variable role being played by the minor mixture component tends to affect the parameters of the major mixture component appreciably. (When the minor mixture component is being used to adjust the low speed range the major mixture component parameters tend to increase while the opposite is the case when used to adjust the high speed range. This roughens the values of σ_2,w_2 so that the statistical variation in fitting the scaling formula is increased.)

The parameters of the empirical formula for the p.d.f. for scalar wind speed by hours of the day are given in Table 16 for January and in Table 17 for July. The same statement can be made for this hourly data as were made for the monthly data here and at Cape Kennedy, namely: (1) The parameters for the major mixture component (σ_2,w_2) are reasonably well identified and have a well defined trend with altitude; (2) The parameters for the minor mixture component (σ_1 and w_1) indicate that it usually serves as an adjustment to fit the formula better in either the high speed or low speed range; (3) The parameter k is usually small, but not uniformly so with the result that on occasion the majority of cases is sometimes switched into the minor mixture component category (i.e., $k>0.5$).

The diurnal variation of the parameters σ_2 and w_2 during January and July at 16, 62, and 120m are shown in Figures 21 through 24. The point at 09 hrs. for the 120m level is marked A in all four figures to indicate that it might be in error. If scaling were perfect, these curves would form a

TABLE 14. PARAMETERS $\sigma_1, w_1, \sigma_2, w_2, k$ FOR THE MID-SEASON MONTHS AT LEVELS ON THE PATRICK TOWER, MONTHLY AND ANNUAL DATA

Ht.	σ_1	w_1	σ_2	w_2	k	RMSE
			(JAN)			
3	0.00	0.00	2.00	2.23	0.0981	0.09
16	0.89	3.57	2.30	4.77	0.3298	0.04
49	0.36	3.47	2.34	5.75	0.1074	0.17
62	1.92	9.09	2.17	5.19	0.3294	0.15
89	1.48	3.94	2.53	8.28	0.2219	0.17
120	0.00	0.00	3.69	6.91	0.0000	0.63
149	1.60	12.18	3.85	7.31	0.1057	0.07
			(APR)			
3	0.00	0.00	1.25	4.65	0.5691	0.00
16	0.51	3.60	2.08	4.94	0.1729	0.03
49	1.23	5.46	2.42	5.94	0.3049	0.02
62	1.84	9.76	2.07	6.17	0.1805	0.15
89	1.61	4.31	2.61	7.51	0.1430	0.07
120	0.00	0.00	3.13	6.83	0.0000	0.45
149	0.00	0.00	3.43	7.23	0.0000	0.63
			(JUL)			
3	1.17	0.00	1.80	2.16	0.3161	0.02
16	1.13	3.34	1.86	4.16	0.3983	0.02
49	2.40	6.13	1.64	4.51	0.0318	0.01
62	4.14	0.00	1.76	5.30	0.1735	0.05
89	4.21	0.00	1.77	5.60	0.2697	0.09
120	0.00	0.00	2.48	5.61	0.0380	0.50
149	0.00	0.00	2.43	5.83	0.1061	0.20
			(OCT)			
3	0.49	1.69	2.14	2.91	0.1920	0.13
16	0.37	3.72	2.62	5.09	0.1867	0.31
49	1.42	5.10	3.66	5.95	0.6014	0.37
62	1.26	6.79	4.40	5.08	0.3205	0.16
89	0.00	0.00	3.10	6.70	0.0178	1.80
120	0.00	0.00	3.74	7.20	0.0192	2.16
149	0.00	0.00	5.16	6.66	0.0000	3.02

TABLE 15. SCALING PARAMETERS FOR σ_2 AND w_2 FOR THE MID-SEASON MONTHS AND ANNUALLY ON THE PATRICK TOWER

	σ_2			w_2		
Mo.	w_o	b	σ_b	w_o	b	σ_b
JAN	2.15	0.138	0.058	3.50	0.301	0.044
APR	1.67	0.229	0.035	5.10	0.124	0.022
JUL	1.79	0.057	0.047	3.18	0.247	0.028
OCT	2.60	0.189	0.050	4.02	0.212	0.032
ALL-A	1.33	0.227	0.067	3.69	0.228	0.025
ALL-B	1.16	0.410	0.075	3.43	0.235	0.028

TABLE 16. DIURNAL VARIATION OF $\sigma_1, w_1, \sigma_2, w_2, k$ AT LEVELS ON THE PATRICK TOWER DURING JANUARY

Ht.	σ_1	w_1	σ_2	w_2	k	RMSE
			(00 hrs)			
3	0.00	0.00	1.82	2.51	0.1676	0.32
16	2.15	5.46	1.21	3.77	0.4577	0.21
49	6.26	0.00	2.04	5.43	0.1128	0.50
62	0.00	0.00	2.85	6.34	0.0767	0.69
89	0.00	0.00	3.19	7.06	0.0000	0.77
120	0.00	0.00	3.69	7.03	0.0000	0.80
149	0.41	0.00	4.05	7.47	0.0038	0.59
			(03 hrs)			
3	2.59	0.00	1.28	0.00	0.5517	0.10
16	0.74	8.18	1.39	3.69	0.1042	0.00
49	4.24	0.00	1.69	5.88	0.3143	0.68
62	0.00	0.00	2.72	6.28	0.0765	0.34
89	5.17	0.00	1.88	8.61	0.3909	0.75
120	0.00	0.00	3.17	7.55	0.0105	0.77
149	0.00	0.00	3.62	8.12	0.0111	0.88
			(06 hrs)			
3	1.21	0.00	1.76	2.44	0.5128	0.01
16	2.00	5.41	1.19	3.52	0.2290	0.04
49	1.68	6.61	1.61	4.18	0.5581	0.00
62	0.35	0.00	2.37	6.35	0.0983	0.39
89	1.55	10.45	2.31	5.75	0.3297	0.17
120	0.00	0.00	3.34	7.40	0.0130	0.77
149	0.00	0.00	3.80	7.99	0.0183	1.05
			(09 hrs)			
3	0.00	0.00	1.82	1.94	0.1784	0.08
16	0.72	8.26	1.48	3.74	0.0801	0.00
49	1.69	7.01	1.42	3.87	0.5692	0.00
62	0.00	0.00	2.75	6.28	0.0952	0.56
89	0.47	10.90	2.54	5.91	0.3170	0.42
120	2.08	10.53	2.16	5.28	0.5184	0.18
149	3.12	9.96	5.34	0.00	0.6209	1.15

TABLE 16
(continued)

Ht.	σ_1	w_1	σ_2	w_2	k	RMSE
			(12 hrs)			
3	0.00	0.00	1.93	2.02	0.1739	0.04
16	0.60	3.26	2.06	4.56	0.3155	0.05
49	0.52	10.54	2.03	5.17	0.0690	0.11
62	0.00	0.00	2.73	6.12	0.0898	0.39
89	0.00	0.00	3.00	7.25	0.0000	0.57
120	0.00	0.00	3.20	7.74	0.0121	0.75
149	--	--	--	--	--	--
			(15 hrs)			
3	0.77	5.22	1.37	2.81	0.2566	0.00
16	0.79	7.71	1.14	3.81	0.4026	0.00
49	1.85	7.72	1.16	3.76	0.5714	0.01
62	0.50	10.84	3.01	4.09	0.2014	1.86
89	4.61	0.00	3.05	8.14	0.4267	2.11
120	1.18	3.77	2.52	8.92	0.3269	0.30
149	--	--	--	--	--	--
			(18 hrs)			
3	1.46	5.24	1.33	3.26	0.2305	0.08
16	0.00	0.00	2.19	5.10	0.0027	1.50
49	1.94	8.46	1.77	3.35	0.3060	0.03
62	0.00	0.00	3.45	5.66	0.0525	0.46
89	0.00	0.00	3.63	6.20	0.0000	1.08
120	0.00	0.00	3.79	6.20	0.0000	0.99
149	--	--	--	--	--	--
			(21 hrs)			
3	0.40	10.09	1.83	2.65	0.0056	0.21
16	1.28	3.73	2.19	5.38	0.3924	0.16
49	0.34	3.42	2.50	5.81	0.1402	0.37
62	0.00	0.00	3.13	5.86	0.0517	0.80
89	0.00	0.00	3.55	6.27	0.0000	1.28
120	0.00	0.00	3.67	6.36	0.0016	0.72
149	--	--	--	--	--	--

TABLE 17. DIURNAL VARIATION OF σ_1,$w_{1\ 2}$,w_2 AND k AT LEVELS ON THE PATRICK TOWER DURING JULY

Ht.	σ_1	w_1	σ_2	w_2	k	RMSE
			(00 hrs)			
3	1.36	0.00	1.19	4.46	0.5967	0.00
16	0.00	0.00	1.77	4.33	0.0000	0.31
49	2.91	0.00	1.39	5.55	0.0784	0.33
62	1.00	0.00	1.58	6.08	0.0808	0.20
89	4.87	0.00	1.65	6.31	0.1423	0.19
120	5.15	0.00	1.50	7.01	0.4687	0.81
149	5.05	0.00	1.77	7.01	0.1683	0.21
			(03 hrs)			
3	0.75	0.00	1.81	2.01	0.2237	0.01
16	1.45	5.12	1.17	3.30	0.3731	0.00
49	3.24	0.00	1.61	5.06	0.0603	0.02
62	0.00	0.00	1.81	5.74	0.0734	0.08
89	0.57	6.01	2.39	5.75	0.1694	0.11
120	0.38	1.57	2.55	6.78	0.0758	0.73
149	1.54	0.00	2.81	6.92	0.0526	0.09
			(06 hrs)			
3	0.00	0.00	1.13	2.12	0.2966	0.00
16	1.03	5.27	1.12	3.40	0.0667	0.00
49	0.00	0.00	1.55	4.45	0.0000	0.51
62	0.00	0.00	1.73	5.26	0.0843	0.62
89	0.70	7.74	1.90	5.25	0.0917	0.13
120	0.00	0.00	2.55	5.90	0.0268	0.50
149	3.55	0.00	2.40	6.60	0.1514	0.87
			(09 hrs)			
3	0.94	0.00	0.87	2.30	0.6186	0.00
16	1.35	5.31	1.14	3.16	0.0108	0.00
49	1.23	5.13	1.19	3.41	0.4860	0.00
62	0.00	0.00	1.90	4.77	0.0574	0.19
89	3.37	0.00	1.75	5.76	0.2844	0.28
120	4.02	0.00	1.41	6.89	0.6140	0.15
149	3.50	0.00	2.17	6.67	0.3136	0.23

TABLE 17
(continued)

Ht.	σ_1	w_1	σ_2	w_2	k	RMSE
			(12 hrs)			
3	2.14	0.00	1.06	1.41	0.3001	0.00
16	1.38	5.28	1.09	3.08	0.1568	0.00
49	1.24	5.27	1.10	3.29	0.3348	0.00
62	3.55	0.00	1.77	4.16	0.3345	0.12
89	1.09	7.46	1.52	3.74	0.2744	0.00
120	1.49	0.00	2.41	4.61	0.0396	0.08
149	1.29	2.83	2.22	5.81	0.2591	0.00
			(15 hrs)			
3	0.43	1.87	1.23	3.93	0.7425	0.00
16	0.79	7.88	1.36	3.49	0.0620	0.00
49	0.43	3.69	2.36	4.17	0.4971	0.07
62	3.70	0.00	0.37	5.19	0.3057	0.97
89	1.21	4.55	1.21	4.13	0.3787	0.01
120	0.00	0.00	2.36	4.57	0.0107	0.79
149	4.45	0.00	1.60	5.26	0.4756	0.36
			(18 hrs)			
3	2.08	0.00	1.32	3.27	0.2966	0.01
16	0.48	5.15	2.22	4.01	0.3682	0.04
49	3.85	0.00	1.16	5.01	0.2896	0.03
62	4.01	0.00	0.47	5.62	0.5288	1.47
89	4.44	0.00	0.44	5.53	0.3929	0.23
120	4.71	0.00	0.43	5.56	0.5989	1.22
149	4.85	0.00	1.38	5.84	0.3788	0.91
			(21 hrs)			
3	1.94	0.00	1.08	4.14	0.4817	0.00
16	0.00	0.00	1.72	4.81	0.0260	0.21
49	0.00	0.00	1.68	5.26	0.0170	0.08
62	0.65	0.00	1.90	5.83	0.0755	0.46
89	4.85	0.00	1.59	5.88	0.2444	0.07
120	5.03	0.00	1.11	6.24	0.6069	0.52
149	5.04	0.00	1.70	6.26	0.3218	0.40

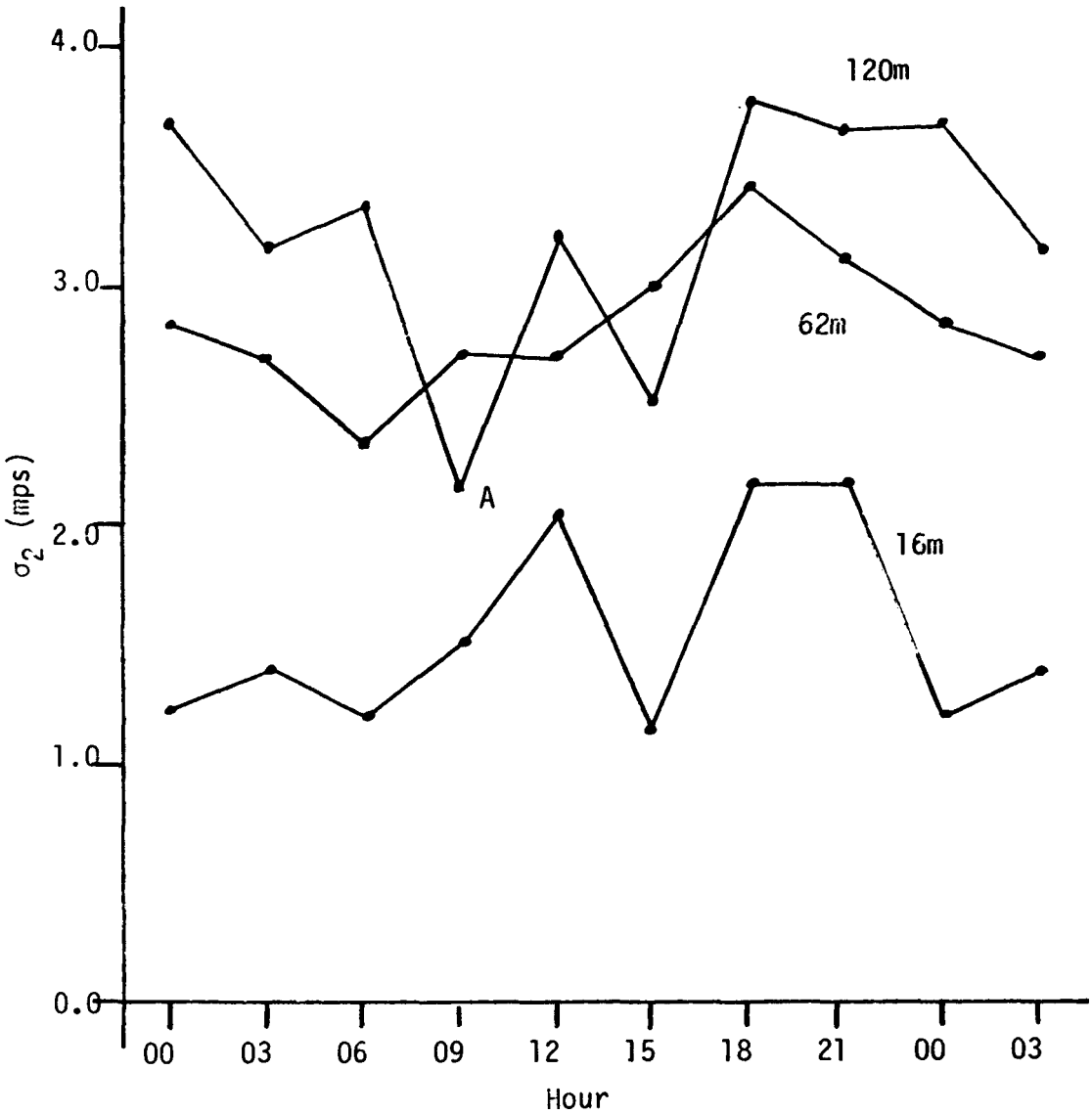

Figure 21. Diurnal Variation of σ_2 during January at 16, 62, 120m on the Patrick Tower

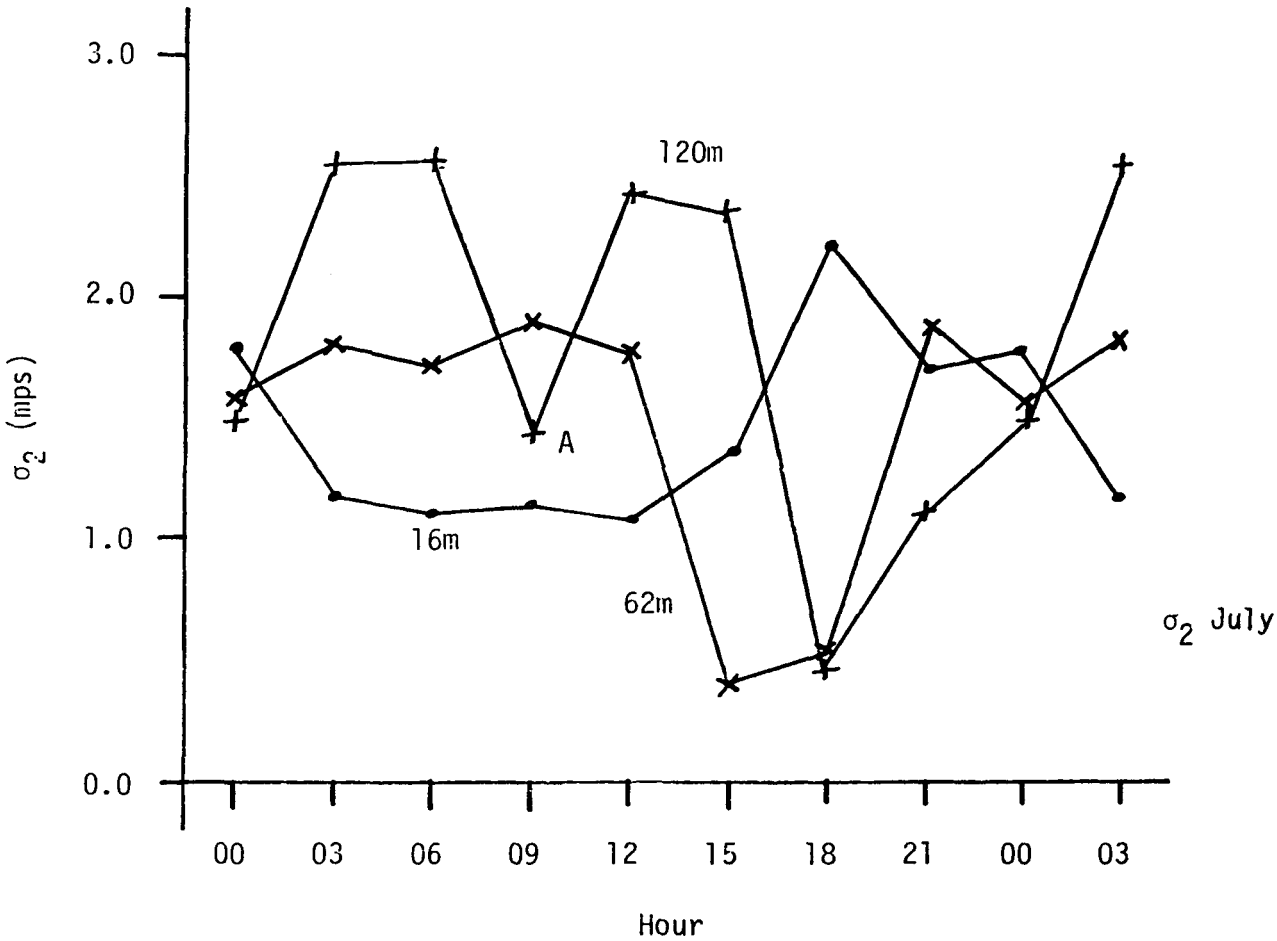

Figure 22. Diurnal Variation of σ_2 During July at 16, 62, 120m on the Patrick Tower

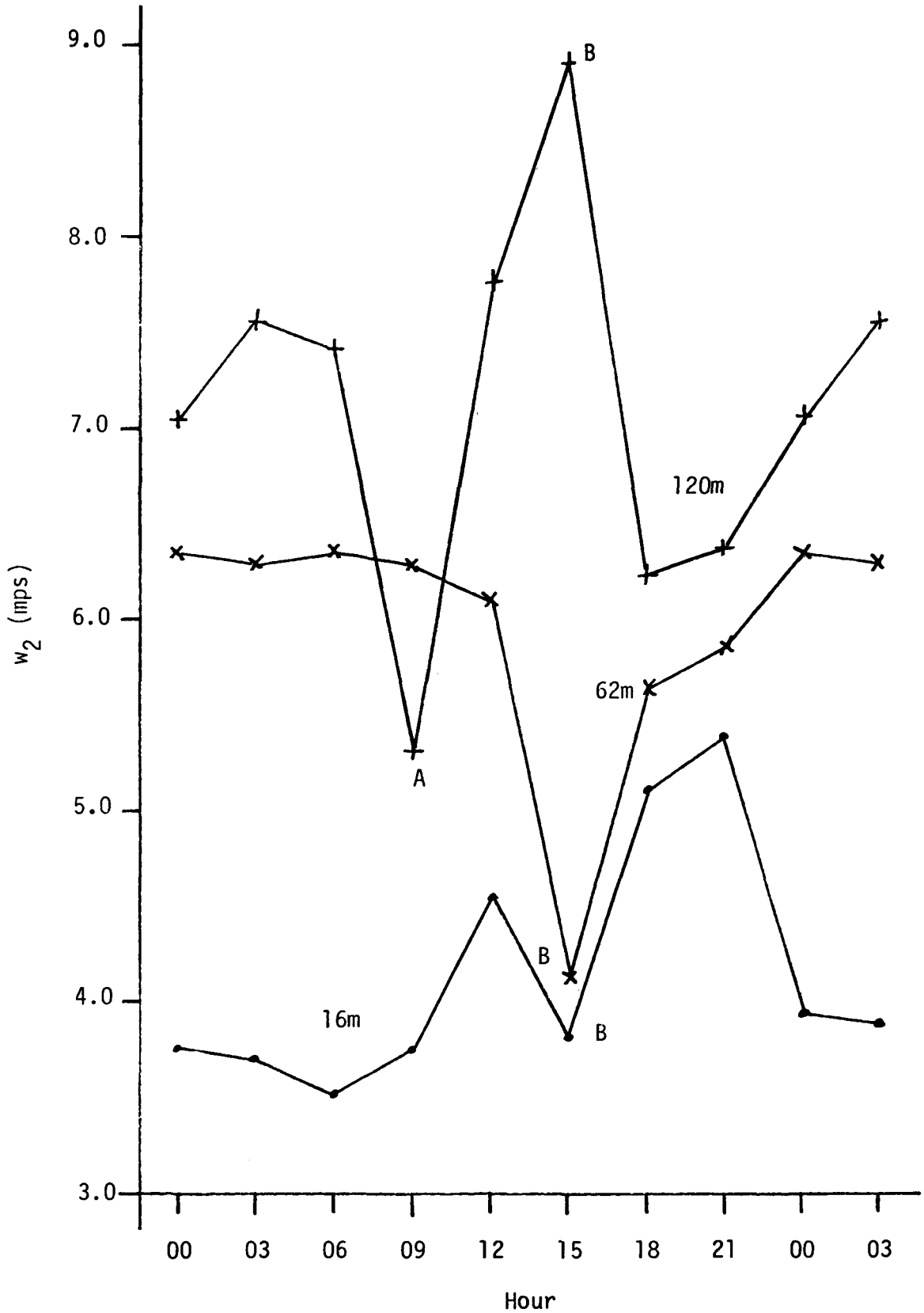

Figure 23. Diurnal Variation of w_2 During January at 16, 62, 120m on the Patrick Tower

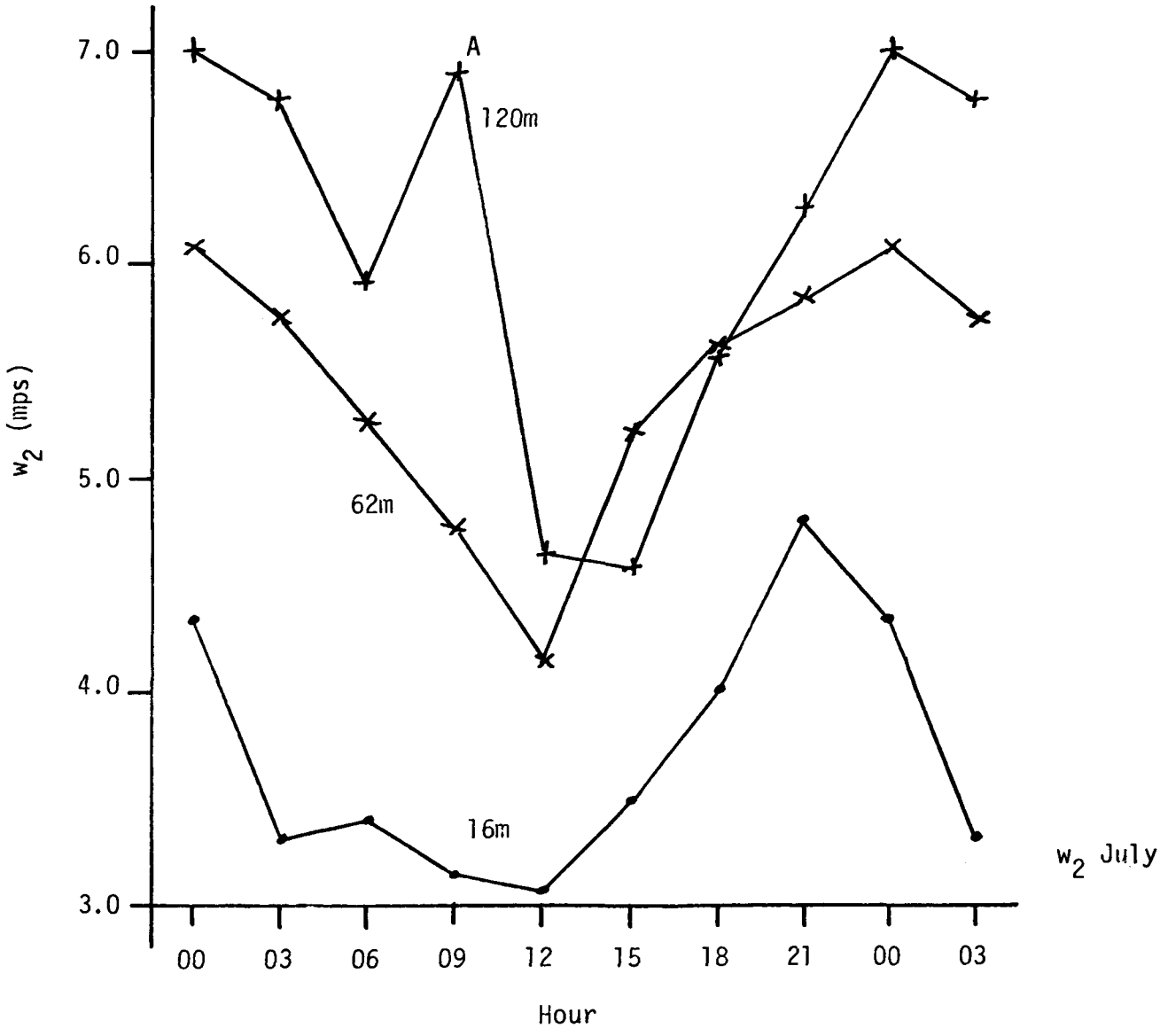

Figure 24. Diurnal Variation of w_2 During July at 16, 62, 120m on the Patrick Tower

family such that for all times, t, if $h_2 > h_1$ (h_2, h_1 are height values), then $y(t,h_2) > y(t,h_1)$; i.e., the curves would lie one above another in the order of increasing anemometer height. This is only roughly the case; and for σ_2 in July (Figure 23) the mix-up is extreme.

Comparing Figures 21 and 22, for σ_2, one notes that the diurnal variation of σ_2 at 16m in January and July are similar, the minimum occurring in early morning and the maximum in the evening. The diurnal variations of σ_2 at 62m and 120m are similar to each other in both January and July but the diurnal variation in these months are opposite; in January σ_2 at both 62m and 120m is a minimum in the morning and a maximum in the evening (as is σ_2 at 16m); in July σ_2 at both 62m and 120m is a maximum in the morning and displays a minimum in the afternoon (the opposite of σ_2 at 16m in July).

Comparing Figures 23 and 24 for w_2 it is to be noted that the diurnal variation of w_2 at 16m for January and July are similar, both being a minimum in the morning and a maximum in the afternoon. This is also the same diurnal variation displayed by σ_2 at 16m noted above. Thus, both σ_2 and w_2 at 16m have the same diurnal behavior in January and July.

Figures 23 and 24 also indicate that for both January and July the diurnal variation of w_2 at 62m and 120m are similar to each other. (The points marked B at 15 hrs. in January, Figure 23, should be ignored since the data at this hour for all levels is suspect.) On the other hand, Figure 23 indicates that w_2 at both 62m and 120m have near sunset minima and near sunrise maxima, the opposite of the variation of w_2 at 16m for this month (January); while Figure 24 indicates that w_2 at both 62m and 120m have mid-day minima and midnight maxima, roughly the same as the variation of w_2 at 16m in this month (July).

In all cases there appears to be a shift in the exact time of minimum or maximum as a function of height. There also appears to be a shift between January and July due to the differences in the time of sunrise and sunset. The data points are too irregular to discuss these items in detail.

The situation on diurnal variation of σ_2 and w_2 may be summarized in the following array. The comparison is with the diurnal variation of σ_2 and w_2 at the 16m level both of which for both January and July have morning minima and evening maxima. The array describes the diurnal variation at the 62m and 120m levels.

	January	July
σ_2	In phase	Out of phase
w_2	Out of phase	In phase

Table 18 contains the scaling parameters w_0 (z_0=10m), b, and the standard deviation of b, σ_b, for January and July. The diurnal variations of the scaling parameter w_0 for σ_2 and w_2 during January and July are shown in Figure 25 while the scaling exponent, b, for January and July are shown in Figure 26 for the parameter σ_2 and in Figure 27 for the parameter w_2. The computed values are shown in Table 18 together with a column indicating the standard deviation of the estimate of the parameter b, σ_b. Values of b for which σ_b is large are marked by A in Figures 26 and 27. (The scaling formula is σ_2 or $w_2 \approx w_0(z/z_0)^b$, z_0=10m.)

The scaling parameter w_0 should track with the observed values of the parameter concerned at 16m since this is close to the reference level z_0=10m. That this is the case is seen in Figure 25 where the diurnal variation of w_0 is the same as that for σ_2 or w_2 at 16m from Figures 21 through 24. The exception is w_0 for σ_2 during July for which the diurnal variation is very small. Even in this case w_0 for σ_2 (July) has its minimum near that of the other cases and differs in that its maximum is shifted a few hours later into the night.

The diurnal variations of the scaling exponent shown in Figures 26 and 27 indicate that b (for σ_2) in July and b (for w_2) during both January and July are in phase with each other and show a sunset minimum/sunrise maximum while b (for σ_2) in January has a midnight maximum and late morning minimum.

TABLE 18. DIURNAL VARIATION OF THE SCALING PARAMETERS FOR σ_2 AND w_2 DURING JANUARY AND JULY ON THE PATRICK TOWER

Hr.	w_o	σ_2 b	σ_b	w_o	w_2 b	σ_b
			JANUARY			
00	1.76	0.243	0.090	3.49	0.293	0.016
03	1.07	0.403	0.126	3.22	0.370	0.057
06	1.62	0.205	0.096	3.24	0.300	0.042
09	1.76	0.090	0.090	2.93	0.295	0.057
12	2.08	0.131	0.047	3.28	0.350	0.034
15	1.42	0.220	0.132	3.43	0.272	0.101
18	1.79	0.273	0.081	3.98	0.151	0.077
21	2.17	0.189	0.035	3.92	0.227	0.042
			JULY			
00	1.40	0.065	0.036	4.75	0.126	0.032
03	1.60	0.135	0.078	2.95	0.326	0.014
06	1.24	0.213	0.048	2.97	0.282	0.012
09	1.07	0.201	0.055	2.92	0.284	0.048
12	1.14	0.198	0.070	2.72	0.241	0.040
15	1.03	0.078	0.252	3.87	0.068	0.046
18	1.27	-0.253	0.186	3.91	0.156	0.013
21	1.38	0.064	0.067	4.65	0.110	0.009

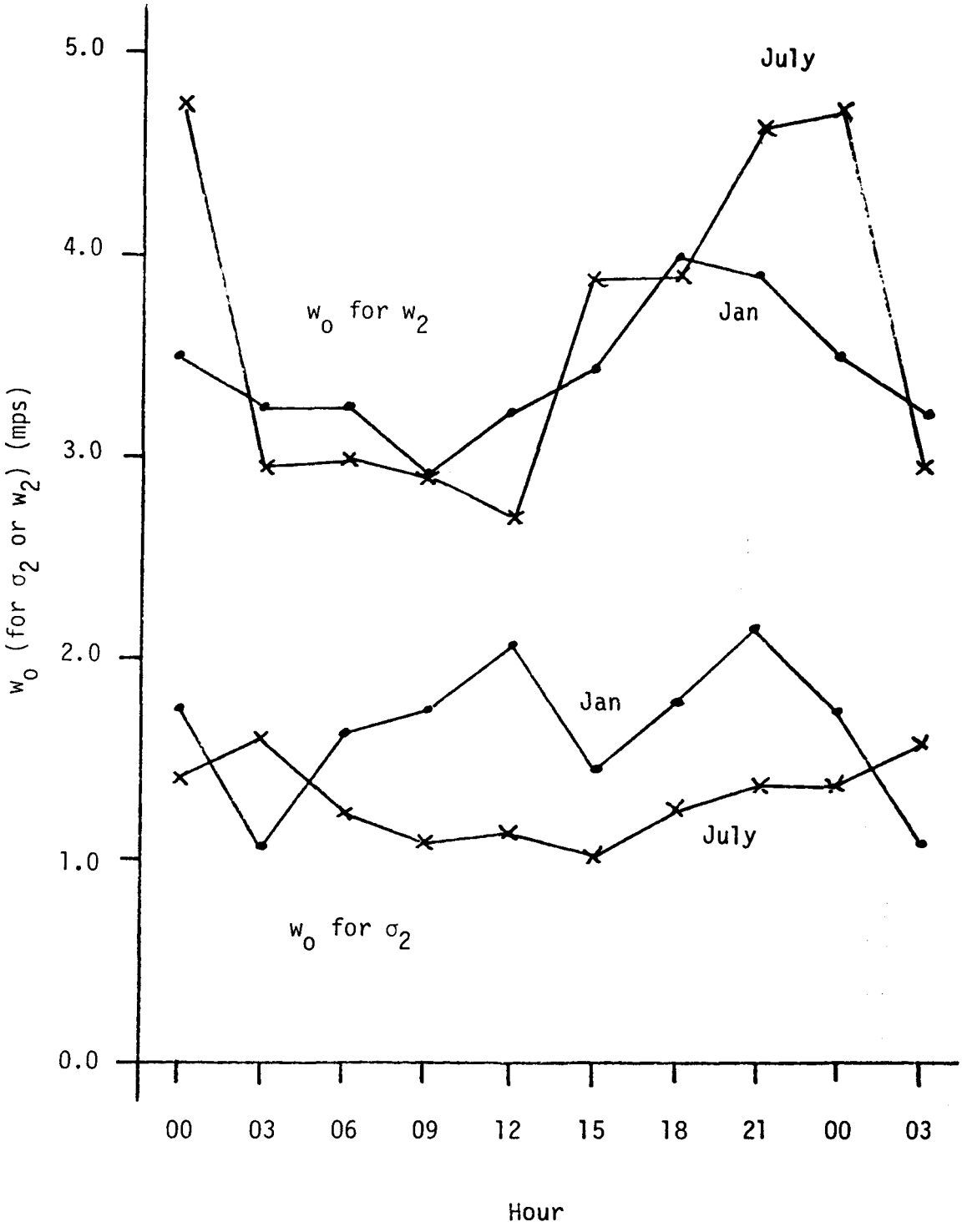

Figure 25. Diurnal Variation of the Scaling Parameter w_o for σ_2 and w_2 During January and July on the Patrick Tower

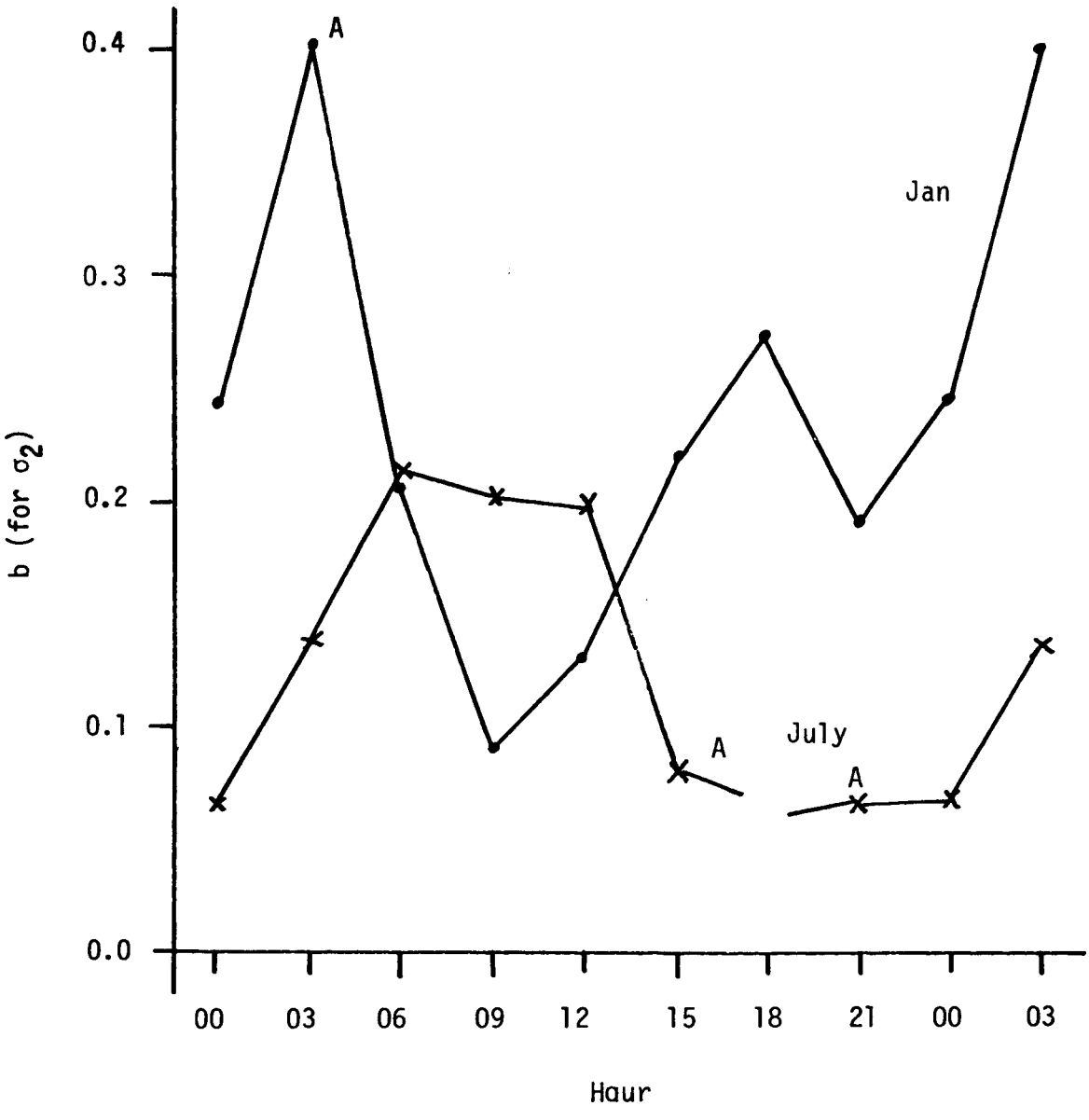

Figure 26. Diurnal Variation of the Scaling Parameter b for σ_2 During January and July on the Patrick Tower

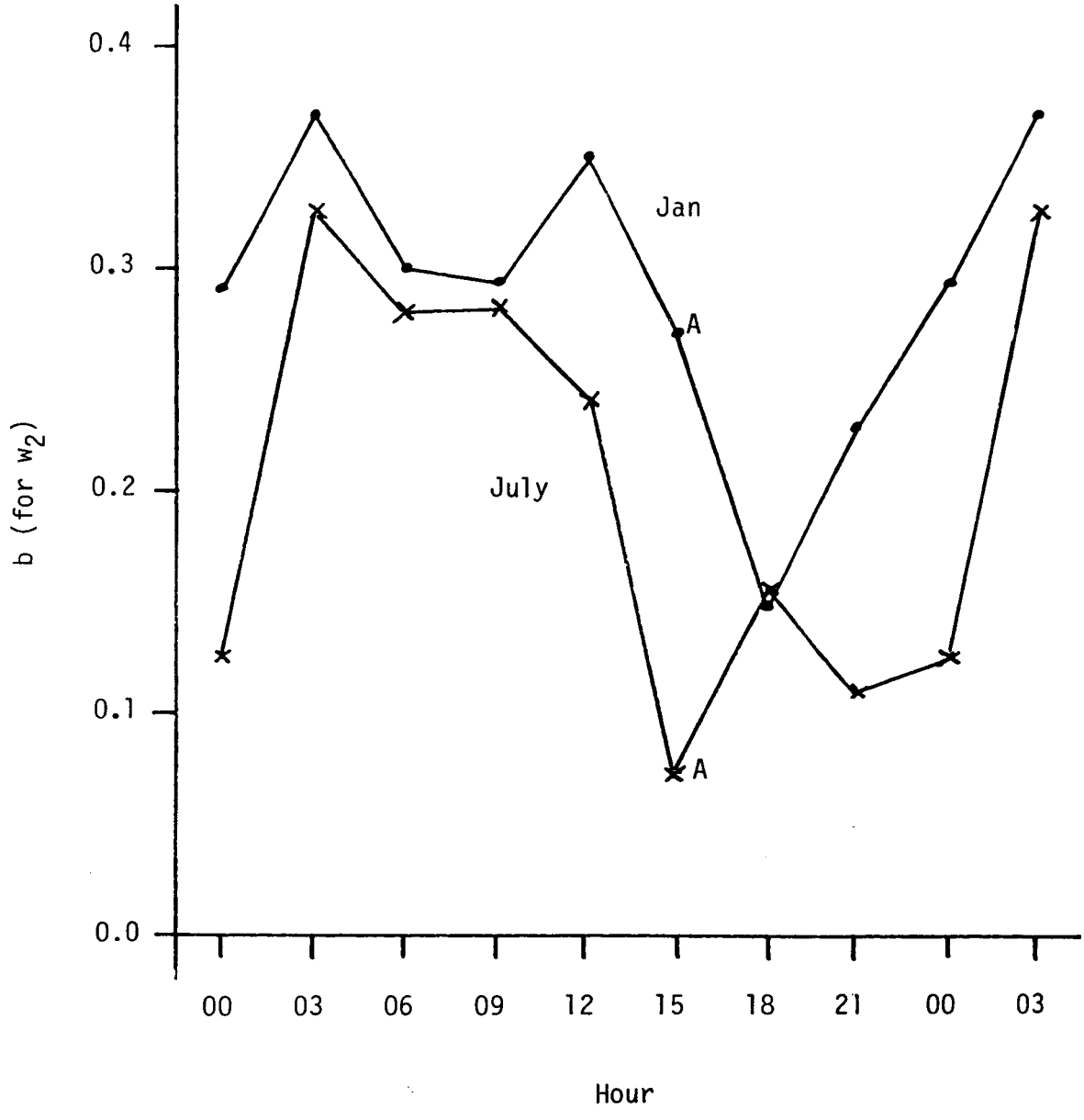

Figure 27. Diurnal Variation of the Scaling Parameter b for w_2 During January and July on the Patrick Tower

One would expect that the diurnal behavior of the parameters σ_2 and w_2 and that of the scaling parameters w_o and b would be easily interpreted in terms of each other. This seems to be very nearly the case for w_o in terms of σ_2 and w_2 at 16m. The "explanation" of the diurnal behavior of σ_2 and w_2 in terms of that of the scaling exponent b apparently does not follow easily. It is expected that when b is large σ_2 or w_2 at the higher levels would also be large. The following breakdown is in terms of the common diurnal behavior of σ_2, w_2 in January and July at 16m (AM minimum, PM maximum).

Case	w_o	b	result at 62/120m
Jan. w_2	in phase	out of phase (ck)	out of phase (ck)
July w_2	in phase	out of phase	in phase
Jan. σ_2	in phase	in phase (ck)	in phase (ck)
July σ_2	neutral	out of phase (ck)	out of phase (ck)

It is readily seen that the observed behavior of w_2 and σ_2 at the 62 and 120m levels checks that of the diurnal behavior of the scaling exponent in three of the four cases. To check the odd-ball case, July, w_2, refer to Figure 24 where the diurnal behavior of w_2 at 62 and 120m is shown. It is reasonably evident that the problem lies in the looseness of the terminology being used. The morning minimum of w_2, July, at 62 and 120m is classed as "in phase" with that at 16m and actually occurs in the range of 12 to 15 hours. The term "out of phase" has been used for a minimum occuring in the range 18 to 21 hours. One is dealing with a situation in which "in" and "out" of phase is not sufficiently precise and for which a 90° phase shift should be included. As pointed out above, it is evident that the situation actually involves shifts of maximum/minimum with altitude and with the time of sunrise/sunset but for which the data shows large irregular variations which make a refined analysis pointless.

NUCLEAR POWER PLANT SITES

The data contained in Verholek (1977) for the annual scalar wind speed frequency by class intervals may be divided into three categories depending on whether there was an anemometer at one, two, or three (or more) levels. The cases in which there is wind speed data at only one level do not provide information on the variation of the parameters of the empirical formula for the p.d.f. with height. Those sites from which wind data are available at two levels provide the minimum amount of data required for this. Where data is listed for three or more levels, the variation of the parameters with height may be checked reasonably well. These last two cases are discussed separately.

DATA LISTED AT TWO LEVELS

General Discussion

The parameter values at the levels concerned are divided into three categories and are tabulated in Tables 19, 20 and 21. In the first instance (Table 19) the cases include those for which reasonably identifiable mixture components can be determined at each level. Table 20 contains the cases for which only one component of the mixture can be identified at both levels. The remaining cases are listed in Table 21.

The RMSE listed in these tables (and others) is the root mean square error of the fit of the empirical formula for the D.F. with parameters shown to the values of the D.F. that are observed. The D.F. may be expressed on the range (0, 1) or on the range (0%, 100%). In listing the RMSE the percentage range is used to avoid tabulating an excessive number of leading zeros.

The values of the parameter b of the scaling formula $w/w_0=(z/z_0)^b$ are listed in Table 22 for each site concerned in cases A and B. These are then summarized at the bottom of the table where the number of cases (n), the mean value ($\bar{b}$), and the standard deviation (σ_b) are listed.

TABLE 19. PARAMETERS FOR NUCLEAR POWER PLANT SITES WITH ANEMOMETERS AT TWO LEVELS - CASES WITH REASONABLY IDENTIFIABLE MIXTURE COMPONENTS AT EACH LEVEL

Height	σ_1	w_1	σ_2	w_2	k(%)	RMSE
			Beaver Valley, PA			
15	2.51	0.00	0.88	0.00	42.13	0.38
46	3.06	0.00	1.03	0.00	49.88	0.76
			Ed. Hatch, GA			
23	3.37	0.00	1.32	2.20	40.60	0.06
46	4.26	0.00	1.64	3.06	35.26	0.07
			Indian Point, NY			
10	1.05	0.00	2.26	0.00	61.42	0.01
122	1.56	0.00	4.19	0.00	23.54	0.35
			Wm. B. McGuire, NC			
10	2.91	0.00	1.56	0.00	44.92	0.26
40	4.73	0.00	2.81	0.00	8.88	1.47
			North Anna, VA			
11	1.38	0.00	3.19	0.00	26.19	0.63
46	1.42	0.00	2.67	0.00	17.62	0.75
			Palo Verde, AZ			
11	1.33	0.00	3.27	0.00	54.95	0.41
61	1.62	0.00	4.03	0.00	41.37	0.38
			Perkins, NC			
9	0.50	1.02	1.94	0.00	34.66	0.25
40	0.95	2.16	2.89	0.00	45.82	0.13
			Phipps Bend, TN			
10	0.66	0.00	1.80	0.00	39.91	1.33
46	1.08	0.00	2.79	0.00	51.10	0.42
			Shoreham, NY			
10	1.35	5.74	1.25	2.42	12.85	0.00
46	2.74	6.11	1.86	3.91	37.34	0.45

TABLE 19 (cont'd)

Height	σ_1	w_1	σ_2	w_2	k(%)	RMSE
			Sasquehanna, PA			
9	0.95	0.00	1.92	2.17	61.48	0.00
91	1.26	0.00	2.30	3.41	31.01	0.13
			Watts Bar, TN (1)			
10	2.13	0.00	0.89	0.00	31.28	0.09
40	2.48	0.00	0.94	0.00	54.25	0.24
			Watts Bar, TN (2)			
10	0.83	0.00	2.38	0.00	45.02	0.68
91	1.91	0.00	3.68	0.00	44.32	0.78
			WPPSS Satsop, WA			
10	0.00	0.00	1.70	0.00	9.50	1.04
60	0.00	0.00	2.82	0.00	3.82	0.76

TABLE 20. PARAMETERS FOR NUCLEAR POWER PLANT SITES WITH TWO ANEMOMETER LEVELS - CASES WITH POORLY IDENTIFIABLE MIXTURE COMPONENTS AT EACH LEVEL

Height	σ_1	w_1	σ_2	w_2	k(%)	RMSE
			Bellefonte, AL			
10	0.82	0.00	2.45	0.00	48.30	0.24
40	1.22	2.39	3.55	0.00	50.54	0.15
			Brown's Ferry, AL			
10	0.83	4.98	1.35	0.00	11.94	0.36
90	2.04	0.00	4.24	0.00	1.91	0.38
			Brunswick, NC			
10	0.89	0.00	2.22	2.76	17.68	0.22
107	0.00	0.00	2.78	5.03	0.00	0.56
			Cherokee, SC			
9	0.98	0.00	1.59	0.00	44.74	0.52
40	0.19	2.43	2.39	0.00	13.89	0.53
			Greene, NY			
10	1.12	0.00	2.46	0.00	14.08	0.04
60	2.26	0.00	2.01	6.13	59.22	0.24
			Oconee, SC			
10	1.08	6.15	1.74	0.00	5.31	1.25
46	0.86	2.00	3.11	0.00	51.72	0.50
			H. B. Robinson, SC			
11	0.00	0.00	1.83	0.00	2.16	0.49
61	1.38	3.28	3.46	0.00	33.10	0.18
			San Onofre, CA			
10	3.15	0.00	1.31	2.24	41.86	0.65
40	4.41	0.00	2.19	0.00	14.36	0.24
			Skagit, WA			
10	1.64	2.96	1.04	0.00	64.78	0.01
60	1.14	0.00	3.65	0.00	11.66	0.79
			Surry, VA			
10	1.65	0.00	2.79	0.00	49.42	1.14
46	3.24	0.00	1.03	2.66	49.48	0.24
			Yellow Creek, MS			
10	0.86	0.00	2.04	0.00	25.46	0.56
46	1.11	2.53	3.22	0.00	40.17	0.03
			Zion, IL			
11	1.79	7.73	2.66	0.00	9.77	0.71
76	3.35	8.65	2.75	4.95	26.53	0.02

TABLE 21. PARAMETERS FOR NUCLEAR POWER PLANT SITES WITH TWO ANEMOMETER LEVELS - CASES WITHOUT IDENTIFIABLE MIXTURE COMPONENTS AT EACH LEVEL

Height	σ_1	w_1	σ_2	w_2	k(%)	RMSE
			Blue Hills, TX			
10	0.46	4.63	1.48	0.00	13.56	0.46
50	0.36	3.04	2.43	3.31	23.27	0.36
			Koshkonong, WI			
10	0.00	0.00	3.21	0.00	0.00	0.11
60	5.41	0.00	2.11	5.05	27.26	0.43
			Perry, OH			
11	1.77	0.00	2.64	3.81	50.12	0.16
61	6.73	0.00	2.91	3.36	19.73	0.11
			River Bend, MS			
9	1.04	0.00	1.87	0.00	41.93	0.00
46	1.88	4.46	1.25	2.38	16.73	0.04
			South Texas, TX			
10	2.70	7.28	3.41	0.00	14.04	0.87
60	0.00	0.00	3.06	6.04	0.00	0.98
			Wolf Creek, KS			
10	0.30	2.96	4.06	0.00	21.98	0.39
60	0.00	0.00	3.07	6.61	0.00	0.31

TABLE 22. THE COMPUTED VALUES OF THE EXPONENT (b) FROM THE SCALING FORMULA COMPUTED FROM THE PARAMETER VALUES OF TABLES 19 AND 20 FOR IDENTIFIABLE MIXTURE COMPONENTS

	Recessive		Dominant	
	σ_1	w_1	σ_2	w_2
		(from Table 19)		
Beaver Valley	0.1768	--	0.1405	--
Ed. Hatch	0.3381	--	0.3132	0.4760
Indian Point	0.1583	--	0.2468	--
W. B. McGuire	0.3489	--	0.4245	--
North Anna	0.0200	--	- 0.1244	--
Palo Verde	0.1151	--	+ 0.1220	--
Perkins	0.4303	0.5030	0.2672	--
Phipps Bend	0.3227	--	0.2872	--
Shoreham	0.4638	0.0409	0.2604	0.3144
Sasquehanna, PA	0.1221	--	0.0781	0.1954
Watts Bar (1)	0.1094	--	0.0394	--
Watts Bar (2)	0.3774	--	0.1974	--
WPPSS Satsop	--	--	0.0282	--
		(from Table 20)		
Bellefonte, AL	--	--	0.2675	--
Brown's Ferry, AL	--	--	0.5209	--
Brunswick, NC	--	--	0.0949	0.2532
Cherokee, SC	--	--	0.2732	--
Greene, NY	0.3918	--	--	--
Oconee, SC	--	--	0.3805	--
H. B. Robinson, SC	--	--	0.3718	--
San Onofre, CA	0.2427	--	--	--
Skagit, WA	--	--	0.7007	--
Surry, VA	0.4422	--	--	--
Yellow Creek, MS	--	--	0.2991	--
Zion, IL	0.3243	0.0582	--	--
n	16	3	21	4
$\bar{b}$	0.2734	0.2007	0.2471	0.3098
σ_b	0.1392	0.2619	0.1825	0.1210

In Tables 19 and 20 the values in the columns headed σ_1, w_1 refer to the recessive component of the mixture ($k<0.5$) while σ_2, w_2 refer to the dominant component ($k>0.5$) whenever such a distinction can be made at both levels simultaneously. There are, however, several cases in which an identifiable component is recessive at one level and dominant at the other. The same situation carries over into Table 21.

As indicated at the bottom of Table 22, one may conclude that:

(1) There are too few cases in which the scaling exponent (b) for the resultant wind speed (w_1 or w_2) was available to form any real conclusions.

(2) There appears to be no significant difference between the average values of the scaling exponent (b) for the dominant and recessive mixture components as applied to the standard deviations σ_1 and σ_2. Combining the dominant and recessive cases gives a grand mean for the exponent of 0.2585 with a standard deviation of 0.1657.

Detailed Analysis

An inspection of Tables 19, 20, and 21 reveals at once that these tables are arranged in increasing order of complexity of the parameters that they contain. Table 19 contains by far the most cases for which $w_1=w_2=0$. Thus, simple wind speed structure is more readily identified at different levels.

It must be kept in mind that the data used in all of these cases is annual data. Thus, the distinction between the dominant and recessive components of the scalar wind speed p.d.f. probably reflect to a large extent an overall measure of the difference between the summer and winter wind regimes. There is virtually no distinction between the frequency of occurrence of the higher wind speed regime in the dominant or recessive categories at either the upper or lower wind observation levels. There

are several cases in which, particularly at the higher anemometer level, the two possible wind speed regimes that can be accounted for by the expirical formula effectively fuse into one. This occurs when the most probable wind speeds for the dominant and recessive regimes are close together but one has a broad and the other a narrow peak (maximum). Examples are at Bellefonte, AL, Yellow Creek, MS, Cherokee, SC, Blue Hills, TX, H. B. Robinson, SC, Koshkonong, WI, and Surry, VA, in all cases at the upper of the two levels.

DATA LISTED AT THREE OR MORE LEVELS

General Discussion

The parameter values and RMSE at the levels concerned are given in Tables 23 and 24. The first table contains the cases for which the two components of the mixture are identifiable at all three levels while the second contains the cases for which only one component of the mixture is identifiable at all three levels. On the other hand, in the second category there are several cases for which the second component of the mixture is identifiable at two adjacent levels (but not all).

In the Tables 23 and 24, the parameter values σ_1, w_1, σ_2, w_2 are not categorized as belonging to the recessive or dominant component of the mixture identified. The reason for this is the fact that in too many cases such a separation does not hold for all three levels concerned.

In Table 25 the parameter values b and w_o of the scaling formula $w/w_o=(z/z_o)^b$, z_o=10m, are shown together with their standard errors σ_b and σ_{w_o} and the standard deviation of the estimate, σ_e. The column headed "param" indicates which of the quantities σ_1, w_1, σ_2, w_2 were used.

The two cases marked by * in the last column are excluded since the value of σ_e is much too large. In those cases in which only two levels are used to identify a component of the mixture only b and w_o are shown. The values of σ_b and σ_{w_o} have no meaning and $\sigma_e \equiv 0$ since the fit is exact. The numbers in parenthesis in the column headed σ_{w_o} are the levels used to

TABLE 23. PARAMETERS FOR NUCLEAR POWER PLANT SITES WITH ANEMOMETERS AT THREE OR MORE LEVELS - CASES WITH IDENTIFIABLE MIXTURE COMPONENTS AT EACH LEVEL

Height	σ_1	w_1	σ_2	w_2	k(%)	RMSE
			Dresden, IL			
11	0.76	2.86	3.84	0.00	31.08	0.07
46	1.68	4.13	4.93	0.00	45.51	0.73
91	2.53	5.12	5.82	0.00	64.58	0.67
			Limerick, PA			
9	3.13	0.00	1.07	0.00	49.37	0.24
53	4.14	0.00	2.29	0.00	47.77	0.50
82	10.13	0.00	3.45	0.00	5.09	0.32
			Montaque, MA			
10	0.87	0.00	2.13	0.00	72.14	0.03
46	1.15	0.00	2.88	0.00	18.33	0.59
99	1.22	0.00	3.75	0.00	16.30	0.43
151	1.63	0.00	4.27	0.00	9.99	0.21
			Monticello, MN			
10	0.24	3.21	3.27	0.00	8.76	0.38
43	2.14	5.08	5.52	0.00	77.39	0.02
100	1.39	8.33	4.90	0.00	27.58	0.25
			Quad Cities, IL			
11	1.00	2.69	3.45	0.00	31.89	0.34
38	1.49	3.54	3.96	0.00	40.03	0.92
91	1.25	7.57	4.86	0.00	9.13	0.56
			WPPSS Hanford, WA			
2	3.02	0.00	1.15	0.00	45.08	0.24
10	4.03	0.00	1.79	0.00	38.59	0.21
75	5.08	0.00	2.27	0.00	54.08	0.62
			WPPS Hanford (HMS), WA			
15	1.36	0.00	3.70	0.00	41.83	0.74
61	1.31	0.00	4.57	0.00	29.48	0.53
122	1.35	0.00	5.18	0.00	30.36	0.73

TABLE 24. PARAMETERS FOR NUCLEAR POWER PLANT SITES WITH ANEMOMETERS AT THREE OR MORE LEVELS - CASES WITH ONLY ONE IDENTIFIABLE MIXTURE COMPONENT AT ALL LEVELS

Height	σ_1	w_1	σ_2	w_2	k(%)	RMSE
			Jamesport, NY			
10	3.91	0.00	0.92	2.73	87.53	0.19
61	6.61	0.00	2.68	5.41	36.30	0.58
122	2.14	4.00	3.95	7.23	16.32	0.41
			Millstone Point, CT			
10	5.74	0.00	2.95	0.00	17.24	0.38
43	0.00	0.00	4.29	0.00	0.00	0.96
114	2.55	5.77	5.75	0.00	47.16	0.36
136	3.32	5.75	5.99	0.00	62.50	0.42
			Pebble Springs, OR			
9	1.41	0.00	4.85	0.00	32.45	0.35
40	0.92	1.97	5.52	0.00	25.78	0.38
70	1.02	1.99	6.22	0.00	23.11	0.48
			Pilgrim, MA (A)			
10	2.95	5.36	1.70	2.75	24.75	0.03
49	0.62	11.11	2.60	4.41	6.69	0.05
67	4.59	9.53	3.14	5.29	8.22	0.39
			Pilgrim, MA (B)			
10	2.95	5.36	1.70	2.75	24.75	0.03
49	5.10	0.00	2.16	4.50	53.37	0.06
67	7.82	0.00	3.15	5.33	10.07	0.39

TABLE 25. THE PARAMETERS OF THE SCALING FORMULA $w/w_o=(z/z_o)^b$, z_o=10m, COMPUTED FROM THE INDICATED PARAMETERS OF THE DISTRIBUTION FUNCTION FORMULA

Location	Param.	b	w_o	σ_b	σ_{w_o}	σ_e
Dresden, IL	σ_2	0.1934	3.75	0.0166	0.10	0.0254
	σ_1	0.5736	0.71	0.0088	0.01	0.0135
	w_1	0.2727	2.77	0.0141	0.06	0.0215
Limerick, PA	σ_2	0.5008	1.10	0.0832	0.14	0.1377
	σ_1	0.4237	3.03	0.3087	1.45	0.5109*
Montaque, MA	σ_1	0.2036	0.85	0.0500	0.08	0.1035
	σ_2	0.2551	2.08	0.0250	0.10	0.0518
Monticello, MN	σ_2	0.1879	3.50	0.1374	0.76	0.2263
	σ_1	0.8440	0.31	0.5261	0.26	0.8677*
Quad Cities, IL	σ_2	0.1588	3.34	0.0342	0.17	0.0513
	σ_1	0.1201	1.06	0.1449	0.23	0.2176
	w_1	0.4717	2.35	0.1799	0.63	0.2701
WPPSS Hanford, WA	σ_2	0.1018	1.79	0.0842	0.25	0.2678
	σ_1	0.1055	3.88	0.0183	0.11	0.0469
WPPSS Hanford	σ_1	- 0.0069	1.35	0.0173	0.04	0.0261
(HMS), WA	σ_2	0.1591	3.46	0.0074	0.05	0.0112
Jamesport, NY	σ_1	0.2904	3.91	--	(10.61)	--
	σ_2	0.5843	0.92	0.0069	0.01	0.0125
	w_2	0.3871	2.72	0.0087	0.04	0.0159

TABLE 25
(continued)

Location	Param.	b	w_o	σ_b	σ_{w_o}	σ_e
Millstone Point, CT	σ_2	0.2735	2.93	0.0071	0.04	0.0147
	σ_1	1.4954	0.07	--	(114,136)	--
	w_1	- 0.0197	6.05	--	(114,136)	--
Pebble Springs, OR	σ_2	0.1142	4.87	0.271	0.1823	0.0407
	σ_1	0.1844	0.71	--	(40,70)	--
	w_1	0.0181	1.92	--	(40,70)	--
Pilgrim, MA (A)	σ_2	0.3046	1.69	0.0463	0.11	0.0668
	w_2	0.3287	2.73	0.0392	0.15	0.0566
	σ_1	0.2324	2.95	--	(10,67)	--
	w_1	0.3025	5.36	--	(10,67)	--
Pilgrim, MA (B)	σ_1	1.3662	0.58	--	(49,67)	--
	σ_2	0.2679	1.65	0.1456	0.35	0.2100
	w_2	0.3355	2.73	0.0319	0.12	0.0460

compute the tabulated values of b and w_o entered in the first two columns for these cases. All of these two-level values of b are excluded from further analysis.

The values of the exponent, b, of the scaling formula may be summarized as:

(a) From the values σ_1 and σ_2 combined, 17 cases with mean value 0.2401 and standard deviation 0.1681.

(b) From the values of w_2, 5 cases with mean value 0.3591 and standard deviation 0.0748.

Detailed Analysis

As was noted in the case of the two-level data, there are several cases in which the most probable wind speed associated with the two components of the mixture that are identified by the empirical formula used to describe the p.d.f. are nearly coincident but of different shape. One is characterized by a value of w_1 (or w_2) of zero so that the most probable speed is the value given for σ_1 (or σ_2). The other is characterized by a value of w_2 (or w_1) rather close to the value of σ_1 (or σ_2) of the former but with a value of σ_2 (or σ_1) that is much smaller than the associated w_2 (or w_1). In this case the most probable wind speed is somewhat larger than w_2 (or w_1) and is rather sharply peaked. Cases and levels that show this are Dresden, IL (11,46,91); Monticello, MN (10,43); Quad Cities, IL (11,38); Millstone Point, CT (114,136); and Pilgrim, MA (B) (49).

Two data analyses are given for Pilgrim, MA as indicated by the A and B flags (Table 24). The 10m level analysis is common to both, the 49m and 67m analyses are different. The RMSE values (in the last column) are so nearly identical at the two upper levels that there seems to be no real difference between the fit of the parameters selected to the distribution function data. The distinction between the two cases lies in the recessive component of the mixture that is selected by the least squares estimation

algorithm (σ_1, w_1 at the 49m and 67m levels). In the first case (A) at the 49m level the least squares algorithm has picked a very narrow spike that peaks near 11.2m sec^{-1} but with an occurrence (k) of only 6.69% while in the second case (B) at 49m the least squares algorithm has selected a rather broad maximum at the 5.10m sec^{-1} point which is no longer considered "recessive" since k=53.37%. This is very close to the peak (most probable speed) of the second component of the mixture which in both cases has a narrower peak near 4.5m sec^{-1}. Apparently, there are three "components" to the mixture while the empirical formula used permits the identification of only two. At the 67m level a similar situation prevails but the mixture component in both cases is definitely recessive (k=8.22 in A and 10.07 in B) and the choice being made by the least squares algorithm is between two different ways of fitting the empirical formula to the higher speed distribution function data.

NORTHWESTERN STATES DATA

GENERAL DISCUSSION

Annual data on the frequency of occurrence of wind speeds at two (or more) anemometer levels for observation locations (airports) in Wyoming, Montana, and Washington was provided by the Pacific Northwest Laboratory. Observations at these different levels were not simultaneous, but came about due to anemometer relocation. For each level the parameters of the empirical formula for the wind speed p.d.f. were determined and are tabulated in Table 26, which also contains the anemometer elevation for each case. The lower anemometer level in all cases was 7m or lower. The higher level is generally above 20m except in the cases of Cut Bank, MT, Glasgow, MT, and Rock Springs, WY. In these cases, the height change of the anemometer was considered too small to provide a reliable estimate of the exponent in the scaling formula.

Calculated values of the exponent, b, and the normalized parameter value (w_0 which may be the normalized value of σ or w_R) are indicated in Table 27 together with an indication for the parameter concerned. In the later case the subscript 1 indicates the minor component of the mixture ($k<0.5$) while the subscript 2 indicates the major component ($k>0.5$) (where this distinction is valid). The cases in which the change in anemometer height is considered to be too small to give reliable estimates of the scaling exponent, b, are marked by the letter (a). The values of w_0 are all normalized to a reference height z_0=10m (i.e., the scaling formula used is $w=w_0(z/z_0)^b$, where w may stand for either the parameter σ or w_R. There are then 7 cases for which scaling exponents for σ were computed with reasonable input data. The mean exponent value was found to be $\bar{b}$=0.2348 with standard deviation estimated at σ_b=0.1524.

DETAILED ANALYSIS

It is only in the cases of Casper, WY, Great Falls, MT, Great Falls (AFB), MT that the model used is exactly the same at the two anemometer levels and hence that thoroughly self-consistent scaling can be accomplished. In view of the small anemometer separations at Cut Bank, MT, Glasgow, MT, and Rock Springs, WY, it would appear that the differences in the parameter models

TABLE 26. PARAMETERS FOR LOCATIONS IN THE NORTHWESTERN STATES WITH DATA AT TWO DIFFERENT ANEMOMETER LEVELS (NOT SIMULTANEOUSLY)

Height (m)	σ_1	w_1	σ_2	w_2	k	RMSE (%)
			Casper, WY			
6	0.00	0.00	4.56	0.00	0.00	1.40
24	0.00	0.00	4.91	0.00	2.45	0.53
			Cut Bank, MT			
6	3.43	6.94	3.00	0.00	47.83	0.60
13	1.75	0.00	5.87	0.00	26.46	0.84
			Glasgow AFB, MT			
4	4.00	0.00	2.47	0.00	68.68	0.60
28	3.70	8.18	3.68	0.00	15.88	1.05
			Glasgow, MT			
6	5.43	0.00	1.00	0.00	31.48	1.39
9	2.67	7.86	3.10	0.00	23.20	0.54
16	1.84	0.00	3.91	0.00	32.68	1.22
			Hawre, MT			
6	1.96	8.76	3.39	0.00	11.83	0.71
20	1.73	0.00	2.74	3.36	26.51	1.50
			Great Falls, MT			
7	0.00	0.00	4.23	0.00	0.00	1.76
23	0.00	0.00	5.23	0.00	3.48	1.95
			Great Falls AFB, MT			
5	1.38	0.00	4.02	0.00	30.23	0.75
33	2.45	0.00	5.51	0.00	28.90	0.97
			Rock Springs, WY			
6	0.00	0.00	4.14	0.00	5.28	1.83
15	2.53	0.00	5.49	0.00	26.97	0.75
			Seatac, WA (A)			
6	3.49	0.00	1.20	3.09	56.18	0.34
33	0.00	0.00	3.00	3.92	5.33	1.33
			Seatac, WA (B)			
6	0.00	0.00	2.14	2.91	0.00	1.78
33	0.00	0.00	3.00	3.92	5.33	1.33

TABLE 27. SCALING PARAMETER, b, AND NORMALIZED PARAMETER, w_o, (σ or w_R) FOR LOCATIONS IN THE NORTHWESTERN STATES

Location	Param.	b	w_o
Casper, WY	σ_2 (b)	0.0533	4.69
Cut Bank, MT	σ_2	0.8681 (a)	4.67
Glasgow AFB, MT	σ_2	0.2049	2.98
Glasgow, MT	σ_2	1.3240 (a)	2.45
Great Falls, MT	σ_2	0.1784	4.51
Great Falls AFB, MT	σ_1	0.3042	1.70
Great Falls AFB, MT	σ_2	0.1671	4.51
Rock Springs, WY	σ_2	0.3080 (a)	4.85
Seatac, WA (A)	σ_2	0.5375	1.58
Seatac, WA (A)	w_2	0.1396	3.32
Seatac, WA (B)	σ_2	0.1982	2.73
Seatac, WA (B)	w_2	0.1748	3.18

(a) Too small height change in anemometer locations.

(b) Subscript 1 indicates a parameter for the minor component of the mixture, 2 for the major component.

are due more to the sampling variation between the different time periods rather than the difference in anemometer height. This effect (sample variation) is without doubt present at locations with larger anemometer separations. In most of the remaining cases one component of the mixture seems to be identifiable at both of the levels concerned but the other component of the mixture seems to be representing different wind speed regimes at the different levels. An example of the different wind speed regimes that may occur is given by Glasgow AFB, MT. In this case the dominant regime at the 4m level is σ= 4.00, w_R = 0.00, (68.68%) while at 28m level σ= 3.68, w_R = 0.00 (84.21%). The recessive regime at 4m is a low speed one σ = 2.47, w_R = 0.00 (31.32%) while at 28m it is a high speed one, σ=3.70, w_R = 8.18 (15.88%). As tabulated in Table 26 the recessive regime at 4m is associated with the dominant regime at 28m due to the increase of σ with anemometer height. This need not be the best association of speed regimes. If the dominant regimes at the two levels are associated as above, then the decrease of σ with height may well be due to the difference between fitting the recessive regime at the low or high speed. A further point in this connection is that very likely the low speed regime is probably present at 28m and that the high speed regime is present at 4m. The model used is confined to identification of only two wind speed regimes. The σ for the dominant regime at 4m may be influenced by an undetected high speed regime and that at 28m by an undetected low speed regime.

If one uses parameter values for other relative minima of the least squares procedure and RMSE's that are unacceptably large, the Glasgow AFB, MT, lines in Table 26 may be replaced by:

4	0.00	0.00	3.61	0.00	4.53%	0.84
28	0.00	0.00	4.27	0.00	2.65%	2.03

This corresponds to a regime of "calms" less than 5% of the time (at both levels and decreasing with height) and a dominant regime (more than 95%) corresponding to a Rayleigh p.d.f. with parameter σ that increases with height as it should. The same things can be said of Cut Bank, MT and Rock Springs, WY.

SURFACE LOCATIONS

This chapter is devoted to the consideration of the effect of site exposure on the parameters of the empirical probability density functions being used and to the diurnal variations of these parameters.

It is understood that the terms such as site, location, exposure, etc. are used to refer to the relation between the anemometer and the surrounding terrain on the scale of up to several kilometers. They are not used in connection with such items as the height of the anemometer above the ground, the effect of neighboring buildings and general airport building arrangement. The data used in the following has been taken from standard wind summaries that cover a span of several years record. In all cases the anemometer has been relocated several times during this period. The summarized wind speed record then represents a mixture of records from different detailed locations, particularly with regard to elevation above the ground. Some of these details are recorded in the text but only to the extent that they may verify some degree of homogeneity in the detailed local instrument exposure. Examples were found in which this was not the case. To discuss these details as they affect the p.d.f. for scalar wind speed requires going to the original records and re-doing the summaries in terms of these exposure details (as was done in the cases discussed in the previous chapter). Such detail is beyond the scope of this report. It is felt that the larger scale effects of surrounding terrain have an effect on the parametric description of the p.d.f. for scalar wind speed that is more important than the effects of detailed instrument exposure and consequently records that include several locations and elevations of the wind instruments may be reasonably valid if used with care.

EFFECT OF THE SITE ON THE PARAMETERS

In order to obtain some information on the effect of the wind measurement site on the parameters that enter the empirical formula being used to describe the p.d.f. for scalar wind speed these parameters were computed

for several groups of observation points located near each other but at which the effects of the surrounding terrain were expected to be different. The station groups used were:

(1) Boston (Logan International Airport), Bedford (L. G. Hanscomb Field), and South Weymouth (NAS), MA

(2) Washington (National Airport), Andrews AFB, Dulles International Airport, D.C., Ft. Mead, MD, Quantico and Ft. Belvoir, VA

(3) Bridgeport and New Haven, CT

(4) Tucson, AZ (Municipal Airport and Davis-Monthan AFB).

Each of these is discussed separately in the following. The parameters for the scalar wind speed p.d.f. were calculated for the months of January, April, July and October, and for the entire year. The frequency function data were extracted from Reed (1975).

The parameters shown in each of the tables are indicated in the column headings as:

σ_1, σ_2 wind component standard deviation

w_1, w_2 mean resultant wind speed

k the fraction due to the part of the mixture indicated by the parameters σ_1, w_1

$\bar{p}$ the approximate average wind power as determined from the computed parameters (see Appendix E for the method of computation)

For the most part, the tables are arranged so that k<50% and hence the component of the mixture with parameters σ_1, w_1 may be called the "minor component" (and that with parameters σ_2, w_2 the "major component") of the mixture. This arrangement is not always strictly possible or is at least inconvenient to follow consistently. The two mixture components usually

differ in that one will have a distinctly larger most probable wind speed. It occasionally happens that for one month this is the minor component of the mixture while for the other months it is the major component of the mixture. When this happens the columns headed σ_1, w_1 (and σ_2, w_2) label the mixture component with the higher (or lower) most probable speed and the value of k for that month will assume a value greater than 50%.

Boston Area

The parameters for the empirical formula for the p.d.f. of scalar wind speed at Boston, MA, (Logan International Airport), Bedford, MA, (L. G. Hanscomb Field), and South Weymouth, MA (Naval Air Station) together with an approximation to the average wind power (watts/m^2) for the midseason months and the entire year are given in Table 28.

Logan International Airport is located about 32 km north northeast of the center of old Boston and is surrounded by Boston Harbor except to the north northwest. The field elevation is about 4.9m. The period of record for Logan International Airport is from 1951 through 1960. During the first 11 months the anemometer was at a height of 18.9m but was moved on November 22, 1951 to a height of 10.1m where it remained for the rest of the period. The total number of observations is 87,672.

L. G. Hanscomb Field is approximately 19 km west northwest of Logan International Airport at an elevation of 38.1m and is surrounded by hills to 91.5m (or more). The airport is in the valley of the Concord River (3 km northwest) and swamp areas lie in all directions. The period of record listed by Reed (1975) is from 1951-1970 (20 years). During this period the anemometer height steadily decreased as follows: 3/53-6/54 at 21.3m, 6/54-11/56 at 18.3m, 11/56-4/62 at 11.3m, 4/62-date at 4.0m. The total number of observations is 58,658.

The South Weymouth Naval Air Station lies 13 km south of Boston Harbor (21 km south southeast of Logan Airport) at an elevation of 46.3m. It is surrounded by swampy areas in all directions with occasional hilltops to 61m.

TABLE 28. PARAMETERS OF THE EMPIRICAL DISTRIBUTION FUNCTION FOR LOCATIONS IN THE BOSTON AREA SHOWING SEASONAL AND ANNUAL VALUES

Month	σ_1	w_1	σ_2	w_2	k(%)	$\bar{P}$ (watts/m^2)
			Boston International Airport, MA			
Jan	4.94	5.27	2.09	7.00	73.91	469.7
April	6.03	0.00	2.11	6.78	59.24	411.7
July	4.47	0.00	1.87	5.63	44.52	183.2
Oct	4.03	4.44	0.56	6.36	74.63	263.8
Annual	5.81	0.00	2.06	6.07	53.37	339.0
			L. G. Hanscomb Field, Bedford, MA			
Jan	0.00	0.00	3.63	0.00	22.93	84.9
April	0.00	0.00	3.54	0.00	17.13	84.7
July	0.00	0.00	2.69	0.00	27.20	32.6
Oct	0.00	0.00	3.17	0.00	28.98	52.1
Annual	0.00	0.00	3.25	0.00	25.18	59.2
			South Weymouth, MA (NAS)			
Jan	0.00	0.00	3.71	0.00	8.54	107.7
April	0.00	0.00	3.83	0.00	3.48	124.9
July	0.00	0.00	2.57	0.00	1.07	38.7
Oct	0.00	0.00	3.03	0.00	11.87	56.5
Annual	0.00	0.00	3.26	0.00	7.48	73.8

The period of record listed by Reed (1975) is 1954-1972 (19 yrs.) (nearly coincident with that at Bedford). During the years 1954-1960 the anemometer height was at 13.7m and 1960-date at 3.7m. The total number of observations is 142,467.

Inspection of the table indicates that while South Weymouth NAS shows somewhat more available wind power than Hanscomb Field, both have only about 25% of that available at Logan Airport. This is not due to the difference in anemometer height since it is much too great to be accounted for by scaling. Further the wind p.d.f. parameters at Logan are of a distinctly different character than those at Hanscomb Field and South Weymouth NAS.

The annual and monthly wind speed p.d.f. parameters at Bedford and South Weymouth are all of the same type; a simple Rayleigh p.d.f. with a spike at zero speed. The numerical values for σ_2 at these two points are very nearly the same. The largest difference lies in the fraction of cases that are assigned to the "calm" category. At Bedford, about 25% of occurrences are so assigned while at South Weymouth generally less than 10%.

The p.d.f. for scalar wind speed at Logan Airport is described as a mixture of p.d.f.'s with somewhat different characteristics. The first "component" of this mixture (parameter σ_1, w_1) is characterized by a rather broad peak (values of σ_1 in the range 4.03 to 6.03). The second "component" is characterized by a much narrower peak (σ_2 in the range 0.56 to 2.11). Table 29 gives the most probable speed for each component of the mixture (w_1* and w_2*) and the "width" of the peak there (the half width of the parabola that fits the maximum measured at half the height of the maximum, L_1, L_2) (see Appendix F for a discussion of these quantities.)

TABLE 29. THE LOCATION OF THE MAXIMUM (w_1^* and w_2^*) AND THE "WIDTH" OF THE PEAK THERE FOR LOGAN AIRPORT

Month	w_1^*	w_2^*	L_1	L_2
Jan	6.71	7.29	5.04	2.17
April	6.03	7.08	4.26	2.19
July	4.47	5.92	3.16	1.95
Oct	5.59	6.38	4.15	0.56
Annual	5.81	6.39	4.11	2.15

Though the two most probable values, w_1^* and w_2^*, are not far apart the half-width of the second component of the mixture, L_2, is about half that of the first component, L_1. It is also to be noted that the proportions in which the mixture occurs are between 45% and 75% so that in all cases each mixture component is well represented. (The column headed k% is the fraction in percent of the mixture that consists of the first component.) The implication of this is that the shape of the overall p.d.f. (for the mixture as a whole) is somewhat more sharply peaked and has more extensive "tails" than would be expected from a simple generalized Rayleigh p.d.f.

At least a part of the difference in apparent wind power at Logan International Airport and Bedford and South Weymouth may well be due to the fact that the anemometer height at Logan was generally at 10.1m while at the other two locations was at various heights but mostly at 4.0m and 3.7m respectively.

At Logan International Airport the wind observations were made hourly throughout 24 hours per day. This is not the case at Bedford and South Weymouth. At Bedford it appears that there were 8 observations/day while at South Weymouth the number turns out to be 20.54. On the basis of the rather odd frequency of observations at South Weymouth one is inclined to assume 24 observations per day during most of the period with an abbreviated schedule for the remainder (as 24 observations/day for 78% and 8 observations/

day for 22%, for example). The record then fairly well represents samples taken reasonably uniformly throughout the day. It is impossible to infer anything from the 8 observations/day at Bedford. If these were made at three hourly intervals, the day would be uniformly covered and the three records would be comparable in this respect. If the 8 observations/day were during daylight hours the lower night wind speeds would be missed and hence the low available wind power at Bedford would be an over-estimate.

It is reasonably evident that the reason for the large wind power differences in the Boston area are due to the differences in anemometer location with respect to the surrounding terrain. Boston Airport is an "exposed" location, with no hills in the immediate area and generally open to the sea. Bedford and South Weymouth are "sheltered" locations, in swampy areas which are completely surrounded by hills. The effect of the hills to decrease valley winds is apparently effective over short distances since South Weymouth is only a few kilometers from the coast.

Washington D.C., Locations

Six locations in the Washington, D.C. area were selected to get information on how the site influenced the parameters of the empirical formula for the p.d.f. of the scalar wind speed. These were: (1) National Airport, (2) Andrews AFB, (3) Dulles International Airport, (4) Quantico, VA, (5) Ft. Belvoir, VA, and (6) Ft. Mead, MD. The parameters and the average available power are shown in Table 30.

The National Airport is located on the west bank of the Potomac River near the center of the city at an elevation of about 4.6m. The river is immediately adjacent to it on the north, east, and south. Hills rise to an elevation of about 76m or more in all directions. The period of record is 10 years (1951-1960) during which the anemometer was occasionally relocated as follows: 9/28/50-12/30/57 at 35.1m, 12/30/57-9/30/59 at 6.1m, 9/30/59-9/20/60 at 35.1m, 9/30/60-date at 6.1m.

TABLE 30. PARAMETERS OF THE EMPIRICAL DISTRIBUTION FUNCTION FOR LOCATIONS IN THE WASHINGTON, D.C. AREA SHOWING SEASONAL AND ANNUAL VALUES

Month	σ_1	w_1	σ_2	w_2	k(%)	$\bar{P}$
			Washington National Airport, DC			
Jan	1.03	0.00	3.40	3.09	8.47	144.9
April	1.65	6.51	3.62	0.00	17.08	127.9
July	1.03	5.06	2.78	0.00	18.18	40.5
Oct	1.38	0.00	2.52	3.43	13.54	81.5
Annual	0.15	0.00	3.13	2.28	1.98	97.7
			Andrews AFB, DC			
Jan	1.12	0.00	3.83	0.00	19.07	105.3
April	0.70	10.65	3.26	0.00	5.59	75.3
July	0.00	0.00	1.95	2.28	12.14	31.7
Oct	0.29	0.00	2.89	0.00	10.49	49.8
Annual	0.94	0.00	3.20	0.00	12.73	66.1
			Dulles International Airport, DC			
Jan	5.15	0.00	2.50	0.00	22.31	98.1
April	6.53	0.00	3.12	0.00	6.98	109.8
July	0.31	0.00	2.49	0.00	8.35	32.6
Oct	1.50	0.00	3.01	0.00	45.67	37.7
Annual	3.92	0.00	2.27	0.00	31.28	61.9
			Quantico, VA			
Jan	3.04	0.00	1.28	0.00	70.33	46.9
April	3.75	0.00	2.45	0.00	23.41	62.9
July	2.38	2.78	1.55	1.73	19.58	26.6
Oct	2.36	3.23	1.42	1.78	26.44	31.6
Annual	3.40	0.00	2.04	0.00	31.74	42.08
			Ft. Belvoir, VA			
Jan	3.18	0.00	0.89	0.00	46.78	35.5
April	2.91	0.00	0.91	0.00	61.82	35.7
July	2.12	0.00	0.83	0.00	45.96	10.8
Oct	2.59	0.00	0.89	0.00	37.37	16.0
Annual	2.83	0.00	0.92	0.00	45.23	24.6
			Ft. Mead, MD			
Jan	0.92	0.00	3.28	0.00	43.30	46.9
April	0.86	0.00	3.14	0.00	27.49	52.1
July	0.32	0.00	2.03	0.00	35.28	12.5
Oct	0.88	0.00	2.63	0.00	55.94	19.3
Annual	0.91	0.00	2.87	0.00	44.55	31.0

Andrews AFB is located near Suitland, MD at an elevation of about 79 m. This is the highest ground in the immediate vicinity although there are hilltops to over 91m, the nearest being 10 km to the northwest. The period of record is 1944-1972 (28 yrs.). The anemometer was relocated several times: 3/44-4/55 at 15.2m, 4/55-9/56 at 18.3m, 9/56-11/61 at 20.7m, 11/61-date at 4.0m.

Dulles International Airport is located west of the city in rolling country at about 91m. Surrounding hilltops reach to over 122m. The airport itself is on the highest ground in the immediate area. The anemometer height is 6.1m. The period record is 1963-1971 (8 years).

Quantico Airport (Marine Corps Air Station) is located south southwest of Washington on the west bank of the Potomac River at the mouth of Chapawamsic Creek which enters the Potomac from the west. The creek valley is broad and swampy with much open water immediately west of the field. There are hills to somewhat over 61m to the northwest and southwest. The field elevation is at about 3m. The record covers the years 1946-1972 (26 years). Before 1958 the anemometer was located 18.3m above ground level and since at 4.3m.

Ft. Belvoir, VA, Davison Airfield, lies between Washington and Quantico 1.6 km west of the head of Gunston Cove (Accotink Bay) with Accotink Creek on the northwest, northeast and southeast sides. The field elevation is about 21.3m. Hills a 0.8 km northwest rise to 43m with more distant hilltops to near 76m. The record is from the years 1958-1970 (12 years). Though the anemometer was moved frequently, the height changes have not been extreme: 2/57-3/59 at 8.5m, 3/59-3/60 at 8.8m, 3/60-3/62 at 6.1m, 3/62-3/68 at 4.6m, 3/68-1/71 at 6.4m.

Ft. Mead, MD, Tipton Airfield, is northwest of Washington at an elevation of 46m. The Little Patuxent River is immediately to the west and south of the field at 30m with large extents of swamp. The Patuxent River itself is 4.8 km southwest with more swamp. The highground rises to 91m in all directions. The period of record is 1960-1970 (10 years). Prior to 9/15/60 the anemometer height was 11.3m and since at 4.0m.

There are significantly higher wind speeds at the high elevation airports (Andrews and Dulles) with Washington in this category due to the unusually high anemometer location for so much of the data period.

The tables are arranged so that generally the parameters (σ_1, w_1) for the minor component of the mixture ($k<50\%$) are listed in the first two columns while those for the major component (σ_2, w_2) follow. Exceptions appear in the cases of Quantico, Ft. Belvoir, and Ft. Mead; these being cases in which the parameters of the mixture component with the higher (lower) most probable speed are listed first.

The outstanding feature of this comparison of mixture parameters is the fact that the fraction of cases (k) attributed to the "minor" component at the airports that are at relatively low level with respect to the surrounding terrain exhibit distinctly larger values of the parameter k (fraction of cases due to the minor component of the mixture); Quantico, Ft. Belvoir and Ft. Mead. At the higher elevation airports (Dulles and Andrews AFB) the minor component of the mixture is usually quite small (usually less than 15%). At Quantico and Ft. Belvoir the minor mixture component has the larger most probable speed and hence the mixture component with the smaller most probable speed tends to occur the larger fraction of the time. The opposite is true at Ft. Mead. (There is an exception of one month in each of these three cases.)

Bridgeport, CT, and New Haven, CT

The parameters for the empirical formulas for the p.d.f. for scalar wind speed at Bridgeport, CT, and New Haven, CT, together with an approximate average power (watts m^{-2}) for the midseason months and the entire year are given in Table 31.

These two airports are on the north shore of Long Island Sound and are about 21 km apart. The anemometer at Bridgeport is at a height of 10.0m while that at New Haven is at 6.1m. The average wind power for each month and for the year at Bridgeport is about twice that at New Haven. The power

TABLE 31. PARAMETERS OF THE EMPIRICAL DISTRIBUTION FUNCTION FOR BRIDGEPORT, CT, AND NEW HAVEN, CT, SHOWING SEASONAL AND ANNUAL VALUES

Month	σ_1	w_1	σ_2	w_2	k(%)	$\bar{P}$ (watts/m^2)
			Bridgeport, CT			
Jan	0.00	0.00	4.70	0.00	2.10	234.1
April	0.40	5.14	4.56	0.00	3.47	213.8
July	1.96	3.68	3.73	0.00	64.40	89.2
Oct	1.21	4.69	4.42	0.00	13.79	182.8
Annual	0.00	4.16	4.26	0.00	3.34	173.6
			New Haven, CT			
Jan	0.46	10.46	3.54	0.00	1.69	112.4
April	0.51	10.68	2.02	4.16	2.81	112.3
July	0.41	0.00	1.36	3.58	4.81	44.8
October	0.60	10.77	2.03	3.54	1.52	81.7
Year	0.55	10.66	2.01	3.58	2.80	90.2

difference may in part be due to the difference in anemometer height but a comparison of the parameter values of the Table 31 indicates that it is probably only a partial explanation of the difference in average power. There are also rather important differences in the terrain around these airports.

At Bridgeport, CT, the airport is southwest of the mouth of the Housatonic River at an elevation of about 3.0m above sea level. There is the river and marsh to the north and northeast while the Long Island Sound lies to the east, through south to northwest with marsh to the west. The surrounding terrain is rather flat for 3 km to 5 km to the northwest. Beyond this distance the terrain becomes hilly (tops to near 61m).

At New Haven the airport is on the east side of New Haven Harbor at an elevation of about 3m. There are hills with tops to 61m or more in all directions except to southeast through south to southwest. These hills are at about 6 km (across New Haven Harbor) to the west but at less than 1.6 km to north through northeast to east.

Had anemometer height differences been a major factor in the average wind power difference, one would expect very similar parameters for the empirical formula with differences due largely to scaling. Inspection of the table indicates quite different wind regimes. At Bridgeport the major wind regime is as though it was independent of direction (resultant wind speed w_1=0 for all months) while at New Haven the major wind regime is characterized by a sizable resultant wind speed (about 4 m/sec) and a ratio w_1/σ_1 of about 2. The minor wind regimes at these locations are also distinctly different though amounting to only a few percent.

At Bridgeport the minor wind regime usually consists of a narrow peak about a resultant wind speed near that of the major wind regime so that in effect overall the wind speed p.d.f. is somewhat more peaked than a generalized Rayleigh p.d.f. (Note 1: January and Annual minor wind regimes are degenerate; January assigns 2.1% to calms [spike at zero speed] while Annual assigns 3.34% to a spike at 4.16 m/sec..) (Note 2: In July the major wind regime at Bridgeport corresponds almost exactly to that at New Haven.)

At New Haven, the minor wind regime is quite different, being a narrow peak at somewhat over 10 m/sec but accounting for only 1% to 2% of the cases. July is again an exception in that the minor regime (4.81%) peaks at 0.41 m/sec.

It would seem reasonable that the proximity of the hilly terrain at New Haven accounts for these differences in the p.d.f. of wind speed.

An adequate discussion of the difference in wind regimes at two locations like Bridgeport and New Haven is not possible on the basis of scalar wind speed data alone. Both locations are subject to sea/land breeze influences in addition to the effects of terrain on the prevailing winds. Consideration of the details of the bivariate vector wind component p.d.f. is required to take these items into account.

The minor component of the mixture displayed at Bridgeport for the annual wind speed frequencies is exceptional in that $\sigma_1=0$ while $w_1\neq 0$. The treatment of the case $\sigma_1=w_1=0$, $k>0$, as a degenerate "spike" at zero speed has been used throughout. In this case there is a "small" spike (k=3.34%) at $w_1=4.16$ m/sec.

The data for New Haven and Bridgeport were taken from Reed (1975). The period covered by the record is tabulated there as 1949-1968 and 1951-1970 respectively. Thus, there are 20 years of record at each location which are also nearly coincident. On the other hand, the total number of observations are listed as 50,769 for Bridgeport and 27,204 for New Haven. The 10 years of record 1951-1960 tabulated in the series Dicennial Census of United States Climate, Summary of Hourly Observations contain 87,672 observations. On this basis the number of observations per day at New Haven averages somewhat less than 4 (3.73) while at Bridgeport it averages somewhat less than 7 (6.95). The effect of the selection of the observation time can significantly affect the apparent power available from the wind. If one assumes observations for air traffic purposes, the implication is that the observation hours are predominantly in the daytime when the wind speeds are

generally larger than at night. One might also infer that at Bridgeport (7 observations/day) covers early morning and late evening hours and hence a larger proportion of low wind speed cases than at New Haven, (4 observations/day). This is at odds with the fact that the apparent wind power available at Bridgeport is nearly twice that at New Haven. One might expect that if wind had been observed hourly at both locations, the difference in wind power available would be even larger.

Tuscon, AZ (Municipal Airport vs. Davis-Monthan AFB)
(A Digression on Class Interval Values)

The Municipal Airport lies to the south of the city about 3 km east of the Santa Cruz River (usually dry). The terrain is rather flat and slopes gradually upward toward the southeast. Ground elevation at the airport is about 793m. The nearest "peak" is Sahwarita Butte about 3 km west southwest which rises to 869m (about 76m above ground level). The city is built up to the north edge of the airport.

Davis-Monthan AFB is on the southeast edge of the city with built-up areas on the north and west. Its elevation is also about 793m. It is about 10 km northeast of the Municipal Airport. The general terrain at the two locations is nearly the same.

Although these locations are close to each other in almost identical terrain, the available wind power at the Municipal Airport is half again larger than that at Davis-Monthan AFB.

The data used is that contained in Reed (1975) which lists the period of record at the AFB as 1942-1970 (28 years). For the Municipal Airport, Reed indicates broken record periods. However, the Summary of Hourly Observations (U.S.W.B.) indicates the period 1956-1960 (5 years), and the values listed check those of Reed. Thus, the 5 years of record at the Municipal Airport is about the middle of the 28 year period of record at the AFB.

Station history sheets indicate that the anemometer at the Municipal Airport was located 10.0m above the ground from October 14, 1948 to October 15, 1958 and at 7.0m from October 15, 1958 to the present (1963). At Davis-Monthan AFB the anemometer height prior to March 1949 is not listed but more recently the record indicates 3/49 to 4/14/54 at 20.1m, 4/14/54 to 5/4/55 at 10.7m, 5/4/55 to 10/17/55 at 7.6m, 10/17/55 to 5/2/56 at 12.2m, 5/2/56 to 2/79 at 4.0m (but at several locations with respect to the runway configuration). During the 29-year period of record, the AFB anemometer was above 7.6m for at least 7 years and perhaps as long as 14 years.

The interesting feature of the wind power available at these two sites lies in the fact that the apparent wind power available at the Municipal Airport is half again as large as that available at Davis-Monthan AFB. Though the anemometer height at the two locations are not strictly comparable, one would expect that the period of 7 (to possibly 14) years of greater anemometer height at the AFB would at least partially compensate for the final period at 4.0m (vs. 7.0m at Municipal). The fact that the AFB is adjacent to the built-up city on the north and west does not seem to account for the lower wind speeds since the prevailing wind direction is from the southeast where the terrain at both locations is essentially open desert sloping downward very gradually to the northwest. (Prevailing down-slope winds; over 50% of occurrences are from east to south.)

In Reed (1975) there are several cases of duplicate data tables for a single location. Tucson, AZ (Municipal Airport) is an example. The only difference between the two tables is that in one the class interval for wind speed is in knots while in the other the class interval is given in miles per hour. In carrying out the calculations for the parameters appearing in the empirical p.d.f. the wind speed at the upper edge of each class interval was used as the speed associated with the D. F. concerned, i.e., Pr ($w<w_i$) for the probability that the wind speed, w, is less than the i'th class interval division point, w_i. The class intervals are listed in ranges such as (knots) 1-3, 4-6, 7-10,--- or (mph) 0-3, 4-7, 8-12,---. In the first case the division points are taken as 3.5, 6.5, 10.5,--- (knots)

while in the other they are 3.5, 7.5, 12.5,--- (mph). Since output is to be in meters per second, these class interval division points are converted to m/sec. The division points in m/sec for these two cases are:

knots	1.80	3.35	5.41	8.49	11.07	14.16	17.25	---
mph	1.56	3.35	5.59	8.27	10.95	14.08	17.21	---
difference	+0.24	0.00	-0.18	+0.22	+0.12	+0.08	+0.04	---

It is readily seen that the difference between the values is always less than a quarter of a m/sec. The question is than whether these discrepancies in the class interval division points has a significant effect on the parameter estimate computed.

The least squares estimates of the parameters concerned are given in Table 32. This table differs from the others appearing in this section in that two sets of parameters are listed for the Municipal Airport, one for class intervals in knots and the other for class intervals in mph (each being so labled). Also a column for the root mean square error (RSME) is included. Values of RMSE are in percent.

The three parts of this table agree in that all indicate a mixture of scalar wind speed p.d.f.'s. The nature of the p.d.f.'s entering into the mixture as computed from Municipal Airport (mph) and the AFB (knots) class intervals agree that the mixture consists of two ordinary Rayliegh p.d.f.'s ($w_1=w_2=0$ throughout). These are tabulated so that σ_1 corresponds to the one with the lower most probable speed, σ_2 to the higher.

In the case of the parameters calculated using the Municipal Airport (knot) class intervals the minimization procedure leads to a mixture of p.d.f.'s one of which is a generalized Rayleigh p.d.f. throughout while the other is an ordinary Rayleigh (except for January when it is also a generalized Rayleigh). Further, the Municipal Airport (knots) part of the table has been rearranged so that the columns headed σ_2, w_2 correspond to a most probable speed that closely matches that in the same columns for

TABLE 32. PARAMETERS OF THE EMPIRICAL DISTRIBUTION FUNCTION FOR TUCSON, AZ, SHOWING SEASONAL AND ANNUAL VALUES

Month	σ_1	w_1	σ_2	w_2	k	RMSE	$\bar{P}$
			Tucson Municipal Airport, AZ (knots)				
Jan	2.47	6.77	1.63	2.20	14.77	0.03	66.3
Apr	3.83	0.00	1.24	2.48	59.02	0.04	84.8
July	3.61	0.00	1.26	2.39	55.59	0.08	68.9
Oct	4.20	0.00	1.47	2.30	35.43	0.10	75.1
Annual	3.82	0.00	1.37	2.28	44.38	0.06	68.2
			Tucson Municipal Airport, AZ (m.p.h.)				
Jan	1.84	0.00	3.55	0.00	46.16	0.70	62.1
Apr	1.88	0.00	3.57	0.00	25.26	0.14	82.2
July	1.74	0.00	3.33	0.00	24.17	0.14	67.4
Oct	2.00	0.00	3.71	0.00	47.90	0.52	70.1
Annual	1.73	0.00	3.37	0.00	30.94	0.26	64.6
			Davis-Monthan AFB, AZ (knots)				
Jan	1.25	0.00	2.86	0.00	38.23	0.57	35.0
Apr	1.49	0.00	3.14	0.00	34.26	0.71	49.5
July	1.09	0.00	2.80	0.00	20.46	0.49	40.8
Oct	1.29	0.00	2.69	0.00	31.85	0.36	32.1
Annual	1.22	0.00	2.70	0.00	28.73	0.36	33.5

Municipal Airport (mph) and AFB (knots). This leaves columns σ_1, w_1 under Municipal Airport (knots) as representing a mixture component having a higher most probable speed. This rearrangement of columns is reflected in the values of the parameter k that appear in the two Municipal Airport sections. Except for January, where the "knots" section picks an unusually high most probable speed (and which appears as a very minor component of the mixture), the values of k agree roughly as to whether the high or low speed mixture component is predominant (large k in the "knots" section favors the high speed mixture component while small k in the "m.p.h." section also favors the predominance of the high speed mixture component).

Nothing in the above has indicated any good reason why there is the large difference in available wind power at these two locations. To further refine the analysis would require a detailed analysis of the exposure of the anemometer with respect to the immediately surrounding structures. Such effects can be significantly large. A refined analysis of instrument exposure requires much more information than is contained in existing wind summaries and is consequently considered beyond the current effort.

Conclusions

One might summarize the preceding discussion by pointing out that:

(1) Wind measurements sites below the general level of the higher terrain tend to have a wind speed p.d.f. that can be adequately represented by a mixture of two simple Rayleigh p.d.f. and that the fraction of occurrences of the lower wind speed regime tends to be quite large.

(2) There is a strong tendency for the wind speed p.d.f. at reasonably sheltered sites to be adequately represented by a combination of ordinary Rayleigh p.d.f.'s one of which has become degenerate at zero speed (spike p.d.f. at w=0 for "calms").

(3) Well exposed sites (either at or near the level of the highest surrounding terrain or due to the immediate proximity for a large water body) tend to have a scalar wind speed p.d.f. that involves at least one mixture component that is a generalized Rayleigh p.d.f.

(4) Rather small changes in input information significantly affect not only parameter values, but also the character of the parametric description of the mixture.

DIURNAL VARIATION OF PARAMETERS FOR SURFACE WINDS

The diurnal variation of the parameters of the empirical formula for the p.d.f. for scalar wind speed is illustrated by examples from Washington, D.C., Montgomery, AL, Mobile, AL, and Great Falls, MT. The data were extracted from the Climatography of the United States No. 30-X (the symbol X refers to the appropriate state index number), Summary of Hourly Observations (Station Name), Table E. Data for each month and hour of the day are given, but only the months of January and July and the hours 00, 03, ---, 18, 21 are included here. All data summarized in this publication are from the years 1950-1955.

In the tables of the parameter values, the mixture component parameters with the lower most probable speed appear in the columns headed σ_1 and w_1 (m/sec) while those for the higher most probable speed are headed σ_2 and w_2 (m/sec). The parameter k is given in percent and refers to the proportion of the mixture due to the component with parameters σ_1, w_1. The final column headed $\bar{P}$ is the nominal wind power available (watts/m^2) computed from the parameter values shown. (See Appendix E for the determination of $\bar{P}$ from the parameters $\sigma_1, w_1, \sigma_2, w_2, k$.) The "hour" refers to local standard time.

Washington D.C. (National Airport)

During this period the anemometer was located at an elevation of 35.1m above the ground. During January the predominant component of the mixture is that with the higher most probable wind speed (k<33% and usually k<12%) except for 09 hrs. (Table 33). The most probable speed (m.p.s.) for this component undergoes a diurnal variation given by (see Appendix F).

Hour	00	03	06	09	12	15	18	21
m.p.s. (m/sec)	3.71	3.74	3.92	3.99	6.34	5.63	4.23	3.74

which accounts for most of the diurnal variation. During the hours 15, 18, 21, 00 a small fraction of the mixture is assigned to "calm" ($\sigma_1=w_1=0$) and at 03 hours σ_1 is so small that this is also essentially the case for this hour. At 09 and 12 hours a sizable fraction of the mixture is associated with a low speed mixture component with an appreciable (non-zero) m.p.s. At 09 hours the situation is exceptional in that the analysis method has picked up a rather infrequent narrow "spike" at 10.95 m/sec.

The situation in July is somewhat different. During most of the hours the dominant fraction of the mixture is that with the smaller m.p.s. which shows a strong diurnal variation in parameters. The diurnal variation of σ_2 and w_2 is much smaller.

With the exception of 09 hours, the January low speed mixture component is an ordinary Rayleigh p.d.f. or the degenerate case thereof ($\sigma_1=w_1=0$) while the high speed component is either an ordinary Rayleigh p.d.f. or a generalized Rayleigh p.d.f. In July the low speed mixture component is an ordinary Rayleigh (at 18 hours it is degenerate) while the high speed mixture component is a generalized Rayleigh p.d.f. at all hours.

Montgomery, AL

Anemometer at 8.5m throughout this period. During both January and July (Table 34) the low speed mixture component had an ordinary Rayleigh p.d.f. (or degenerate version thereof) while the high speed mixture component

TABLE 33. PARAMETERS OF THE EMPIRICAL DISTRIBUTION FUNCTION FOR WASHINGTON, D.C. (NATIONAL AIRPORT) SHOWING DIURNAL VARIATION

Hour	σ_1	w_1	σ_2	w_2	k	RMSE (%)	$\bar{P}$
				January			
00	0.00	0.00	3.71	0.00	11.31	1.32	104.3
03	0.76	0.00	3.74	0.00	10.85	0.79	107.5
06	1.19	0.00	3.92	0.00	20.36	0.70	111.3
09	0.53	10.95	2.62	3.31	9.74	1.80	88.6
12	3.64	0.00	2.88	5.74	32.88	1.21	208.2
15	0.00	0.00	2.77	5.02	1.89	1.31	188.7
18	0.00	0.00	2.93	3.43	2.95	0.89	118.8
21	0.00	0.00	3.74	0.00	4.55	0.82	115.0
				July			
00	1.56	0.00	1.00	4.91	68.32	0.00	33.3
03	1.55	0.00	1.17	4.29	69.43	0.00	25.8
06	0.41	0.00	1.72	2.68	16.52	0.04	30.2
09	3.66	0.00	0.41	3.43	55.95	0.82	74.8
12	3.81	0.00	1.12	4.47	73.49	0.07	112.3
15	3.95	0.00	1.66	4.29	29.45	0.17	99.8
18	0.00	0.00	1.27	4.46	2.43	0.10	72.8
21	2.93	0.00	1.11	2.77	52.85	0.02	41.4

TABLE 34. PARAMETERS OF THE EMPIRICAL DISTRIBUTION FUNCTION FOR MONTGOMERY, AL, SHOWING DIURNAL VARIATION

Hour	σ_1	w_1	σ_2	w_2	k (%)	RMSE (%)	$\bar{P}$
				January			
00	0.00	0.00	2.06	2.77	25.46	0.22	37.6
03	1.14	0.00	3.22	0.00	46.08	0.08	43.0
06	0.00	0.00	2.85	0.00	29.23	0.66	37.7
09	0.00	0.00	2.23	3.85	7.40	0.48	84.9
12	1.58	0.00	2.52	4.95	14.06	0.38	144.7
15	2.50	0.00	1.65	6.06	45.68	1.18	115.6
18	1.31	0.00	3.57	0.00	42.56	0.62	62.4
21	0.72	0.00	2.01	3.47	27.27	0.00	49.5
				July			
00	0.97	0.00	2.14	0.00	69.94	0.01	8.3
03	0.94	0.00	2.20	0.00	74.82	0.01	7.6
06	1.23	0.00	0.68	3.20	68.30	0.00	10.6
09	1.69	0.00	0.68	4.88	65.76	0.00	33.8
12	0.00	0.00	1.81	3.01	0.00	0.60	46.5
15	0.00	0.00	2.37	2.63	0.67	0.68	60.7
18	1.10	0.00	1.46	2.96	43.76	0.01	20.7
21	0.93	0.00	2.01	0.00	51.91	0.00	10.0

had either ordinary or generalized Rayleigh p.d.f. In the month of January there was a strong tendency for the high speed mixture component to be dominant while in July the reverse was generally the case (exceptions at 12 and 15 hours).

In both January and July the low speed mixture component had a most probable speed that was quite small. These are shown explicitly in the table (since where w_1=0, the value of σ_1 is itself the m.p.s.). However, when both ordinary and generalized Rayleigh p.d.f.'s are present the most probable speed tendency from hour to hour is not so easily visualized. These are listed here on the lines headed w_2* for both January and July:

Hour	00	03	06	09	12	15	18	21
				January				
w_2*	3.29	3.22	2.85	4.35	5.48	6.27	3.57	3.93
				July				
w_2*	2.14	2.20	3.27	4.93	3.47	3.30	3.26	2.01

The diurnal trend is evident and the fact that generally the most probable speed for this component of the mixture is larger in January than in July. Also in July the m.p.s. is a maximum at 09 hours while in January it is a maximum at 15 hours.

The major difference between the two months lies in the fact that in January the dominant component tends to be that with the larger m.p.s. while in July it is the one with the lower m.p.s., exceptions being at 12 and 15 hours.

Mobile, AL

Anemometer height at 17.0m except for the first 9 months during which it was at 9.1m. The Mobile, AL, (Table 35) wind speed data differs radically from the two preceding examples in that at nearly all hours it requires a pair of generalized Rayleigh p.d.f. to represent it adequately. In fact the only exception are at 00, 03 and 21 in July. It also is different in that

TABLE 35. PARAMETERS OF THE EMPIRICAL DISTRIBUTION FUNCTION FOR MOBILE, AL, SHOWING DIURNAL VARIATION

Hour	σ_1	w_1	σ_2	w_2	k (%)	RMSE (%)	$\bar{P}$
				January			
00	0.38	3.44	2.26	5.20	48.31	0.24	96.9
03	0.93	3.42	1.98	7.03	67.89	0.00	115.5
06	1.65	3.89	0.52	10.47	94.60	0.17	65.0
09	1.70	4.95	0.66	10.04	89.01	0.03	110.6
12	2.81	4.96	0.62	8.50	79.47	0.57	168.3
15	1.84	4.69	2.58	7.35	63.45	0.18	210.0
18	0.40	3.48	2.14	6.14	64.27	0.19	96.8
21	0.39	3.52	2.06	4.99	46.16	0.35	101.0
				July			
00	2.21	0.00	0.18	2.96	47.74	0.02	20.3
03	2.11	0.00	1.05	2.59	25.69	0.01	21.5
06	1.23	2.67	1.31	3.92	77.02	0.01	30.2
09	1.09	3.20	1.64	5.61	72.56	0.01	63.7
12	0.99	3.44	1.62	5.55	48.85	0.01	91.4
15	1.47	3.65	0.75	7.77	74.24	0.00	46.9
18	1.22	3.21	0.72	8.02	97.40	0.00	33.6
21	2.32	0.00	0.36	3.02	54.17	0.05	23.8

in both January and July there is a very strong tendency for the mixture component with lower m.p.s. to be dominant. The diurnal variation of the m.p.s. is evident from the data tables since it is given by σ_1 or σ_2 when $w_1=0$ or $w_2=0$ respectively and is a few tenths of a m.p.s. larger than w_1 or w_2 depending on the size of σ_1 or σ_2 respectively.

Another feature is the fact that the sharper the maximum the more this case is avoided regardless of whether it is the high or low speed mixture component.

Great Falls, MT

The diurnal variation of parameters for Great Falls, MT (Table 36) is a mixture of the variations exhibited by the preceding examples. The outstanding feature of the January situation is that the low speed mixture component (σ_1, w_1) is an ordinary Rayleigh p.d.f. while the high speed mixture component (σ_2, w_2) is a generalized Rayleigh p.d.f. The diurnal variation of σ_1 is not well defined, nor is that for the parameter w_2, but σ_2 has a well defined diurnal variation. The parameter k is always less than 35% so that the low speed mixture component is a minor contributor to the overall p.d.f., but again it does not show a well defined diurnal variation.

In July both the high and low speed mixture component switch between an ordinary and generalized Rayleigh p.d.f.'s. The low speed mixture component appears as a generalized Rayleigh p.d.f. except for one hour (03 hours). This may be a property of the data reduction method since when $w_1<\sigma_1$ the procedure sets $w_1=0$ and accepts this form if the mean square error is not significantly increased (it usually is not). In the case of the high speed mixture component the shift from the generalized Rayleigh to ordinary Rayleigh p.d.f. during daylight hours is also accompanied by the diurnal increase in σ_2. As with the January case, the low speed mixture component occurs the smaller fraction of the time (k<50%) except for 03 and 09 hours. The diurnal variation of k is not significant.

TABLE 36. PARAMETERS OF THE EMPIRICAL DISTRIBUTION FUNCTION FOR GREAT FALLS, MT, SHOWING DIURNAL VARIATION

Hour	σ_1	w_1	σ_2	w_2	k (%)	RMSE (%)	$\bar{P}$
				January			
00	1.69	0.00	4.38	6.74	11.68	0.72	517.8
03	2.51	0.00	2.70	9.52	33.39	0.31	494.2
06	2.68	0.00	2.87	9.51	33.56	0.28	511.7
09	1.00	0.00	4.93	6.04	5.31	0.48	582.1
12	2.14	0.00	5.09	8.35	25.08	1.79	764.5
15	2.63	0.00	4.18	7.80	31.00	0.49	492.6
18	2.09	0.00	3.80	7.22	16.94	1.37	451.3
21	2.46	0.00	2.64	9.38	37.46	0.33	443.9
				July			
00	0.32	2.96	2.63	4.41	30.58	0.53	111.1
03	3.20	0.00	1.91	5.77	67.43	1.41	108.6
06	1.07	2.65	4.21	0.00	44.33	0.44	108.7
09	1.82	2.19	5.59	0.00	58.34	0.69	185.2
12	1.23	2.83	5.17	0.00	37.52	0.83	208.7
15	1.15	3.56	5.66	0.00	41.17	0.31	262.5
18	1.94	3.29	2.73	7.15	44.89	0.00	246.2
21	0.99	2.67	2.43	5.58	49.14	0.00	112.2

The parameter tables tend to mask what is really going on since the parameter selection procedure introduces zeros that appear to interrupt the trend of the information. A better picture of the situation is presented by a tabulation of the most probable wind speed for each mixture components, w_1^* and w_2^*, and a measure of the sharpness (breadth) of the peak (maximum) there, L_1 and L_2, (the half width at half height of the parabola that fits the maximum). These are shown in Table 37.

It will be noted that neither w_1^* nor L_1 show any significant diurnal variation. The breadth of the low speed mixture component maximum (L_1) for January and July appear to be about the same. The most probable speed, w_1^*, is significantly larger in July than in January (the opposite of what would seem reasonable).

The situation with regard to w_2^* and L_2 for the higher speed mixture component is somewhat different. L_2 for January is somewhat larger than for July and both show a definite diurnal variation with a minimum near 03 hours and a maximum near 12 hours. The most probable speed, w_2^*, for July also exhibits a diurnal variation but with a minimum at about 06 hours and a maximum at about 18 hours. The diurnal variation of w_2^* for January is very small and masked by its variation from point to point.

TABLE 37. MOST PROBABLE WIND SPEED AND WIDTH OF THE PEAK AT GREAT FALLS, MT

Hour	00	03	06	09	12	15	18	21
				January				
w_1*	1.69	2.51	2.68	1.00	2.14	2.63	2.09	2.46
L_1	1.20	1.78	1.90	0.71	1.51	1.86	1.48	1.74
w_2*	7.81	9.88	9.92	7.34	9.52	8.71	8.04	9.93
L_2	4.17	2.65	2.81	4.56	4.86	4.05	3.64	2.59
				July				
w_1*	2.98	3.20	2.84	2.68	3.06	3.73	3.73	2.84
L_1	0.32	2.26	1.03	1.68	1.19	1.12	1.85	0.96
w_2*	5.01	6.06	4.21	5.59	5.17	5.66	7.62	6.04
L_2	2.51	1.86	2.98	3.95	3.65	4.00	2.65	2.35

CONCLUSIONS

GENERAL OBSERVATIONS

It is evident from elementary considerations that the probability density function for the scalar wind speed at low speeds must have a series expansion that starts with the first power of the speed and the series expansion contains only terms of odd powers of the speed. The Weibull probability density function fails to meet this criterion and consequently is not a physically acceptable probability density function for the scalar wind speed. Further, inspection of scalar wind speed frequency function data turns up a number of cases in which the probability density function is definitely bimodal which clearly indicates that to be generally adequate an empirical probability density function must be expressed as a mixture of at least two probability density functions with different parameters. The generalized Rayleigh probability density function was selected for this purpose since it is the exact function resulting from the bivariate circularly normal probability density of the vector wind. Further, a wide variety of bivariate wind vector probability densities reduce to a single generalized Rayleigh distribution.

The parameters of the generalized Rayleigh distribution have definite physical significance in terms of the bivariate density function of the vector wind; the parameter σ is the magnitude of the standard deviation of a component of the vector wind while the parameter w_R is the magnitude of the mean resultant vector wind. On the other hand, since so many mixtures of bivariate vector wind distributions lead to a single parameter pair σ, w_R it is not possible to infer from these parameter values what the parent bivariate distribution would be.

The mixture of two generalized Rayleigh distributions is specified by five parameters which we write as the pentad $(\sigma_1, w_1, \sigma_2, w_2, k)$ where the subscripts indicate which of the two mixture components is concerned. The R is dropped from the mean resultant wind speed symbol to avoid writing

subscripts on subscripts. The first component of the mixture, parameters σ_1, w_1, is usually the low speed component (the smaller most probable wind speed) while the second component parameters σ_2, w_2, is usually the high speed component (the larger most probable wind speed). In any case the mixing fraction, k, $0<k<1$ always indicates the fraction of the mixture with parameters σ_1, w_1. Five parameters appears to be the minimum required to handle the cases of a bimodal probability density for the scalar wind speed (which occur with sufficient frequency that they cannot be ignored).

In general, it may be said that the more varied the situations that contribute to the data collected into the scalar wind speed frequency function table the simpler the parameter collection (pentad) of the mixture that can be used to describe it. Thus, yearly data (a mixture of months and hours of the day within months) may usually be described with the simplest collection of parameters. The monthly data tends to require a more complex collection of parameters. Hourly data within months seems to require a still more complicated ensemble of parameters.

The mixture parameters (σ_1, w_1, σ_2, w_2, k) were fitted to the frequency function data by the method of least squares using the probability distribution function rather than the probability density function. It is typical of the method when several parameters are involved that there is not only a combination that gives a least sum of squares of the errors but that there are other combinations that give relative (or local) minima. It frequently happens that such a relative minimum may have a sum of squares of the errors that for all practical purposes is just as satisfying as the absolute minimum. When such is the case an arbitrary selection was made, usually picking the parameter pentad with the larger number of zeros. Also the selection was influenced by the parameter pentad at adjacent tower levels or for adjacent months or hours of the day.

VARIATION OF PARAMETERS WITH ALTITUDE

The variation of the mixture parameters with altitude was determined from data collected at various levels on meteorological towers at various locations. To adequately discuss parameter variation with altitude it is necessary that the parameter description of the scalar wind speed be the same (or nearly the same) from level to level. This is generally not the case. For example, the higher speed component of the mixture tends to be an ordinary Rayleigh distribution at lower levels and shifts to a generalized Rayleigh distribution as the altitude increases. The exception to the rule is the tower data from the White Sands Missile Range, NM, which for all months of the year could be described as the particularly simple combination of a degenerate and an ordinary Rayleigh distribution, $(0,0,\sigma_2,0,k)$, $k>0$.

For the tower data in general, it may be said that over those altitudes which permit a common parameter mix, the parameters $\sigma_1,w_1,\sigma_2,w_2$ may be approximated by a simple power law $w=w_o(z/z_o)^b$.

The values of the exponent, b, in the power law has been computed in previous sections under a wide variety of conditions. In Table 38 the values of this exponent from annual wind speed frequency function data have been summarized. The first column contains the location and the table number concerned. The column heading indicates the parameter in the empirical formula for the p.d.f. which is being scaled. The data blocks are arranged so that the first item is the number of cases, the second item is the average value of the exponent, $\bar{b}$, for these cases, and the last item is the standard deviation, σ_b, for this group of cases. The row labeled "Combined" contains the result of combining all of the values on the rows above into one batch with the resulting total cases, grand mean, and standard deviation about the new mean. On the last row the data on the exponent, b, are further combined so that the data pertaining to σ_1 and σ_2 form one batch and that pertaining to w_1 and w_2 another as indicated by new inserted column headings. It is obvious that in an overall sense the values $\bar{b}\approx 0.25$

TABLE 38. SUMMARY OF ANNUAL VALUES OF THE SCALING EXPONENT, b.

Location	σ_1	w_1	σ_2	w_2
Hanford, WA (HMS) (Table 5)			1 0.1590 --	
Cape Kennedy (Table 12)			2 0.3505 0.3033	1 0.2370 --
Patrick (Table 15)			2 0.3185 0.1294	2 0.2315 0.0049
NPPS (2 levels) (Table 22)	16 0.2734 0.1392	3 0.2007 0.2619	21 0.2471 0.1825	4 0.3098 0.1210
NPPS (3+ levels) (Table 25)	9 0.2363 0.1751	5 0.2091 0.2056	12 0.2585 0.1482	3 0.3504 0.0319
N.W. States (Table 27)	1 0.3042 --		6 0.2232 0.1636	2 0.1572 0.0249
Combined	26 0.2617 0.1514	8 0.2060 0.1924	44 0.2529 0.1773	12 0.2754 0.0991
	σ_1 and σ_2		w_1 and w_2	
Further Combined	70 0.2562 0.1680 For σ		20 0.2476 0.1479 For w_R	

and $\sigma_b \approx 0.15$ are reasonably representative. (Note: In this table, and also the ones that follow, there are a few cases in which isolated odd values of b from the previous tables have been omitted.

The values of the scaling exponent, b, determined from monthly data are summarized in Table 39. The format is the same as that of Table 38. It is to be noted that in these cases the combined mean value, $\bar{b}$, is somewhat smaller than that obtained from annual data and its standard deviation is also somewhat smaller. This is due at least in part to the fact that data from the large number of nuclear power plant sites was available only in annual summary form and thence does not appear here. The values of $\bar{b}$ and σ_b would be even smaller, σ_b especially, if the Cape Kennedy data (only one year of record) had been excluded. In the previous discussions of the monthly data it was pointed out that a distinct annual variation of the exponent, b, was present. In this table such annual variation has been eliminated, but is reflected as an increase in σ_b.

The values of the scaling exponent, b, from hourly data are summarized in Table 40 in the same format as used in Tables 38 and 39. The results are nearly the same as for the monthly data, a reduction of the value of $\bar{b}$ for the parameter σ_2 and especially of σ_b as compared with the annual data.

VARIATION OF PARAMETERS WITH EXPOSURE

At sites below the general level of the higher terrain the p.d.f. for scalar wind speed tends to be that of a mixture of ordinary Rayleigh p.d.f.'s with a large fraction of occurrences in the lower speed mixture component. This lower speed mixture component has a tendency to become degenerate at zero speed (spike p.d.f. at w=0 for "calms").

At sites near the level of the highest surrounding terrain or in the immediate proximity of a large body of water the p.d.f. for scalar wind speed tends to have one mixture component that is a generalized Rayleigh p.d.f.; usually the mixture component representing the higher wind speeds.

TABLE 39. SUMMARY OF MONTHLY VALUES OF THE SCALING EXPONENT, b.

Location	σ_2	w_2
WSMR	12	
(Table 3)	0.2141	
	0.0391	
Hanford, WA (HMS)	12	
(Table 5)	0.1455	
	0.0292	
Cape Kennedy	12	12
(Table 12)	0.2650	0.2610
	0.1656	0.1391
Patrick	4	4
(Table 15)	0.1783	0.2210
	0.0398	0.0743
	40	16
Combined	0.2052	0.2510
	0.1065	0.1272

TABLE 40. SUMMARY OF HOURLY VALUES OF THE SCALING EXPONENT, b.

	Jan		July	
Location	σ_2	w_2	σ_2	w_2
HMS	8		8	5
(Tables 7 & 9)	0.1676		0.1633	0.2546
	0.0326		0.1323	0.1631
Patrick	8	8	7	8
(Table 18)	0.2193	0.2823	0.1506	0.1991
	0.0947	0.0689	0.0639	0.0958
	16	8	15	13
Combined	0.1935	0.2823	0.1574	0.2204
	0.0638	0.0689	0.1062	0.1290

The observations above are based primarily on data from the Boston, MA, and Washington, DC, areas. There are some exceptions (or modification of definitions) that should be noted. Logan Airport (Boston) is virtually at sea level, almost surrounded by Boston harbor, and well away from hills. It must be considered as an "exposed" location. This "sea" effect does not extend far inland. South Yarmouth NAS is only a few kilometers from the sea, but is indeed a "sheltered" location. One would normally consider Washington National Airport "sheltered" but the data summarized includes mostly years during which the anemometer was located about 35.1m above the ground so that the distribution function is that for an "exposed" location.

ANNUAL AND DIURNAL VARIATION

The annual variation of parameters and the type of distribution appearing in the mixture components may be summarized by stating that the low speed component is more frequent in the summer and tends to be an ordinary Rayleigh distribution while in the winter the high speed component tends to be most frequent and to be a generalized Rayleigh distribution. A notable feature of the monthly distribution functions is that the generalized Rayleigh distribution appears more frequently than in the annual data.

The diurnal variation of the parameters and the distribution types that appear in the mixture are similar to those that appear in the annual variation but in a more extreme way (early morning corresponding to summer and late afternoon to winter).

REFERENCES

Abramowitz, M., and I. A. Stegun, 1964: Handbook of Mathematical Functions with Formulas, Graphs, and Mathematical Tables, National Bureau of Standards, Applied Mathematics Series No. 55, Sup. Doc., U.S.G.P.O., Washington, D.C., 20402, June 1964, 1046 p.

Alexanderson, Hans, 1979: A Statistical Analysis of Wind, Wind Profiles and Gust Ratios at Granby, Uppsala, Meteorologiska Institutionen vid Kunegl. Universitatat, Uppsala, 1979, Reports No. 55, 39+21 p.

Anon., 1976: Monthly Wind Summary, Patrick Tower 313 (Computer Print-out, Loaned by Jack W. Reed, Div. 4533, Sandia Laboratories, Albuquerque, N.M., 87185)

Anon., 1971: Cape Kennedy Wind Tower Statistics, 18m and 15m Towers, National Weather Records Center, Ashville, N.C., Job. No. 06913 (W-1280), July 26, 1971

Beardsley, W. E., 1980: Note on the Use of the Inverse Gaussian Distribution for Wind Energy Applications, J. Appl. Meteor., Vol. 19, pp. 1126-1130

Boehm, A. R., 1976: Transnormalized Regression Probability, AWS-TR-75-259, Air Weather Service (MAC), U.S. Air Force, (pp. 18 and 19, 7 Fits to Pittsburgh Surface Wind Speed Data)

Brooks, C.E.P., et al, 1950: Upper Winds Over the World, Geophysical Memoirs, No. 85, Meteorological Office, Air Ministry, London, 57 p. also Q. J. Roy. Meteor, Soc., Vol. 195, pp. 55-73

Buell, C. E., 1976: Comments on "Estimation of Long-Term Concentrations using a 'Univerisal' Wind Speed Distribution," J. Appl. Meteor., Vol. 15, pp. 515-516

Cliff, W. C., 1977: The Effect of Generalized Wind Characteristics on Annual Power Estimates from Wind Turbine Generators. PNL-2436, Pacific Northwest Laboratory, Richland, Washington.

Crawford, J. C., and H. R. Hudson, 1970: Behavior of Winds in the Lowest 1500 Feet in Central Oklahoma, June 1966-May 1967, ESSA Tech. Memo., ERL, TM-MSSL 48, 57 p.

Davies, M., 1958: Non-circular normal wind distributions, Q. J. Roy, Meteor. Soc., Vol. 84, No. 361, pp. 277-279.

Dinkelacker, O., 1948: Die Verteilungsfunktion der Windgeschwindigkeit für die Hockrkön, Wetter und Klima, Vol. 1, Nos. 9/10, p. 257-270.

Dinkelacker, O., 1949: Über spezielle Windverteilungsfunktionen, Wetter und Klima, Vol. 2, Nos. 5/6, pp. 129-138

Doran, J. C. and M. G. Verholek, 1978: A Note on Vertical Extrapolation Formulas for Weibull Velocity Distribution Parameters. J. Appl. Meteor., Vol. 17, pp. 410-442

Essenwanger, O., 1959: Probleme der Windstatistik, Meteorologische Rundschau, Vol. 12, No. 2, pp. 37-47

Gloyne, R. W., 1959: Note on a tabulated function for use with two-dimensional wind distributions, Meteorological Magazine, Vol. 88, pp. 170-171

Gomes, L., and B. J. Vickery, 1974: On the Prediction of Extreme Wind Speeds from the Parent Distribution, Sidney University, Sidney, Australia

Guterman, I. G., 1961: On the Statistical Law of Wind Velocity Distribution, Meteorologiya y Gidrologize, No. 9, pp. 13-24 (In: Studies of Temperature Distribution, Wind Velocity, and Weather Forecasting, U.S.S.R., January 9, 1962, Office of Technical Services, U.S. Dept. of Commerce, Washington, D.C. JPRS:11845, pp. 14-27)

Hansen, Frank V., and V. D. Neil, 1964: Monthly Wind and Temperature Distributions in the First 62 Meters of the Atmosphere for White Sands Missile Range, New Mexico, Environmental Science Department, U.S. Army Electronics Research and Development Activity, White Sands Missile Range, N.M., ERDA-113, February 1964, 33 p.

Hennessey, Joseph P., 1977: Some Aspects of Wind Power Statistics, J. Appl. Meteor., Vol. 16, pp. 119-128

Hesselberg, Th., and E. Björkdal, 1929: Über das Verteilungsgesetz der Windunruhe, Beitrag zur Physik der Frien Atmosphare, Vol. 15, pp. 121-133

Jahnke, E., F. Emde, and F. Lösch, 1960: Tables of Higher Functions, McGraw-Hill Book Co., Inc., New York, N.Y., 1960

Justus, C. G., W. R. Hargraves, and Ali Yalcin, 1976: Nationwide Assessment of Potential Output from Wind-Powered Generators, J. Appl. Meteor., Vol. 15, No. 7, pp. 673-678

Justus, C. G., W. R. Hargraves, Amir Mikhail, and Denise Graber, 1978: Methods for Estimating Wind Speed Frequency Distributions. J. Appl. Meteor., Vol. 17, pp. 350-353

Justus, C. G., 1978: Winds and Wind System Performance, The Franklin Institute Press, Philadelphia, PA, 120 p.

Knighting, E., 1954: Upper Winds over the World, Q. Jour. Roy. Meteor. Soc., Vol. 80, No. 344, p. 239-240

Luna, R. E., and H. W. Church, 1974: Estimation of long-term concentrations using a "universal" wind speed distribution, J. Appl. Meteor., Vol. 13, pp. 910-916

Miller, K. S., 1964: Multidimensional Gaussian Distributions, John Wiley & sons, N.Y., 129 p.

Nash, J. C., 1979: Compact Numerical Methods for Computers: Linear Algebra and Function Minimization, Halsted Press, John Wiley and Sons, New York, 1979, ix+227 p.

Peterson, E. W., and J. P. Hennessey, Jr., 1978: On the Use of Power Laws for Estimates of Wind Power Potential. J. Appl. Meteor., Vol. 17, pp. 390-394

Reed, Jack W., 1975: Wind Power Climatology of the United States, Sandia Corporation, Albuquerque, N.M., SAND74-0348, June 1975, 163 p.

Reed, Jack W., 1978: Wind Speed Distribution Changes with Height at Selected Weather Stations, Sandia Corporation, Albuquerque, NM, SAND76-0714, August 1978

Reed, Jack W., 1979: Wind Power Climatology of the United States, Supplement. Sandia Corporation, Albuquerque, NM, SAND78-1620, April 1979

Reynolds, George W., 1976: Threshold Values in Wind Speed Measurements, Third Symposium on Atmospheric Turbulence, Diffusion, and Air Quality, Oct. 19-22, 1976, Raliegh, N.C., American Meteorological Society, 45 Beacon St., Boston, MA 02108, 596 p. (pp. 130-133)

Smith, O. E., 1976: Vector Wind and Vector Wind Shear Models 0 to 27 km Altitude for Cape Kennedy, Florida, and Vandenberg AFB, California, NASA TM X-73319, George C. Marshall Space Flight Center, Marshall Space Flight Center, Alabama 35812, 95 p.

Stewart, D. A., and O. M. Essenwanger, 1978: Frequency Distribution of Wind Speed Near the Surface. J. Appl. Meteor., Vol. 17, pp. 1633-1642

Stone, W. A., D. E. Jenne, and J. M. Thorp, 1972: Climatography of the Hanford Area. BNWL-1605, Pacific Northwest Laboratory, Richland, Washington.

Takle, E. S., and J. M. Brown, 1977: Note on the Use of Weibull Statistics to Characterize Wind Speed Data. J. Appl. Meteor., Vol. 17, pp. 556-559

U. S. Weather Bureau, 1963: Summary of Hourly Observations (Various Locations), 1951-1960, Supt. of Documents, U. S. Govt. Print. Off., Washington, D.C.

Van der Auwera, L., F. de Meyer, and L. M. Malet, 1980: The Use of the Weibull Three-parameter Model for Estimating Mean Wind Power Densities. J. Appl. Meteor., Vol. 19, pp. 819-825

Verholek, M. Gary, 1977: Summary of Wind Data from Nuclear Power Plant Sites, BNWL-2220, WIND-4. Pacific Northwest Laboratory, Richland, Washington.

Wagner, A., 1929: Theorie der Böegkeit and der Häufigkeitsverteilung von Windstärke and Windrichtung, Gerl. Beitr. Geophys., Vol. 24, pp. 386-436

Wanner, E., 1939: Über die Frequenz der Windstärke auf dem Sante's 1932-39, Annalen der Schweitz Meteorologische Sentralanet, Vol. 76, No. 7, pp. 1-3 (Uses a Poisson distribution)

Wax, N., 1954: Noise and Stochastic Processes, Dover Publications, Inc., New York 19, New York, 1954, 337 p. (A source for Rice, S.O., 1945 Mathematical Analysis of Random Noise, Bell System Technical Journal, Vols. 23 and 24)

Weil, H., 1954: The Distribution of Radial Error, Ann. Math. Statist., Vol. 25, pp. 168-170

White, R. G., 1975: Distribution and Moments of Radial Error, NASA TM X-64962, George C. Marshall Space Flight Center, Marshall Space Flight Center, Alabama 35812, 52 p.

Widger, W. K., 1976: Estimating Wind Power Feasibility. Power Eng., Vol. 80, pp. 58-61

Widger, W. K., 1977: Estimation of Wind Speed Frequency Distributions Using only the Monthly Average and Fastest Data. J. Appl. Meteor., Vol. 16, pp. 244-247

APPENDIX A

THE SERIES REPRESENTATION FOR THE PROBABILITY DENSITY FUNCTION FOR WIND SPEED FROM A GENERAL BIVARIATE VECTOR WIND

THE SERIES REPRESENTATION FOR THE PROBABILITY DENSITY FUNCTION FOR WIND SPEED FROM A GENERAL BIVARIATE VECTOR WIND

Consider a general bivariate vector wind with orthogonal components u, v and let $p_2(u,v)$ be the corresponding probability density function (p.d.f.). The fraction of cases falling in a rectangle of sides du, dv will then be given by $p_2(u,v)dudv$. To obtain wind speed, this expression is transformed so that speed and direction are used instead of orthogonal components; $u=w\cos\theta$, $v=w\sin\theta$ and the fraction of the cases then becomes $p_2(w\cos\theta,w\sin\theta)wdwd\theta$. To obtain the fraction of cases in the interval w, w+dw one integrates over wind direction so that the probability density function for speed regardless of direction, p(w), is given by

$$p(w)dw = wdw \int_0^{2\pi} p_2(w\cos\theta,\ w\sin\theta)d\theta$$

or

$$p(w) = w \int_0^{2\pi} p_2(w\cos\theta,\ w\sin\theta)d\theta \qquad (1)$$

Returning to the orthogonal wind components form of the bivariate p.d.f., $p_2(u,v)$, and assuming that this has a power series expansion about the zero vector, u=0, v=0,

$$p_2(u,v) = p_{2o}+(\partial p_2/\partial u)_o u+(\partial p_2/\partial v)_o v$$
$$+\left[(\partial^2 p_2/\partial u^2)_o u^2+2(\partial^2 p_2/\partial u\,\partial v)_o uv+(\partial^2 p_2/\partial v^2)_o v^2\right]/2!+\cdots \qquad (2)$$

where (u,v) on the right side of (2) are considered small quantities and the coefficients are evaluated at (0,0). Then substituting $u=w\cos\theta$, $v=w\sin\theta$ into (2) one obtains

$$p_2(w\cos\theta,\ w\sin\theta) = p_{2o}+w\left[(\partial p_2/\partial u)_o\cos\theta+(\partial p_2/\partial v)_o\sin\theta\right]+$$
$$w^2\left[(\partial^2 p_2/\partial u^2)_o\cos^2\theta+2(\partial^2 p_2/\partial u\,\partial v)_o\sin\theta\cos\theta+(\partial^2 p_2/\partial v^2)_o\sin^2\theta\right]/2!+\cdots$$

Integrating this expression over the range of θ reduces it to

$$\int_0^{2\pi} p_2(w\cos\theta, w\sin\theta)d\theta = 2\pi p_{2o}+(1/2)\left[(\partial^2 p_2/\partial u^2)_o+(\partial^2 p_2/\partial v^2)_o\right](w^2/2!)+---$$

and (1) then becomes

$$p(w) = (2\pi p_{2o})w + (1/2)\left[(\partial^2 p_2/\partial u^2)_o + (\partial^2 p_2/\partial v^2)_o\right](w^3/2!)+--- \quad (3)$$

It may be shown that on integration over θ all of the odd power terms of (2) vanish. Thus, (except for some very unlikely cases) the power series expansion of the p.d.f. for wind speed about the point w=0 starts with a term in w to the first power and thereafter contains only odd power terms in w.

(The unlikely cases involve the behavior of the function $p_2(u,v)$ at the origin, u=v=0. In particular those cases in which $p_2(u,v)$ has an infinite singularity ($p_2(u,v)\to\infty$ when $u^2+v^2 \to 0$) or in which $p_2(u,v)$ (and some of its partial derivatives) are zero at the origin. The determination of the existence of such cases involves the interpretation of the calm and lowest wind speed frequency. Reynolds (1976) clearly shows that when reasonably sensitive anemometers are used, the frequency of "calms" virtually vanishes and that the phenomena is essentially an aspect of the fact that standard instruments for measuring wind speed are not capable of measuring speeds below a reasonably large threshold value.

The first paragraph of Appendix B indicates the method of constructing the bivariate p.d.f. for the vector wind from the tabulated frequency function by speed and direction class intervals. When "calms" are included in the lowest speed intervals, it is a matter of experience that no instances have been found that would give the slightest hint that the p.d.f. had an infinite singularity at u=v=0. In fact the only hint of exceptional behavior of the bivariate p.d.f. of the vector wind near u=v=0 that we have noted is at Gatwick Airport (London, England) where the p.d.f. has a distinct minimum slightly offset from (0,0).)

Application. Tabulated data on the frequency of occurrence of wind in speed ranges is usually in terms of the frequency function $f(w_i, w_{i+1})$, the number or fraction (or %) of cases of wind in the range $w_i < w < w_{i+1}$, $i=0,1,2,---$, where w_0 may or may not be zero. The frequency function and the p.d.f. are related by

$$f(w_i, w_{i+1}) = \int_{w_i}^{w_{i+1}} p(w)dw \qquad (4)$$

To obtain a value of the p.d.f., one uses the first mean value theorem to obtain

$$f(w_i, w_{i+1})/(w_{i+1}-w_i) = p(\xi), \; w_i < \xi < w_{i+1} \qquad (5)$$

in which it is to be noted that the location of the point ξ (a wind speed) is only very loosely specified as somewhere in the interval (w_i, w_{i+1}) (and in fact there may be more than one such location as is shown in Figure 28). One may then construct a bar-chart for the p.d.f. for wind speed from the frequency function data using (5) to adjust for varying widths of the interval (w_i, w_{i+1}) without specifying the point (or points) ξ at which the value of the p.d.f. is actually realized. Note: In forming $p(\xi)$ from (5) for the first interval (w_0, w_1) one should use $w_0=0$ and include the number (or fraction or percent) of calms. This number has little or no real significance in itself and represents more the sensitivity of the measuring equipment than it does a property of the air motion (See Reynolds, 1976).

The importance of the series representation, (3), for the p.d.f. for wind speed is manifest if one now attempts to form a more reasonable representation of the p.d.f. for speed from the bar-chart representation. If $p(w)$ is to be represented by a continuous smooth curve rather than a series of horizontal lines, then (4) and (5) imply that in each interval (w_i, w_{i+1}) the area under this curve must exactly equal the area under the bar representing $p(\xi)$ in this interval. In addition, the series representation, (3), specifically states that this smooth curve for $p(w)$ must start on a straight line from the point $w=0$, $p(0)=0$; the origin of coordinates for a plot of $p(w)$ as ordinate with w

as abscissa. Figure 28 shows the result from such an exercise. The smooth curve representing p(w) is definitely bimodal (two humps) which is hardly noticeable in the bar-graph representation of the data. (The smooth curve in Figure 28 actually represents points interpolated from a differentiated cubic spline through the distribution function points. The area property in each interval is preserved exactly. On the other hand it is not precisely of the form specified by the series (3) in the first interval and at the higher wind speeds shows small oscillations since no polynomial can be asymptotic to zero.)

Conclusion. When the basic physics of the p.d.f. for wind speed derived from an abritrary bivariate vector distribution is taken into account it is obvious that an adequate representation must include provision for (at least) bimodality.

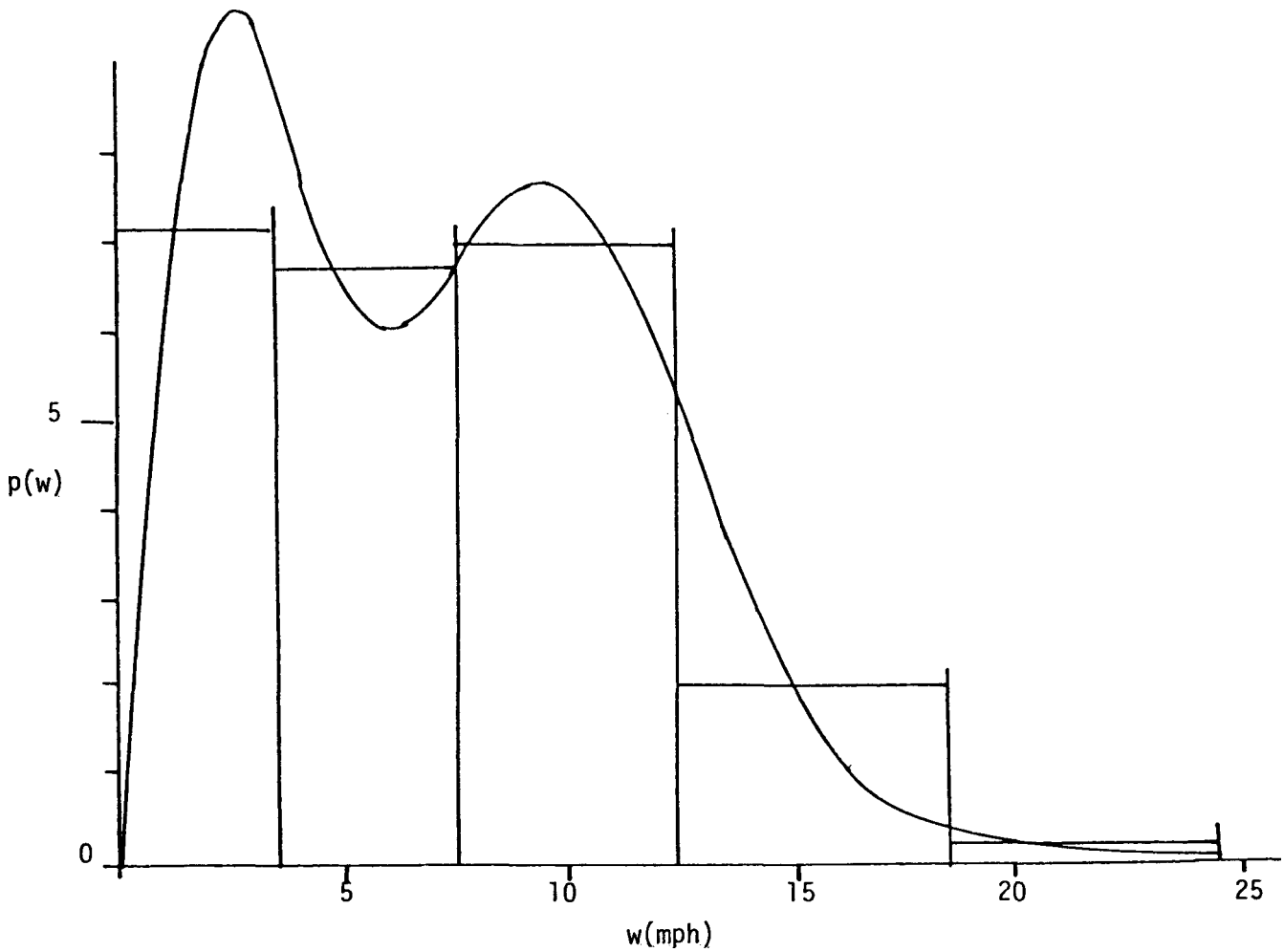

Figure 28. Bar Chart and Smooth Representation of the Probability Density Function. Data for Birmingham, AL, 18 hrs. Abscissa is in m.p.h. The smooth curve is the differentiated cubic spline fit to the distribution function values at the division points between class intervals. The area under the smoother curve in each class interval is equal to the rectangular area of the bar chart representation in that class interval. Note that the bimodal nature of the p.d.f. is much more pronounced in the differentiated cubic spline representation than that of the bar chart.

APPENDIX B

THE BIVARIATE PROBABILITY DENSITY FUNCTIONS OF THE WIND VECTOR AND SOME REASONABLE APPROXIMATIONS TO THE PROBABILITY DENSITY FUNCTION FOR WIND SPEED

THE BIVARIATE PROBABILITY DENSITY FUNCTIONS OF THE WIND VECTOR AND SOME REASONABLE APPROXIMATIONS TO THE PROBABILITY DENSITY FUNCTION FOR WIND SPEED

THE BIVARIATE P.D.F. OF THE WIND VECTOR IN THE REAL WORLD

The published tables of the frequency of occurrence of the wind vector by speed and direction intervals disply data related to the bivariate p.d.f. of the wind vector based on the relation

$$f(i,\ j) = \int_{w_i}^{w_{i+1}} \int_{\theta_j}^{\theta_{j+1}} P_2(w,\theta)\,w\,dw\,d\theta \qquad (1)$$

where f(i,j) is the frequency of occurrence of speed in the i'th speed interval (w_i, w_{i+1}) and direction in the j'th direction interval $(\theta_j,\ \theta_{j+1})$. The bivariate p.d.f. for the wind speed is obtained from the theorem of the mean with the result that

$$p_2(\hat{w}, \hat{\theta}) = f(i,j)/A_{ij} \qquad (2)$$

where A_{ij} = the area of the (i,j)'th cell

$$A_{ij} = \int_{w_i}^{w_{i+1}} \int_{\theta_j}^{\theta_{j+1}} w\,dw\,d\theta$$

and where $w_i<\hat{w}<w_{i+1}$, $\theta_j<\hat{\theta}<\theta_{j+1}$ but cannot be more exactly specified at this point. A reasonable (but not necessarily correct) plotting position for $(\hat{w},\hat{\theta})$ is at the center of gravity of the area A_{ij}.

Figure 29 shows a typical bivariate p.d.f. for the wind vector. (The labels on the contours of Figure 29 represent the percent of occurrences per 5^2 units of area on the plane of the paper, in this case $(5\ \text{mph})^2$.) There are two items displayed in Figure 29 that deserve specific mention: (1) it certainly is not like any form of the bivariate normal distribution and (2)

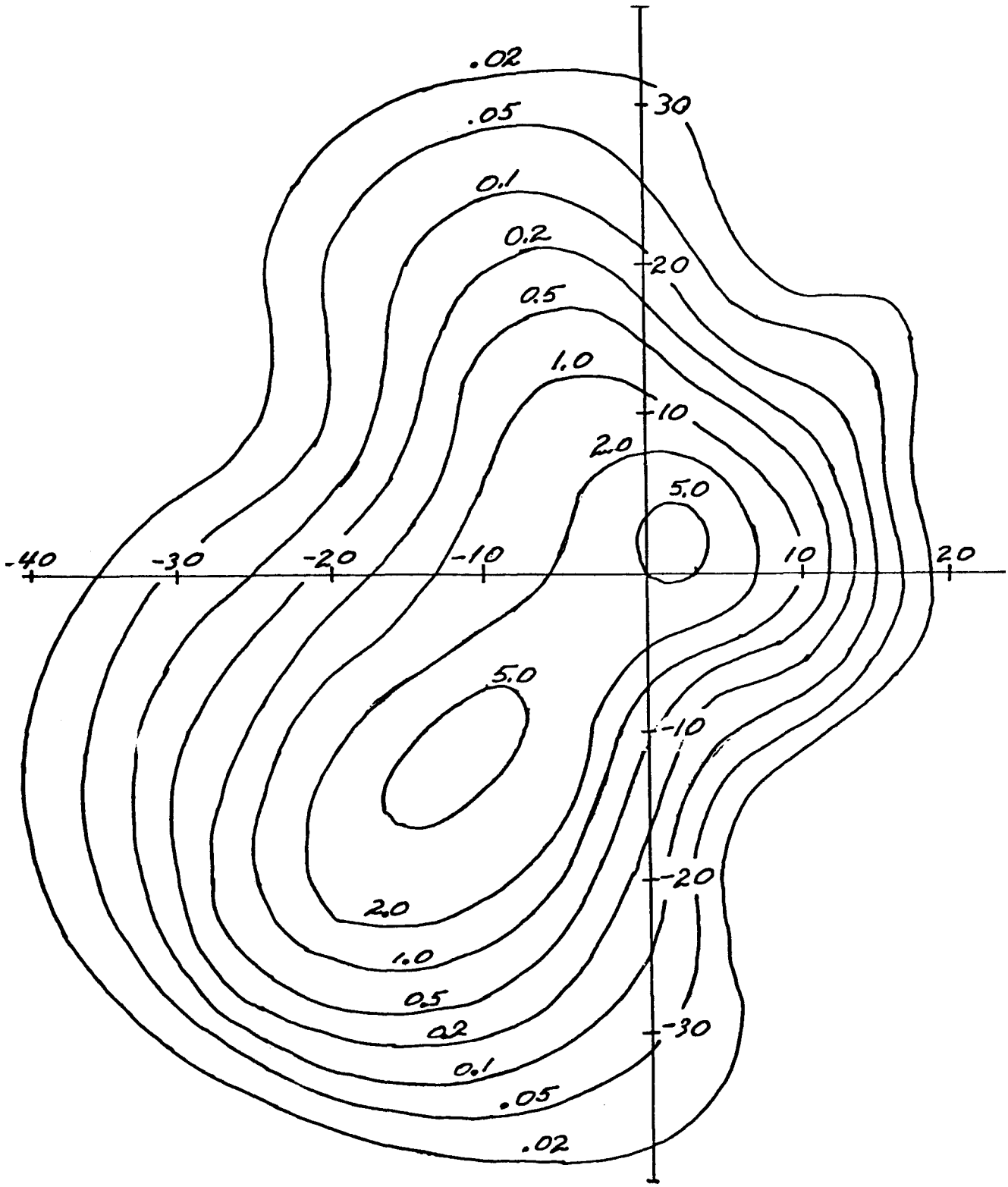

Figure 29. The Bivariate p.d.f. for the wind velocity vector at Great Falls, MT, for January. Note that the p.d.f. is defintely bimodal and thence cannot be represented by a single unimodal bivariate p.d.f. (in particular not by a general bivariate normal p.d.f.). It can be approximated by a mixture of two circularly normal p.d.f.s.

it is definitely bimodal. Many bivariate p.d.f.'s for the wind vector are much simpler while many are more complex. The derivation of a reasonable p.d.f. for wind speed from a general bivariate normal p.d.f. for the wind vector seems to be entirely out of the question since it does not reasonably represent the data. The bimodality of the wind vector p.d.f. suggests that at least this aspect of the data could be represented by a mixture of two unimodal bivariate p.d.f.'s. The simplest possible representation of this kind appears to be a mixture of two circularly normal p.d.f.'s.

THE P.D.F. FOR WIND SPEED FROM THE BIVARIATE CIRCULARLY NORMAL P.D.F.

The p.d.f. of the bivariate circularly normal distribution is expressed in terms of orthogonal components (u,v) as

$$p_2(u,v) = (1/2\pi\sigma^2)\exp\left\{-\left[(u-\bar{u})^2+(v-\bar{v})^2\right]/2\sigma^2\right\}$$

where $(\bar{u},\bar{v})$ are the mean values of the wind components and σ is the wind component standard deviation (common to both components). Now let $u=w\cos\theta$, $v=w\sin\theta$ where w is wind speed and θ is wind direction; and $\bar{u}=w_R\cos\theta_R$, $\bar{v}=w_R\sin\theta_R$ where w_R is the speed of the mean resultant wind and θ_R is its direction. Then

$$(u-\bar{u})^2+(v-\bar{v})^2 = w^2+w_R^2-2ww_R\cos(\theta-\theta_R)$$

and thence as in (1) of Appendix A, the p.d.f. for wind speed is given by $(\phi=\theta-\theta_R)$

$$p(w;\sigma,w_R) = (w/2\pi\sigma^2)\exp\left[-(w^2+w_R^2)/2\sigma^2\right]\int_0^{2\pi}\exp\left\{-(ww_R/\sigma^2)\cos\phi\right\}d\phi \qquad (3)$$

The integral factor on the far right is given by Abramowitz and Stegun (1964) p. 376, 9.616, as $2\pi I_0(ww_R/\sigma 2)$ so that the p.d.f. for wind speed from a circularly normal p.d.f. for wind vector components is

$$p(w;\sigma,w_R) = (w/\sigma^2)\exp\left[-(w^2+w_R^2)/2\sigma^2\right] I_o(ww_R/\sigma^2) \qquad (4)$$

where $I_o(x)$ is the Modified Bessel Function of zero order. This function is tabulated extensively; Abramowitz and Stegen, 1964; Jahnke and Emde, 1960, etc.

The p.d.f. (4) is well known and goes by several names depending on the application being made. In statistics it is a non-central Chi-squared p.d.f., in operations analysis it is the offset circle p.d.f., in electrical engineering it is a generalized Rayleigh p.d.f., etc.

The parameters that appear in (4) have definite physical meaning in terms of the circularly normal p.d.f. from which it was derived. As they appear in (4), σ may be interpreted as a scale parameter and w_R as a location parameter. In terms of the bivariate circularly normal p.d.f. the parameter σ is the (common) wind component standard deviation and w_R is the resultant mean wind speed, $w_R^2 = (\bar{u})^2+(\bar{v})^2$. If $s=w/\sigma$, $\lambda=w_R/\sigma$ (dimensionless variables) one may write (4) in the form

$$p(s,\lambda) = s\exp\left\{-(s^2+\lambda^2)/2\right\} I_o(s\lambda) \qquad (5)$$

Figure 30 shows the function in terms of $p(s,\lambda)$ as ordinate s as abscissa, for various values of the parameter λ. The curve for $p(s,0)$ is skew but for only moderate values of λ it is shaped very much like the Gaussian p.d.f. with mean value near $\lambda=w_R/\sigma$ and unit standard deviation. The location of the maximum and of the two inflection points on either side of the maximum (when they exist) is illustrated in Figure 31. See Appendix F for details. The parallel dashed lines in Figure 31 represent the asymptotes to the curves concerned.

Although it is convenient to use the dimensionless form of the generalized Rayleigh p.d.f. (i.e., plotted to a scale corresponding to $\sigma=1$), the behavior of this function as it depends on σ is of considerable importance. In Figure 32 the curves for σ = 1, 2, 3, 4, 5, 6 with $w_R=5$ are shown. The

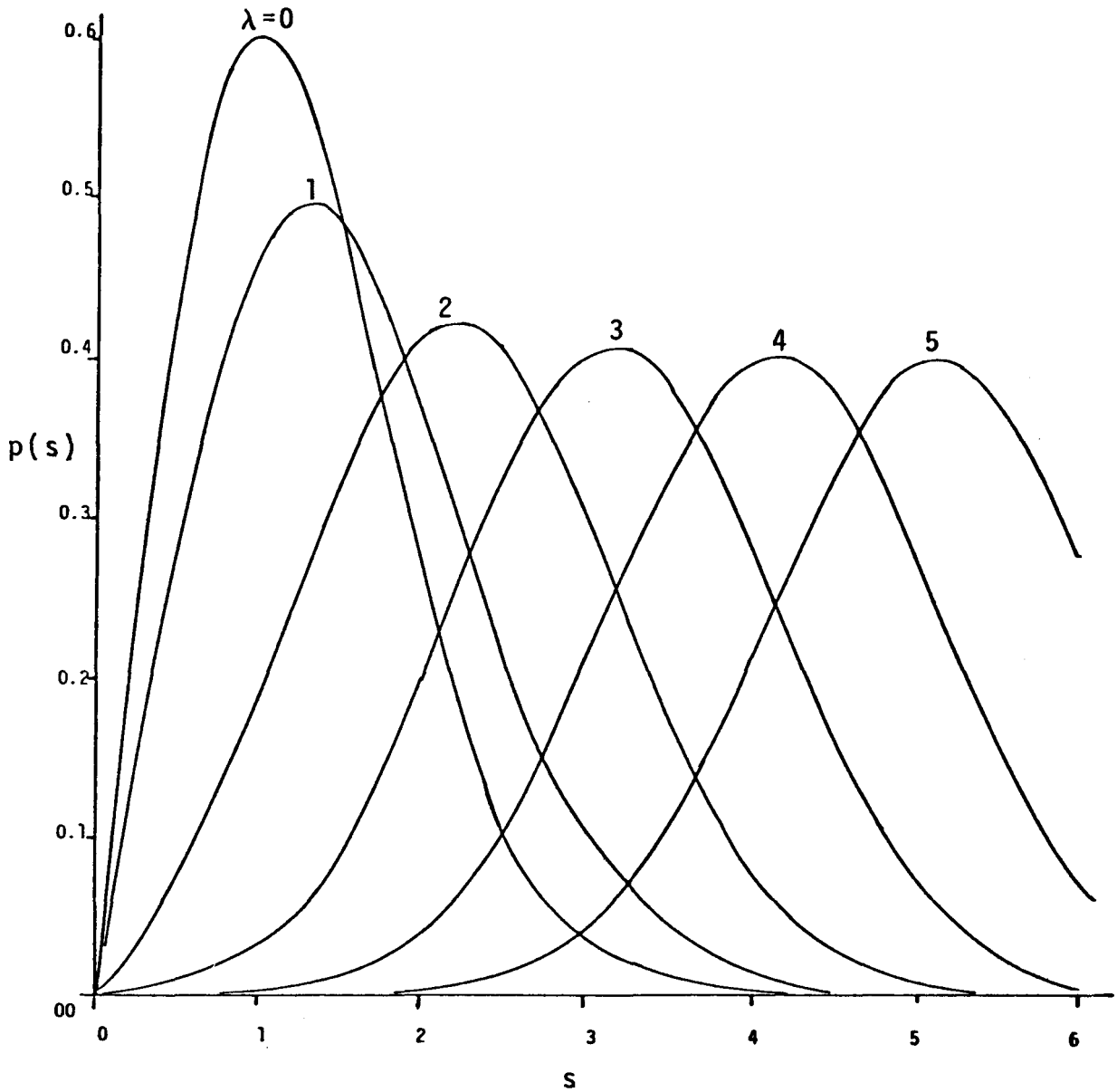

Figure 30. The family of generalized Rayleigh p.d.f.'s. in dimensionless units $s = w/\sigma$, $\lambda = w_R/\sigma$.

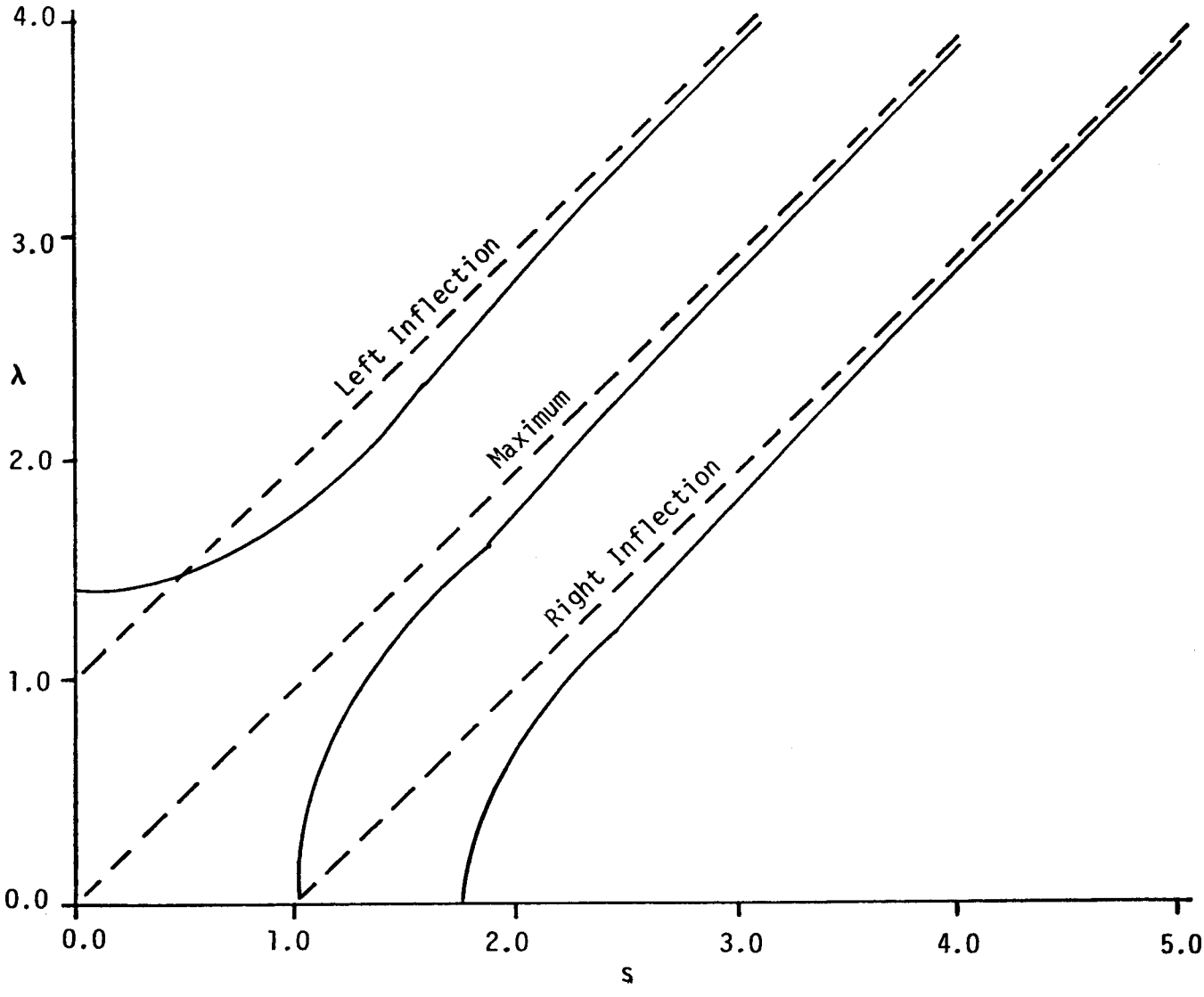

Figure 31. The location of the maximum (most probable value) and the inflection points of the generalized Rayleigh p.d.f. as a function of the parameter $\lambda(\lambda = w_R/\sigma)$.

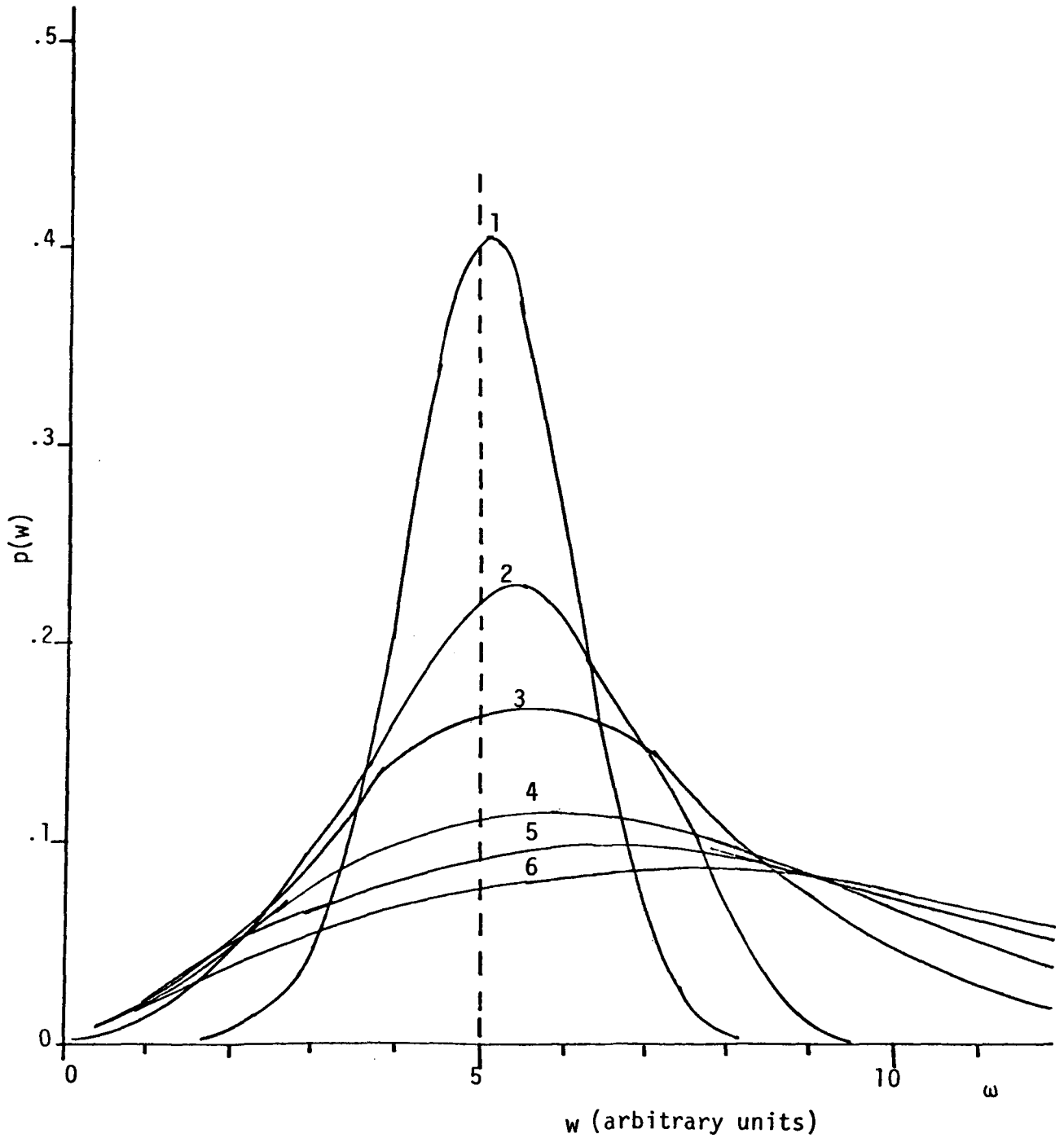

Figure 32. The behavior of p(w) from (3) as a function of w with w_R=5 and values of σ shown on each curve (same units as w and w_R). In the limit $\sigma \to 0$, the curve is an infinite spike along the vertical at w_R=5 enclosing a unit area.

maximum in all cases is to the right of w_R=5. The area under each curve is 1. As σ decreases the hump near w_R=5 increases. In the limit for $\sigma \rightarrow 0$, the function p(w) becomes a slender spike of infinite height but containing a unit of area. The case for w_R=0 is illustrated in Figure 33. In this case the leftward displacement of the maximum is more pronounced. The infinite spike of unit area in the limit for $\sigma \rightarrow 0$ lies along the vertical coordinate axis (w=0). This behavior for $\sigma \rightarrow 0$ makes it possible to identify important degenerate cases in practical applications, particularly those in which the frequency of low wind speeds or calms is large.

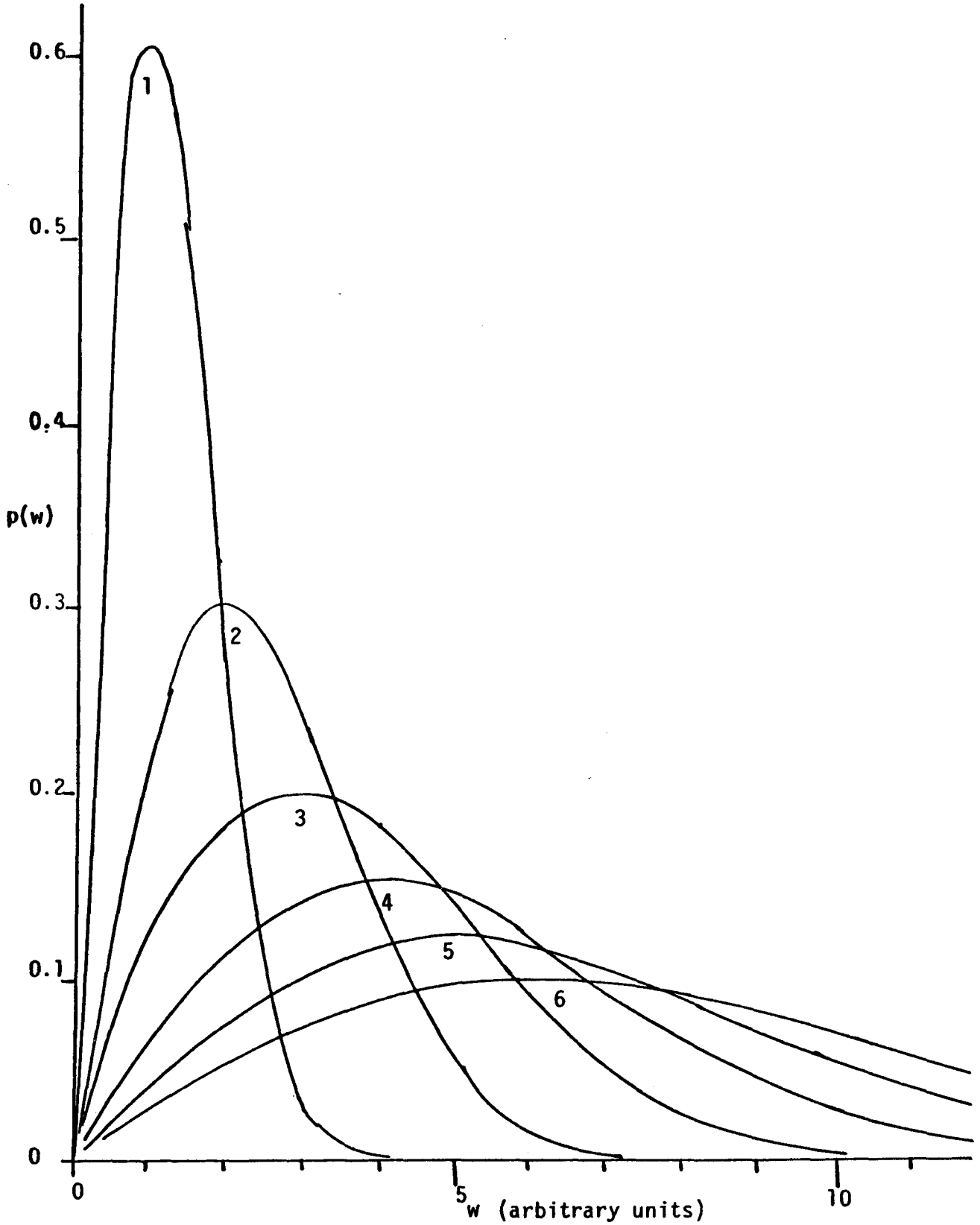

Figure 33. The behavior of p(w) from (3) as a function of w with w_R=0 and values of σ shown on each curve (same units as w and w_R). The area under each curve is 1. In the limit for σ=0, the curve is an infinite spike along the vertical coordinate axis enclosing a unit area.

APPENDIX C

SOME MIXING PROPERTIES OF THE GENERALIZED RAYLEIGH P.D.F. FOR SCALAR WIND SPEED

SOME MIXING PROPERTIES OF THE GENERALIZED RAYLIEGH P.D.F. FOR SCALAR WIND SPEED

Consider the case of a two component mixture of distributions with circularly normal p.d.f.'s $p_1(u,v)$ and $p_2(u,v)$ and let k be the fraction due to the first component and (1-k) the fraction due to the second component. The p.d.f. of the mixture will then be

$$p(u,v) = kp_1(u,v) + (1-k)p_2(u,v)$$

If we write these expressions in terms of speed, w, and direction, θ, and the corresponding parameters, one has

$$p(w,\theta;---) = kp_1(w,\theta;\sigma_1,w_1,\theta_1)+(1-k)p_2(w,\theta;\sigma_2,w_2,\theta_2)$$

The p.d.f. for wind speed for the mixture is obtained by integrating over θ

$$p(w;---) = \int_0^{2\pi} p(w,\theta;---)d\theta$$
$$= k\int_0^{2\pi} p_1(w,\theta;\sigma_1 w_1,\theta_1)d\theta+(1-k)\int_0^{2\pi} p_2(w,\theta;\sigma_2,w_2,\theta_2)d\theta$$

As in (3) of Appendix B above, introduce $\phi' = \theta - \theta_1$ in the first term and $\phi'' = \theta - \theta_2$ in the second term and integrate to obtain the p.d.f. for the mixture as

$$p(w;---) = kp(w;\sigma_1,w_1)+(1-k)p(w;\sigma_2,w_2) \qquad (1)$$

where the functions on the right are given by (4) of Appendix B. In the case that $\sigma_1=\sigma_2=\sigma$, $w_1=w_2=w_R$ the probability density functions on the right of (1) are identical so that the appearance of a mixture (the parameter k) is no longer present,

$$p(w;---) = \left[k+(1-k)\right]p(w;\sigma,w_R) = p(w;\sigma,w_R) \qquad (2)$$

One then obtains the result that if the mixture of circularly normal distributions is such that the two (or more) components of the mixture have the same parameters σ, and w_R the resulting p.d.f. for wind speed is independent of the orientation of the resultant wind speeds θ_1, θ_2 and is independent of the proportions of the mixture, k, (1-k). This implies that, though specialized, there are a wide variety of wind vector bivariate circularly normal mixtures of distributions that will appear to be the same when only the p.d.f. for scalar wind speed is considered.

The situation is illustrated in Figures 34 and 35. Figure 34 represents a bivariate circularly normal p.d.f. with parameters $\sigma=3$, $w_R=5$, ($\theta_R=0^o$). The contour interval is on a roughly logarithmic scale---,10, 5, 2, 1, 0.5, 0.2, 0.1,---; i.e., as though the logarithm of $p(w,\theta;---)$ was a vertical coordinate perpendicular to the plane of the paper. In this case the surface concerned is a paraboloid of revolution, most easily seen in rectangular coordinate form as

$$z = \log p(u,v;---) = \left[(u-5)^2+v^2\right]/2\cdot 3^2 - \log(2\pi\cdot 3^2)$$

The labeling on the contours expresses $p(u,v;\ -\ )$ in terms of percent per 5^2 units of area on the horizontal (plane of the paper). If one then integrates this p.d.f. over the angular parameter θ the resulting p.d.f. for scaler wind speed is a generalized Rayleigh p.d.f. as in (4) in Appendix B with parameters $\sigma=3$, $w_R=5$.

In Figure 35 the mixtures of bivariate circularly normal p.d.f.'s are illustrated with the following parameter assignments:

	σ_1,	w_1,	θ_1,	σ_2,	w_2,	θ_2,	k
A	3	5	0°	3	5	+90°	0.50
B	3	5	0°	3	5	+90°	0.25
C	3	5	-90°	3	5	+90°	0.50
D	3	5	-90°	3	5	+90°	0.75

When the integration is carried out over the angle θ the dependence on the

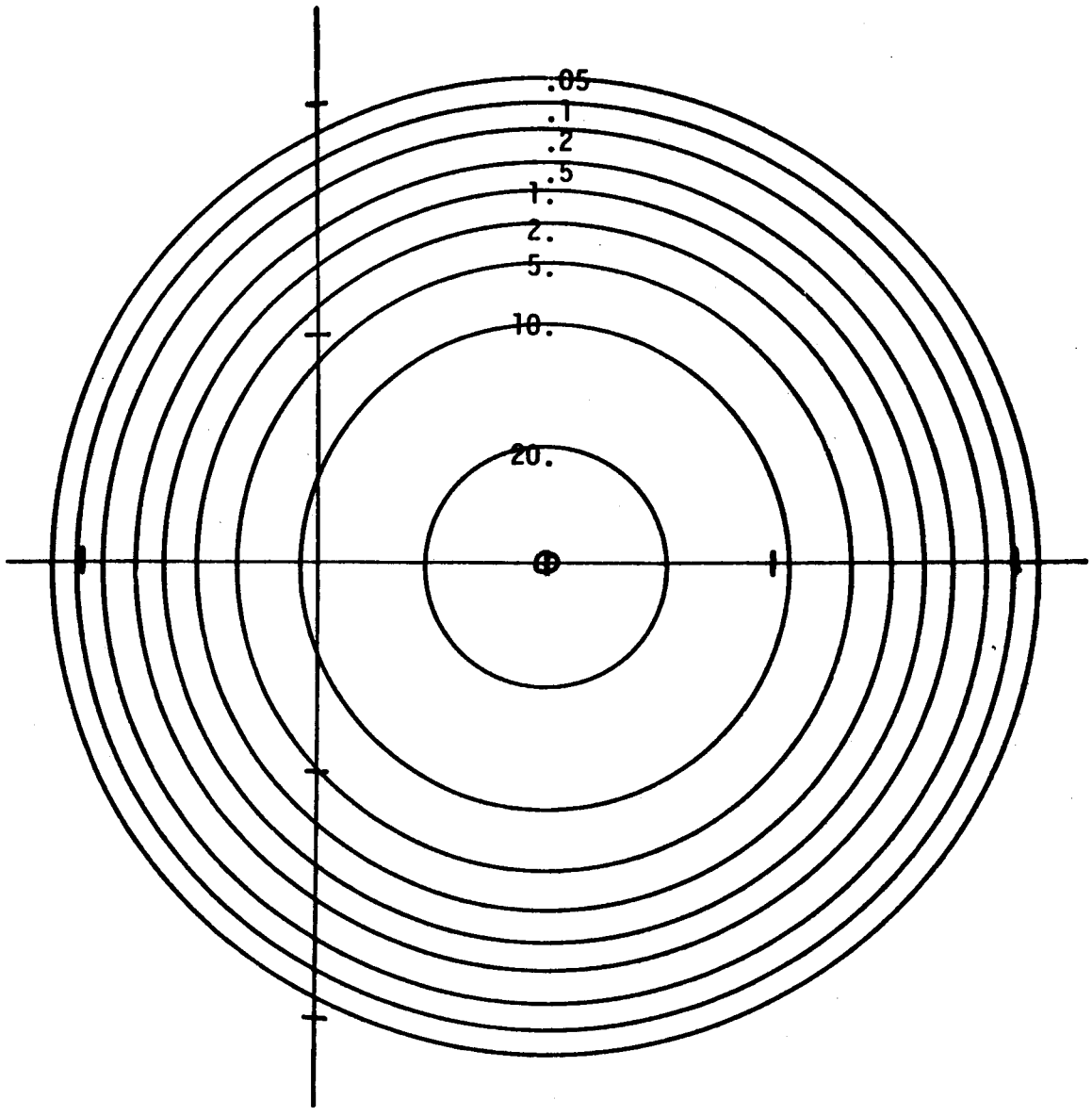

Figure 34. Contours for the Bivariate Circularly Normal p.d.f. with Parameters $\sigma=3$, $w_R=5$, $\theta_R=0^0$.

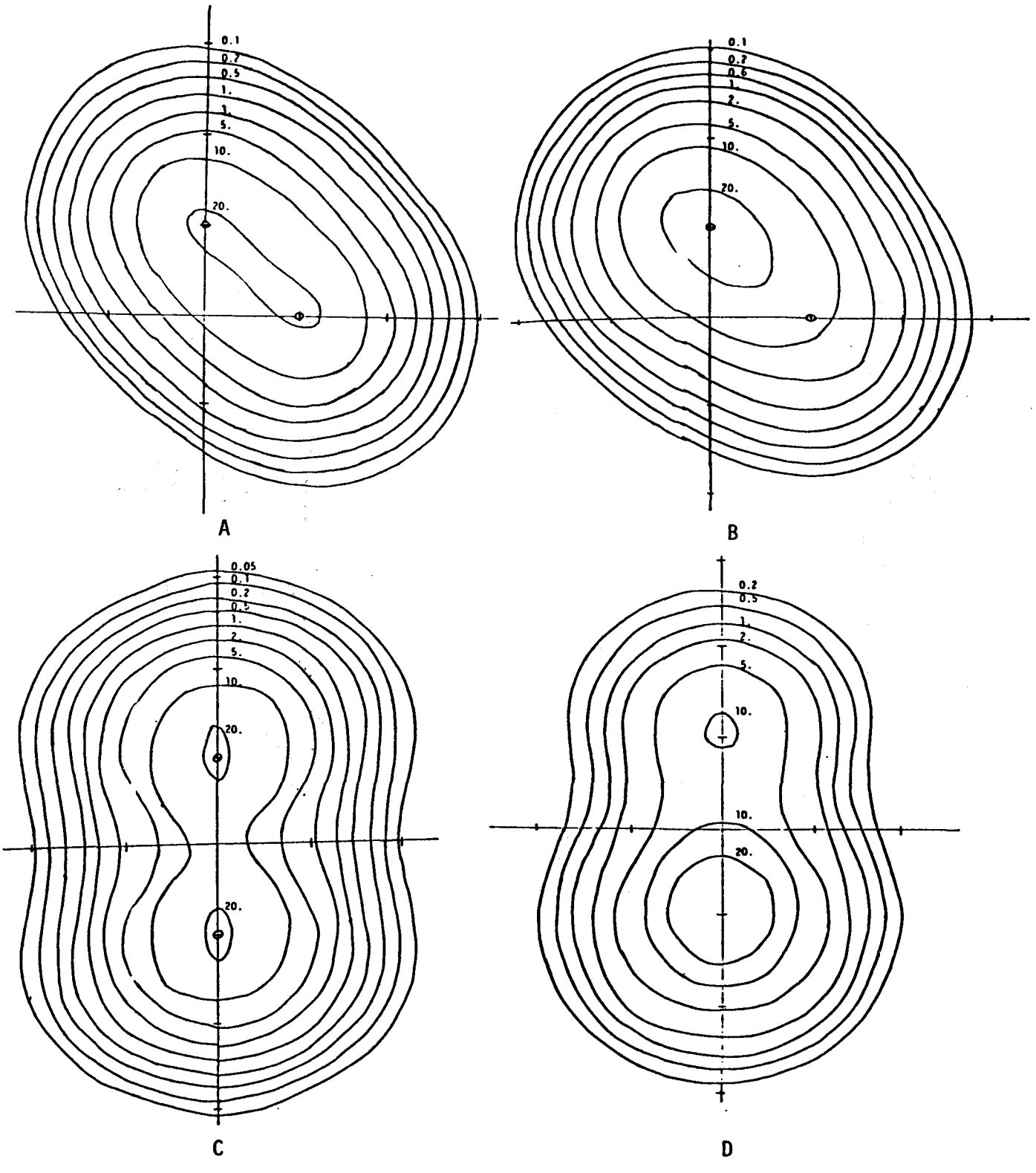

Figure 35. Contours for the Mixture of Bivariate Circularly Normal p.d.f.'s with Parameter Values Listed in the Text. All of these reduce to the same single generalized Rayleigh p.d.f. for scalar wind speed as obtained from Figure 34 (no mixture) when the angular dependence is removed by integration.

angles θ_1 and θ_2 is eliminated and since $\sigma_1=\sigma_2=\sigma$, $w_1=w_2=w_R$ one is lead from (1) to (2); i.e., that each of these mixtures reduces to a single generalized Rayleigh p.d.f. for wind speed which also was valid for the "pure" bivariate circularly normal p.d.f. of Figure 7.

These are only four special cases that would lead to this generalized Rayleigh p.d.f. For a two component mixture with $\sigma_1=\sigma_2=\sigma$, $w_1=w_2=w_R$ there is actually a triple-infinity (∞^3) of such cases; an infinity of cases for each parameter that is dropped: $0 \le \theta_1 < 2\pi$, $0 \le \theta_2 < 2\pi$, $0 \le k < 1$.

The situation is even more general since one need not be limited to a two component mixture. The same is true for an n-component mixture with mixing ratios $k_1,---,k_n$, $k_1+k_2+---+k_n=1$, provided that $\sigma_1=\sigma_2=---=\sigma_n=\sigma$, $w_1=w_2=---=w_n=w_R$.

In the above a mixture of two discrete components has been considered such that the probability of the occurrence of the first component is k_1, the probability of occurrence of the second component is k_2, and $k_1+k_2=1$. The situation may be extended to a class of continuous mixtures; let $p(x;\lambda)$ be a p.d.f. depending on the parameter λ and let λ itself have a p.d.f., say $q(\lambda)$, and let $p_m(x)$ be the p.d.f. of the mixture of $p(x,\lambda)$ in which occurs with p.d.f. $q(\lambda)$. Then

$$p_m(x) = \int p(x,\lambda)q(\lambda)d\lambda$$

where integration takes place over the range of the parameter λ.

In the case of interest for wind speed p.d.f.'s one may show that the following statement is valid. Consider an ensemble of circularly normal wind component p.d.f.'s, $p_2(w,\theta;\ \sigma_1,\hat{w}_R,\hat{\theta}_R)$ where σ_1 is a common parameter and for which the direction of the resultant mean wind, $\hat{\theta}_R$, may be dependent on the speed of the resultant mean wind, $\hat{w}_R$ (i.e., $\hat{\theta}_R=f(\hat{w}_R)$). Let the speed of the resultant mean wind, $\hat{w}_R$, be distributed in accordance with the generalized

Rayleigh distribution (as in (4) of Appendix B) with parameters σ_2 and w_R. Then the p.d.f. for wind speed from this mixture of distributions will be of the same form as that in (4) of Appendix B with scale parameter, σ, given by $\sigma^2=\sigma_1^2+\sigma_2^2$ and with the location parameter (resultant mean speed) the same as that of the mixing distribution, w_R.

The point of the argument lies in the fact that, given a particular generalized Rayleigh p.d.f. for wind speed, it is virtually impossible to infer the combination of circularly bivariate normal p.d.f.'s from which it might have been derived.

Though a single generalized Rayleigh p.d.f. for scalar wind speed may come from a wide variety of mixtures, one may refer to Figure 29 to be reminded that bivariate p.d.f.'s of the real world may require a mixture of at least two generalized Rayleigh p.d.f.'s for an adequate representation of the resulting scalar wind speeds. In Figure 29 it is obvious that $\sigma_1 \neq \sigma_2$ and $w_1 \neq w_2$.

APPENDIX D

GRAPHIC REPRESENTATION OF THE DISTRIBUTION FUNCTION FOR WIND SPEED

GRAPHIC REPRESENTATION OF THE DISTRIBUTION FUNCTION FOR WIND SPEED

The use of normal or log-normal probability paper to represent the distribution function for wind speed always leads to confusion since in both cases the low wind speeds are unduly distorted. In the following section a representation for the Rayleigh distribution is given after which the use of such a representation for mixtures of generalized Rayleigh or actual wind speed distributions is taken up.

THE BASIC PLOTTING PAPER

Let p(w) be the p.d.f. for wind speed (parameters omitted). Then the distribution function (D.F.) for wind speed is given by

$$P(w) = \int_0^w p(x)dx \tag{1}$$

When p(w) is the generalized Rayleigh p.d.f., the corresponding D.F. cannot be expressed in closed form. However, the expression for the Rayleigh distribution (w_R=0) is handily given by

$$P(w) = 1-\exp(-w^2/2\sigma^2) \tag{2}$$

which may be solved for w explicitly

$$w = \sigma \sqrt{-2\ln(1-P)} \tag{3}$$

If we let y=w, $x = \sqrt{(-2)\ln(1-P)}$, then (3) becomes $y=\sigma x$ which in (x,y) coordinates is the equation of a straight line with slope σ. The abscissa may be marked in terms of x=0,1,2,--- (sometimes called "probits") or in terms of the probability function P (in percent). The ordinate, y, has a uniform scale in terms of wind speed and may be arbitrary to fit the data at hand. The ordinate may also be taken as $y=w/\sigma$ in which case it is dimensionless.

When one is concerned with the generalized Rayleigh D.F. the parameter w_R (resultant mean wind speed) is also involved. Figure 36 illustrates the case in which the ordinate is the non-dimensional speed w/σ. The curves for the ratio w_R/σ are labeled with values of this ratio. It is to be noted that for $w_R=0$ the curve concerned is a straight line and that for $w_R>0$ the curves have a slope greater than 1 (or σ) at the origin, are concave downward, and eventually become parallel to the curve for $w_R=0$.

MIXTURES OF DISTRIBUTIONS

Consider the theoretical case in which the D.F. concerned corresponds to a two component mixture of generalized Rayleigh D.F.'s.

$$P(w) = kP_1(w;\sigma_1,w_1)+(1-k)P_2(w;\sigma_2,w_2) \qquad (4)$$

where the "R" of the resultant mean wind speed is dropped to prevent the accumulation of multiple subscripts in the functions on the right. The two extreme cases k=1, $P=P_1$, and k=0, $P=P_2$ will then consist of curves from the family represented in Figure 37. One cannot easily use a dimensionless ordinate since the parameters σ_1 and σ_2 need not be the same. For values of k in the range $0<k<1$ one obtains a family of curves that will lie between the curves for the extreme cases.

The plotting diagram can be used to estimate the parameters of a mixture of generalized Rayleigh distributions only in a rather limited sense. (This is equally true for estimating the parameters of a mixture of Gaussian distributions using a plot of data points on ordinary probability paper.) Some of the special cases that are easily recognized are discussed in the following paragraphs.

(a) Ordinary Rayleigh Distribution. Straight line with slope σ.

(b) Generalized Rayleigh Distribution. See Figure 36 for typical curves. Note that all of these curves are concave downward. They will not be asymptotic to any straight line through x=y=0.

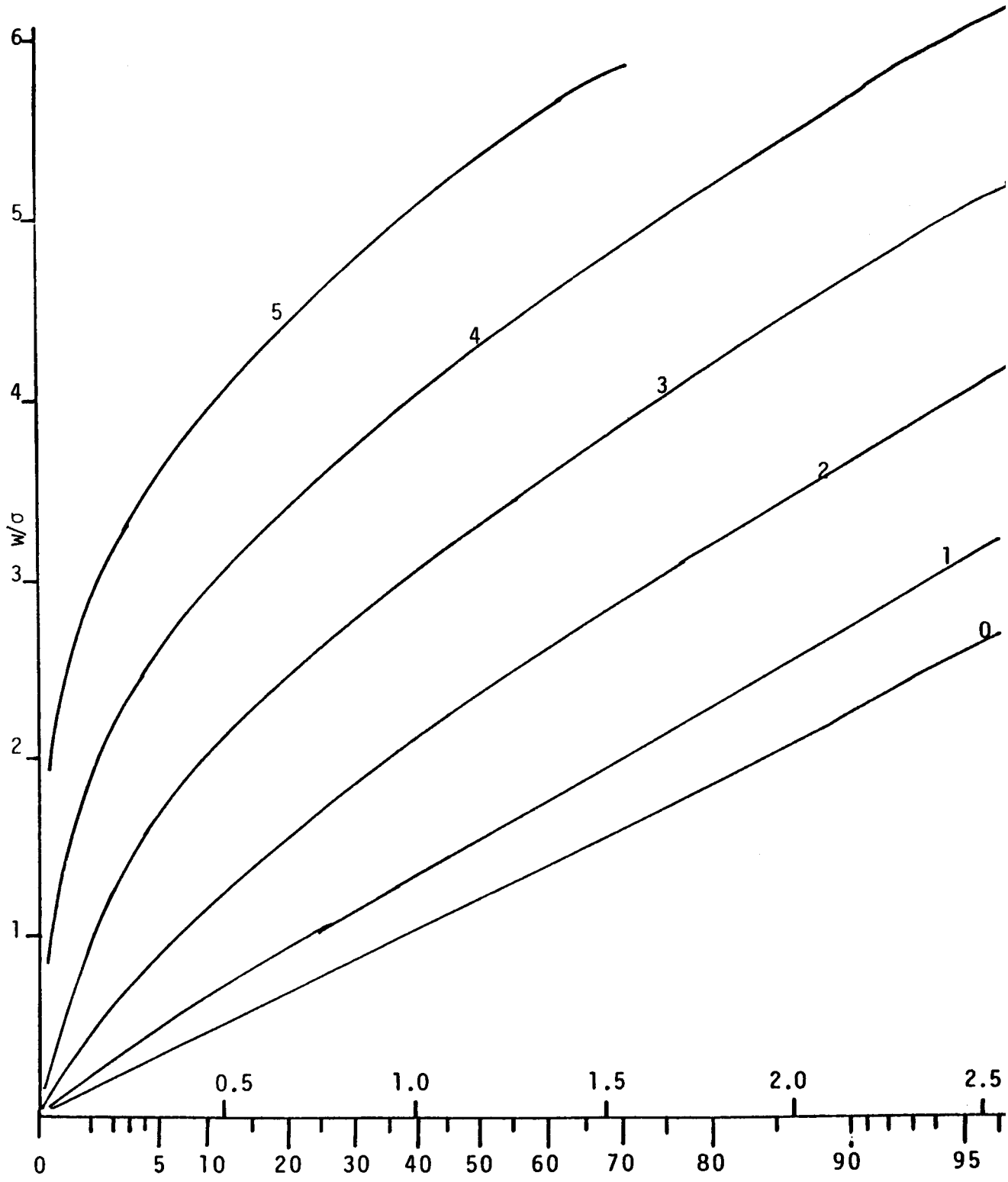

Figure 36. A Plotting Paper for Wind Speed Distributions. The abscissa is shown in terms of both "probits" (0,1,2,...) and the probability. The ordinate is the dimensionless ratio w/σ. The curves are for the values of the ratio w_R/σ shown of a generalized Rayleigh D.F. The straight line (labled 0) corresponds to the Rayleigh D.F.

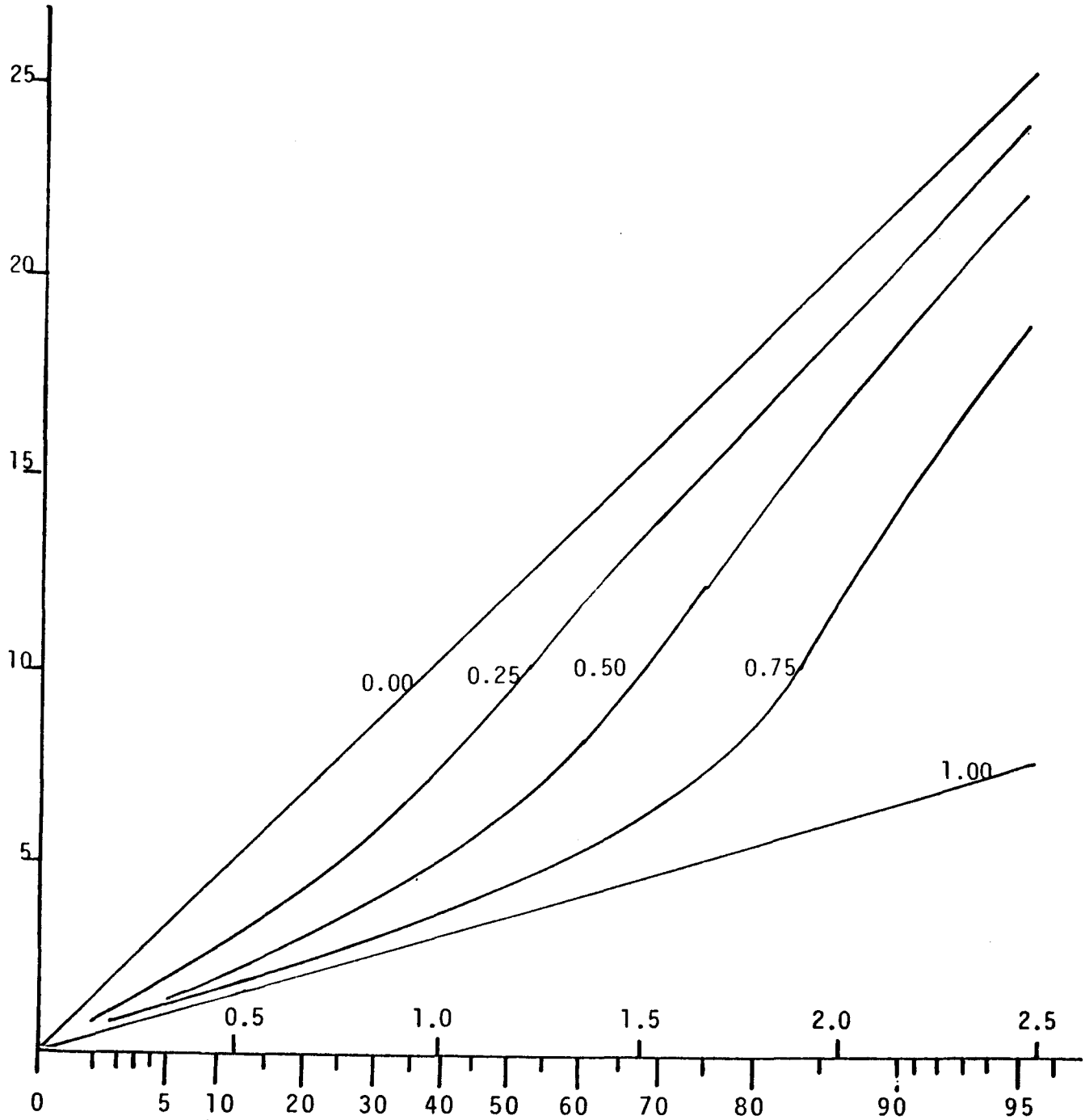

Figure 37. A Plot of Mixtures of Two Rayleigh Distributions. The parameters are σ_1=3, w_1=0, σ_2=10, w_2=0. Values of the mixing ratio k are shown beside the corresponding curves. The ordinate is wind speed in the same units as are used for the parameters σ_1, w_1, σ_2, w_2.

(c) Mixture of Two Ordinary Rayleigh Distributions. In this case the curve lies in the wedge shaped area bounded by the lines $y=\sigma_1 x$ and $y=\sigma_2 x$, $0<\sigma_1<\sigma_2$, and the curve will be asymptotic to the upper line $y=\sigma_2 x$. Its slope at the origin is given by $\left[k/\sigma_1^2+(1-k)/\sigma_2^2\right]^{-\frac{1}{2}}$ which is within the angle formed by the wedge at x=y=0. See Figure 37.

(d) Mixture of Ordinary Rayleigh and a Degenerate Rayleigh. If one component of the mixture is degenerate at the origin then $w_1=0$, $\sigma_1=0$, but $0<k$. Then for $w>0$ one has for the mixture

$$P = k+(1-k)\left[1-\exp(-w^2/2\sigma_2^2)\right].$$

Then a bit of algebra gives (for $x = \sqrt{-2\ln(1-P)}$, $y=w$) the relation

$$x^2/A^2 = 1+y^2/A^2\sigma^2,\ A^2=(-2)\ln(1-k)$$

which is the equation of an hyperbola that opens to the right in standard form. The x-intercept is at x=A (where the tangent is vertical) and the asymptote (in the first quadrant) is the line $y=\sigma x$. If the probability scale (P) is plotted along the x-axis, the value of k corresponds to the value of P where the curve meets the x-axis. See Figure 38.

(e) Other Mixtures. Other mixtures are illustrated in Figures 39 and 40. In both of these the upper curve for k=0 is that for $\sigma_2=10$, $w_2=10$ and corresponds to the curve $\lambda=w_R/\sigma=1$ of Figure 36. When displayed alone this is scarcely distinguished from a straight line. In practical problems it is found that with minor adjustments of other parameters the value $w_2=0$ gives about the same results as far as the data fit is concerned. The fact that the curves for $w_R/\sigma>0$ (as in Figure 36) are concave downward leads to a useful rule of thumb: Set a straight-edge at the origin, (i) if the data points look like they could approach this straight line from below, it is possible that the high-speed component of the mixture is an ordinary Rayleigh D.F.; (ii) if the data points at lower wind speeds lie above the line that seems

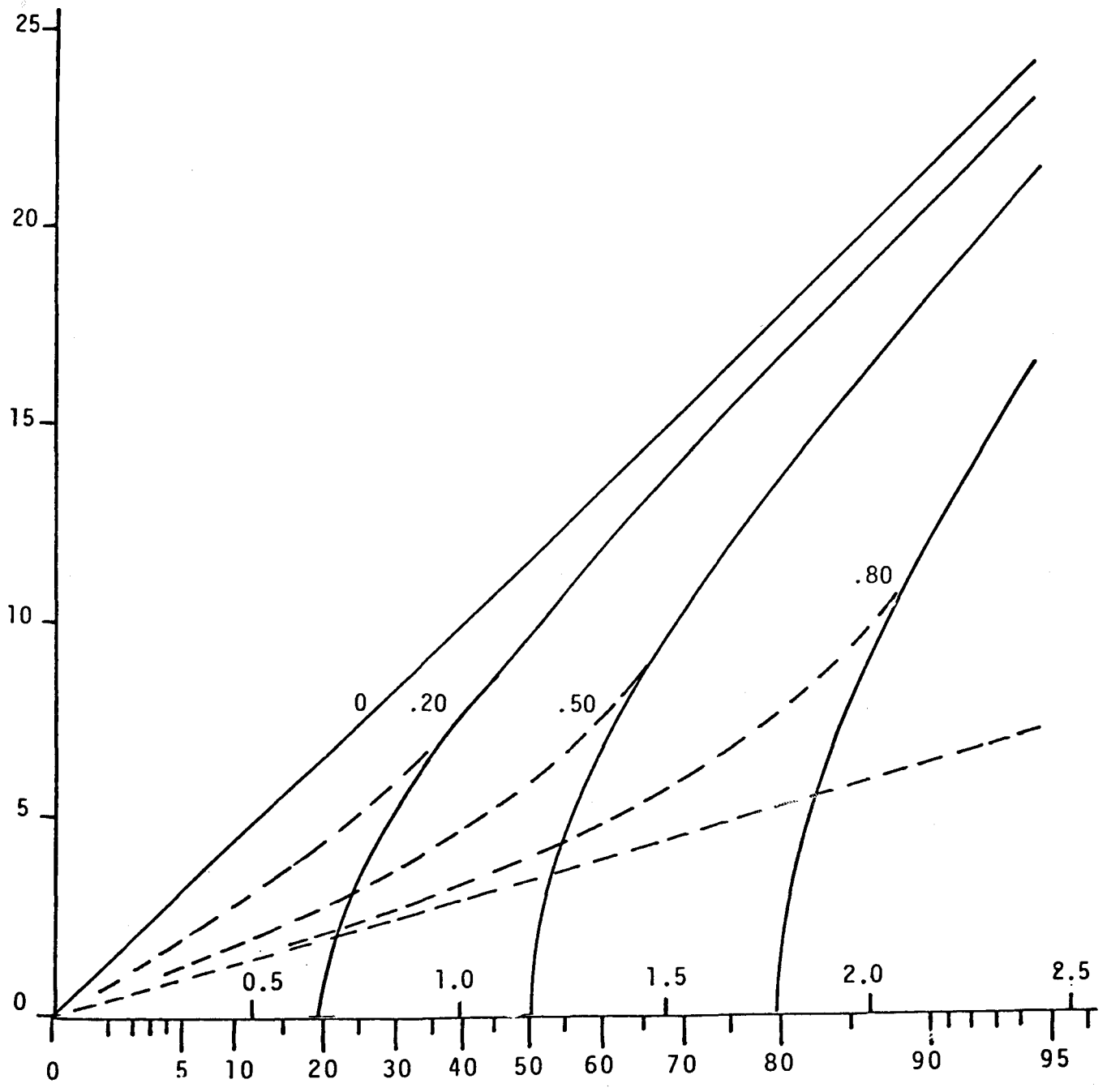

Figure 38. A Plot of a Mixture of a Rayleigh and a Degenerate Rayleigh Distribution. The parameters are (0,0,10,0,k) with the value of k labeling the curves. The dashed curves are those for the mix (3,0,10,0,k) as in Figure 10. As $\sigma_1 \to 0$ the lower dashed straight line approaches the axis of abscissae and brings the dashed part of the curves along to also coincide with the x-axis.

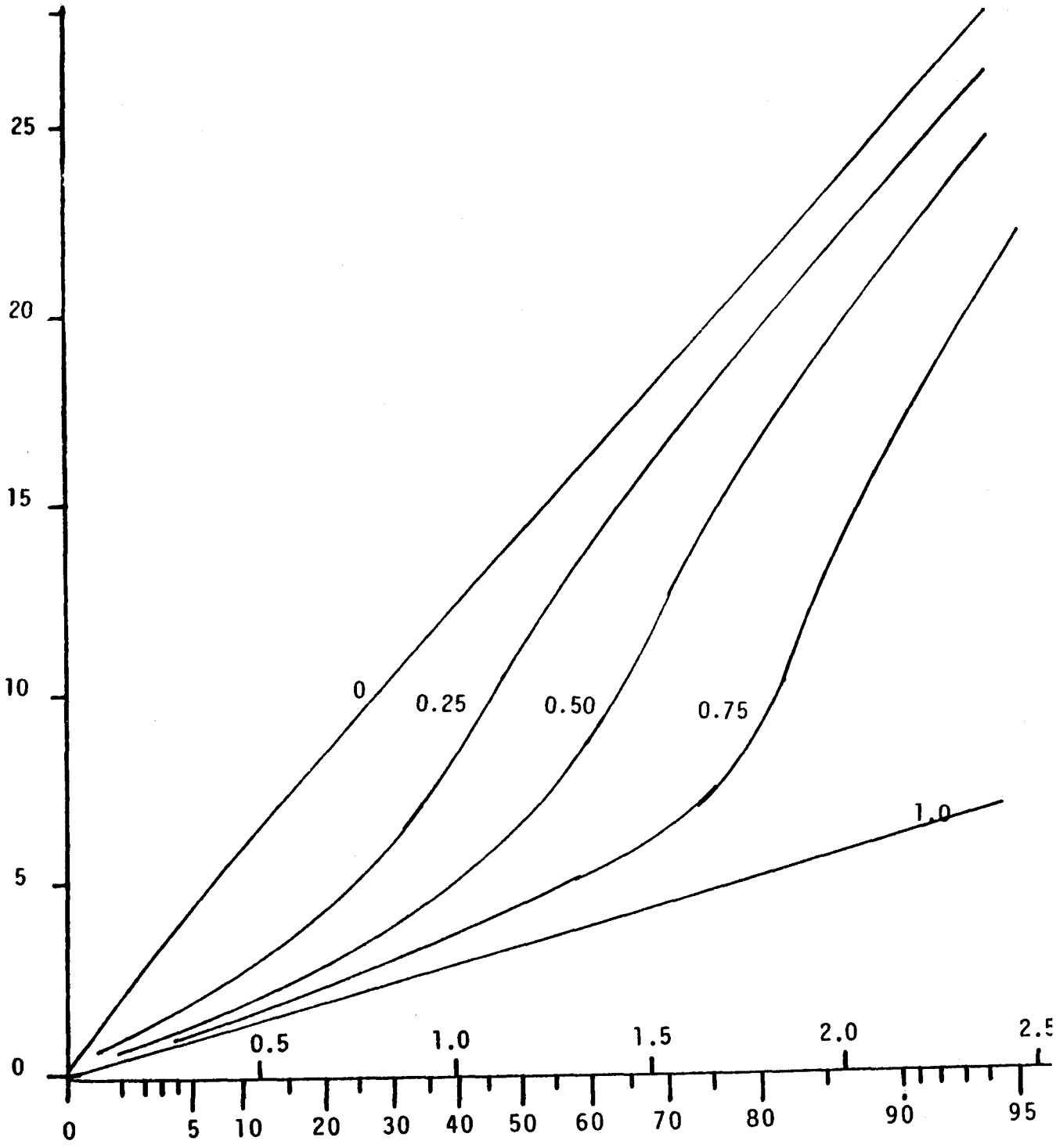

Figure 39. A Plot of a Mixture of a Rayleigh and a Generalized Rayleigh Distribution. The parameters are (3,0,10,10,k) with the values of k shown beside the corresponding curve. Compare the curve for k=0 with that labeled 1 (= w_R/σ) in Figure 9.

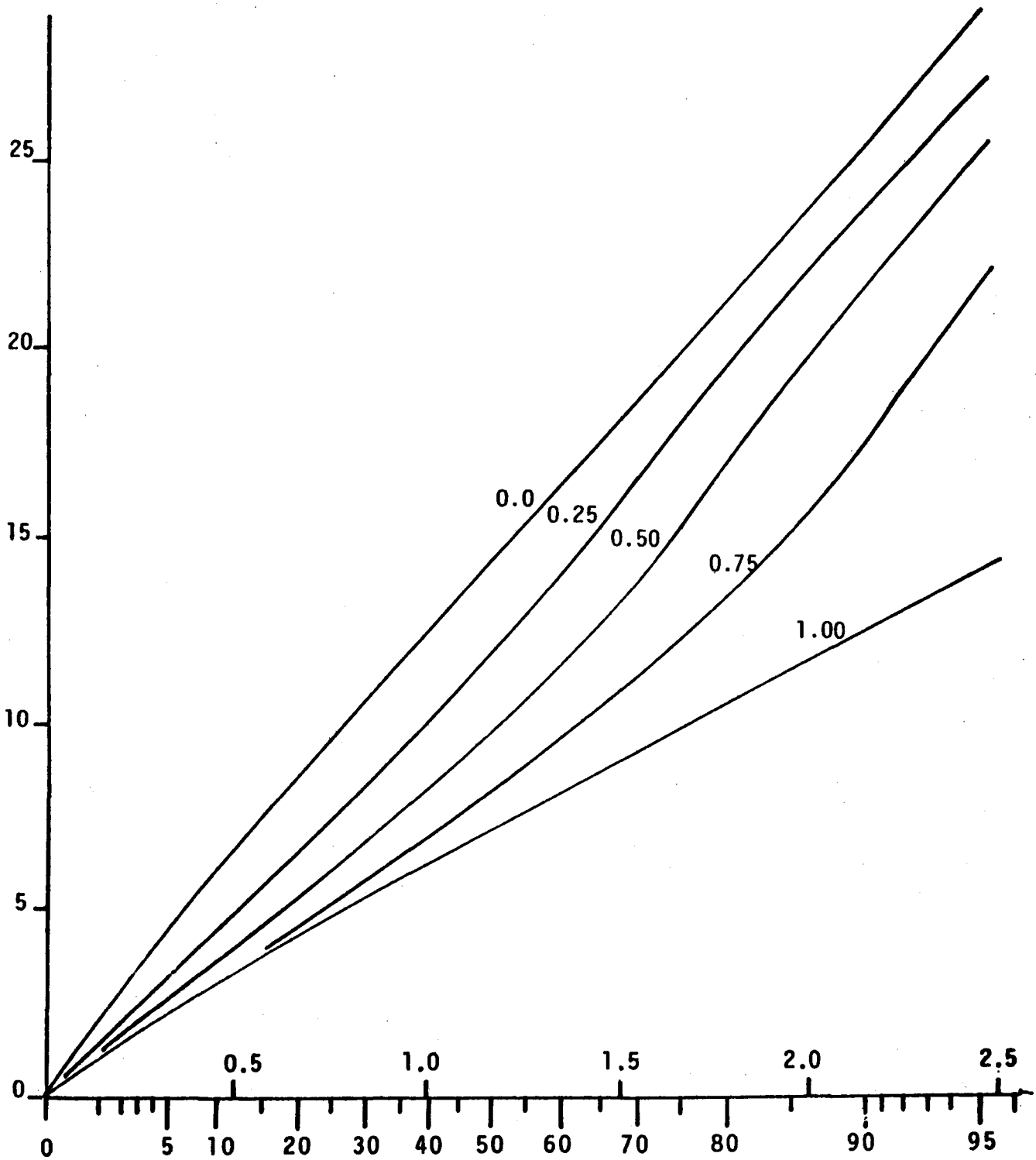

Figure 40. A Plot of a Mixture of Two Generalized Rayleigh Distributions. The parameters are (5,5,10,10,k) where the values of k label the curves.

to be an asymptote for the higher wind speed points or (iii) if the higher wind speed points are asymptotic from below to a line that has as y-intercept a value of w>0, then at least one component of the mixture is a generalized Rayleigh D.F. This rule of thumb does not always work.

APPENDIX E

MOMENTS OF WIND SPEED ABOUT ZERO

MOMENTS OF WIND SPEED ABOUT ZERO

The moments of the wind speed about zero (the average of some power of the wind speed) are defined by the relation

$$\overline{w^a} = \int_0^\infty w^a p(w)dw \tag{1}$$

where p(w) is the p.d.f. for the wind speed. When the p.d.f. for wind speed is represented in terms of a mixture of different p.d.f.'s

$$p(w) = kp_1(w;\sigma_1,w_1)+(1-k)p_2(w;\sigma_2,w_2) \tag{2}$$

(or at least a mixture of p.d.f.'s with different parameters) then

$$\overline{w^a} = k\int_0^\infty w^a p_1(w;\sigma_1,w_1)dw+(1-k)\int_0^\infty w^a p_2(w;\sigma_2,w_2)dw \tag{3}$$

If the p.d.f.'s concerned are those of the generalized Rayliegh distribution

$$p(w;\sigma,w_R) = (w/\sigma^2)\exp\left[-(w^2+w_R{}^2)/2\sigma^2\right] I_0(ww_R/\sigma^2) \tag{4}$$

it is necessary to carry out the integration

$$I = \sigma^{-2}\exp(-w_R{}^2/2\sigma^2)\int_0^\infty w^{a+1}\exp(-w^2/2\sigma^2)I_0(ww_R/\sigma^2)dw \tag{5}$$

This is easily done (using Abramowitz and Stegun (1964), 11.4.28, p.486) with the result that

$$I = 2^{a/2}\,\Gamma(\tfrac{a}{2}+1)\sigma^a\,\exp(-w^2{}_R/2\sigma^2)M(\tfrac{a}{2}+1,\ 1;\ w_R{}^2/2\sigma^2) \tag{6a}$$

or

$$I = 2^{a/2}\,\Gamma(\tfrac{a}{2}+1)\sigma^a\,M(-\,a/2,\ 1;\ -w_R{}^2/2\sigma^2) \tag{6b}$$

where M(a,b;x) is the comfluent hypergeometric function of x with parameters a and b, and $\Gamma(x)$ is the gamma function. The confluent hypergeometric function is easily computed from the series

$$M(a,b;x) = 1+\frac{a}{b}x+\frac{a(a+1)}{b(b+1)}\frac{x}{2!}+\frac{a(a+1)(a+2)}{b(b+1)(b+2)}\frac{x}{3!}+\text{---}. \qquad (7)$$

It is readily seen that if α is an even integer, $\alpha=2n$, then in (6b) $a=-\frac{\alpha}{2}=-n$ and the series (7) terminates with the n'th term so that (7) reduces to a polynomial. These are the Laguerre polynomials $M(-n,1;x)=L_n^{(0)}(x)$ of degree n and order zero. In particular

$$L_0^{(0)}(x) = 1$$

$$L_1^{(0)}(x) = 1-x$$

$$L_2^{(0)}(x) = 2-4x + x^2)/2$$

$$L_3^{(0)}(x) = (6-18x + 9x^2 - x^3)/6$$

etc.

The numerical coefficients in (6a) or (6b) are given by the table:

α	$2^{\alpha/2}\Gamma(\frac{\alpha}{2}+1)$
1	$\sqrt{\pi/2}$
2	2
3	$1\cdot 3\sqrt{\pi/2}$
4	8
5	$1\cdot 3\cdot 5\sqrt{\pi/2}$
6	48
---	---

For the two-component mixture (3), the moments may then be written as

$$\overline{w^{\alpha}}\left[2^{\alpha/2}\Gamma(\alpha/2+1)\right]^{-1} = k\sigma_1^{\alpha}M(-\alpha/2,\ 1;-w_1^2/2\sigma_1^2) + (1-k)\sigma_2^{\alpha}M(-\alpha/2,1;-w_2^2/2\sigma_2^2) \tag{8}$$

The confluent hypergeometric function is easily computed using a hand-held calculator with a modest memory. This series is always convergent for negative values of the argument, as is the case in (8), and the error is always less than the first term neglected and of opposite sign. Still, for large values of $w_R^2/2\sigma^2$, a large number of terms may be required leading to unreasonably long computing time. This problem is solved by using the asymptotic expansion

$$M(a,b;-x) = \left[\Gamma(b)/\Gamma(b-a)x^a\right]\left\{1+a(1+a-b)/1!x + a(a+1)(1+a-b)(2+a-b)/2!x^2+---\right\} \tag{9}$$

(See Rice, in Wax, 1954.)

The use of the confluent hypergeometric series to compute the moments $\overline{w^{\alpha}}$ from (8) and (9) provides the mean scalar wind speed, $\overline{w}$, for α=1 and (using the appropriate factors for air density) the mean kinetic energy from $\overline{w^2}$, for α=2, and the mean wind power from $\overline{w^3}$, for α=3. When the parameters give a reasonably good fit to the frequency function data, the results of this method should be more reliable than using the frequency function data directly for this computation.

To obtain mean wind power for a particular device the function that describes its performance must be included in the integrand of (5) with the result that a numerical quadrature is required.

APPENDIX F

ANALYTICAL AND GEOMETRICAL PROPERTIES OF THE GENERALIZED RAYLEIGH P.D.F.

ANALYTICAL AND GEOMETRICAL PROPERTIES

In the following paragraphs, some analytical details concerning the generalized Rayleigh p.d.f. are derived in detail. Some of these were mentioned in Appendix A in a qualitative manner.

The generalized Rayleigh p.d.f. may be written as

$$p(w;\sigma,w_R) = (w/\sigma^2)e^{-(w^2+w_R^2)/2\sigma^2} I_o(ww_R/\sigma^2) \qquad (1)$$

where w = scalar wind speed

w_R = mean resultant wind speed

σ = component standard deviation of wind speed

The generalized Rayleigh p.d.f. for scalar wind speed is obtained exactly if the bivariate wind component p.d.f. is circularly normal. If $s=w/\sigma$ and $\lambda=w_R/\sigma$, then (1) becomes

$$p(s,\lambda) = s \cdot \exp\left[-(s^2+\lambda^2)/2\right] I_o(\lambda s) \qquad (2)$$

in which σ has been used as a scaling factor.

MOST PROBABLE WIND SPEED

The most probable wind speed is that for which $p(s,\lambda)$ attains its maximum as a function of s given λ (or where $p(w;\sigma,w_R)$ attains its maximum in w given the parameters σ,w_R).

Differentiating (2) with respect to s one obtains

$$\partial p/\partial s = \left[I_o(\lambda s)(1-s^2)+\lambda s I_1(\lambda s)\right] \exp\left[-(s^2+\lambda^2)/2\right]$$

and thence for the maximum one must solve the transcendental equation

$$I_0(\lambda s)(1-s^2)+\lambda s I_1(\lambda s)=0 \qquad (3)$$

for s given the parameter value λ. A workable procedure is to use an iteration technique with (3) written in the form

$$s_{n+1} = \left[1+\lambda s_n I_1(\lambda s_n)/I_0(\lambda s_n)\right]^{1/2} \qquad (4)$$

An initial value, s_0, is needed to start the iterations. The better the starting value, the more quickly will the sequence, s_n, n=1,2,---, converge to the solution of (3). Some manipulation of (3) using the power series (for small λs) and asymptotic series (for large λs) indicates that reasonable starting values are

$$s_0 = 1/\sqrt{1-\lambda^2/2} \quad , \quad \lambda \leq 0.8$$

and

$$s_0 = (\lambda+\sqrt{2+\lambda^2})/2, \quad \lambda \geq 0.8$$

The most probable value of s as a function of λ is shown as the central curve in Figure 31 of Appendix B.

Another method of computing the most probable value, s*, in terms of λ is to introduce the parameter $\xi=\lambda s$ so that one has the two equations

$$s^* = \left\{1+\xi\, I_1(\xi)/I_0/\xi)\right\}^{1/2}$$

$$\lambda = \xi/s^*$$

in parametric form. For each assignment of the independent variable ξ, a suitable pair s*,λ is obtained. Suitable tables of $I_0(\xi)$ and $I_1(\xi)$ are contained in Abramowitz and Stegun (1964).

INFLECTION POINTS

The inflection points of (1) or (2) are those at which the second derivative is zero. Differentiating (2) twice and setting the second

derivative with respect to s equal to zero gives the relation

$$s^4 I_0(\lambda s) - s^2 \left[3I_0(\lambda s) + 2\lambda s I_1(\lambda s) \right] + \lambda s \left[\lambda s I_0(\lambda s) + I_1/\lambda s) \right] = 0 \qquad (5)$$

which is another transcendent equation to be solved for s given λ. The results are illustrated in Figure 31 of Appendix B. One may also write (5) in terms of the variable $\xi = \lambda s$. Then if we let $B = \xi I_1(\xi)/I_0(\xi)$, (5) becomes

$$s^4 - s^2(3+2B) + (\xi^2+B) = 0$$

and

$$\lambda = \xi/s$$

so that the above may be considered as expressions for s, λ in terms of the parameter ξ. The quartic in s will have two positive roots corresponding to the left and right inflection points.

For $\xi=0$, the quartic has the root $\sqrt{3}$ for the righthand inflection point and a double root at s=0.

One may write the quartic in s as a quartic in λ (and the parameter ξ)

$$\xi^4 - \lambda^2\xi^2(3+2B) + \lambda^4(\xi^2+B) = 0$$

or

$$\lambda^4(1+B/\xi^2) - \lambda^2(3+2B) + \xi^2 = 0$$

Then for $\xi \to 0$, note that $B/\xi^2 \to 1/2$, $B \to 0$ so that in the limit for $\xi=0$ one has

$$\lambda^4(3/2) - \lambda^2 \cdot 3 = 0$$

which has roots $\lambda^2 = 0, 2$. The lefthand inflection point is then at s=0, $\lambda = \sqrt{2}$. On the range $0 < \lambda < \sqrt{2}$ the lefthand inflection point is at s=0. For $\lambda \geq \sqrt{2}$ both left and right inflection points are present (as shown in Figure 31 of Appendix B).

THE SHARPNESS OF THE MAXIMUM

The peakedness of the p.d.f. at the point of most probable scalar wind speed may be measured in terms of the parabolic approximation at that point. If one expands the p.d.f. in a power series about the most probable scalar wind speed, then

$$p(s,\lambda) = p(s^*,\lambda) + \frac{\partial^2 p}{\partial s^2}\Big|_{s^*} (s-s^*)^2/2! + \cdots$$

which may be written as

$$p(s,\lambda) = p(s^*,\lambda)\left[1-(s-s^*)^2/2L^2+\cdots\right]$$

in which L^2 is given by

$$L^2 = -\left[p/(\partial^2 p/\partial s^2)\right]_{s^*}$$

and L is the half width of the parabola that approximates the p.d.f. at its maximum measured at half the height of the maximum.

Since $\partial^2 p/\partial s^2 = e^{-(s^2+\lambda^2)/2}\left\{s^4 I_0(\lambda s) - s^2\left[3I_0(\lambda s)+2\lambda s I_1(\lambda s)\right] + \lambda s\left[\lambda s I_0(\lambda s)+I_1(\lambda s)\right]\right\}$

then

$$p/(\partial^2 p/\partial s^2) = s\left\{s^4 - s^2\left[3+2\lambda s I_1(\lambda s)/I_0(\lambda s)\right]+(\lambda s)^2+ s I_1(\lambda s)/I_0(\lambda s)\right\}^{-1}$$

Evaluating $\lambda s I_1(\lambda s)/I_0(\lambda s)$ at $s\approx s^*$ from (3) one has $\lambda s^* I_1(\lambda s^*)/I_0(\lambda s^*) = s^{*2}-1$

so that

$$L = \sigma/(s^{*2}+1/s^{*2}-\lambda^2)^{1/2}$$

For $\lambda=0$, $s^*=1$ and $L=\sigma/\sqrt{2}$. For large λ, note that s^* approaches λ in such a way that $s^{*2}\cong\frac{1}{2}+\lambda s^*$. Then

$$L \approx \sigma \left[(1/2+\lambda s^*)/(5/4+\lambda s^*)\right]^{1/2}$$

whence for $\lambda s^* \to \infty$ then $L \to \sigma$. Thus, the half width of the maximum at the half height has a small range and lies in the interval $0.707\sigma \leq L < \sigma$.

ASYMPTOTIC FORM OF THE P.D.F.

If the parameter product λs is large, then $I_0(\lambda s)$ in (2) may be replaced by its asymptotic form

$$I_0(\lambda s) \approx \left[e^{\lambda s}/\sqrt{2\pi\lambda s}\right]\left\{1+\frac{1}{8\lambda s}+\frac{1\cdot 9}{2!(8\lambda s)^2}+\frac{1\cdot 9\cdot 25}{3!(8\lambda s)^3}+\cdots\right\}.$$

Using only the first factor on the right above in (2) one obtains

$$p(s,\lambda) \approx \sqrt{s/2\pi\lambda}\,\exp\left[-(s-\lambda)^2/2\right] \qquad (6)$$

Since the factor $\sqrt{s/\lambda} = \sqrt{w/w_R}$ varies slowly compared with the exponential near $s=\lambda$, it is evident that for large λs, the p.d.f. is very much like the ordinary Gaussian p.d.f. with mean value λ and unit variance.

VALUES OF W_R, σ FOR GIVEN MOST PROBABLE SPEED W^*

It is convenient to know the functional relationship between w_R and σ for a given value of the most probable speed w^*. Two extreme cases may be set down at once. If $w_R=0$ (or $\lambda=0$) and $\sigma\neq 0$, it then follows from (3) (since $I_0(0)=1$, $I_1(0)=0$) that $s=1$, i.e., that $\sigma=w^*$. From (6) it is readily seen that for large values of the product λs, the maximum of the p.d.f. is near $s=\lambda$ for small values of σ. This then means that for $\sigma\to 0$ one has $w^*=w_R$.

The functional relation between w_R and σ for a given w^* follows immediately from the solution of (3). Let this solution be $s^*=w^*/\sigma$ for which $\lambda=w_R/\sigma$. Then $\lambda=(w_R/w^*)/(\sigma/w^*)$ and so $(\sigma/w^*)=1/s^*$ and $w_R/w^*=\lambda/s^*$.

Thus, given λ, the computation of s^* leads to the ratios σ/w^* and w_R/w^*. These values are shown in Figure 41.

SERIES EXPANSION FOR SMALL s

The behavior of the p.d.f. for small values of s is conveniently given by the series expansion about s=0. When $e^{-s^2/2}$ and $I_0(\lambda s)$ are expanded in series and the product formed, one obtains

$$p(s,\lambda) = e^{-\lambda^2/2}\left[s+(\lambda^2-2)s^3/4+(\lambda^4-8\lambda^2-8)s^5/(2!)^2 4^2 + (\lambda^6-18\lambda^4+72\lambda^2-48)s^7/(3!)^2 4^3+---\right].$$

Differential Equation

The generalized Rayleigh p.d.f. contains the factor $I_0(\lambda s)$, $\lambda=w_R/\sigma$, $s=w/\sigma$ and since $I_0'(x) = I_1(x)$ and $I_n'(x) = I_{n-1}(x)-(n/x)I_n(x)$ one may eliminate $I_0(\lambda s)$ and $I_1(\lambda s)$ from the p.d.f. and its first two derivatives with respect to s to obtain the linear homogeneous differential equation

$$s^2(\partial^2 p/\partial s^2)+s(2s^2-1)(\partial p/\partial s)+(1+s^4-\lambda^2 s^2)p = 0$$

or in terms of the original variables

$$\sigma^4 w^2(\partial^2 p/\partial w^2)+\sigma^2 w(2w^2-\sigma^2)(\partial p/\partial w)+(\sigma^4+w^4-w_R{}^2 w^2)p = 0.$$

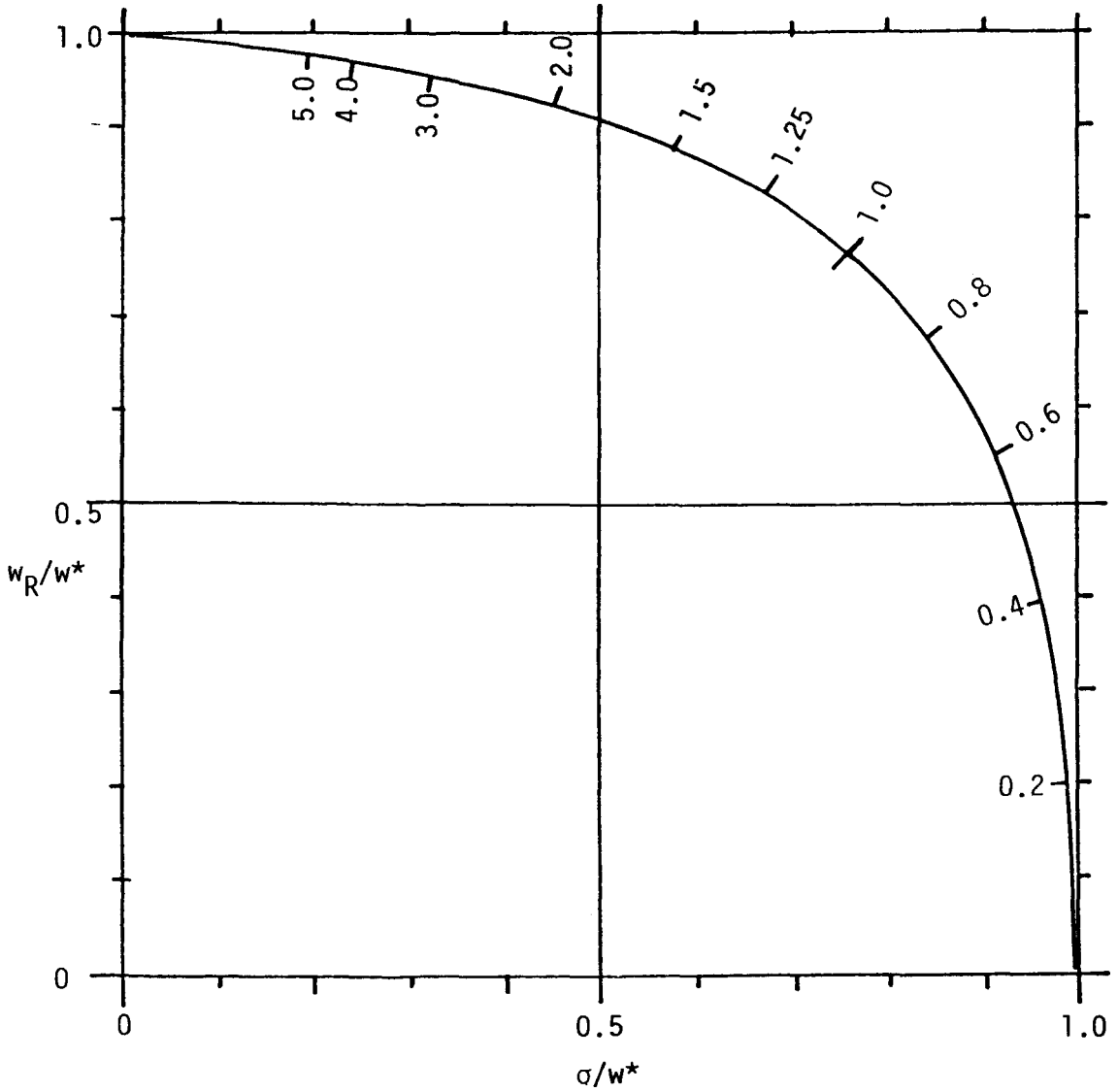

Figure 41. The Relation Between w_R and σ for a Given Value of the Most Probable Wind Speed, w^*. The labled points on the curve indicate the values of $\lambda=w_R/\sigma$.

APPENDIX G

EXPRESSIONS FOR THE GENERALIZED RAYLEIGH D.F.

EXPRESSIONS FOR THE GENERALIZED RAYLEIGH D.F.

Scalar wind speed data is usually tabulated in terms of the "frequency function;" i.e., the fraction of occurrences (usually in percent) of wind speed in a system of class intervals. The frequency function is related to the probability density function (p.d.f.) in that it is equal to the integral of the p.d.f. over the range of each class interval. If (w_{i-1}, w_i) represents a class interval, f_i the frequency function, and $p(w)$ the p.d.f., then

$$f_i = \int_{w_{i-1}}^{w_i} p(w)dw$$

it then follows that

$$f_i/(w_i - w_{i-1}) = p(\xi),\ w_{i-1} \leq \xi \leq w_i$$

so that the p.d.f. at the point ξ is the frequency function divided by the width of the class interval. The difficulty here lies in the fact that the location of ξ on the range (w_{i-1}, w_i) is not known. All that is explicitly known is that such a point exists, in fact there may be several such points. In the case of data on the scalar wind speed the nominal choice as $\xi \sim (w_i + w_{i-1})/2$ turns out to be rather poor in general.

One can do a little better by considering the distribution function (D.F.) rather than the p.d.f. The D.F. is defined as

$$P(w_i) = \int_0^{w_i} p(w)dw$$

and is the probability that the scalar speed of the wind is less than (or equal to) the value w_i. If the wind speed data is given in terms of the frequency function, f_i, i=1,---,n, over class intervals (w_{i-1}, w_i), then one has

$$\sum_{k=1}^{i} f_k = \int_0^{w_i} p(w)dw = P(w_i);$$

i.e., the D.F. at the class interval division point w_i is the sum of the frequency function values over all class intervals with upper end points less than or equal to w_i. The values of w_i can be specified with reasonable accuracy.

In the case of the generalized Rayleigh p.d.f., the D.F. is given by the expression

$$P(w;\sigma,w_R) = \int_0^w (v/\sigma^2)e^{-(v^2+w_R^2)/2\sigma^2} I_0(vw_R/\sigma^2)dv \qquad (1)$$

This integral cannot be evaluated explicitly in terms of a finite number of elementary functions.

SERIES EXPANSIONS

If one makes the substitution $x=w^2/2\sigma^2$, $y=w_R^2/2\sigma^2$ in (1), expands the factor $I_0(-)$ in infinite series, and integrates term by term, the resulting infinite series for $P(x,y)$ becomes

$$1-P(x,y) = e^{-(x+y)} \sum_{n=0}^{\infty}(y^n/n!) \sum_{k=0}^{n}(x^k/k!) \qquad (2)$$

In the form (2) the series is in terms of increasing powers of y and $y^n/n!$ has as coefficient a polynomial of n'th degree in x. To obtain the power series

$$P(x,y) = \sum_{n=0}^{\infty} a_n x^n$$

where the coefficients a_n are functions of y, one merely expands (2) and collects terms in like powers of x after converting e^{-x} to a power series in x and multiplying the two. The end result is the expression

$$P(x,y) = e^{-y} \sum_{n=1}^{\infty}(-1)^{n-1}\left[\sum_{k=0}^{n-1}(-1)^k\binom{n-1}{k}(y^k/k!)\right](x^n/n!) \qquad (3)$$

or showing the leading terms

$$P(x,y) = e^{-y}\left\{x-(1-y)x^2/2+(1-2y+y^2/2)x^3/6 - (1-3y+y^2/3-y^3/6)x^4/24+---\right\} \tag{3a}$$

and in terms of the original variable and parameters

$$P(w;\sigma,w_R) = \exp(-w_R^2/2\sigma^2)\left\{w^2/2\sigma^2-(1-w_R^2/2\sigma^2)w^4/8\sigma^4 +(1-w_R^2/\sigma^2+w_R^4/8\sigma^4)w^6/48\sigma^6-(1-3w_R^2/2\sigma^2+w_R^4/12\sigma^4-w_R^6/48\sigma^6)w^8/384\sigma^8+---\right\} \tag{3b}$$

In Appendix D it was noted that the diagram with coordinates $x = \sqrt{-2\ln(1-P)}$, $y=w$ was useful for a graphical representation of the distribution function. The series expansion permits the determination of the shape of the curve $p=p(w)$ for small values of w. If, however, one has a two-component mixture of distribution functions, one must combine these before taking the logarithm of (1-P). Thus, for the mixture

$$P = kP_1(w;\sigma_1,w_1)+(1-k)P_2(w;\sigma_2,w_2)$$

one must form the series

$$\begin{aligned} 1-P &= k(1-P_1)+(1-k)(1-P_2) \\ &= 1-\left[ke^{-y_1/\sigma_1^2}+(1-k)e^{-y_2/\sigma_1^2}\right](w^2/2) \\ &+\left[k(1+y_1)e^{-y_1/\sigma_1^4}+(1-k)(1+y_2)e^{-y_2/\sigma_2^4}\right](w^2/2)^2/2!+--- \end{aligned}$$

Then

$$\sqrt{-2\ln(1-P)} = \left[ke^{-y_1/\sigma_1^2}+(1-k)e^{-y_2/\sigma_2^2}\right]^{1/2}w+---$$

where only the first power term is included. The slope of the curve representing the mixture at w=0 is then given by m (if y=mx in the diagram) where

$$m = \left\{(k/\sigma_1^2)\exp(-w_1^2/2\sigma_1^2) + \left[(1-k)/\sigma_2^2\right]\exp(-w_2^2/2\sigma_2^2)\right\}^{-1/2}.$$

ASYMPTOTIC EXPRESSIONS

In terms of the variables $s=w/\sigma$, $\lambda=w_R/\sigma$ one may write

$$P(s,\lambda) = \exp\left[-(s^2+\lambda^2)/2\right] \sum_{n=1}^{\infty} (s/\lambda)^n I_n(\lambda s) \tag{4}$$

and

$$1-P(s,\lambda) = \exp\left[-(s^2+\lambda^2)/2\right] \sum_{n=0}^{\infty} (\lambda/s)^n I_n(\lambda s) \tag{5}$$

The relation (4) is given by Rice (see Wax, 1954). The asymptotic expansion for $I_n(z)$ is (Abramowitz and Stegun, 1964)

$$I_n(z)\sim(e^z/\sqrt{2\pi z})\left\{1-(4n^2-1)/8z+(4n^2-1)(4n^2-9)/2!(8z)^2 + (4n^2-1)(4n^2-9)(4n^2-25)/3!(8z)^3+---\right\} \tag{6}$$

Using only the first term of the series factor of (6) in (4) and (5) leads to the asymptotic approximations for $\lambda s \gg 1$, $s<\lambda$

$$P(s,\lambda)\sim(s/2\pi\lambda)^{1/2}\left\{\exp\left[-(s-\lambda)^2/2\right]\right\}/(\lambda-s) \tag{7a}$$

and for $\lambda s \gg 1$, $\lambda<s$

$$P(s,\lambda)\sim 1-(s/2\pi\lambda)^{1/2}\left\{\exp\left[-(s-\lambda)^2/2\right]\right\}/(s-\lambda). \tag{7b}$$

Rice (see Wax, 1954, p. 241) gives the form

$$P(s,\lambda) = (1/2)\left\{1+\mathrm{erf}\left[(s-\lambda)/2\right]\right\} - (2\lambda\sqrt{2\pi})^{-1}\left\{\exp\left[-(s-\lambda)^2/2\right]\right\}\left\{1-(s-\lambda)/4a+\left[1+(s-\lambda)^2\right]/8a^2\right\} \tag{8}$$

which is valid for $\lambda s \gg 1$ and $\lambda \gg |s-\lambda|$.

THE DERIVATIVES

Termwise differentiation of (2) gives the expressions

$$\partial P/\partial x = \exp\left[-(x+y)\right] \sum^{\infty} (xy)^n/n!)^2 \tag{9}$$

$$\partial P/\partial y = -\exp\left[-(x+y)\right] \sum x^{n+1}y^n/(n+1)!n! \tag{10}$$

which may be written in terms of the modified Bessel function as

$$\partial P/\partial x = \exp\left[-(x+y)\right] I_0(2\sqrt{xy}) \tag{11}$$

and

$$\partial P/\partial y = -(\sqrt{x/y})\exp\left[-(x+y)\right] I_1(2\sqrt{xy}) \tag{12}$$

In terms of the original variables, note that

$$\partial P/\partial w = (\partial P/\partial x)(\partial x/\partial w)+(\partial P/\partial y)(\partial y/\partial w) \tag{13}$$

$$\partial P/\partial \sigma = (\partial P/\partial x)(\partial x/\partial \sigma)+(\partial P/\partial y)(\partial y/\partial \sigma) \tag{14}$$

$$P/\partial w_R = (\partial P/\partial x)(\partial x/\partial w_R)+(\partial P/\partial y)(\partial y/\partial w_R) \tag{15}$$

and since $x=w^2/2\sigma^2$, $y=w_R^2/2\sigma^2$, then

$$\partial x/\partial w = w/\sigma^2 = 2x/w,\ \partial x/\partial \sigma = -w^2/\sigma^3 = -2x/\sigma,\ \partial x/\partial w_R = 0$$

$$\partial y/\partial w = 0,\ \partial y/\partial \sigma = -w_R^2/\sigma^3 = -2y/\sigma,\ \partial y/\partial w_R = w_R/\sigma^2 = 2y/w_R$$

so that

$$\partial P/\partial w = (2/w)(x\partial P/\partial x) \tag{16}$$

$$\partial P/\partial \sigma = (-2/\sigma)\left[x\partial P/\partial x+y\partial P/\partial y\right] \tag{17}$$

$$\partial P/\partial w_R = (2/w_R)(y\partial P/\partial y) \tag{18}$$

APPENDIX H

DETERMINATION OF THE PARAMETERS

DETERMINATION OF THE PARAMETERS

METHOD OF NON-LINEAR LEAST SQUARES

The parameters σ_1, w_1, σ_2, w_2, k of the two component mixture of distribution functions (D.F.s)

$$P(w;-) = kP_1(w;\sigma_1,w_1)+(1-k)P_2(w;\sigma_2,w_2) \qquad (1)$$

where $P_i(w;\sigma_i,w_i)$, i=1,2 are generalized Rayleigh D.F.s was carried out using the method of least squares. The symbol P(w;-) is used to indicate dependence on parameters not explicitly listed. Let the data given consist of the sequence of wind speeds w_i, i=1,---,n and let $P_o(w_i)$ consist of the values of the probability that the wind speed is less than w_i. Then the sum of the squares of the errors for given values of the parameters is given by

$$\sum_{j=1}^{n}\left[P_o(w_j)-P(w_j;-)\right]^2 = F(\sigma_1,w_1,\sigma_2,w_2k) \qquad (2)$$

which is a function of the five parameters concerned.

It is required that values of the parameters be determined that minimize this function. There are many procedures for doing this. Nash (1979), p. 118-209, is devoted to this subject and gives references to the more important original papers. The method used here is a combination of the Newton-Raphson method and the method of steepest descent (see Nash (1979), p. 175, Algorithm 23). An outline of the technique is given here to clarify the steps required in the computer program (Appendix J).

The function $F(\sigma_1,w_1,\sigma_2,w_2,k)$ in (2) will be a minimum if the five partial derivatives with respect to the parameters are set equal to zero. This gives five equations which in theory provide the required solution, but which cannot be solved by elementary methods. To simplify the situation, $P(w_j;-)$ in (2) is approximated by estimating the parameters, say $\hat{\sigma}_1,\hat{w}_1,\hat{\sigma}_2,\hat{w}_2,\hat{k}$, and expanding as a series through the linear terms

$$P(w_j;-) = P_{jo}+(\partial P_j/\partial\sigma_1)_o\,\Delta\sigma_1+---+(\partial P_j/\partial k)_o\,\Delta k+--- \qquad (3)$$

where P_{jo} is the function evaluated at wind speed w_j using the estimates and $(\partial P_j/\partial\sigma_1)_o$,--- are the partial derivatives evaluated in the same way. The increments $\Delta\sigma_1$,---, Δk are unknown parameter increments to be found in anticipation that $\sigma_1=\sigma_1+\Delta\sigma_1$,---,$k=k+\Delta k$ when substituted in (2) will give a smaller value of the sum of the squares of the errors.

To shorten the notation, let $x_1=\Delta\sigma_1$, $x_2=\Delta w_1$, $x_3=\Delta\sigma_2$, $x_4=\Delta w_2$, $x_5=\Delta k$ and let $(\partial P_j/\partial\sigma_1)_o = P_{1j}$,$(\partial P_j/\partial w_1)_o = P_{2j}$, $(\partial P_j/\partial\sigma_2) = P_{3j}$,$(\partial P_j/\partial w_2) = P_{4j}$, $(\partial P_j/\partial k)_o - P_{5j}$ so that (2) becomes

$$\sum_{j=1}^{n}\left\{\left[P_o(w_j)-P_{jo}\right] -P_{1j}x_1-P_{2j}x_2-P_{3j}x_3-P_{4j}x_4-P_{5j}x_5\right\}^2 = G(x_1,x_2,--,x_5) \qquad (4)$$

which is to be minimized in x_1,---,x_5. This is now a linear problem for which the solution process is elementary. The partial derivatives with respect to the x's are easily obtained with the result that on being set equal to zero one has five linear equations

$$(\sum_j P_{1j}^2)x_1+(\sum_j P_{1j}P_{2j})x_2+---+(\sum_j P_{1j}P_{5j})x_5 = \sum_j\left[P_o(w_j)-P_{jo}\right]P_{1j}$$

$$(\sum_j P_{2j}P_{1j})x_1+(\sum_j P_{2j}^2)x_2+---+(\sum_j P_{2j}P_{5j})x_5 = \sum_j\left[P_o(w_j)-P_{jo}\right]P_{2j} \qquad (5)$$

$$(\sum_j P_{5j}P_{1j})x_1+(\sum_j P_{5j}P_{2j})x_2+---+(\sum_j P_{5j}^2)x_5 = \sum_j\left[P_o(w_j)-P_{jo}\right]P_{5j}$$

which may be written as

$$\sum_{j=1}^{5}a_{ij}x_j = g_i,\ i = 1,---,5 \qquad (6)$$

One should note that in using the empirical distribution function of (1) that there are some simplifications (as far as computation is concerned but not in writing the expressions). Then

$$a_{11} = k^2 \sum_j (\partial P_1/\partial \sigma_1)^2_j,\ a_{12} = k^2 \sum_j (\partial P_1/\partial \sigma_1)(\partial P_1/\partial w_1)_j$$
$$a_{21} = a_{12} \qquad ,\ a_{22} = k^2 \sum_j (\partial P_1/\partial w_1)^2_j \tag{7}$$

$$a_{33} = (1-k)^2 \sum_j (\partial P_2/\partial \sigma_2)^2_j\ ,\ a_{34} = (1-k)^2 \sum_j (\partial P_2/\partial \sigma_2)(\partial P_2/\partial w_2)_j$$
$$a_{43} = a_{34} \qquad ,\ a_{44} = (1-k)^2 \sum_j (\partial P_2/\partial w_2)^2 \tag{8}$$

$$a_{13} = k(1-k) \sum_j (\partial P_1/\partial \sigma_1)(\partial P_2/\partial \sigma_2)_j,\ a_{14} = k(1-k) \sum_j (\partial P_1/\partial \sigma_1)(\partial P_2/\partial w_2)_j$$
$$a_{23} = k(1-k) \sum_j (\partial P_1/\partial w_1)(\partial P_2/\partial \sigma_2)j,\ a_{24} = k(1-k) \sum_j (\partial P_1/\partial w_1)(\partial P_2/\partial w_2)_j \tag{9}$$

$$a_{31} = a_{13},\ a_{41} = a_{14},\ a_{32} = a_{23},\ a_{42} = a_{24} \tag{10}$$

$$a_{15} = a_{51} = k \sum_j (P_1-P_2)(\partial P_1/\partial \sigma_1)j,\ a_{25} = a_{52} = k \sum (P_1-P_2)(\partial P_1/\partial w_1)j$$
$$a_{35} = a_{53} = (1-k) \sum_j (P_1-P_2)(\partial P_2/\partial \sigma_2)j,\ a_{45} = a_{54} = (1-k) \sum (P_1-P_2)(\partial P_2/\partial w_2)j \tag{11}$$

$$a_{55} = \sum_j (P_1-P_2)^2 \tag{12}$$

$$g_1 = k \sum_j (P_o-P)(\partial P_1/\partial \sigma_1)j,\ g_2 = k \sum_j (P_o-P)(\partial P_1/\partial w_1)j$$
$$g_3 = (1-k) \sum_j (P_o-P)(\partial P_2/\partial \sigma_2)j,\ g_4 = (1-k) \sum_j (P_o-P)(\partial P_2/\partial w_2)j \tag{13}$$
$$g_5 = \sum (P_o-P)(P_1-P_2)j$$

The computation of the increments $x_1,---,x_5$ was carried out using a modification of Nash (1979) which in turn is based on a method of Marquardt (see Nash 1979). This involves a modification of the diagonal terms of the matrix of coefficients of (6) to

$$a_{ii}(1+\lambda)+a\lambda$$

where a=1 is used to avoid singularity of the equations and λ is Marquardt's parameter, initially taken as 0.0001. For λ=0 the method corresponds to the Newton-Raphson technique; for relative large λ it approaches the method of steepest descent. If, at the end of an iteration step the sum of square has decreased, the Marquardt parameter λ is decreased to 0.4λ for the next step (in which the coefficients a_{ij},g_i of (6) are reevaluated). If the sum of squares has not decreased the Marquardt parameter is increased to 10λ and a solution obtained without recomputation of the coefficients. Iteration was stopped when the parameter increments were small (0.0001).

A further modification was made to take advantage of the fact that this particular least squares problem is linear in the mixing ratio k. Given the parameter values $\sigma_1,w_1,\sigma_2,w_2$ the best value of k is readily obtained from

$$k = \sum_j (P_o-P)(P_1-P_2) / \sum_j (P_1-P_2)^2 \qquad (14)$$

where in (14) the values of P_o are the observed values of the distribution function $P_o(w_j)$ and those of P are computed at w_j from (1). The values of P_1 and P_2 are those of the individal terms on the right of (1).

INITIAL ESTIMATES

The direct minimization of the sum of the squares of the errors described in the preceding section requires as input information reasonable estimates of the parameters $\sigma_1,w_1,\sigma_2,w_2$. No estimate for k is required

in general since the minimization problem is linear in k (i.e., given σ_1, w_1, σ_2, w_2 a best k may be obtained easily from (14)).

The problem of the initial estimates of the parameters may be handled graphically using techniques outlined in Appendix D (if only a few cases are to be investigated) or it may be handled analytically. This later case is described in this section.

A basic assumption is made to simplify the work required: that one may estimate the parameters σ_1, w_1 that determine the low wind speed shape of the distribution function from low wind speed data ignoring the effect of σ_2, w_2 and conversely that the parameters σ_2, w_2 may be determined from the high wind speed data ignoring the effect of the low wind speed parameters σ_1, w_1. This assumption is not necessarily true, but seems to provide a good operating basis that straightens itself out in subsequent steps of the computations.

Another aspect of the initial estimate problem lies in the fact that one must be prepared to handle several special cases that may lead to simple satisfactory solutions, simple solutions of sufficient accuracy being preferred to complex solutions of only a little more accuracy.

ESTIMATION OF THE HIGH WIND SPEED PARAMETERS

The estimation of the high wind speed parameters is carried out on a highly simplified basis from the tabulated values of the frequency function. In general the speed ranges in the various intervals is not uniform, but the range changes between adjacent intervals at the high speed end is relatively small so that the estimates are sufficiently accurate. The frequency function is checked starting at the high speed end until a maximum is reached or until two ranges show the same value. The wind speed at the upper end of such an interval is taken as an estimate of w_2. The estimate of σ_2 is based on the assumption that the decrease in the frequency function is Gaussian toward the higher wind speeds, i.e.,

$$f(w) = f(w_2)\exp\left[-(w-w_2)^2/2\sigma_2^2\right] \qquad (1)$$

Then if $w_0>w_2$ is the next higher wind speed tabulated and f_0 the tabulated frequency function, $f_0=f(w_0)$, $f_2=f(w_2)$, it follows from (1) that

$$\sigma_2 = (w_0-w_1)/\sqrt{2\ln(f_2/f_0)} \qquad (2)$$

ESTIMATION OF THE LOW WIND SPEED PARAMETERS

The low wind speed parameters are estimated from the first three points of the D.F. using the infinite series expansion of this function about zero speed

$$P(w) = (e^{-y}/2\sigma^2)w^2 - \left[(1-y)e^{-y}/8\sigma^4\right]w^4 + \left[(1-2y+y^2/2)e^{-y}/48\sigma^6\right]w^6 + \cdots \qquad (5)$$

where $y=w_R^2/2\sigma^2$ (see Appendix G).

Degenerate Case

The first test is made for the presence of the degenerate case $P(w) = k+(1-k)P(w;\sigma_1,w_1)$ in which case (5) is used for $P(w;\sigma_1,w_1)$. In this case the D.F. is fitted to the polynomial

$$P(w) = A+Bw^2 + Cw^4 \qquad (6)$$

and the parameters identified with the coefficients using

$$A=k,\ B=(1-k)e^{-y}/2\sigma^2,\ C=-(1-k)\left[(1-y)e^{-y}/8\sigma^4\right] \qquad (7)$$

Obviously, for a proper degenerate case $0<A<1$ and $B>0$ so the degenerate case is ruled out if these inequalities are not satisfied. Also one notes that

$$\left[B^2 + 2(1-A)C\right]/B^2 = 1-(1-y)e^{+y} \qquad (8)$$

is independent of k and is positive for all y. If the expression on the left is positive, this relation is solved for y. Then

$$\sigma_d = 0.5\left[(1-y)B/(-C)\right]^{1/2}$$
$$w_d = \sigma_d\sqrt{2y} \tag{9a}$$

are used as the parameters for the degenerate case. If the left side of (8) is not positive it is assumed that y=0 and the estimates

$$\sigma_d = 0.5\sqrt{8/(-C)}$$
$$w_d = 0 \tag{9b}$$

are used.

NON-DEGENERATE LOW WIND SPEED ESTIMATES

The non-degenerate low wind speed parameter estimated are made by letting

$$P(w)/w^2 = A+Bw^2 + Cw^4 \tag{10}$$

to the first three data points and using

$$A = e^{-y}/2\sigma^2,\ B = -(1-y)e^{-y}/8\sigma^4,\ C = (1-2y+y^2/2)e^{-y}/48\sigma^6 \tag{11}$$

If $A>0$ and $B\neq 0$ it follows that

$$R^2 = (2B^2-3AC)/B^2 = y^2/(1-y)^2,\ y = w_R^2/2\sigma^2 \tag{12}$$

so that if $R^2>0$ then there are two possible positive roots for y. For $B<0$, $y=R/(R+1)$ while for $B>0$ then $y=R/(R-1)$, so that one must have $R>1$ for $y>0$ in this case. One then obtains two estimates for σ_1, w_1 given by

$$\sigma_1 = \sqrt{A(1-y)/(-B)} \tag{13}$$

$$w_1 = \sigma_1 \sqrt{2y} \tag{14}$$

depending on the selection of the root for y.

Another expression that may be used is

$$Q = (A^2+2B)/A^2 = 1-(1-y)e^y \tag{15}$$

In this case if $Q > 0$ the transcendental relation (15) may be easily solved for y with the resulting estimates for σ_1, w_1

$$\sigma_1 = \sqrt{e^{-y}/2A} \tag{16}$$

$$w_1 = \sigma_1 \sqrt{2y} \tag{17}$$

There are then three possible non-degenerate estimates of the parameters σ_1, w_1 for the low wind speeds. Of these, usually only two occur in any particular case and occasionally only one.

The special case for $w_1=0$, $\sigma_1 \neq 0$, is of considerable importance and is always tested. In this case one uses y=0 in (11) from which $\sigma_1=(1/2)\sqrt{A/(-B)}$ or $\sigma_1=(1/2)\sqrt{(-B)/C}$ or both depending on the signs of A,B,C and whether $B \neq 0$ and/or $C \neq 0$. Where both exist the average value is used as the estimate of σ_1.

In the above parameter estimates from (10) only the first three data points are used. Data irregularities in this region are frequent and may easily lead to no valid parameter estimates. This is particularly the case in which $P(w_i)$, $w_1 < w_2 < w_3$ is very small. In this event one may solve

$$P/w^2 = A+Bw^2 \tag{18}$$

for A and B using w_2 and w_3. If this yields A>0 and Q>0 from (15) the estimates (16) and (17) remain valid.

If the data is so irregular that even this fails to give a reasonable estimate of the parameters σ_1, w_1, then one may use $A \approx \left[P(w_1)/w_1^2+P(w_2)/w_2^2+P(w_3)/w_3^2\right]/3$ to obtain the special case estimate

$$\sigma_1 = \sqrt{1/2A} \tag{19}$$

$$w_1 = 0 \tag{20}$$

The following flow charts indicate the logic in making the various initial estimates. In most cases it has been found that all of the valid initial estimates should be tried. This is due to the fact that the least squares solution process does not necessarily converge to a unique minimum. In fact it is not infrequent that given two not widely different initial estimates one (or even both) may not converge to a reasonable minimum at all.

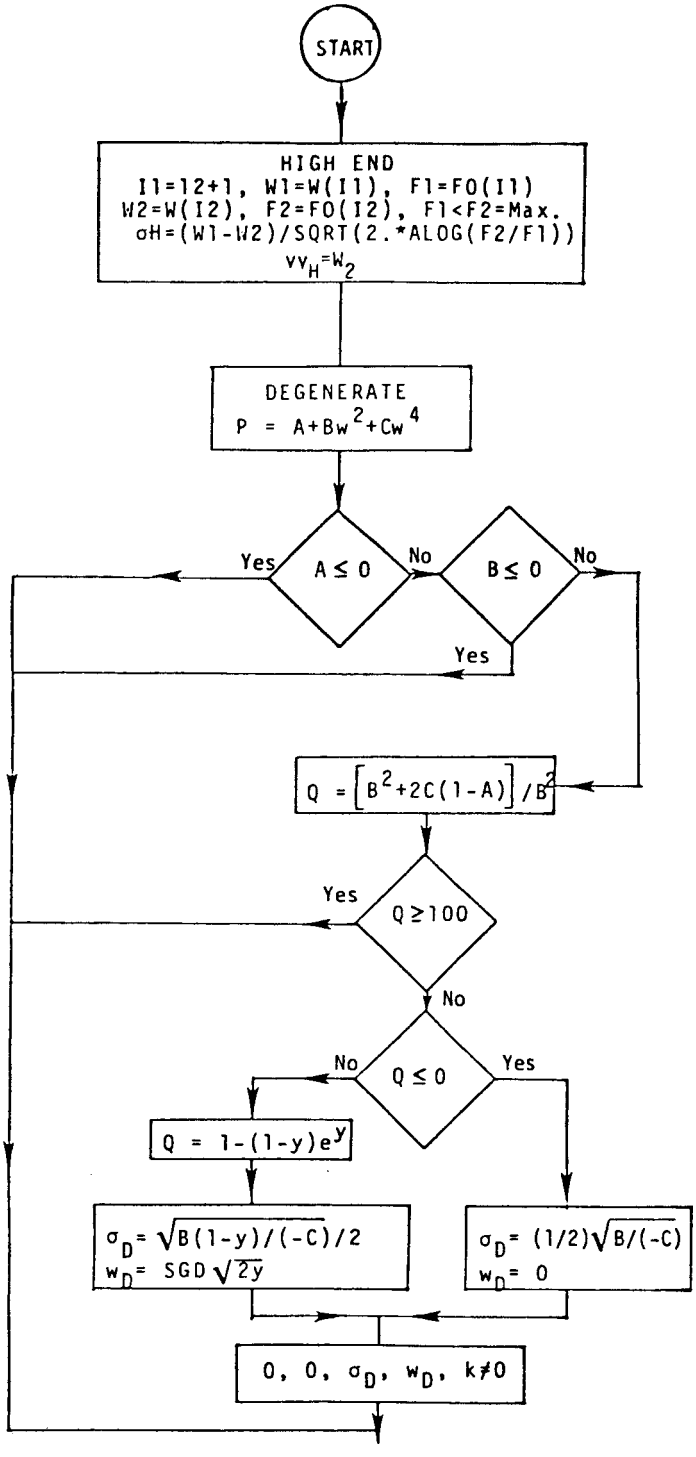

(CONT.)

Figure 42. Flow Chart for Parameter Estimation, High Speed Estimate and Degenerate Case

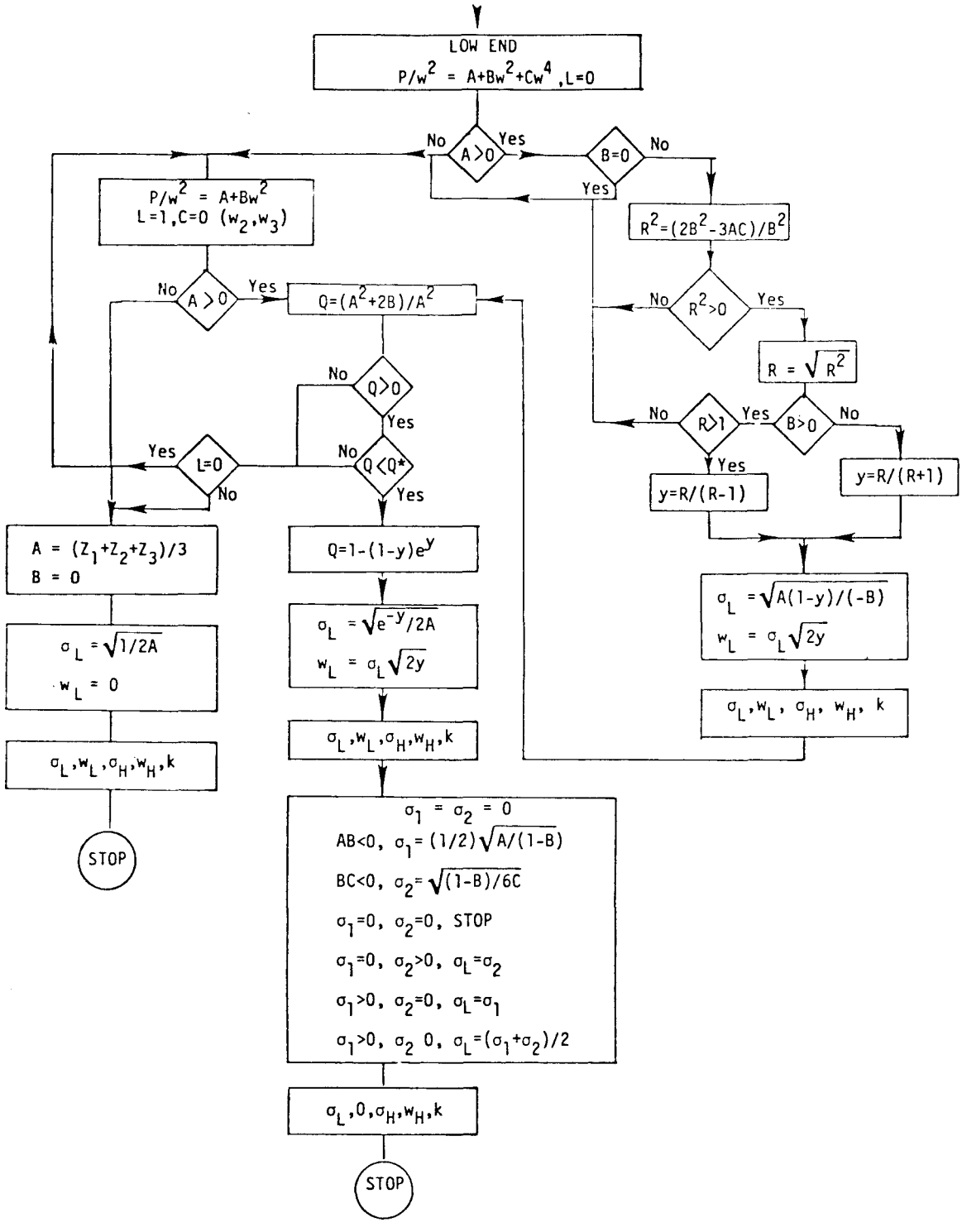

Figure 43. Flow Chart for Parameter Estimation, Non-degenerate Cases

APPENDIX J

COMPUTER PROGRAM

COMPUTER PROGRAM

The main program, PARAMS, is listed beginning on page 210. The subroutines are listed as PROB, p. 217; CHOL1, p. 219; CHOL2, p. 220; KBEST, p. 221; MARQ, p. 222, COEF, p. 224; SOLV, p. 225; ROOT, p. 225. These are discussed under the headings indicated in the following sections.

PROGRAM PARAMS

The main program (1) accepts a variety of housekeeping parameters, and (2) the input frequency function table. This information is (3) organized into a standard format and (4) output for reference. It then either (5) accepts initial estimates of the parameters or (6) computes such estimates from the frequency function. The initial estimates are then (7) subjected to an iteration procedure from which final values that minimize the sum of the squares of the errors are obtained.

The data input requires housekeeping procedures since data from various sources differed widely one from another. The basic inputs for program control are listed with the format statement number under which they are read:

IWE (1002) = 0, skip error details
= 1, write error details

IWD (1002) = 0, skip iteration parameters below
= 1, write IT = iteration number, SS = sum of squares, EMQ = Marquardt parameter
= 2, write also G(I) = righthand term of normal equation (modified) and X(I) = computed parameter increments (I = 1,---,5)

IUI (1002) = wind speed input units, 1=mph, 2=kts, 3=mps

IUO (1002) = wind speed output units, 1=mph, 2=kts, 3=mps

IMI (1002) = anemometer height input, 1=ft, 2=m

IMMO (1002) = anemometer height output, 1=ft, 2=m

EMQQ (1024) = Marquardt parameter

PX (1024) = smallest frequency function value used in high end parameter estimates

M (2004) = number of wind speeds in the frequency function table

W(I), I=1, M, (1004) = wind speed frequency function table (the speed at the high end of each class interval)

MS (2004) = number of stations in a batch (used where several stations have identified frequency function table formats)

ISTN (1005) = station name

JA, JB, JD (7000) JD = 1,2,3 to assign hour, month, and level

MB (7000) = number of frequency function tables in a batch

NC (2005) = index for level, month, hour

N (2005) = number of items in the frequency function table

CT (2005) = number of cases tabulated (100 if frequency function given in percent) CT=0 leaves frequency function table unchanged

NE (2005) = 0 to use last parameter values as estimates for next frequency function table, =-1 to compute initial parameter estimates

FO(I), I=1, N, (1007) = input frequency function table

The first step of the computations consists of checking the frequency function table and where necessary inserting the frequency of calms in the lowest wind speed class interval. At the same time distribution function values are calculated. The whole is then printed out for reference and checking.

The initial parameter estimates (XE(I), I=1,5) are then input or initial estimates are computed from the values of the probability density function (or frequency function) and the final estimates calculated by iteration in the subroutine MARQ. The details of calculating the initial estimates are covered in Appendix H.

SUBROUTINES

The subroutines are discussed in the order in which they appear in the program listing.

PROB(-) -- This subroutine is used to compute the generalized Rayleigh distribution function and its derivatives with respect to the parameters at the given wind speed points.

CHOL1(-) -- The lower triangular matrix corresponding to the symmetric matrix input is computed.

CHOL2(-) -- The triangular matrix from CHOL1(-) is used to solve the equations for the increments to be added to the parameter estimates to obtain a smaller sum of squares of the errors.

KBEST(-)-- This subroutine serves two functions. It uses the most recent estimates of the first four parameters to get the value of k=x(5) that yields the smallest sum of squares of the errors, (x(I), I=1,4) being fixed. It also is used to compute the sum of squares of the errors.

MARQ(-) -- This subroutine could have been included as a part of the main program. It is used to control the iteration process. The method used is described in Nash (1979), Algorithm 23, p. 175. Some inconsequential modifications have been made so that iterations are terminated when the required accuracy is obtained. Otherwise they would continue till the results are comparable to the machine accuracy. This shortened the iteration process considerably.

COEF(-) -- The matrix of coefficients and vector of non-homogeneous terms is calculated for new parameter estimates.

SOLV(-) -- Solves a set of three equations used in the computation of parameter estimates.

ROOT(-) -- Solves a transcendental equation to obtain the root used in the computation of parameter estimates.

```
      PROGRAM PARAMS
C     DETERMINE UP TO 5 PARAMETERS OF WIND SPEED DISTRIBUTION FUNCTION
C     FROM FREQUENCY TABLE DATA
      INTEGER DEVICE
      LOGICAL CHAR(1),ISTN(16),IFILE(11)
      DIMENSION FACT(3,3),UN(2),VEL(3),E1(5),FO(20),EE(20),STD(5),XE(5)
     *          ,FAC2(2,2),WW(20),FF(20),Z(5),TT(5)
      COMMON/BK1/N,W(20),FO(20),X(5)/BK2/A(15),G(5)
      COMMON/DEVICE/DEVICE
      DATA PI/3.141596/,FACT/1.,0.8684,0.44705,1.1516,1.,0.5148,
     *2.2369,1.94250,1./,UN/2HFT,1HM/,VEL/3HMPH,3HKTS,3HMPS/
     *,FAC2/1.0,3.2808,0.3048,1.0/
C     READ/WRITE CONTROLS. E1(I),I=1,5,=BOUND FOR INCREMENTS
      CALL OPEN(6,'WINDDATADAT',2)
      WRITE(3,9999)
      READ(3,9991)DEVICE
 9999 FORMAT(' ENTER DEVICE NO. FOR OUTPUT - CRT=3,PRINTER=2,DISKB=10 '
 9991 FORMAT(I2)
      CALL OPEN(10,'DATAFILEDAT',2)
      READ(6,1102)IFILE
 1102 FORMAT(11A1)
      CHAR(1)=IFILE(1)
      IF(CHAR(1).EQ.'0')GO TO 1
      CALL OPEN(7,IFILE,2)
    1 READ(6,1000)(E1(I),I=1,5)
 1000 FORMAT(5E10.1)
      WRITE(DEVICE,1001)(E1(I),I=1,5)
 1001 FORMAT(' INCREMENT TESTS:',5E10.1)
C     IWE=0,SKIP; =1,WRITE ERROR DETAILS
C     IWD=0,SKIP; =1,WRITE IT,SS,EMQ;=2 WRITE ALSO G(I),X(I)
C     IUI=UNITS INPUT, IUO=UNTS OUTPUT, 1=MPH, 2=KTS, 3=MPS
C     MAX=MAXIMUM ITERATIONS
C     IMI,IMMO; INPUT/OUTPUT FOR HEIGHT, 1=FT,2=M
      READ(6,1002)IWE,IWD,IUI,IUO,IMI,IMMO,MAX
 1002 FORMAT(7I5)
      ISAVE=IUI
      WRITE(DEVICE,1003)IWE,IWD,IUI,IUO,IMI,IMMO,MAX
 1003 FORMAT(' IWE =',I2,3X,'IWD =',I2,3X,'IUI =',I2,3X
     1 'IUO =',I2,3X,'IMI =',I2,3X,'IMMO =',I2,3X,'MAX =',I3,3X,//)
C     EMQQ=SCALE FACTOR IN MARQ, J2=NO. PTS. IN HI END ESTIMATE
C     PX =SMALLEST FF VALUE IN HI END ESTIMATES
      READ(6,1024)EMQQ,PX
 1024 FORMAT(2(E10.1))
      WRITE(DEVICE,1026)EMQQ,PX
 1026 FORMAT(' EMQ =',E8.1,5X,'PX =',F6.4)
  896 READ(6,2004)M
 2004 FORMAT(I5)
      IF(M.EQ.0)STOP
C     WIND SPEED AT DIVISIONS OF F-TABLE
      READ(6,1004)(W(I),I=1,M)
 1004 FORMAT(F7.2)
```

```
      B=FACT(IUO,IUI)
      DO 20 I=1,M
   20 W(I)=W(I)*B
C     MS=NO. OF STATIONS IN BATCH
      READ(6,2004)MS
      MT=0
  898 MT=MT+1
      IF(MT.GT.MS)GO TO 896
C     DATA IDENTIFICATION
C     ISTN=STATION INDEX
C     JD=1 GETS JA=HR,JB=MO,JC=LVL
C     JD=2 GETS JA=HR,JC=MO,JB=LVL
C     JD=3 GETS JC=HR,JA=MO,JB=LVL
C     MB=NUMEROF F-TABLES TO BE PROCESSED IN A BATCH
      READ(6,1005)ISTN
 1005 FORMAT(16A1)
      READ(6,7000)JA,JB,JD,MB
 7000 FORMAT(4I5)
C     RETURN POINT FOR BATCH
      MM=0
  900 MM=MM+1
      IF(MM.GT.MB)GO TO 898
C     JC=LVL, MO, HR, INDEX
C     N=NO. OF DATA ITEMS IN F-TABLE
C     CT=TOTAL NO. OF CASES IN F-TABLE OR 100. IN PERCENT
C     CT=0 LEAVES F-TABLE UNCHANGED
C     NE=0 USES LAST X(I),I=1,5, AS ESTIMATES FOR NEXT F-TABLE
C     NE=-1, COMPUTES ESTIMATES
      READ(6,2005)JC,N,CT,NE
 2005 FORMAT(2I5,F5.1,I5)
      GO TO(2,4,6),JD
    2 IHR=JA
      IMO=JB
      LVL=JC
      GO TO 8
    4 IHR=JA
      IMO=JC
      LVL=JB
      GO TO 8
    6 IHR=JC
      IMO=JA
      LVL=JB
    8 WRITE(DEVICE,2006)
 2006 FORMAT(/////)
      LVL=IFIX(FLOAT(LVL)*FAC2(IMI,IMMO))
      WRITE(3,1006)(ISTN(NN),NN=2,16),IHR,IMO,LVL
      WRITE(DEVICE,1006)(ISTN(NN),NN=2,16),IHR,IMO,LVL
 1006 FORMAT('0ISTN = ',15A1,2X,'HR =',I3,2X,'MO =',I3,2X,'LVL =',I3)
      READ(6,1007)(FO(I),I=1,N)
 1007 FORMAT(F7.2)
      IF(CT.EQ.0.)GO TO 13
```

```
C       CHECKS SUMS, ADJUSTS FOR CALMS
        SUM=0.
        DO 10 I=1,N
        SUM=SUM+FO(I)
   10   CONTINUE
        IF(CT.LT.SUM)CT=SUM
        FO(1)=FO(1)+CT-SUM
        B=100./CT
        DO 12 I=1,N
        FO(I)=FO(I)*B
   12   CONTINUE
C       GETS DISTRIBUTION FUNCTION
   13   PO(1)=FO(1)
        DO 14 I=2,N
        I1=I-1
        PO(I)=PO(I1)+FO(I)
   14   CONTINUE
        N1=N
        IF(N.GE.8)N1=8
        WRITE(DEVICE,1008)VEL(IUO),(W(I),I=1,N1)
 1008   FORMAT(' W, ',A3,2X,8F7.2)
        WRITE(DEVICE,1009)(FO(I),I=1,N1)
        WRITE(3,1009)(FO(I),I=1,N1)
 1009   FORMAT(' F(%)',4X,8F7.2)
        WRITE(DEVICE,1010)(PO(I),I=1,N1)
        WRITE(3,1010)(PO(I),I=1,N1)
 1010   FORMAT(' P(%)',4X,8F7.2/)
        IF(N.LE.8)GO TO 16
        N1=9
        N2=N
        IF(N.GT.16)N2=16
        WRITE(DEVICE,1008)VEL(IUO),(W(I),I=N1,N2)
        WRITE(DEVICE,1009)(FO(I),I=N1,N2)
        WRITE(DEVICE,1010)(PO(I),I=N1,N2)
        IF(N.LE.16)GO TO 16
        N1=17
        WRITE(DEVICE,1008)VEL(IUO),(W(I),I=N1,N)
        WRITE(DEVICE,1009)(FO(I),I=N1,N)
        WRITE(DEVICE,1010)(PO(I),I=N1,N)
C       CHANGES % TO FRACTION
   16   DO 18 I=1,N
        FO(I)=FO(I)/100.
        PO(I)=PO(I)/100.
   18   CONTINUE
        IF(NE)197,23,21
   21   NF=0
C         RETURN POINT FOR ESTIMATES
  902   NF=NF+1
        IF(NF.GT.NE)GO TO 900
        READ(6,1007)(XE(I),I=1,5)
        B=FACT(IUO,IUI)
```

```
      DO 22 I=1,4
   22 X(I)=XE(I)*B
      X(5)=XE(5)
   23 WRITE(DEVICE,1011)
 1011 FORMAT(/14X,'SG1',6X,'WR1',6X,'SG2',6X,'WR2',6X,'K',
     1 8X,'RMSE',5X,'EMAX')
      IF(NE.GT.0) ISW=0
      WRITE(DEVICE,1012)ISW,(X(I),I=1,5)
 1012 FORMAT(' INITIAL',I1,4(F9.2),F9.4)
      KK=1
      CALL MARQ(5,MAX,E1,IWD,SS,KK,EE,EMAX,EMQQ,ID2,IT)
   30 RMSE = SQRT(SS/N)*100
      EMAX=EMAX*100.
      DO 24 I=1,4
   24 Z(I)=0.
      AK=X(5)
      IF(AK.EQ.0.) GO TO 25
      Z(1)=X(1)
      Z(2)=X(2)
      IF(AK.EQ.1.) GO TO 26
   25 Z(3)=X(3)
      Z(4)=X(4)
   26 Z(5)=AK
      WRITE(DEVICE,1013)IT,(Z(I),I=1,5),RMSE,EMAX
 1013 FORMAT(' FINAL ',I2,4(F9.2),F9.4,2(F9.2))
      IF(ID2.EQ.0)GO TO 31
      WRITE(DEVICE,1022)
 1022 FORMAT(' NO CONVERGENCE')
   31 IF(IWE.EQ.0)GO TO 196
      DO 32 I=1,N
   32 EE(I)=EE(I)*100.
      N1=N
      IF(N.GE.7)N1=7
      WRITE(DEVICE,1016)VEL(IUO),(W(I),I=1,N1)
 1016 FORMAT(' W   ',A3,2X,7F9.2)
      WRITE(DEVICE,1018)(EE(I),I=1,N1)
 1018 FORMAT(' ERRORS  ',7(F9.2))
      IF(N.LE.7)GO TO 196
      N1=N1+1
      N2=N
      IF(N.GE.14)N2=14
      WRITE(DEVICE,1016)VEL(IUO),(W(I),I=N1,N2)
      WRITE(DEVICE,1018)(EE(I),I=N1,N2)
      IF(N.LE.14) GO TO 196
      N2=N2+1
      WRITE(DEVICE,1016)VEL(IUO),(W(I),I=N2,N)
      WRITE(DEVICE,1018)(EE(I),I=N2,N)
C     CHECKS FOR NON-ZERO BUT SMALL WR
C     SETS SMALL WR=0 AND RECOMPUTES ESTIMATES
  196 IF(X(2).EQ.0.) GO TO 192
      IF(X(1).LE.X(2)) GO TO 192
```

```
      X(2)=0
      GO TO 23
  192 IF(X(4).EQ.0.) GO TO 194
      IF(X(3).LE.X(4)) GO TO 194
      X(4)=0.
      GO TO 23
  194 IF(NE.GE.0) GO TO 902
      GO TO (208,900,224,220,220,900),ISW
C     CALCULATED PARAMETER ESTIMATES
C     HIGH END ESTIMATES
  197 DO 198 I=1,N
      I2=N+1-I
      I1=I2-1
      IF(I1.EQ.0)GO TO 199
      F1=FO(I1)
      F2=FO(I2)
      IF(FO(I2).LT.PX) GO TO 198
      IF(F1-F2) 199,199,198
  198 CONTINUE
  199 W2 = W(I2)
      F2 = FO(I2)
      I1=I2+1
      W1=W(I1)
      F1=FO(I1)
      SGH=(W1-W2)/SQRT(2.*ALOG(F2/F1))
      WRH=W2
      IF(WRH.LE.SGH/2) WRH=SGH/2
C     LOW END ESTIMATES. DEGENERATE CASE
  200 DO  202 I=1,3
      W1=W(I)
      WW(I)=W1*W1
  202 Z(I)=PO(I)
      CALL SOLV(Z,WW,AA,BB,CC)
      IF((AA.LE.0).OR.(BB.LE.0))GO TO 208
      QQ=(BB*BB+2.*CC*(1-AA))/(BB*BB)
      IF(QQ.GE.100.)GO TO 208
      IF(QQ.LT.0.)GO TO 204
      CALL ROOT(QQ,YY)
      SGD=0.5*SQRT((1.-YY)*BB/(-CC))
      WRD=SGD*SQRT(2.*YY)
      GO TO 206
  204 SGD=0.5*SQRT(BB/(-CC))
      WRD=0.
  206 ISW=1
      X(1)=0
      X(2)=0
      X(3)=SGD
      X(4)=WRD
      X(5)=0.5
      GO TO 23
```

```
C     NON DEGENERATE LOW END ESTIMATES
  208 DO 210 I=1,3
      W1=W(I)
      WW(I)=W1*W1
  210 Z(I)=PO(I)/(W1*W1)
      CALL SOLV(Z,WW,AA,BB,CC)
      L=0
      IF(AA.LE.0.) GO TO 218
      IF(BB.EQ.0.) GO TO 218
      R=(2.*BB*BB-3.*AA*CC)/(BB*BB)
      IF(R.LE.0.)GO TO 218
      R=SQRT(R)
      IF(BB)212,218,214
  212 YY=R/(R+1)
      ISW=4
      GO TO 216
  214 IF(R.LE.1)GO TO 218
      YY=R/(R-1)
      ISW=5
  216 SGL=SQRT(AA*(1.-YY)/(-BB))
      WRL=SGL*SQRT(2.*YY)
      GO TO 226
  218 BB=(Z(3)-Z(2))/(WW(3)-WW(2))
      AA=Z(2)-BB*WW(2)
      L=1
      IF(AA.LE.0.)GO TO 222
  220 QQ=(AA*AA-2.*BB)/(AA*AA)
      IF(QQ.LE.0.) GO TO 222
      IF(QQ.GT.1500.) GO TO 222
      CALL ROOT(QQ,YY)
      SGL=SQRT(EXP(-Y)/(2.*AA))
      WRL=SGL*SQRT(2.*YY)
      ISW=3
      GO TO 226
  222 IF(L.EQ.0) GO TO 218
      AA=(Z(1)+Z(2)+Z(3))/3.
      SGL=1./SQRT(2.*AA)
      WRL=0.
      ISW=2
      GO TO 226
  224 SG1=0.
      SG2=0.
      IF(AA*BB.LT.0.) SG1=SQRT((AA)/(-BB))/2
      IF(BB*CC.LT.0.) SG2=SQRT((-BB)/(6.*CC))
      IF((SG1.EQ.0.).AND.(SG2.EQ.0.)) GO TO 900
      IF((SG1.EQ.0.).AND.(SG2.GT.0.)) SGL=SG2
      IF((SG1.GT.0.).AND.(SG2.EQ.0.)) SGL=SG1
      IF(SG1*SG2.GT.0.) SGL=(SG1+SG2)/2.
      WRL=0
      ISW=6
```

```
226 X(1)=SGL
    X(2)=WRL
    X(3)=SGH
    X(4)=WRH
    X(5)=.5
    GO TO 23
    END
```

```
      SUBROUTINE PROB(W,SG,WR,P,I)
C     GIVEN W,SG,WR,COMPUTES P(1)=PROB.,P(2)=DP/DSG,P(3)=DP/DWR
C     WHERE E=ACCURACY
C     FOR CONVERGENCE CRITERIA. I=UPPER INDEX REQUIRED 1,3.
C
      DIMENSION P(3)
      E=1.E-07
      IF(SG.NE.0)GO TO 10
C     CASE SG=0
    1 IF(W.LE.WR)P(1)=0
      IF(W.GT.WR)P(1)=1
      P(2)=0
      P(3)=0
      RETURN
   10 Y=2.*SG*SG
      X=W*W/Y
      Y=WR*WR/Y
      IF(Y.NE.0)GO TO 15
C     CASE WR=0
      IF(X.GT.50)GO TO 1
      Z=EXP(-X)
      P(1)=1-Z
      P(2)=-2.*X*Z/SG
      P(3)=0.
      RETURN
   15 IF(ABS((W-WR)/(2.*SG)).GT.2.5) GO TO 1
      IF((X+Y).GT.60.) GO TO 40
   16 EX=EXP(-X-Y)
      SUM1=1
      SUM2=1
      SUM3=1
      SUM4=1
      SUM5=X
      A=1
      TX=1
      TY=1
      TZ=1
   20 TX=TX*X/A
      TY=TY*Y/A
      SUM1=SUM1+TX
      SUM2=SUM2+TY
      SUM3=SUM3+TY*SUM1
      A=A+1
      B=A
      IF(I.EQ.1) GO TO 25
      TXY=TX*TY
      SUM4=SUM4+TXY
      TZ=TXY*X/A
      SUM5=SUM5+TZ
   25 T1=1-Y/B
      T2=1-(X*Y)/(B*B)
```

```
      IF(T1.LE.0)GO TO 20
      IF(T2.LE.0)GO TO 20
      IF(EX*TX*TY/(T1*T2)-E)30,20,20
   30 SUM3=SUM3+SUM1*(EXP(Y)-SUM2)
      P(1)=1-EX*SUM3
      IF(I.EQ.1)RETURN
      P(3)=-2.*Y*EX*SUM5/WR
      P(2)=-2.*EX*(X*SUM4-Y*SUM5)/SG
      RETURN
C     ASYMPTOTIC FORM FROM RICE P. 109(P.241)
   40 X1=W/SG
      X2=WR/SG
      DX=ABS(X1-X2)
      TE=1./(1.+0.33267*DX)
      ZE=EXP(-DX*DX/2.)/2.50662829
      PP=1.-ZE*TE*(0.4361836+TE*(-0.1201676+TE*0.9372980))
      IF(X2.GT.X1) PP=1.-PP
      RAT=(X1-X2)/(2.*X2)
      AA=1./(8.*X2*X2)
      P(1)=PP-(ZE/(2.*X2))*(1.+AA-0.5*RAT*(1.-RAT))
      IF(I.EQ.1) RETURN
      PS=ZE*(1.+AA+RAT*(1.-AA-0.5*RAT*(1.-RAT)))
      PC=ZE*(1.+3.*AA+RAT*(-1.+1.5*RAT))/(2.*WR)
      P(2)=-(X1-X2)*PS/SG-PC
      P(3)=-PS/SG+PC/X2
      RETURN
      END
```

```
      SUBROUTINE CHOL1(M)
      COMMON/BK2/A(15),G(5)
C     GETS LOWER TRIANGULAR FACTOR,L,A=LTL,A=SYMMETRIC,RETURNS
C     L IN A
      DO 14 J=1,M
      IQ=J*(J+1)/2
      IF(J.EQ.1)GO TO 5
      DO 4 I=J,M
      IM=I*(I-1)/2+J
      S=A(IM)
      J1=J-1
      DO 2 K=1,J1
      I3=IM-K
      I2=IQ-K
      S=S-A(I3)*A(I2)
    2 CONTINUE
      A(IM)=S
    4 CONTINUE
    5 IF(A(IQ).GT.0) GO TO 6
      A(IQ)=0
    6 S=SQRT(A(IQ))
      DO 12 I=J,M
      IM=I*(I-1)/2+J
      IF(S)8,8,10
    8 A(IM)=0
      GO TO 12
   10 A(IM)=A(IM)/S
   12 CONTINUE
   14 CONTINUE
      RETURN
      END
```

```
      SUBROUTINE CHOL2(M)
      COMMON/BK2/A(15),G(5)
C     FORWARD SUBSTITUTION
      IF(A(1))2,2,4
    2 G(1)=0
      GO TO 6
    4 G(1)=G(1)/A(1)
    6 IF(M.EQ.1)GO TO 13
      IQ=1
      DO 11 I=2,M
      IM=I-1
      DO 8 J=1,IM
      IQ=IQ+1
      G(I)=G(I)-A(IQ)*G(J)
    8 CONTINUE
      IQ=IQ+1
      IF(A(IQ))10,10,12
   10 G(I)=0
      GO TO 11
   12 G(I)=G(I)/A(IQ)
   11 CONTINUE
C     BAC SOLUTION
   13 MM=M*(M+1)/2
      IF(A(MM))14,14,16
   14 G(N)=0
      GO TO 18
   16 G(M)=G(M)/A(MM)
   18 IF(M.EQ.1) GO TO 28
      DO 26 I1=2,M
      I=M-I1+2
      IQ=I*(I-1)/2
      IM=I-1
      DO 20 J=1,IM
      I8=IQ+J
      G(J)=G(J)-G(I)*A(I8)
   20 CONTINUE
      IF(A(IQ))22,22,24
   22 I9=I-1
      G(I9)=0
      GO TO 26
   24 I9=I-1
      G(I9)=G(I9)/A(IQ)
   26 CONTINUE
   28 RETURN
      END
```

```
      SUBROUTINE KBEST(SS,EMAX,EE,KK)
C     GETS BEST K IN X(5) AND SUM OF SQUARES OF ERRORS .
C     GETS INDIVIDUAL ERRORS,EE(I),I=1,N, AND
C     PICKS OUT LARGEST ABSOLUTE EMAX, KK=1, USUAL, =0,SETS X(5)=0.
C
      DIMENSION Q1(20),Q2(20),EE(20),P1(3),P2(3)
      COMMON/BK1/N,W(20),PO(20),X(5)
      B=0.
      SUM1=0.
      SUM2=0.
      SUM3=0.
      DO 2 I=1,N
      W1=W(I)
      X1=X(1)
      X2=X(2)
      CALL PROB(W1,X1,X2,P1,1)
      X3=X(3)
      X4=X(4)
      CALL PROB(W1,X3,X4,P2,1)
      Q1(I)=P1(1)
      Q2(I)=P2(1)
      A1=P1(1)-P2(1)
      B1=PO(I)-P2(1)
      SUM1=SUM1+A1*A1
      SUM2=SUM2+B1*B1
      SUM3=SUM3+A1*B1
    2 CONTINUE
      AK=SUM3/SUM1
      IF(AK-1.)6,4,4
    4 AK=1.
      SS=SUM1-2.*SUM3+SUM2
      GO TO 12
    6 IF(AK)8,8,10
    8 AK=0.
   10 SS=SUM2-AK*SUM3
      IF(SS .LT. 0.) SS = 0.
   12 X(5)=AK
      BIG=0.
      DO 14 I=1,N
      AA=Q1(I)-Q2(I)
      E3=PO(I)-Q2(I)-AK*AA
      EE(I)=E3
      E2=ABS(E3)
      IF(E2.LE.BIG)GO TO 14
      BIG=E2
   14 CONTINUE
      EMAX=BIG
      RETURN
      END
```

```
      SUBROUTINE MARQ(M,MAX,E1,IWD,SS,KK,EE,EMAX,EMQQ,ID2,IT)
C     MODIFIED MARQUARDT ADAPTED FROM NASH.
C     M=NO. OF VARIABLES;IWD=0,NO WRITE, =1,WRITE EACH ITERATION
C     MAX=MAX NO. ITERATIONS, E1(I),I=1,M,TEST ON
C     CONVERGENCE OF INCREMENTS, SS=SUM OF SQUARES OF ERRORS,
C     ID2=0 FOR OK, =1 FOR NO CONVERGENCE.  KK=1,USUAL, =0,SETS X
C
      INTEGER DEVICE
      DIMENSION P1(3),P2(3),BB(20),Y(5),E1(5),EE(20),GG(5)
      COMMON/BK1/N,W(20),PO(20),X(5)/BK2/A(15),G(5)
      COMMON/DEVICE/DEVICE
      EMQ=EMQQ
      JM=M*(M+1)/2
      IT=0
      ID2=0
C     GET INITIAL SUM OF SQUARES
      CALL KBEST(SS,EMAX,EE,KK)
      AKO=X(5)
      IF(IWD.EQ.0)GO TO 100
      WRITE(DEVICE,2600)(X(I),I=1,5)
      WRITE(DEVICE,1014)IT,SS,EMQ
C     RETURN FOR ITERATIONS
  100 IF(IT.EQ.MAX)GO TO 16
      SO=SS
      IT=IT+1
      ITT=IT
      EMQ=EMQ*.4
      CALL COEF(KK)
C     STORES COEFFICIENTS AND PARAMETRS
      DO 2 I=1,M
      Y(I)=X(I)
      GG(I)=G(I)
    2 CONTINUE
      DO 4 I=1,JM
      BB(I)=A(I)
    4 CONTINUE
C     AUGMENTS DIAGONAL
   99 DO 5 I=1,JM
      A(I)=BB(I)
    5 CONTINUE
      DO 6 I=1,M
      IQ=I*(I+1)/2
      A(IQ)=BB(IQ)*(1.+EMQ)+EMQ
    6 CONTINUE
      DO 7 I=1,5
      G(I)=GG(I)
    7 CONTINUE
      IF(IWD.LE.1)GO TO 20
      WRITE(DEVICE,2400)(G(I),I=1,5)
 2400 FORMAT(' G'/10E10.4)
```

```
C       SOLVES FOR INCREMENTS
   20   CALL CHOL1(M)
        CALL CHOL2(M)
C       ADD INCREMENTS, ADJUST IF OUT OF RANGE
        M1=M-1
        DO 8 I=1,M1
        X(I)=Y(I)+G(I)
        IF(X(I).LT.0.)X(I)=0
    8   CONTINUE
        CALL KBEST(SS,EMAX,EE,KK)
        IF(IWD.LE.1)GO TO 22
        WRITE(DEVICE,2600)(X(I),I=1,5)
 2600   FORMAT(' X',/5E10.4)
   22   IF(IWD.EQ.0)GO TO 9
        WRITE(DEVICE,1014)IT,SS,EMQ
 1014   FORMAT(' IT =',I4,4X,'SS =',E11.5,4X,'EMQ =',E10.5)
    9   G(5)=X(5)-AK0
C       CHECKS SIZE OF INCREMENTS
        IC=0
        DO 10 I=1,M
        IF(ABS(G(I)).LE.E1(I))IC=IC+1
   10   CONTINUE
        AK0=X(5)
   12   IF(IC.EQ.M)GO TO 18
        IF(SS.EQ.0.) GO TO 18
        IF(SS.LE.S0)GO TO 100
        IF(EMQ.EQ.0.)EMQ=1.E-07
        EMQ=EMQ*10
        GO TO 99
   16   ID2=1
   18   IT=ITT
        RETURN
        END
```

```
      SUBROUTINE COEF(KK)
C     COMPUTES COEFFICIENTS FOR LEAST SQUARES
C     KK=1,USUAL, KK=0,SETS X(5)=K=0.
      DIMENSION D(5),P1(3),P2(3)
      COMMON/BK1/N,W(20),PO(20),X(5)/BK2/A(15),G(5)
C     ZEROS COEFFICIENTS
      DO 2 I=1,5
      G(I)=0.
    2 CONTINUE
      DO 4 I=1,15
      A(I)=0.
    4 CONTINUE
C     COMPUTES COEFFICIENTS
      AK=X(5)
      BK=1-AK
      DO 10 I=1,N
      W1=W(I)
      CALL PROB(W1,X(1),X(2),P1,3)
      CALL PROB(W1,X(3),X(4),P2,3)
      DP=P1(1)-P2(1)
      S=PO(I)-P2(1)-AK*DP
      D(1)=AK*P1(2)
      D(2)=AK*P1(3)
      D(3)=BK*P2(2)
      D(4)=BK*P2(3)
      D(5)=DP
      DO 8 J=1,5
      G(J)=G(J)+S*D(J)
      JQ=J*(J-1)/2
      DO 6 K=1,J
      K1=JQ+K
      A(K1)=A(K1)+D(J)*D(K)
    6 CONTINUE
    8 CONTINUE
   10 CONTINUE
      DO 12 I=1,5
      IQ=I*(I+1)/2
      IF(A(IQ).EQ.0)A(IQ)=1
   12 CONTINUE
      IF(KK.EQ.1)RETURN
      DO 13 I=11,14
      A(I)=0
   13 CONTINUE
      G(5)=0.
      A(15)=1.
      RETURN
      END
```

```
      SUBROUTINE SOLV(Z,WW,AA,BB,CC)
C     FITS QUADRATIC TO THREE POINTS AND OUTPUTS COEFFICIENTS
C     OF Z=AA+BB*WW+CC*WW**2
      DIMENSION Z(3),WW(3)
      Z1=Z(1)
      Z2=Z(2)
      Z3=Z(3)
      W1=WW(1)
      W2=WW(2)
      W3=WW(3)
      Y12=(Z1-Z2)/(W1-W2)
      Y23=(Z2-Z3)/(W2-W3)
      CC=(Y23-Y12)/(W3-W1)
      BB=Y12-CC*(W1+W2)
      AA=Z1-BB*W1-CC*(W1*W1)
      RETURN
      END
```

```
      SUBROUTINE ROOT(QQ,YY)
C     SOLVES 1-(1-Y) EXP(Y)-Q=0 FOR Y.
      Z1=SQRT(2.*QQ)
    2 Z2=Z1-(1.-QQ-(1.-Z1)*EXP(Z1))/(Z1*EXP(Z1))
      IF (ABS(Z2-Z1)-0.001) 6,6,4
    4 Z1=Z2
      GO TO 2
    6 YY=Z2
      RETURN
      END
```


☆U.S. GOVERNMENT PRINTING OFFICE: 1981-740-145/2917